2018

Carbon Catalysts for Liquid Phase Reactions

Raquel Pinto Rocha

Dissertation presented to obtain the Doctor of Philosophy (PhD) degree in Chemical and Biological Engineering

Laboratory of Separation and Reaction Engineering - Laboratory of Catalysis and Materials (LSRE-LCM)

Department of Chemical Engineering, Faculty of Engineering, University of Oporto, Portugal

SUPERVISOR | Emeritus Professor José Luís Cabral Da Conceição Figueiredo

CO-SUPERVISOR | Associate Professor Manuel Fernando Ribeiro Pereira

SRE CM Shaking the Present Shaping the Future
ASSOCIATE LABORATORY
LABORATORY OF SEPARATION AND REACTION ENGINEERING
LABORATORY OF CATALYSIS AND MATERIALS

U.PORTO FEUP FACULDADE DE ENGENHARIA UNIVERSIDADE DO PORTO

FCT Fundação para a Ciência e a Tecnologia

(This page intentionally left blank)

This work was financially supported by Fundação para a Ciência e a Tecnologia (FCT) through the PhD scholarship SFRH/BD/95411/2013.

Additional funding was provided from the following projects: Project POCI-01-0145-FEDER-006984 – Associate Laboratory LSRE-LCM funded by FEDER through COMPETE2020 - Programa Operacional Competitividade e Internacionalização (POCI) – and by national funds through FCT - Fundação para a Ciência e a Tecnologia.

(This page intentionally left blank)

Play is the Highest Form of Research

- Albert Einstein -

…and I played a lot.

- Raquel Rocha –

(This page intentionally left blank)

Preface

This PhD thesis was written on the basis of experiments carried out at the Catalysis and Carbon Materials group of the Associate Laboratory LSRE-LCM (Laboratory of Separation and Reaction Engineering - Laboratory of Catalysis and Materials), at the Department of Chemical Engineering, Faculty of Engineering of the University of Porto. The research described herein was supervised by Professors José Luís Figueiredo and Fernando Pereira.

It represents the end of a journey, a journey that had initiated in 2010 when I joined the Laboratory of Catalysis and Materials and started my career in science, as a researcher in the project *Nanostructured catalysts based on carbon nanofibers for environmental applications*, my first contact with the field of carbon nanomaterials and their application as catalysts. This project led to my preliminary results on the subject and to the desire to go deeper into the use of carbon materials as catalysts. This PhD reflects that ambition and the reaped fruits of a gladly hard work.

The thesis is divided into five parts. Part I briefly introduces the theme of carbon materials for catalysis applications and presents the state of the art on this subject. Part II is exclusively dedicated to the presentation of the methodologies adopted for tuning carbon materials properties for further catalytic application in a typical acid catalysed reaction (PART III) and in a liquid-phase oxidation process (Part IV). Part V summarizes the main conclusions and offers suggestions for future work.

The main core of the text (Parts II, III and IV) has already been reported in scientific papers, carefully indicated throughout the work; however, it does not follow the typical article structure.

I hope that this work may be useful for those researchers starting in the field and for experts in related topics.

The journey ended, but all endings are also beginnings.

Raquel Rocha

Porto, January 2018

Acknowledgements

Foremost, I would like to express my sincere gratitude to my supervisors, Professor José Luís Figueiredo and Professor Manuel Fernando Pereira, for the continuous support, motivation and guidance during all my research journey since 2010. Their belief and encouragement were crucial to lead me to this stage. To both I would like to thank the attentive and close supervision, but with enough freedom to promote my autonomy and personal and professional growth.

I would like to thank Professor José Luís Figueiredo, in addition to the provided practical support and access to the laboratory facilities, for his teachings based on his extensive experience and knowledge, not only technical but also human, his stimulating discussions, and his inspiration for a research career.

To Professor Manuel Fernando Pereira, my sincere thanks for all the positive words, his serene availability, his insightful comments which incited me to widen my research, and all the trust always shown.

This thesis would not be possible without the financial support through the PhD scholarship received from Fundação para a Ciência e a Tecnologia, SFRH/BD/95411/2013, for which I am grateful.

My sincere thanks also go to Professor Madalena Dias, as Director and scientific coordinator of the Associate Laboratory LSRE-LCM, who promptly accepted my request to develop this thesis within this host institution and allowed me to join their team. Without this support, it would have been impossible to accomplish this work.

To the Department of Chemical Engineering, I would like to express my gratitude for the access to the facilities and kind assistance.

To Doctor Carlos Sá, Director of the Materials Centre of the University of Porto (CEMUP), I am indebted for allowing access to materials characterization techniques, and precious assistance.

I want to thank all my current fellow labmates for their support, availability and cooperation, and also those whom in the meantime left us for further journeys: Juliana, João, Alexandra, Luísa, Sérgio and Marina, eternal friends. To Salomé and Carla, for all cooperation, help, support on work, but more importantly, for their friendship on every coffee-break, after work meetings, all the conversations and fun; with you, it was much easier. I would like also to thank Adrián Silva who enlightened me at the first glance at the research in the laboratory and in scientific writing.

To all my co-authors, on this work and all the others performed, I express my gratitude for their cooperation. I am sure that without their help and collaboration I would not achieve these results.

I would like to thank, in advance, all members of the jury for the time devoted to reading and evaluating this thesis.

Last but not least, I will always be grateful to my parents, to Rodrigo, my brothers and sisters, my grandparents and friends, for their support in life, their unbeatable patience, their encouragement, and their love.

Abstract

This work deals with the chemical functionalization of carbon materials and their evaluation as heterogeneous catalysts in liquid-phase reactions, traditionally catalysed by noble metals, rare earth oxides and homogeneous catalysts.

Chemical, mechanical and thermal treatments were applied to carbon materials in order to incorporate O-, N- and S-containing groups onto the carbon surface. Commercial multiwalled carbon nanotubes (CNTs), carbon xerogels synthesized by the sol–gel process (CXs) and graphene-based materials (rGOs) prepared by the modified Hummers method were selected as carbon samples.

O-containing groups were successfully introduced onto CNT and CX samples by nitric acid (HNO_3) oxidation at boiling temperature (BT). The HNO_3 treatment affects the textural properties (the effect is more pronounced in the case of CNTs than in CXs) promoting an increase of surface area (S_{BET}) and a decrease of total pore volume. In addition, it induces a pronounced acidic character to the carbon materials, creating a large amount of carboxylic acids and anhydrides, phenol groups, and, in less extent, lactones and some neutral and basic groups, as carbonyl-quinones. Subsequent thermal treatments allow to induce basicity of the samples, by the selective removal of the acidic groups. In addition to the BT approach, controlled functionalization of CNTs was demonstrated by HNO_3 hydrothermal oxidation at 200 °C. The formation/evolution of oxygen functional groups and the degree of surface functionalization were described by exponential functions in terms of HNO_3 concentration. A

progressive increase of the S_{BET} upon hydrothermal functionalization was observed. Hydrothermal oxidation competes well with the BT treatment regarding the total amount of oxygen functionalities, while requiring much lower amounts of oxidizing agent.

Treatments with sulphuric acid (H_2SO_4), or with HNO_3/ H_2SO_4 mixture, performed over CNT and CX samples, led to the introduction of S-containing groups, more precisely sulphonic acid groups (-SO_3H). Larger content of -SO_3H groups was introduced on CXs (up to 2.1 % wt. S content), in comparison with the CNT sample. A decrease of S_{BET} was observed with the H_2SO_4 treatment.

A hydrothermal approach was developed to incorporate N-functionalities onto CNTs surface. The method involves pre-oxidation of the surface by HNO_3 treatment at BT, followed by liquid-phase urea treatment at 200 °C, and gas-phase thermal treatment with nitrogen at 600 °C. In spite of its effectiveness for N-incorporation, low amounts of nitrogen were reached (< 1 % wt.). In alternative, an easy to handle method, combining a mechanical treatment under ball milling followed by thermal treatments, was developed. This novel approach leads to the incorporation of large amounts of N-groups (up to 7.6 % wt.), namely quaternary nitrogen, pyridinic and pyrrolic groups. Different nitrogen precursors (melamine, urea, ammonia), different precursor/CNT ratios, the presence/absence of solvent, the effect of O-containing surface groups and final temperatures of the thermal treatment were evaluated towards the generation of active and stable N-species. The highest efficiency for N-doping was obtained with melamine, by a solvent-free approach which avoids the production of wastes. The method was extended to rGO materials, and melamine was also found to be the most

suitable precursor to incorporate large amounts of nitrogen groups, while keeping adequate surface area.

Nitrogen adsorption isotherms at -196 °C, temperature programmed desorption coupled with mass spectrometry, thermogravimetry, point of zero charge, elemental analysis and X-ray photoelectron spectroscopy were used to characterize the prepared and modified carbon materials.

The catalytic activity of selected heteroatom-modified carbon materials was studied in two liquid phase reactions: in the esterification of acetic acid with ethanol (as a model acid-catalysed reaction) and in the catalytic wet air oxidation (CWAO) process, using oxalic acid and phenol as model compounds.

In the esterification reaction, carried out at 70 °C using 1:10 acetic acid/ethanol molar ratio, CNT and CX samples treated with H_2SO_4 and HNO_3, were tested as catalysts. The rate of formation of ethyl acetate (EtAc) was found to depend strongly on the chemical properties of the carbon materials, the presence of $-SO_3H$ groups being more adequate for this reaction than carboxylic acids. A good correlation was obtained between the rate of formation of EtAc and the concentration of $-SO_3H$ groups. The sample with the best performance, a H_2SO_4 treated CX sample, underperformed compared with the traditional H_2SO_4 homogeneous catalyst; however, a turn-over frequency (TOF) of 1.9 min^{-1} was obtained, which is competitive with the conventional strong solid acid catalyst Nafion resin NR50 (TOF = 1.5 min^{-1}).

Regarding the CWAO process, experiments were performed at 40 bar of total pressure and 140 and 160 °C, for oxalic acid and phenol, respectively. Both model compounds are very stable under non-catalytic conditions; but they can be degraded in the presence of carbon materials.

CNT, CX and rGO materials were tested as catalysts with strongly different textural and chemical properties. Some general trends were observed, and correlations between the catalytic activity and the surface chemistry of the carbon materials were established. It was found that the oxidation of oxalic acid and phenol depends on the textural and chemical properties of the carbon materials. The catalytic oxidation of model pollutants is faster in the presence of samples rich in nitrogen, and also favoured in the absence of O-containing surface groups on the CNT surface; however, the introduction of sulphonic acid groups enhanced the removal rate of the model compounds, particularly in the of phenol oxidation. Nitrogen functionalities improved the catalytic performance of the carbon materials, regardless of the pollutant. Using N-doped CXs, the apparent reaction rate constant for oxalic acid oxidation correlates with the concentration of surface nitrogen, the rate constant increasing by two orders of magnitude in comparison with the nitrogen-free material. The CNT sample prepared by ball milling with melamine without solvent was the most promising sample, combining an easy preparation with high amount of N-functionalities and leading to faster oxalic acid and phenol removals. Under the operation conditions used, oxalic acid was completely mineralized in 5 min (initial concentration of 1000 mg L^{-1}), while total phenol degradation was achieved after 2 h of reaction (initial concentration of 75 mg L^{-1}). The sample also revealed good stability under cyclic runs. Additional experiments were performed with a radical scavenger and sodium persulfate, in order to clarify the reaction mechanism. Oxalic acid oxidation appears to proceed mainly on the carbon surface using undoped and N-doped carbon materials; while the

reaction pathway in the presence of sulphonic acid groups possibly involves sulphate radicals in the liquid phase.

Metal-free carbon materials were found to be very active catalysts for CWAO, their activity strongly depending on the stability of their surface chemistry.

(This page intentionally left blank)

Resumo

Este trabalho explora diferentes métodos de funcionalização da química superficial de materiais de carbono e a avaliação dos materiais resultantes como catalisadores heterogéneos em reações de fase líquida, tradicionalmente catalisadas por metais nobres, óxidos de terras raras e/ou catalisadores homogéneos.

A incorporação de grupos superficiais contendo O, N e S foi promovida por tratamentos químicos, mecânicos e térmicos, aplicados a nanotubos de carbono comerciais de parede múltipla (NTC), xerogéis de carbono sintetizados pelo processo sol-gel (XC) e materiais derivados de grafeno preparados por adaptação do método de Hummers.

Diferentes grupos oxigenados foram introduzidos com sucesso em NTC e XC por oxidação com ácido nítrico (HNO_3) à temperatura de ebulição (T_e). As propriedades texturais dos materiais são afetadas pela oxidação (o efeito é mais pronunciado no caso dos NTC do que nos CX), promovendo um aumento da área superficial (S_{BET}) e uma diminuição do volume total de poros. Além disso, a oxidação induz um forte caráter ácido às amostras, pela incorporação de uma grande quantidade de ácidos carboxílicos, anidridos e grupos fenólicos. Em menor extensão, são introduzidas lactonas e alguns grupos neutros ou básicos, como os grupos carbonilo/quinonas. A aplicação de tratamentos térmicos subsequentes permite recuperar a basicidade das amostras, pela remoção seletiva dos grupos ácidos. A funcionalização controlada de NTC foi demonstrada por oxidação hidrotérmica com HNO_3 a 200 °C. A formação/evolução dos grupos oxigenados e o grau de funcionalização da superfície foram descritos por uma função exponencial em função da concentração de

HNO_3. Observou-se um aumento progressivo da S_{BET} após a funcionalização hidrotérmica. A oxidação hidrotérmica é competitiva com o tratamento com HNO_3 à temperatura de ebulição no que respeita à quantidade de grupos introduzidos, com a vantagem de requerer quantidades muito menores de agente oxidante.

Tratamentos com ácido sulfúrico (H_2SO_4) ou com mistura de HNO_3/H_2SO_4, realizados com NTC e XC, levaram à introdução de grupos contendo S, mais concretamente grupos ácido sulfónico ($-SO_3H$). Consegui-se maior introdução de grupos $-SO_3H$ em XC (até 2,1 %), tendo-se observado uma diminuição da S_{BET} com o tratamento com H_2SO_4.

Para a incorporação de grupos N em NTC foi desenvolvida uma abordagem hidrotérmica que envolve pré-oxidação da superfície com HNO_3 à temperatura de ebulição, um tratamento com ureia em fase líquida a 200 °C e, por fim, um tratamento térmico em atmosfera inerte a 600 °C. Contudo, a incorporação de grupos N atingida é pequena (<1 %). Em alternativa, foi desenvolvido um novo método que combina um tratamento mecânico num moinho de bolas, seguido de tratamentos térmicos. Esta abordagem permite a incorporação de maiores quantidades de grupos N (até 7,6 %), nomeadamente grupos quaternários, piridínicos e pirrólicos. Foram testados diferentes precursores de N (melamina, ureia, amoníaco), diferentes razões precursores/NTC, na presença ou não de solventes, e foi estudado o efeito de grupos oxigenados na superfície e diferentes temperaturas finais no tratamento térmico. A amostra tratada com melamina sem solvente e sem produção de resíduos resultou na maior incorporação de grupos N na superfície dos NTC. Esta metodologia foi ainda alargada a materiais derivados de grafeno, tendo-se verificado novamente que a amostra

tratada com melamina incorporou maior quantidade de grupos N, preservando a área específica.

Os materiais preparados e modificados pelos tratamentos anteriormente descritos foram caraterizados com recurso a diferentes técnicas: isotérmicas de adsorção de N_2 a -196 °C, dessorção a temperatura programada, termogravimetria, análise elementar, ponto de carga nula e espectroscopia de fotoelectrões de raios-X.

Os materiais resultantes foram estudados como catalisadores em duas reações em fase líquida: na esterificação do ácido acético com etanol (como reação modelo de catálise ácida) e na oxidação do ácido oxálico e do fenol por oxidação catalítica húmida.

A reação de esterificação foi realizada a 70 °C, utilizando uma razão molar de ácido acético/etanol de 1:10, com catalisadores ácidos de NTC e XC previamente tratados com H_2SO_4 e HNO_3. Constatou-se uma forte dependência entre a formação de acetato de etilo e as propriedades da química superficial dos materiais de carbono; os grupos $-SO_3H$ revelaram-se mais adequados para a reação do que os ácidos carboxílicos. Uma correlação forte foi obtida entre a velocidade de formação do éster e a concentração de grupos $-SO_3H$. O melhor desempenho alcançou-se com uma amostra de XC tratada com H_2SO_4. Apesar de demostrar um desempenho inferior comparado com o catalisador homogéneo convencionalmente utilizado (H_2SO_4), esta amostra revelou-se competitiva em comparação com a resina Nafion NR50, um catalisador sólido convencional. Usando a amostra de XC obteve-se uma atividade, avaliada pela frequência de *Turnover,* de 1,9 min^{-1} contra 1,5 min^{-1} da resina NR50.

A oxidação do ácido oxálico e do fenol por oxidação húmida foi realizada a 40 bar de pressão total e a 140 e 160 °C, respetivamente. Ambos os compostos modelo são muito estáveis em condições não catalíticas, mas podem ser degradados na presença de materiais de carbono. NTC, XC e materiais derivados do grafeno com diferentes heteroátomos na superfície foram testados como catalisadores. A oxidação do ácido oxálico e do fenol depende das propriedades texturais e da química superficial dos materiais. A oxidação catalítica dos poluentes modelo é alcançada mais rapidamente na presença de amostras dopadas com N e é também favorecida na ausência de grupos oxigenados. Com surpresa, a introdução de grupos ácidos -SO_3H revelou-se benéfica na degradação dos compostos, em particular, no caso do fenol. Independentemente do poluente, os melhores resultados foram obtidos com amostras dopadas com N. No caso dos N-XC testados, foi obtida uma correlação linear entre a constante de velocidade aparente de oxidação do ácido oxálico e a quantidade de N na superfície. A constante de velocidade aparente aumenta quase duas ordens de grandeza usando N-CX em comparação com a amostra não dopada. De todas as amostras testadas, a amostra de NTC preparada no moinho de bolas com melamina (sem solvente) revelou o melhor desempenho catalítico: o ácido oxálico foi completamente mineralizado em 5 min (concentração inicial de 1000 mg L^{-1}), enquanto a degradação total do fenol foi alcançada após 2 h de reação (concentração inicial de 75 mg L^{-1}). A amostra combina uma metodologia de fácil preparação, incorporando grupos N e ainda apresenta boa estabilidade em ensaios cíclicos. Em reações com materiais de carbono dopados com N, a oxidação do ácido oxálico parece prosseguir por um mecanismo na superfície do material de carbono; enquanto na

presença de grupos -SO_3H a reação parece envolver radicais sulfato na fase líquida.

(This page intentionally left blank)

TABLE OF CONTENTS

PART III | ACID CATALYSED REACTIONS

PART IV | CATALYTIC WET AIR OXIDATION

LIST OF FIGURES

PART I | INTRODUCTION AND STATE OF THE ART

PART II | TUNING CARBON MATERIALS PROPERTIES

APPENDIX| SUPPORTING INFORMATION

LIST OF TABLES

PART II | TUNING CARBON MATERIALS PROPERTIES

PART III | ACID CATALYSED REACTIONS

PART IV | CATALYTIC WET AIR OXIDATION

ABBREVIATION LIST

AC – activated carbon
Ads – adsorption experiment
AOP – advanced oxidation process
BE – binding energy
BM – ball mill
CBs – carbon black
CCVD - catalytic chemical vapor deposition
CNF – carbon fibre
CNT – carbon nanotube
CWAO - catalytic wet air oxidation
CX – carbon xerogel
DT – dry treatment
EA – elemental analysis
EtAc – ethyl acetate
GO – graphene oxide
HT – hydrothermal treatment
M – melamine
N5 – pyrrolic nitrogen
N6 – pyridinic nitrogen
NLDFT – non-local density functional theory
NQ – quaternary nitrogen
ORR – oxygen reduction reaction
OxAc – oxalic acid
pH_{PZC} – point of zero charge
rGO – graphene-based material
ROI – region of interest
t-BuOH – tert-butyl alcohol
TEM – transmission electron microscopy
TGA – thermogravimetric analysis
TOC – total organic carbon
TOF – turnover frequency
TPD – temperature programmed desorption
U – urea
WAO – wet air oxidation
WT – wet treatment
XPS – X-ray photoelectron spectroscopy
k – apparent initial reaction rate constant

PART I

Introduction and State of the Art

CONTENT

Introductory Note, Motivation, Objectives

1. State of the Art

References

(This page intentionally left blank)

Introductory Note

"Carbons of large specific surface area (…) are assuming increasing importance in the control of air and water pollution, in purifying and controlling the general chemical environment, and in certain biomedical applications", Robert W. Couglhin, 1969 [1]. Almost fifty years later, carbon materials are still the focus of extensive research by the scientific community, now with the emphasis on the novel nanomaterials discovered at the end of the last century. Since the catalytic activity of carbon materials has been recognized, the intersection of the fields of catalysis and carbon has become a major subject of research. Current research includes environmental technologies, energy production and fine chemicals synthesis. The increasing role assumed by carbon materials is intrinsically linked to a better understanding of the carbon surface chemistry, as result of reliable methods of analysis. This work addresses the chemical functionalization of carbon materials and their evaluation as catalysts for liquid-phase reactions. Two reactions were selected for this study: the acid catalysed esterification of acetic acid, and the catalytic wet air oxidation of model organic compounds.

(This page intentionally left blank)

Motivation

Most industrial processes use suitable catalysts to enhance the rate of a thermodynamically feasible reaction; therefore, the importance and economical significance of catalysis is enormous. Heterogeneous catalysts are easier to separate from products and reactants by unit operations such as filtration, and therefore are usually preferred as an alternative to homogeneous catalysts. However, in some cases, their performance is not yet competitive with homogeneous catalysts. The use of sulphuric acid in esterification reactions is a good example, for which only a few cases of heterogeneous catalysts have been developed with good performances. Nevertheless, complex routes for their synthesis makes their effective application difficult in real conditions. In this context, it is crucial to continue searching for alternatives to replace the high consumption of liquid-phase homogeneous catalysts like sulphuric acid for acid catalysed reactions.

Regarding the solid heterogeneous catalysts, metal and transition metal oxides, metal salts, metal alloys and metal-organic frameworks, carbides and nitrides, carbons, ion-exchange resins, have been developed to replace homogeneous catalysts in a large variety of applications. In environmental catalysis there are several applications, such as oxidation of organic pollutants, which are currently based on the use of noble metals and rare earth oxides as catalysts. However, these materials are becoming scarce and expensive due to their overall demand for multiple applications. Therefore, the development of metal-free catalysts to replace precious metals can represent a real breakthrough in catalytic processes. The use of metal-free catalysts can also avoid the common

drawbacks of supported metal catalysts, like metal leaching and deactivation phenomena that traditionally occur in liquid-phase reactions. In this context, carbon materials are receiving an increasing scientific and industrial attention. They have been used as catalyst supports for many years, but they can also be used as catalysts on their own. High efficiency, environmental compatibility, low energy consumption, and corrosion resistance are some of the advantages that carbons offer compared with metal-based catalysts, in addition to high selectivity and long-term stability under mild conditions in many catalytic processes. Therefore, metal-free catalysts can become more cost-effective and eco-sustainable than metal-based catalysts. Further investigation is necessary for the development of reliable methods to tune the physicochemical properties of the carbon materials by thermal or chemical post-treatments in order to achieve the high performance required for their use as catalysts in liquid-phase reactions.

Objectives

The main goal of this work is to demonstrate the effectiveness of carbon-based materials as promising catalysts for real liquid-phase chemical reactions, emphasizing the importance of the fine and controllable tuning of surface chemistry to obtain stable and highly active catalysts and, therefore, to replace metal-based and homogeneous catalysts traditionally used in the selected reactions, namely, the oxidation of organic compounds by catalytic wet air oxidation (CWAO) and the acid catalysed reaction of esterification of acetic acid with ethanol.

For that propose, carbon materials were designed, developed and tested in lab-scale catalytic tests. The thesis is organized in four main parts, addressing several individual goals previously defined and, hereafter, identified.

In the first part, *Introduction and State of the Art*, the main objective is to present a literature survey and to establish the state of the art concerning the application of carbon catalysts in the field of heterogeneous catalysis, in order to clearly identify the opportunity of carbon materials as catalysts for different applications.

Part II, *Tuning Carbon Materials Properties*, is focused on the design and development/modification of carbon-based materials (carbon nanotubes, CNTs; carbon xerogels, CXs; and graphene-based materials, rGOs) with different heteroatoms (oxygen, O; nitrogen, N; sulphur, S) by suitable chemical and thermal treatments. Specific objectives are: i) functionalization of carbon materials with O-, N- and S-containing surface groups; ii) development of easier and controllable functionalization methodologies; iii) to avoid the use of solvents and to develop effortlessly

scalable procedures; iv) thorough textural and surface characterization of the carbon materials.

Parts III and IV are dedicated to the evaluation of the prepared materials as catalysts in two distinct reactions, namely the esterification of acetic acid with ethanol in *Part* III, and the oxidation of model compounds by CWAO in *Part* IV. In both cases, individual targets were taken into consideration: i) identification of the most suitable properties of the carbon materials for each application; ii) identification of the active sites in these reactions, iii) whenever possible, to establish correlations between the catalytic activity and the nature/concentration of the active centres involved, in order to clarify the mechanism of the reaction; iv) comparison of catalytic performance of the prepared materials with others in the literature; v) reuse and stability studies of the most promising catalysts in the two selected reactions.

Last but not least, the work is also expected to contribute to the generation of new knowledge in the field of metal-free and acid carbon catalysts for sustainable chemical reactions, hopefully with an impact on tomorrow's industrial and economic sustainable development.

1. State of the art

Carbon is one of the most fascinating and abundant elements in the universe. Although known since ancient times, it only was first recognized as an element in the second half of the 18th century, by the "father" of modern chemistry Antoine Lavoisier. Due to its ability to change in the sp-hybridization, carbon is present in a wide range of allotropes, from the oldest known, as graphite and diamond, to the recently discovered nanocarbons (such as fullerene, CNTs and graphene).

Carbon materials such as activated carbons (ACs), carbon blacks (CBs), graphite, and graphitic materials have been used for decades as adsorbents and in heterogeneous catalysis, either as catalysts or catalyst supports [1-4]. Furthermore, the importance and potential of carbon based materials have been recognized in recent decades by some of the highest scientific awards including the 1996 Nobel Prize in Chemistry (fullerenes), the 2008 Kavli Prize in Nanoscience (carbon nanotubes), and the 2010 Nobel Prize in Physics (graphene) [5, 6] (Figure I- 1).

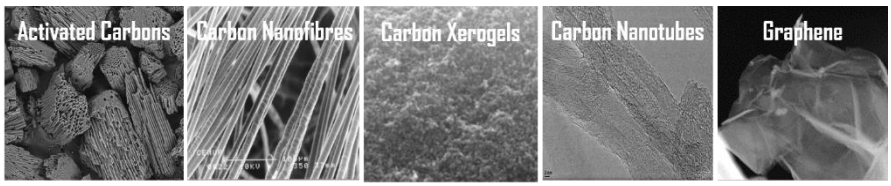

Figure I- 1. Examples of conventional and nanostructured carbon materials.

Due to the ability of carbon atoms to bond with each other in various ways to form linear, planar, and tetrahedral bonding arrangements, the production of carbon materials with a large range of properties is possible.

Nanocarbons (or carbon nanomaterials), adopting the definition proposed by Inagaki et al. [7, 8], include both nanosized carbons (CNTs, carbon nanofibres, CNFs; graphene-based materials; nanodiamonds) and nanostructured porous carbons (carbon gels and templated carbons).

Most of the carbon materials used in catalysis have a graphitic structure [9, 10]. The unsaturated carbon atoms at the edges of the graphene layers and at basal plane defects are able to react with different compounds containing O, N, H, Cl, S, B, P, etc., forming various types of surface functional groups. Such groups can play the role of active sites for catalysis, but they may also act as promoters or inhibitors, enhancing or diminishing the activity of the carbon catalyst, respectively [11]. As result, carbon materials have been reported to perform well in reactions typically catalysed by metals (such as dehydrogenations), non-stoichiometric oxides (such as oxidations and reductions) and acids (such as alkylation and dehydration) [10].

However, the number of industrial applications using carbon materials as catalysts is still limited. For instance, ACs are used in the synthesis of phosgene and of thionyl chloride, and in the production of a biodegradable herbicide, Glyphosate. It is also used industrially in the SO_2/NOx removal in flue gases [10].

The importance and economical significance of catalysis is enormous, because more than 80 % of industrial chemical processes are catalytic [12]. Solid catalysts have been considered an important feature for a sustainable progress in the field of heterogeneous catalysis [13]. Metal-based catalysts have played a major role in various industrial processes, since many reactions involve metals, especially noble metals or metal oxides as catalysts. However, they present multiple drawbacks, including

high cost, susceptibility to poisoning, and detrimental effects on the environment. In this context, metal-free carbon materials exhibit several advantages over metal catalysts, including high efficiency, environmental compatibility, low energy consumption, corrosion resistance, stability in basic and acidic media and unique surface properties and wide availability [14, 15].

The performance of any catalyst depends on the availability of suitable active sites, capable of chemisorbing the reactants and forming surface intermediates of adequate strength. Therefore, the catalytic properties of carbon materials are mostly determined by their textural properties and surface chemistry [2]. The potential growth of the market for carbons in catalysis depends on (1) better understanding of the chemistry of carbon surfaces and its fine tuning, leading to the design of unique catalysts; and (2) improvements in quality control and production methods, to supply constant-quality materials (synthetic carbons) [16].

Although different heteroatoms can be incorporated into carbon surfaces, O, N and S have been most studied and tested in recent years. The concentration of these groups can be further tuned in order to suit specific requirements [2, 10]. Acidic oxygenated groups include carboxylic acids and anhydrides, lactones or lactols, and phenols, and can be easily incorporated by oxidative treatments with nitric acid, oxygen peroxide and oxygen [17-20]. Carbonyls/quinones, chromene and pyrone are considered to be neutral or basic and can also be introduced by oxidative treatments. In addition, the π-electron system of the graphitic basal planes also contributes to the carbon basicity. To increase carbon basicity, nitrogen-containing groups can be incorporated into the graphene structure, including pyridinic (N6), pyrrolic (N5), and quaternary nitrogen

(NQ) [21, 22]. Carbon materials can also be functionalized with sulphur atoms, as sulphonic acid groups (-SO_3H), providing efficient acid catalysts [23-27].

The better understanding of the carbon surface chemistry became possible as a result of reliable methods of analysis available to explore the chemical and structural properties of carbon materials: scanning tunneling microscopy (STM), transmission electron microscopy (TEM), X-ray diffraction (XRD), X-ray photoelectron spectroscopy (XPS), infrared (IR), and Raman spectroscopies, chemical titration methods, electron energy loss spectroscopy (EELS), temperature programmed desorption (TPD), thermogravimetry (TG), and point of zero charge (pH_{PZC}) [10, 28-35]. Some techniques do not allow quantitative characterization, others require relatively large amounts of sample and are time consuming or difficult to implement as a routine analysis [30]. XPS and TPD techniques yield qualitative and quantitative information on individual functional groups on the carbon surface, with TPD being especially adequate for characterization of oxygen functional groups on carbon materials with extended porosity [10]. Nitrogen and sulphur can be properly quantified by elemental analysis (EA), while the nature of N-containing and S-containing groups is commonly identified by suitable deconvolution of the N1s and S2p XPS spectra. Therefore, suitable methods of analysis of the carbon functional groups are now available, including TPD-MS assisted (mass spectroscopy) and XPS. The nature of the functional surface groups and their characteristic binding energies (XPS) and/or temperature ranges of desorption in TPD analyses are indicated in Figure I- 2.

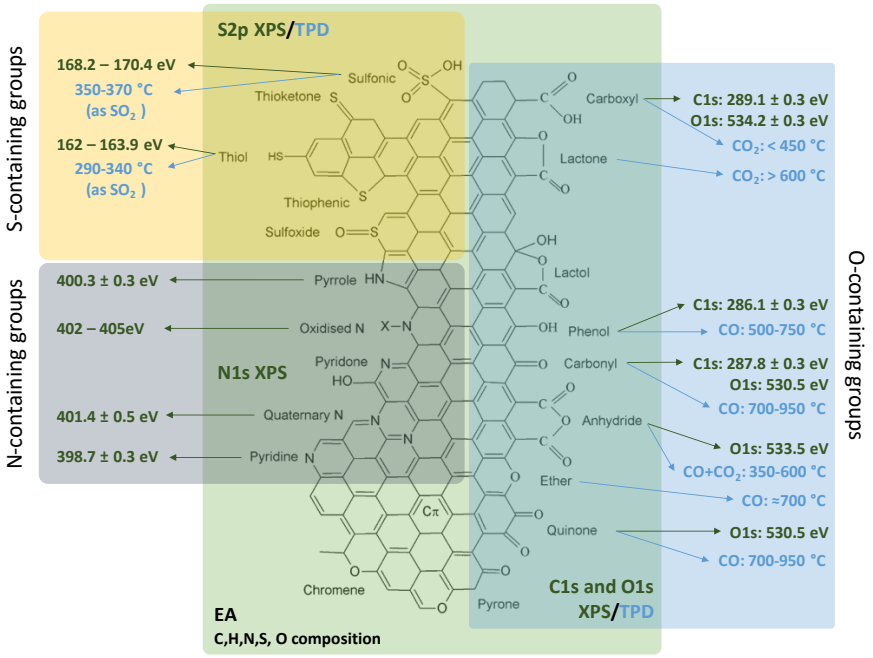

Figure I- 2. Oxygen, nitrogen and sulphur surface groups incorporated on carbon materials and techniques for their identification/quantification[1].

In the meantime, the clear identification of the surface functionalities by suitable methods has allowed to identify the most adequate active sites or the type of surface chemistry required in different reactions catalysed by carbon materials. From the application of ACs as heterogeneous catalysts [13], to graphene and its derivatives as carbocatalysts [36], to overviews on the role O-containing surface groups [10, 15] or nitrogen-, boron-, phosphorous-, sulphur-(N,B,P,S) doped nanomaterials [10, 27, 37], including nanocarbons [11] and nanoporous materials [11] in liquid and gas phase reactions [2, 14, 38], several reviews have been published in the last 10 years. Therefore, the idea here is only to highlight the range of applications of metal-free carbon-based catalysts, commenting on the

[1] Adapted from Journal of Carbon Research C, 2 (2016) 17.

eventual identification of suitable functional groups and active sites, by class of materials or reactions.

Regarding gas-phase reactions, the oxidative dehydrogenation of hydrocarbons represents the most studied reaction catalysed by nanocarbons, with carbonyl/quinones as active sites. Dehydration of alcohols (involving carboxylic acids) and alcohol dehydration (involving both Lewis acids and basic sites) have been also reported. Basic surface groups were also recognised as appropriate for gas phase NO and H_2S oxidation, in addition to the identification of pyridinic nitrogen sites for SO_2 oxidation and dehydrohalogenation reactions [2, 10, 11, 36, 39].

The field of carbocatalysis for liquid-phase reactions, especially for organic synthesis, has undergone rapid development in recent years. Typical liquid-phase reactions catalysed by carbons include oxidation reactions of alcohols and benzene, selective oxidation of cyclohexane, ethylbenzene and toluene, reduction reactions of nitroarenes, alcohol amination, coupling reactions and acid/base reactions. Among the latter, transesterification reactions, hydrolysis, and Knoevenagel condensation reactions stand out. In transesterification, both acid and base catalysts can catalyse the reaction, but base-catalysed processes are more widely studied. Mesoporous carbon nitride nanoparticles and carbon materials grafted with organic amine or imine groups showed to be promising catalysts for transesterification. Also SO_3H-grafted carbon catalysts exhibited good activity in the acid-catalysed transesterification reaction. Hydrolysis of biomass can also be promoted by carbocatalysts with weak acid (carboxylic acid group) and strong acid (sulphonated group) sites. Carbon materials exhibit weak intrinsic basicity, and hence they typically cannot catalyse Knoevenagel condensations. However, nitrogen doping or

amine grafting can enhance the basic strength of carbon materials, such as CNTs, carbon nitrides, and graphene-based materials [38]. In addition, the strongly acidic -SO_3H groups onto carbon materials have been claimed as potential catalysts for acetalization, esterification, acylation, alkylation and alcoholysis of epoxides [2, 10, 39]. Still regarding the use of carbon materials in liquid phase reactions, basic sites have been identified as active sites in catalytic wet peroxide oxidation, catalytic ozonation and CWAO, a group of technologies designed to remove organic contaminants from water and wastewater by oxidation [2, 10, 39]. For CWAO further details will be given ahead.

Different electronegative non-metal heteroatoms incorporated in several carbon materials (CNTs, CNFs, ordered mesoporous carbons, graphene-based materials, carbon gels) have been tested for the oxygen reduction reaction (ORR). From the higher electronegative heteroatoms (as nitrogen), to less electronegative (phosphorus and boron) or those with similar electronegativity as carbon (as sulphur) have been tested in ORR [37]. All types of heteroatoms promote changes in the catalytic reactivity of carbon surface for the ORR, but the mechanism involved in each case is still unclear.

Photocatalytic reactions can also be used for the production of renewable, non-polluting fuels and organic chemicals. This has been proposed as a promising and effective route to be environment-friendly and to relieve the energy crisis. Besides the applications of g-C_3N_4 composite materials containing nanocarbons and other metal-free catalysts can also provide new routes for photocatalysis [14].

In the absence of functional groups, the number of reactive sites in pristine carbon materials is too low, the active sites being only located at

the unsaturated carbons at the edges or defects of the graphene layers [15]. Nonetheless, a clear evidence for the ability of carbon materials to enhance reactivity has been reported in Friedel-Crafts, reduction, oxidation and cycloaddition reactions using graphite, oxidation and oxidative dehydrogenation reactions using carbon nanotubes and in photocatalytic reduction and oxidation and thermal reduction reactions using fullerenes [15]. Muradov et al. found a clear correlation between the catalytic activity of more than 30 types of carbon (including ACs, CBs, graphite, fullerene, CNT and diamond) and the degree of structural order in the methane decomposition into hydrogen at high temperature [40]. However, a significant improvement of the catalytic activity of carbons can be obtained through functionalization or heteroatom-doping.

The huge development of catalysis promoted by carbon materials was boosted by the discovery, synthesis or identification of new carbon materials, such as CNTs, CNFs, nanoporous carbon gels and the isolation of GO.

The work published in 1991 by Ijima [41] ignited the interest for CNTs. Their unusual mechanical, electronic, and thermal properties [42], allowed them to be currently used in a wide range of technological applications [43, 44], including as catalysts or catalyst supports in the fields of renewable energy (storage and conversion) and environmental technologies (oxidation/remediation/adsorption). They have been also applied in multifaceted applications in human healthcare: drug delivery, sensing, water purification, composite materials, and bone scaffolds [45].

Since its isolation and characterization in 2004 [46], graphene and derivatives have emerged as materials of great technological interest due to their remarkable mechanical, thermal, optical and electrical properties

[47, 48]. In particular, graphene oxide (GO) has attracted huge interest as a graphene precursor because oxygen functional groups attached on the GO surface can be partly removed, resulting in the partial restoration of the conjugated structure [49, 50]. To date, the majority of carbocatalysis studies carried out with graphene-based materials have applied graphite and graphene oxides as well as reduced graphene oxide and functionalized or doped graphene [36, 47, 51]. Tested reactions include organic redox reaction, Friedel–Crafts reaction, esterification, condensation, dehydration, hydration, hydrogenation/dehydrogenation and hydrolysis, among others.

The recent advances on the development of nanostructured mesoporous carbons with tunable texture and surface chemistry led to materials that meet the requirements of the targeted applications, like catalysis, adsorption and energy storage. Unlike conventional carbons, the textural properties of nanostructured carbons can be easily adjusted during synthesis [52]. This includes carbon gels (like aerogels, cryogels and xerogels) that are synthesized by sol-gel processing through the polymerization of suitable precursors [5, 53, 54].

Hierarchically structured reactors containing nanocarbons for intensification of chemical reactions have started to be developed [55]. They present a reliable alternative to cross the line that for so long separated the laboratory scale to the industrial reality. Most of the catalytic results reported with carbon materials are in powder form, which represents a number of drawbacks for industrial applications, including the problems of transport and handling, high-pressure drop for gas phase processes and agglomeration with time on stream. Alternatives can be found by using hierarchically structured reactors, combining a nanoscopic

coating layer for active phase dispersion (nanocarbons), or directly as metal-free catalysts, and a macroscopic host matrix (structured reactor), for numerous relevant catalytic processes where mass and heat transfer can be significantly optimized leading to better catalytic performance and stability [55-57].

Several new carbon materials have become widely available and the knowledge about the surface chemistry of carbon materials has increased substantially. Controllable incorporation of functional groups on the surface of carbon materials and identification and quantification of the surface groups provide correlations between the catalytic activity and the functional groups that act as active sites in catalysis, and allow the preparation of high-performance nanostructured catalysts.

Carbon Materials in Water Treatment by Catalytic Wet Air Oxidation

A large part of the work developed during this thesis was dedicated to test carbon materials in CWAO of organic compounds, a process that can be used for wastewater treatment. The abatement of environmental pollution and, especially, the availability of clean water are among the most significant concerns of society. With the increasing global usage of water and the continuous addition of contaminants (from industrial processes, agricultural practices and synthetic chemicals) to the water sources, new challenges associated with their effective removal have arisen. Particularly, the presence of organic pollutants that show some resistance to conventional treatment technologies for water and wastewater led to a growing interest in the development of more efficient methods for their removal [58, 59], such as the so-called advanced oxidation processes, which include CWAO [60].

Advanced oxidation processes (AOPs), based on the production and use of strongly reactive radicals, are a group of technologies designed to remove organic contaminants from water and wastewater by oxidation, the radicals being generated from different oxidants, such as oxygen (wet air oxidation, WAO), hydrogen peroxide (wet peroxide oxidation) or ozone (ozonation). The aim of the process is to oxidize the organic compounds preferably into carbon dioxide and water, or alternatively into easily biodegradable by-products. In the case of WAO, the technology can play an important role as primary treatment for highly concentrated wastewaters that are refractory to biological treatments, or that are toxic, offering high versatility and efficiency in the abatement of several classes of pollutants and remarkable cost advantages [60, 61].

Both homogeneous and heterogeneous catalysts, including supported metals and metal oxides, can be used to enhance the efficiency of these AOPs, and notably to decrease the severity of the operating conditions required in the case of WAO (200–320 °C and 20–200 bar) [60]. Commercially implemented processes of WAO are homogeneous, based on the use of copper and iron, but they require catalyst separation from the treated effluent. Only a few heterogeneous plants are operating, using noble metal catalysts (Ru, Pd and Pt) [62, 63], but several heterogeneous catalysts based on supported or unsupported metal oxides (e.g., Cu, Zn, Mn, Fe, Co, and Bi) and noble metals (e.g., Ru, Pt, Pd and Rh) have been investigated for CWAO in the last four decades [60, 61, 64-75]. In spite of advances in the development of heterogeneous catalysts with minimal leaching effects [76, 77], deactivation phenomena are frequent, in particular the leaching of active metals to the liquid phase [60, 66, 67], which severely limits the efficiency of these heterogeneous catalytic processes. In addition, noble metal and metal oxides (mainly those involving rare-earth elements) are facing an increasing price due to the scarcity of some elements, and they also cause harmful impacts on the environment.

In this context, the use of metal-free carbon materials as catalysts has been recently preferred for many CWAO applications [67, 78-85], not only to avoid possible lixiviation of metals, but also because these materials are stable in both acidic and alkaline media and their texture and surface chemistry can be easily modified in order to provide adequate active sites for the reactions [2, 3, 10].

AC is one of the most studied carbon materials to remove contaminant from water. However, they are essentially microporous

materials and the organic pollutants cannot diffuse so easily as in meso- and macropores [67, 86]. In this context, mesoporous carbons with high external surface area are usually more efficient for liquid-phase oxidation processes than ACs. Alternatives can be found using mesoporous CXs, CNTs, graphene-based materials, carbon fibres and foams and CBs [42, 87-98]. It has been demonstrated that carbon materials are able to enhance the removal of organic pollutants as catalysts in CWAO due to their outstanding textural and chemical properties. While the effect of the textural properties, such as pore size and surface area, is well understood [91], the role of surface chemistry is still not completely established. Basic sites (or low acidic character) have been identified by some authors as the most favourable for CWAO [10, 67, 91]. In contrast, other authors [95-99] have reported a positive effect of oxygen acidic surface groups; therefore, there is a controversy in the literature regarding the active sites of carbon required to achieve the best performance in the CWAO process.

The more recently discovered CNTs and the developments in their mass production, which decreased their cost and increased their accessibility, gradually allowed them to be useful for a wide range of applications [42-44]. The unusual mechanical, electrical, and thermal properties make CNTs suitable to catalyse CWAO reactions and they have been investigated as catalytic supports, for instance, for Fe [100], Cu [42, 100], Ru [100-102], and Pt [42, 103-105], but, less often as catalysts in CWAO [91, 95, 97-99, 106]. Short chain carboxylic acids that are typical refractory compounds in non-catalytic advanced oxidation processes, or low molecular weight probe species as aniline [42, 101, 104, 105] and phenol [95, 96, 99, 106], and, in some cases, some dyes [104, 107] are usually selected as model compounds to evaluate the process efficiency.

The potentialities of carbon materials as metal-free catalysts in liquid phase reactions can be substantially enhanced by tailoring the textural and chemical properties with appropriate thermal or chemical treatments. Next sections will demonstrate different methodologies to tune carbon materials properties and the effect of those modifications on the catalytic performance over selected liquid-phase reactions.

References

[1] R.W. Coughlin, Carbon as Adsorbent and Catalyst, Product R&D, 8 (1969) 12-23.
[2] J.L. Figueiredo, M.F.R. Pereira, Carbon as Catalyst, Carbon Materials for Catalysis, John Wiley & Sons, Inc.2009, pp. 177-217.
[3] F. Rodríguez-Reinoso, The role of carbon materials in heterogeneous catalysis, Carbon, 36 (1998) 159-175.
[4] Y. Yang, K. Chiang, N. Burke, Porous carbon-supported catalysts for energy and environmental applications: A short review, Catalysis Today, 178 (2011) 197-205.
[5] M.M. Titirici, R.J. White, N. Brun, V.L. Budarin, D.S. Su, F. del Monte, J.H. Clark, M.J. MacLachlan, Sustainable carbon materials, Chem Soc Rev, 44 (2015) 250-290.
[6] J. Zhang, M. Terrones, C.R. Park, R. Mukherjee, M. Monthioux, N. Koratkar, Y.S. Kim, R. Hurt, E. Frackowiak, T. Enoki, Y. Chen, Y. Chen, A. Bianco, Carbon science in 2016: Status, challenges and perspectives, Carbon, 98 (2016) 708-732.
[7] M. Inagaki, L.R. Radovic, Nanocarbons, Carbon, 40 (2002) 2279-2282.
[8] M. Inagaki, K. Kaneko, T. Nishizawa, Nanocarbons—recent research in Japan, Carbon, 42 (2004) 1401-1417.
[9] A. Bianco, H.-M. Cheng, T. Enoki, Y. Gogotsi, R.H. Hurt, N. Koratkar, T. Kyotani, M. Monthioux, C.R. Park, J.M.D. Tascon, J. Zhang, All in the graphene family – A recommended nomenclature for two-dimensional carbon materials, Carbon, 65 (2013) 1-6.
[10] J.L. Figueiredo, M.F.R. Pereira, The role of surface chemistry in catalysis with carbons, Catalysis Today, 150 (2010) 2-7.
[11] J.L. Figueiredo, Application of Nanocarbon Materials to Catalysis, Nanotechnology in Catalysis, Wiley-VCH Verlag GmbH & Co. KGaA2017, pp. 37-56.
[12] O. Deutschmann, H. Knözinger, K. Kochloefl, T. Turek, Heterogeneous Catalysis and Solid Catalysts, Ullmann's Encyclopedia of Industrial Chemistry, Wiley-VCH Verlag GmbH & Co. KGaA2000.
[13] I. Matos, M. Bernardo, I. Fonseca, Porous carbon: A versatile material for catalysis, Catalysis Today, 285 (2017) 194-203.
[14] X. Sun, R. Wang, D. Su, Research progress in metal-free carbon-based catalysts, Chinese Journal of Catalysis, 34 (2013) 508-523.
[15] B.M. Philippe Serp, CHAPTER 5 Nanostructured Carbon Materials as Catalysts, Nanostructured Carbon Materials for Catalysis, The Royal Society of Chemistry2015, pp. 223-267.
[16] P. Serp, J.L. Figueiredo, Carbon materials for catalysis, John Wiley & Sons, Hoboken, N.J., 2009.
[17] N. Mahata, M.F.R. Pereira, F. Suárez-García, A. Martínez-Alonso, J.M.D. Tascón, J.L. Figueiredo, Tuning of texture and surface chemistry of carbon xerogels, Journal of Colloid and Interface Science, 324 (2008) 150-155.

[18] A.G. Gonçalves, J.L. Figueiredo, J.J.M. Órfão, M.F.R. Pereira, Influence of the surface chemistry of multi-walled carbon nanotubes on their activity as ozonation catalysts, Carbon, 48 (2010) 4369-4381.
[19] Y.-C. Chiang, W.-H. Lin, Y.-C. Chang, The influence of treatment duration on multi-walled carbon nanotubes functionalized by H2SO4/HNO3 oxidation, Applied Surface Science, 257 (2011) 2401-2410.
[20] V. Datsyuk, M. Kalyva, K. Papagelis, J. Parthenios, D. Tasis, A. Siokou, I. Kallitsis, C. Galiotis, Chemical oxidation of multiwalled carbon nanotubes, Carbon, 46 (2008) 833-840.
[21] J.R. Pels, F. Kapteijn, J.A. Moulijn, Q. Zhu, K.M. Thomas, Evolution of nitrogen functionalities in carbonaceous materials during pyrolysis, Carbon, 33 (1995) 1641-1653.
[22] H.-P. Boehm, Catalytic Properties of Nitrogen-Containing Carbons, in: P. Serp,J.L. Figueiredo (Eds.), Carbon Materials for Catalysis, pp. 219-265, John Wiley & Sons, Inc. Hoboken, NJ 2009.
[23] H.T. Gomes, S.M. Miranda, M.J. Sampaio, J.L. Figueiredo, A.M.T. Silva, J.L. Faria, The role of activated carbons functionalized with thiol and sulfonic acid groups in catalytic wet peroxide oxidation, Applied Catalysis B: Environmental, 106 (2011) 390-397.
[24] F. Peng, L. Zhang, H. Wang, P. Lv, H. Yu, Sulfonated carbon nanotubes as a strong protonic acid catalyst, Carbon, 43 (2005) 2405-2408.
[25] R. Liu, X. Wang, X. Zhao, P. Feng, Sulfonated ordered mesoporous carbon for catalytic preparation of biodiesel, Carbon, 46 (2008) 1664-1669.
[26] H.T. Gomes, S.M. Miranda, M.J. Sampaio, A.M.T. Silva, J.L. Faria, Activated carbons treated with sulphuric acid: Catalysts for catalytic wet peroxide oxidation, Catalysis Today, 151 (2010) 153-158.
[27] W. Kiciński, M. Szala, M. Bystrzejewski, Sulfur-doped porous carbons: Synthesis and applications, Carbon, 68 (2014) 1-32.
[28] J.L. Figueiredo, M.F.R. Pereira, M.M.A. Freitas, J.J.M. Órfão, Modification of the surface chemistry of activated carbons, Carbon, 37 (1999) 1379-1389.
[29] J.L. Figueiredo, M.F.R. Pereira, M.M.A. Freitas, J.J.M. Órfão, Characterization of active sites on carbon catalysts, Industrial and Engineering Chemistry Research, 46 (2007) 4110-4115.
[30] K.A. Wepasnick, B.A. Smith, J.L. Bitter, D. Howard Fairbrother, Chemical and structural characterization of carbon nanotube surfaces, Analytical and Bioanalytical Chemistry, 396 (2010) 1003-1014.
[31] K.A. Wepasnick, B.A. Smith, K.E. Schrote, H.K. Wilson, S.R. Diegelmann, D.H. Fairbrother, Surface and structural characterization of multi-walled carbon nanotubes following different oxidative treatments, Carbon, 49 (2011) 24-36.
[32] C. Herrero-Latorre, J. Álvarez-Méndez, J. Barciela-García, S. García-Martín, R.M. Peña-Crecente, Characterization of carbon nanotubes and analytical methods for their determination in environmental and biological samples: A review, Analytica Chimica Acta, 853 (2015) 77-94.

[33] T. Belin, F. Epron, Characterization methods of carbon nanotubes: a review, Materials Science and Engineering: B, 119 (2005) 105-118.
[34] J.-P. Tessonnier, D. Rosenthal, T.W. Hansen, C. Hess, M.E. Schuster, R. Blume, F. Girgsdies, N. Pfänder, O. Timpe, D.S. Su, R. Schlögl, Analysis of the structure and chemical properties of some commercial carbon nanostructures, Carbon, 47 (2009) 1779-1798.
[35] M. Pérez-Cadenas, C. Moreno-Castilla, F. Carrasco-Marín, A.F. Pérez-Cadenas, Surface Chemistry, Porous Texture, and Morphology of N-Doped Carbon Xerogels, Langmuir, 25 (2008) 466-470.
[36] C.K. Chua, M. Pumera, Carbocatalysis: The State of "Metal-Free" Catalysis, Chemistry – A European Journal, 21 (2015) 12550-12562.
[37] B.M. Philippe Serp, CHAPTER 6 Doped Nanostructured Carbon Materials as Catalysts, Nanostructured Carbon Materials for Catalysis, The Royal Society of Chemistry2015, pp. 268-311.
[38] D.S. Su, G. Wen, S. Wu, F. Peng, R. Schlögl, Carbocatalysis in Liquid-Phase Reactions, Angewandte Chemie International Edition, 56 (2017) 936-964.
[39] J.L. Figueiredo, Functionalization of porous carbons for catalytic applications, Journal of Materials Chemistry A, 1 (2013) 9351-9364.
[40] N. Muradov, Catalysis of methane decomposition over elemental carbon, Catalysis Communications, 2 (2001) 89-94.
[41] S. Iijima, Helical microtubules of graphitic carbon, Nature, 354 (1991) 56-58.
[42] G. Ovejero, J.L. Sotelo, M.D. Romero, A. Rodríguez, M.A. Ocaña, G. Rodríguez, J. García, Multiwalled carbon nanotubes for liquid-phase oxidation. Functionalization, characterization, and catalytic activity, Industrial and Engineering Chemistry Research, 45 (2006) 2206-2212.
[43] M. Paradise, T. Goswami, Carbon nanotubes - Production and industrial applications, Materials & Design, 28 (2007) 1477-1489.
[44] V.N. Popov, Carbon nanotubes: properties and application, Materials Science and Engineering: R: Reports, 43 (2004) 61-102.
[45] S. Kumar, R. Rani, N. Dilbaghi, K. Tankeshwar, K.-H. Kim, Carbon nanotubes: a novel material for multifaceted applications in human healthcare, Chemical Society Reviews, 46 (2017) 158-196.
[46] K.S. Novoselov, A.K. Geim, S.V. Morozov, D. Jiang, Y. Zhang, S.V. Dubonos, I.V. Grigorieva, A.A. Firsov, Electric Field Effect in Atomically Thin Carbon Films, Science, 306 (2004) 666-669.
[47] A.K. Geim, Graphene: Status and Prospects, Science, 324 (2009) 1530-1534.
[48] A.K. Geim, K.S. Novoselov, The rise of graphene, Nature Materials, 6 (2007) 183.
[49] S. Pei, H.-M. Cheng, The reduction of graphene oxide, Carbon, 50 (2012) 3210-3228.
[50] L.M. Pastrana-Martínez, S. Morales-Torres, V. Likodimos, P. Falaras, J.L. Figueiredo, J.L. Faria, A.M.T. Silva, Role of oxygen functionalities on the synthesis of photocatalytically active graphene–TiO2 composites, Applied Catalysis B: Environmental, 158–159 (2014) 329-340.

[51] K.S. Novoselov, V.I. Fal'ko, L. Colombo, P.R. Gellert, M.G. Schwab, K. Kim, A roadmap for graphene, Nature, 490 (2012) 192.
[52] M. Enterría, J.L. Figueiredo, Nanostructured mesoporous carbons: Tuning texture and surface chemistry, Carbon, 108 (2016) 79-102.
[53] N. Job, A. Théry, R. Pirard, J. Marien, L. Kocon, J.-N. Rouzaud, F. Béguin, J.-P. Pirard, Carbon aerogels, cryogels and xerogels: Influence of the drying method on the textural properties of porous carbon materials, Carbon, 43 (2005) 2481-2494.
[54] N. Job, R. Pirard, J. Marien, J.-P. Pirard, Porous carbon xerogels with texture tailored by pH control during sol–gel process, Carbon, 42 (2004) 619-628.
[55] E. Garcia-Bordeje, Y. Liu, D.S. Su, C. Pham-Huu, Hierarchically structured reactors containing nanocarbons for intensification of chemical reactions, Journal of Materials Chemistry A, 5 (2017) 22408-22441.
[56] D.-V. Cuong, H. Ba, Y. Liu, T.-P. Lai, J.-M. Nhut, P.-H. Cuong, Nitrogen-doped carbon nanotubes on silicon carbide as a metal-free catalyst, Chinese Journal of Catalysis, 35 (2014) 906-913.
[57] H. Ba, Y. Liu, L. Truong-Phuoc, C. Duong-Viet, X. Mu, W.H. Doh, T. Tran-Thanh, W. Baaziz, L. Nguyen-Dinh, J.-M. Nhut, I. Janowska, D. Begin, S. Zafeiratos, P. Granger, G. Tuci, G. Giambastiani, F. Banhart, M.J. Ledoux, C. Pham-Huu, A highly N-doped carbon phase "dressing" of macroscopic supports for catalytic applications, Chemical Communications, 51 (2015) 14393-14396.
[58] Z.-h. Liu, Y. Kanjo, S. Mizutani, Removal mechanisms for endocrine disrupting compounds (EDCs) in wastewater treatment — physical means, biodegradation, and chemical advanced oxidation: A review, Science of The Total Environment, 407 (2009) 731-748.
[59] N. Bolong, A.F. Ismail, M.R. Salim, T. Matsuura, A review of the effects of emerging contaminants in wastewater and options for their removal, Desalination, 239 (2009) 229-246.
[60] J. Levec, A. Pintar, Catalytic wet-air oxidation processes: A review, Catalysis Today, 124 (2007) 172-184.
[61] S.K. Bhargava, J. Tardio, J. Prasad, K. Föger, D.B. Akolekar, S.C. Grocott, Wet oxidation and catalytic wet oxidation, Industrial and Engineering Chemistry Research, 45 (2006) 1221-1258.
[62] A. Quintanilla, C.M. Dominguez, J.A. Casas, J.J. Rodriguez, Emerging catalysts for wet air oxidation process, Focus on Catalysis Research: New Developments2012, pp. 237-259.
[63] F. Luck, Wet air oxidation: past, present and future, Catalysis Today, 53 (1999) 81-91.
[64] V.S. Mishra, V.V. Mahajani, J.B. Joshi, Wet Air Oxidation, Industrial & Engineering Chemistry Research, 34 (1995) 2-48.
[65] D. Mantzavinos, M. Sahibzada, A.G. Livingston, I.S. Metcalfe, K. Hellgardt, Wastewater treatment: wet air oxidation as a precursor to biological treatment, Catalysis Today, 53 (1999) 93-106.

[66] A. Cybulski, Catalytic Wet Air Oxidation: Are Monolithic Catalysts and Reactors Feasible?, Industrial & Engineering Chemistry Research, 46 (2007) 4007-4033.
[67] F. Stüber, J. Font, A. Fortuny, C. Bengoa, A. Eftaxias, A. Fabregat, Carbon materials and catalytic wet air oxidation of organic pollutants in wastewater, Topics in Catalysis, 33 (2005) 3-50.
[68] A.M.T. Silva, I.M. Castelo-Branco, R.M. Quinta-Ferreira, J. Levec, Catalytic studies in wet oxidation of effluents from formaldehyde industry, Chemical Engineering Science, 58 (2003) 963-970.
[69] A.M.T. Silva, R.M. Quinta-Ferreira, J. Levec, Catalytic and Noncatalytic Wet Oxidation of Formaldehyde. A Novel Kinetic Model, Industrial & Engineering Chemistry Research, 42 (2003) 5099-5108.
[70] A.M.T. Silva, R.R.N. Marques, R.M. Quinta-Ferreira, Catalysts based in cerium oxide for wet oxidation of acrylic acid in the prevention of environmental risks, Applied Catalysis B: Environmental, 47 (2004) 269-279.
[71] A.M.T. Silva, A.C.M. Oliveira, R.M. Quinta-Ferreira, Catalytic wet oxidation of ethylene glycol: kinetics of reaction on a Mn–Ce–O catalyst, Chemical Engineering Science, 59 (2004) 5291-5299.
[72] L. Oliviero, J. Barbier, D. Duprez, H. Wahyu, J.W. Ponton, I.S. Metcalfe, D. Mantzavinos, Wet air oxidation of aqueous solutions of maleic acid over Ru/CeO2 catalysts, Applied Catalysis B: Environmental, 35 (2001) 1-12.
[73] L. Oliviero, H. Wahyu, J. Barbier Jr, D. Duprez, J.W. Ponton, I.S. Metcalfe, D. Mantzavinos, Experimental and Predictive Approach for Determining Wet Air Oxidation Reaction Pathways in Synthetic Wastewaters, Chemical Engineering Research and Design, 81 (2003) 384-392.
[74] A. Quintanilla, J.A. Casas, J.J. Rodríguez, Catalytic wet air oxidation of phenol with modified activated carbons and Fe/activated carbon catalysts, Applied Catalysis B: Environmental, 76 (2007) 135-145.
[75] A. Quintanilla, N. Menéndez, J. Tornero, J.A. Casas, J.J. Rodríguez, Surface modification of carbon-supported iron catalyst during the wet air oxidation of phenol: Influence on activity, selectivity and stability, Applied Catalysis B: Environmental, 81 (2008) 105-114.
[76] P. Gao, C. Li, H. Wang, X. Wang, A. Wang, Perovskite hollow nanospheres for the catalytic wet air oxidation of lignin, Chinese Journal of Catalysis, 34 (2013) 1811-1815.
[77] A. Xu, X. Lu, M. Yang, H. Du, C. Sun, Activity and Stability of ZnFe0.25Al1.75O4 Catalyst in Catalytic Wet Air Oxidation of Phenol, Chinese Journal of Catalysis, 28 (2007) 395-397.
[78] C. Aguilar, R. García, G. Soto-Garrido, R. Arriagada, Catalytic wet air oxidation of aqueous ammonia with activated carbon, Applied Catalysis B: Environmental, 46 (2003) 229-237.
[79] A. Eftaxias, J. Font, A. Fortuny, A. Fabregat, F. Stüber, Kinetics of phenol oxidation in a trickle bed reactor over active carbon catalyst, Journal of Chemical Technology & Biotechnology, 80 (2005) 677-687.

[80] A. Eftaxias, J. Font, A. Fortuny, A. Fabregat, F. Stüber, Catalytic wet air oxidation of phenol over active carbon catalyst: Global kinetic modelling using simulated annealing, Applied Catalysis B: Environmental, 67 (2006) 12-23.
[81] M. Santiago, F. Stüber, A. Fortuny, A. Fabregat, J. Font, Modified activated carbons for catalytic wet air oxidation of phenol, Carbon, 43 (2005) 2134-2145.
[82] M.E. Suarez-Ojeda, F. Stüber, A. Fortuny, A. Fabregat, J. Carrera, J. Font, Catalytic wet air oxidation of substituted phenols using activated carbon as catalyst, Applied Catalysis B: Environmental, 58 (2005) 105-114.
[83] T. Cordero, J. Rodríguez-Mirasol, J. Bedia, S. Gomis, P. Yustos, F. García-Ochoa, A. Santos, Activated carbon as catalyst in wet oxidation of phenol: Effect of the oxidation reaction on the catalyst properties and stability, Applied Catalysis B: Environmental, 81 (2008) 122-131.
[84] A. Quintanilla, J.A. Casas, J.J. Rodriguez, Hydrogen peroxide-promoted-CWAO of phenol with activated carbon, Applied Catalysis B: Environmental, 93 (2010) 339-345.
[85] A. Fortuny, J. Font, A. Fabregat, Wet air oxidation of phenol using active carbon as catalyst, Applied Catalysis B: Environmental, 19 (1998) 165-173.
[86] M. Sweetman, S. May, N. Mebberson, P. Pendleton, K. Vasilev, S. Plush, J. Hayball, Activated Carbon, Carbon Nanotubes and Graphene: Materials and Composites for Advanced Water Purification, C, 3 (2017) 18.
[87] S. Morales-Torres, A.M.T. Silva, A.F. Pérez-Cadenas, J.L. Faria, F.J. Maldonado-Hódar, J.L. Figueiredo, F. Carrasco-Marín, Wet air oxidation of trinitrophenol with activated carbon catalysts: Effect of textural properties on the mechanism of degradation, Applied Catalysis B: Environmental, 100 (2010) 310-317.
[88] J.P.S. Sousa, A.M.T. Silva, M.F.R. Pereira, J.L. Figueiredo, Wet Air Oxidation of Aniline Using Carbon Foams and Fibers Enriched with Nitrogen, Separation Science and Technology, 45 (2010) 1546 - 1554.
[89] Â.C. Apolinário, A.M.T. Silva, B.F. Machado, H.T. Gomes, P.P. Araújo, J.L. Figueiredo, J.L. Faria, Wet air oxidation of nitro-aromatic compounds: Reactivity on single- and multi-component systems and surface chemistry studies with a carbon xerogel, Applied Catalysis B: Environmental, 84 (2008) 75-86.
[90] H.T. Gomes, B.F. Machado, A. Ribeiro, I. Moreira, M. Rosário, A.M.T. Silva, J.L. Figueiredo, J.L. Faria, Catalytic properties of carbon materials for wet oxidation of aniline, Journal of Hazardous Materials, 159 (2008) 420-426.
[91] M. Soria-Sánchez, A. Maroto-Valiente, J. Álvarez-Rodríguez, V. Muñoz-Andrés, I. Rodríguez-Ramos, A. Guerrero-Ruíz, Carbon nanostrutured materials as direct catalysts for phenol oxidation in aqueous phase, Applied Catalysis B: Environmental, 104 (2011) 101-109.
[92] M. Soria-Sánchez, E. Castillejos-López, A. Maroto-Valiente, M.F.R. Pereira, J.J.M. Órfão, A. Guerrero-Ruiz, High efficiency of the cylindrical mesopores of MWCNTs for the catalytic wet peroxide oxidation of C.I. Reactive Red 241 dissolved in water, Applied Catalysis B: Environmental, 121–122 (2012) 182-189.
[93] A. Katsoni, H.T. Gomes, L.M. Pastrana-Martínez, J.L. Faria, J.L. Figueiredo, D. Mantzavinos, A.M.T. Silva, Degradation of trinitrophenol by sequential catalytic

wet air oxidation and solar TiO2 photocatalysis, Chemical Engineering Journal, 172 (2011) 634-640.
[94] V. Tukač, J. Hanika, Catalytic effect of active carbon black Chezacarb in wet oxidation of phenol, Collection of Czechoslovak Chemical Communications, 61 (1996) 1010-1017.
[95] S. Yang, X. Li, W. Zhu, J. Wang, C. Descorme, Catalytic activity, stability and structure of multi-walled carbon nanotubes in the wet air oxidation of phenol, Carbon, 46 (2008) 445-452.
[96] S. Yang, X. Wang, H. Yang, Y. Sun, Y. Liu, Influence of the different oxidation treatment on the performance of multi-walled carbon nanotubes in the catalytic wet air oxidation of phenol, Journal of Hazardous Materials, 233–234 (2012) 18-24.
[97] J. Wang, W. Fu, X. He, S. Yang, W. Zhu, Catalytic wet air oxidation of phenol with functionalized carbon materials as catalysts: Reaction mechanism and pathway, Journal of Environmental Sciences (China), 26 (2014) 1741-1749.
[98] S. Yang, Y. Sun, H. Yang, J. Wan, Catalytic wet air oxidation of phenol, nitrobenzene and aniline over the multi-walled carbon nanotubes (MWCNTs) as catalysts, Frontiers of Environmental Science & Engineering, (2014).
[99] S. Yang, W. Zhu, X. Li, J. Wang, Y. Zhou, Multi-walled carbon nanotubes (MWNTs) as an efficient catalyst for catalytic wet air oxidation of phenol, Catalysis Communications, 8 (2007) 2059-2063.
[100] A. Rodríguez, G. Ovejero, M. Mestanza, V. Callejo, J. García, Degradation of methylene blue by catalytic wet air oxidation with Fe and Cu catalyst supported on multiwalled carbon nanotubes, 2009, pp. 145-150.
[101] J. Garcia, H.T. Gomes, P. Serp, P. Kalck, J.L. Figueiredo, J.L. Faria, Carbon nanotube supported ruthenium catalysts for the treatment of high strength wastewater with aniline using wet air oxidation, Carbon, 44 (2006) 2384-2391.
[102] A.B. Ayusheev, O.P. Taran, I.A. Seryak, O.Y. Podyacheva, C. Descorme, M. Besson, L.S. Kibis, A.I. Boronin, A.I. Romanenko, Z.R. Ismagilov, V. Parmon, Ruthenium nanoparticles supported on nitrogen-doped carbon nanofibers for the catalytic wet air oxidation of phenol, Applied Catalysis B: Environmental, 146 (2014) 177-185.
[103] G. Ovejero, J.L. Sotelo, A. Rodríguez, C. Díaz, R. Sanz, J. García, Platinum Catalyst on Multiwalled Carbon Nanotubes for the Catalytic Wet Air Oxidation of Phenol, Industrial & Engineering Chemistry Research, 46 (2007) 6449-6455.
[104] J. Garcia, H.T. Gomes, P. Serp, P. Kalck, J.L. Figueiredo, J.L. Faria, Platinum catalysts supported on MWNT for catalytic wet air oxidation of nitrogen containing compounds, Catalysis Today, 102-103 (2005) 101-109.
[105] H.T. Gomes, P.V. Samant, P. Serp, P. Kalck, J.L. Figueiredo, J.L. Faria, Carbon nanotubes and xerogels as supports of well-dispersed Pt catalysts for environmental applications, Applied Catalysis B: Environmental, 54 (2004) 175-182.

[106] X. Li, S.X. Yang, W.P. Zhu, J.B. Wang, L. Wang, Catalytic wet air oxidation of phenol and aniline over multi-walled carbon nanotubes, Huanjing Kexue/Environmental Science, 29 (2008) 2522-2528.
[107] A. Rodríguez, J. García, G. Ovejero, M. Mestanza, Wet air and catalytic wet air oxidation of several azodyes from wastewaters: The beneficial role of catalysis, Water Science and Technology, IWA Publishing, 2009, pp. 1989-1999.

PART II

Tuning Carbon Materials Properties

CONTENT

(This page intentionally left blank)

Introductory note

Carbon materials are available in a wide range of forms, such as ACs, CBs, CNTs, CNFs, carbon gels, graphite and ordered mesoporous carbons. Tailoring their properties to specific needs is the major challenge to increase their potential market and applications as catalysts. The performance of any catalyst depends on the availability of suitable active sites, capable of chemisorbing the reactants and forming surface intermediates of adequate strength. Therefore, the surface chemistry of carbon materials plays an important role on the catalytic performance of carbon materials for different applications [1]. A better understanding of their surface chemistry and the development of controlled fine-tuning methodologies are required. The high reactivity of the carbon surface towards O-/N-/S-containing compounds allows the incorporation of different functional groups, extending the application of the carbon materials to a wide range of processes. In this part, relevant methods for the chemical functionalization of CNTs, CXs and rGOs are presented and their properties discussed, with emphasis on their use as catalysts in heterogeneous and metal-free processes.

Outline

The first chapter (*Chapter 1*) of this part is dedicated to the presentation of the carbon materials selected for this study, including an overview of the properties of commercial CNTs and the synthesis methodologies adopted for the lab-made carbon materials (CXs and rGOs). Detailed information regarding the techniques used to characterize the chemical and textural properties of the carbon materials, as well as information regarding the chemicals used for the liquid and gas phase treatments applied are presented in *Chapter 2*. The three subsequent chapters present the different methodologies adopted to incorporate: oxygen functionalities onto the carbon surface (*Chapter 3*), nitrogen doping of the carbon matrix (*Chapter 4*) and sulphur groups (*Chapter 5*), including the discussion of the properties promoted by each methodology. This part ends with a closing section (*Chapter 6*) where the most important conclusions achieved are summarized.

1. Carbon Materials

Three classes of carbon materials have been studied in this work: commercial CNTs, and, lab-made CXs and rGOs. In this first chapter, a description of the as-received CNTs will be presented, as well as the methodologies adopted for the synthesis of the CXs and rGOs. It was not the aim of this work to perform a detailed study of the synthesis routes of these materials, which are well described in the literature.

1.1. Carbon nanotubes

The CNTs used in the present work were purchased from NANOCYL™ (NC3100 series). According to the manufacturers, NANOCYL® NC3100™ series are thin multiwalled carbon nanotubes produced via the Catalytic Chemical Vapor Deposition (CCVD) process and then purified up to 95 % (wt.), as determined by thermogravimetric analysis (TGA) [4]. Characterizations performed by other authors confirm that the purity is higher than the product specifications, ie, higher than 95 % (wt.). However, CNTs contain impurities from the growth catalyst, mainly iron, cobalt [5, 6], and sulphur (probably due to the purification process), and aluminium as trace impurity [8]. The CNTs are available as a solid black powder with a bulk density around 150 g L^{-1}, and present an average length of 1.5 μm and a average diameter of 9.5 nm, measured by TEM and high resolution TEM, respectively [4]. Furthermore, most of the tubes exhibit well-aligned walls, parallel to the main axis, thus being relatively close to the perfect multiwalled CNT structure [8]. This NC3100 series presents also high electrical conductivity. Differences found in the characterization of

pristine CNTs are likely due to batch-to-batch variations. Henceforward, the as-received CNTs are referred as CNT-O.

1.2. Carbon xerogels

The CXs were produced by the conventional polycondensation of resorcinol with formaldehyde solubilized in water followed by carbonization. The procedure followed was based on a simplified method that reduces the preparation time without compromising the material synthesis [9, 10], adopted from published procedures [11, 12]. Bearing in mind the intended application of these carbon materials in the liquid phase, the operating variables, namely the pH during the sol-gel processing and the drying method (direct drying method), were chosen to produce a CX with high surface area and a monomodal mesoporous texture [10].

Briefly, 25 g of resorcinol were added to 40 mL of distilled water under magnetic stirring and 34 mL of formaldehyde were introduced after complete dissolution. The pH was adjusted to 6.0 (in order to produce a mesoporous structure [11]) by dropwise addition of a sodium hydroxide solution. The gelation step was completed after 3 days at 85 °C in a paraffin bath. Once finished, the red brown opaque solid gel was then cut into powder form. The material was dried in an oven from 60 to 120 °C during 4 days, increasing the temperature 20 °C/day. After drying, the material was further subjected to a carbonization procedure: using a heating ramp of 2 °C min^{-1} under N_2 flow (100 cm^3 min^{-1}), the material was heated until 150, 400, 600 and 800 °C holding each temperature between 1 and 6 h (higher temperature), resulting in a carbon xerogel henceforward referred to as CX-O.

1.3. Graphene oxide

Reduced graphene oxide (rGO) used in the work was obtained by reduction of lab-synthetized graphene oxide (GO). The GO was prepared by strong chemical oxidation of graphite, by using natural graphite (20 μm, from Sigma-Aldrich) and a modified Hummers method [13-15], followed by the sonicated-assisted exfoliation of the obtained graphite oxide.

Briefly, 50 mL of concentrated sulphuric acid was slowly added, under appropriate cooling and stirring conditions, to a flask containing 2 g of graphite. Then, 6 g of potassium permanganate were slowly added to the mixture and the suspension kept at 35 ^{o}C for 2 h under stirring. The solution was diluted in 350 mL of distilled water. Afterwards, hydrogen peroxide (30 % w/v) was added in order to reduce residual permanganate to soluble manganese ions. The oxidized material was purified with a hydrochloric acid solution (10 % wt.) and the suspension was then filtered, washed several times with distilled water until neutrality of the rinsing waters, and dried at 60 ^{o}C for 24 h to obtain graphite oxide. The resulting material was dispersed in a given volume of water and sonicated in an ultrasound bath (ultrasonic processor UP400S, 24 kHz) for 1 h, GO being obtained in this way. The sonicated dispersion was centrifuged for 20 min at 3000 rpm to remove unexfoliated graphite oxide particles from the supernatant. The obtained suspension of graphene oxide was then dried at 80 ^{o}C for 24 h to remove water. The solid graphene oxide material was recovered for further use.

The GO was prepared in the LCM by Doctor Luisa Pastrana-Martínez assisted by Bruno C. Bordoni.

(This page intentionally left blank)

2. Chemicals and Characterization Techniques

2.1. Chemicals

Liquid formaldehyde 37 % (wt.) in H_2O (CH_2O), hydrogen peroxide 30 % (H_2O_2), nitric acid 69 % (HNO_3) and sulphuric acid 95-98 % (H_2SO_4) and granulated sodium hydroxide (NaOH) and potassium permanganate ($KMnO_4$) were purchased from Sigma-Aldrich. Resorcinol ($\geq$ 99 %; $C_6H_6O_2$) and melamine ($C_3H_6N_6$) were acquired from Fluka, and urea ($\geq$ 99 %; CH_4N_2O) from Acros. Hydrochloric acid 37 % (HCl) from Riedel-de Haën was also used. All solutions were prepared with distilled water or with absolute ethanol (C_2H_5OH) from Panreac. High purity standards of sulphanilamide ($C_6H_8N_2O_2S$) and benzoic acid ($C_7H_6O_2$) from Elementar were used in characterization techniques.

Pure nitrogen (N_2), oxygen (O_2), carbon monoxide (CO), carbon dioxide (CO_2), helium (He), ammonia (NH_3) in compressed gas cylinders ALPHAGAZ 1 grade with a purity higher than 99.99 % from Air Liquide were used in characterization techniques and in the thermal treatments.

2.2. Characterization Techniques

The carbon materials synthesized and/or modified were exhaustively characterized to assess their main textural and surface properties and changes promoted by the chemical and thermal treatments applied. This section describes the characterization techniques used and the procedures followed. Most of the techniques are available in the Laboratory of Catalysis and Materials (LCM) or accessible at the Materials Centre of the University of Porto (CEMUP).

2.2.1.Textural Properties

The gas physisorption technique is an important tool for the characterisation of porous solids and fine powders [16]. The textural characterization of the materials was based on the N_2 adsorption-desorption isotherms, determined at -196 °C in the relative pressure range 10^{-5} – 0.995 with a Quantachrome NOVA 4200e multi-station apparatus. Each sample (around 100 mg) was outgassed under high vacuum at 150 °C between 3 and 5 h, prior to analysis. The available surface area of the carbon samples was determined according to the standard Brunauer, Emmett and Teller method (S_{BET}). A linear plot of the BET equation was ensured within the range 0.05 – 0.30 of relative pressure. The estimated experimental error for S_{BET} was ± 20 $m^2 g^{-1}$.

The total pore volume (V_P) was determined from the N_2 uptake at p/p_0= 0.95 (in most cases) or at p/p_0= 0.99 (duly indicated).

The non-local density functional theory (NLDFT) was used to obtain the pore size distribution of selected samples by applying the kernel file provided by Quantachrome's data reduction software, where a cylindrical-pore model is assumed.

In the case of CX samples, the average mesopore diameters (d_P) of the samples were obtained by the method of Barrett, Joyner and Halenda (BJH). The mesopore surface area (S_{meso}), and micropore volume (V_{micro}) were calculated by the *t*-method, using the standard isotherm for carbon materials.

2.2.2.Surface Chemistry Characterization

Bulk composition of the carbon samples was determined by Elemental Analysis (EA) carried out on a Carlo Erba instrument, model EA 1108a or on a vario MICRO cube analyser from Elemental GmbH in CHNS mode. Each element (CHNS) was determined by combustion of the sample at 1050 °C and calculated by the mean of three independent measurements, using a per-day calibration with a standard compound (sulphanilamide). Oxygen analysis was carried out on a rapid OXY cube analyser from Elemental GmbH. Oxygen composition was determined by pyrolysis of the sample at 1450 °C and calculated by the average of three independent measurements, using a per-day calibration with a standard compound (benzoic acid), with the exception of the cases specifically indicated, where O was determined by difference of CHNS EA. The samples were previously dried at 110 °C in the oven to remove any water.

Thermogravimetric analyses (TGA) were carried out using an STA 409 PC/4/H Luxx Netzsch thermal analyser. Samples were heated at

10 °C min^{-1} from 50 until 900 °C, under He flow. At the final temperature, He was replaced by air for 13 min, for burning-off the carbon. Proximate analysis was based on the method described by Ottaway [17].

The pH at the point of zero-charge (pH_{PZC}) was determined by analysis of the pH change of NaCl solutions of different initial values of pH when exposed to a sample of the prepared materials using a drift method described elsewhere [18]. Briefly, 0.050 g of each sample was placed in a closed Erlenmeyer flask with 20 mL of NaCl 0.01 M solution with the pH previously adjusted between 2 and 12 by adding HCl 0.1 M or NaOH 0.1 M. Samples were stirred at room temperature during 24 h and the final pH measured. A blank experiment (without the carbon material) was carried out in order to subtract the variation of pH caused by the effect of CO_2 present in the head space. The pH_{PZC} is the point where the curve pH_{final} vs. $pH_{initial}$ crosses the line $pH_{initial}$ =pH_{final}.

The surface O-groups were characterized by temperature programmed desorption (TPD) analysis. The TPD profiles were obtained with a fully automated AMI-200 or AMI-300 Catalyst Characterization apparatus (Altamira Instruments) connected to a Dycor Dymaxion Mass Spectrometer. The sample (0.100 g) was placed in a U-shaped quartz tube located inside an electrical furnace and heated up to 1100 °C at 5 °C min^{-1} using a constant flow rate of He equal to 25 cm^3 min^{-1}. The CO and CO_2 released during the thermal analysis were monitored, and calibrated at the end of each analysis. The SO_2 signals were also monitored for samples treated with H_2SO_4. A sulphanilamide standard was used in this case for SO_2 mass signal calibration. Deconvolution of TPD-MS profiles was done following the method previously developed by Figueiredo et al. [19, 20].

The elemental chemical analyses of carbon material surfaces were performed at CEMUP by X-Ray Photoelectron Spectroscopy (XPS). Samples were characterized using two apparatus, accordingly to their availability at CEMUP. Therefore, some XPS analyses were performed using an ESCALAB 200A, VG Scientific (UK) with PISCES software for data acquisition and analysis. For analysis, an achromatic Al (Kα) X-ray source (1486.6 eV) operating at 15kV (300 W) was used, and the spectrometer, calibrated with reference to Ag 3d5/2 (368.27 eV), was operated in CAE mode with a pass energy of 20 eV (regions of interest -ROI) and 50 eV (survey). The effect of the electric charge was corrected by reference to the carbon peak (285 eV). Additional analyses were performed using a Kratos AXIS Ultra HSA, with VISION software for data acquisition, CASAXPS software for data analysis. The analyses were carried out with a monochromatic Al Kα X-ray source (1486.7 eV), operating at 15 kV (90 W), in Fixed Analyser Transmission (FAT) mode, with a pass energy of 40 eV for ROI and 80 eV for survey. Data acquisition was performed with a pressure lower them 10^{-6} Pa. Modelling of the spectra was performed using the XPSPEAK4.1 program, in which an adjustment of the peaks was performed using peak fitting with Gaussian-Lorentzian peak shape and Shirley type background subtraction.

(This page intentionally left blank)

3. Oxygen-containing surface groups

The recent advances in the development of reliable methods to tune physicochemical properties of carbon materials by suitable thermal or chemical post-treatments provide a major asset for their use as catalysts in several applications [21-23]. The most important and at the same time the most abundant heteroatom that affects the use of carbon materials is oxygen [24]. Different chemical and thermal treatments can be applied to carbon materials in order to produce materials with oxygenated surface groups. The most common liquid-phase oxidation treatments include HNO_3, mixtures of H_2SO_4/HNO_3, H_2O_2 and ozone (O_3). Alternative gas-phase functionalization techniques involve oxidation with O_2 (usually diluted with N_2), O_3, CO_2, oxidative plasmas or by means of HNO_3 vapours, which can avoid the multi-step procedure of the liquid-phase functionalization [25-27]. Carboxyl, carbonyl, phenol, quinone, and lactone groups, have been identified on carbon surfaces [19].

This chapter describes the methodologies adopted for the incorporation of oxygen-containing surface groups on the carbon materials. Liquid-phase oxidation treatments, controllable surface functionalization by hydrothermal treatments and selective removal of O-surface groups have been applied to carbon materials (CNTs and CXs) to incorporate O-contain groups onto the carbon structure.

The results presented in this section have been already reported in the following papers:

Carbon as a catalyst: Esterification of acetic acid with ethanol, authored by Raquel P. Rocha, Manuel F.R. Pereira and José L. Figueiredo, and published in the journal Catalysis Today Volume 218– 219 pages 51-56 (2013). Author Contributions: Raquel Rocha carried out the experimental work described and wrote the manuscript, with substantial supervision of the other authors.

Supported Pt-particles on multi-walled carbon nanotubes with controlled surface chemistry, authored by Raquel P. Rocha, Adrián M.T. Silva, Goran Dražić, Manuel F.R. Pereira and José L. Figueiredo, and published in the journal Materials Letters Volume 66 pages 64-67 (2012). Author Contributions: Raquel P. Rocha performed the modification and substantial characterization of the samples. The manuscript was written by R.P. Rocha with substantial supervision of all authors.

Controlled surface functionalization of multiwall carbon nanotubes by HNO_3 hydrothermal oxidation, authored by Vlassis Likodimos, Theodore A. Steriotis, Sergios K. Papageorgiou, George Em. Romanos, Rita R.N. Marques, Raquel P. Rocha, Joaquim L. Faria, Manuel F.R. Pereira, José L. Figueiredo, Adrián M.T. Silva and Polycarpos Falaras, and published in the journal Carbon Volume 69 pages 311-326 (2014). Author Contributions: Raquel P. Rocha performed the modification and substantial characterization of the NANOCYL multiwalled carbon nanotube samples. The manuscript was written with contributions from all authors.

3.1. Methodologies

3.1.1.Liquid-Phase Oxidation Treatments

In a typical liquid-phase oxidation run, carbon materials in powder form were treated with HNO_3 by direct contact at boiling temperature for 3 h. A fixed ratio of 1 g of carbon material to 75 mL of HNO_3 solution was used in all oxidations performed. A round bottom flask equipped with a condenser was used and the suspension was kept under magnetic stirring. After cooling, the suspension was washed up to a neutral pH of the rinsing water and the recovered material was dried overnight at 110 °C. This methodology was used both with CNT and CX samples, using different HNO_3 concentrations. The corresponding samples will be designated as CNT-N and CX-N, followed by the HNO_3 concentration used, e.g., CNT-N7 (treated with a HNO_3 solution of 7 mol L^{-1}; Nc - concentrated HNO_3).

3.1.2.Selective removal of O-surface Groups

An alternative way to create basic or neutral surfaces after oxidation with HNO_3 consists in performing thermal treatments under inert atmosphere at specific temperatures, in order to selectively remove the acidic groups introduced during the oxidation. In order to produce different samples with successively lower acid character, thermal treatments under N_2 were applied to oxidized CNTs (CNT-N7). Briefly, 1 g of the CNT-N sample was heated to 200 °C at 10 °C min^{-1} under N_2 flow (100 cm^3 min^{-1}) and kept at this temperature for 1 h (CNT-N200). The same procedure was repeated at higher temperatures, 400, 600 and 900 °C,

resulting in the samples labelled as CNT-N400, CNT-N600 and CNT-N900, respectively.

3.1.3.Hydrothermal Oxidation

Controlled surface functionalization of CNTs was performed by hydrothermal oxidation treatment performed in a 160 mL autoclave (Parr Instruments). The procedure was adapted from a methodology recently developed for controlled functionalization of carbon xerogels and single-walled CNTs [28, 29]. In a typical run, 75 mL of a solution with the desired HNO_3 concentration (0.05, 0.10, 0.20 or 0.30 mol L^{-1}) was transferred to the autoclave and 0.5 g of the pristine CNTs was added. The autoclave was flushed with N_2, in order to remove dissolved oxygen, stirred at 300 rpm and heated until 200 °C at autogenous pressure. After 2 h, the material was recovered, washed several times with distilled water until neutral pH and dried overnight. Samples were labelled as CNT-N-HT-X, where X indicates the HNO_3 concentration used. Samples prepared by hydrothermal treatment were compared with oxidized CNTs treated by direct contact with HNO_3 boiling temperature (2.0 g of CNTs to 150 mL of a 7 mol L^{-1} HNO_3 solution), sample CNT-N-BT-7.

3.2. Induced Properties

3.2.1.Liquid-Phase Oxidation Treatments

HNO_3 is the most common reagent for the oxidation of carbon materials. Typically, liquid-phase oxidation can be performed in a Soxhlet extractor or just by boiling the carbon material in HNO_3. The method chosen depends on the chemical resistance of the carbon material, the concentration of acid used, and on the ratio of carbon material/oxidant [30, 31].

Table II- 1 shows modifications promoted by HNO_3 oxidation over commercial CNTs and CX samples using different oxidant concentrations, in the case of CNTs. Regarding the textural properties determined from the N_2 adsorption isotherms, the changes in S_{BET} resulting from HNO_3 oxidation are smaller than 100 $m^2 g^{-1}$. However, the total pore volume of the CNT samples (determined from the N_2 uptake at p/p_0= 0.99) decreases by increasing the HNO_3 concentration.

Table II- 1. Textural characterization of oxidized CNT and CX samples with nitric acid at boiling temperature.

Sample	S_{BET}	V_p	S_{Meso}	V_{Micro}	d_p
	($m^2 g^{-1}$)	($cm^3 g^{-1}$)	($m^2 g^{-1}$)	($cm^3 g^{-1}$)	(nm)
CNT-O	302	2.90	- - - - - - - - - -	n.a.	- - - - - - - - - -
CNT-N7	358	1.62	- - - - - - - - - -	n.a.	- - - - - - - - - -
CNT-N10	330	1.32	- - - - - - - - - -	n.a.	- - - - - - - - - -
CNT-Nc	312	0.54	- - - - - - - - - -	n.a.	- - - - - - - - - -
CX-O	672	1.16	244	0.173	17.4
CX-N7	697	1.14	234	0.188	17.5

n.a. – not applicable.

According to IUPAC, the isotherms of the CNT samples (Figure II- 1) can be classified as type II [16, 32], characteristic of nonporous materials such as CNTs. In this carbon material, the pore volume is mostly associated to the free space between filaments occurring in CNT bundles [29]; therefore, the decrease of the pore volume could be related to the combined effect of CNTs disentanglement, by a better alignment of the tubes, promoted by the oxidation treatment [33], and the incorporation of oxygen surface groups. On the other hand, the changes in S_{BET} may be connected to changes in length and perfection of the nanotubes, as a result of the applied treatments [34] or by opening the tips of the tubes [35]. Increase of the HNO_3 concentration results in severe degradation effects, especially for the total pore volume that decreases more than 80 %, indicating that tube shortening as well as the formation of structural defects, may be occurring during boiling in HNO_3, as in fact is suggested by other authors [36, 37].

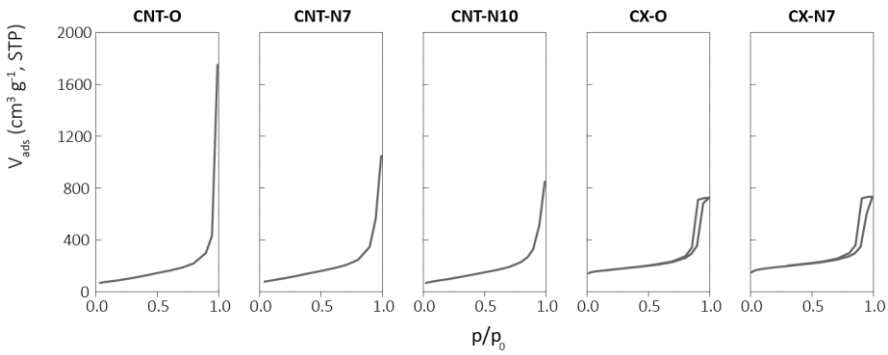

Figure II- 1. N_2 adsorption-desorption isotherms at -196 °C for pristine and nitric acid treated CX and CNT samples[2].

[2] Adapted from Catalysis Today 218-219 (2013) 51-56.

Regarding the CX samples, they presented type IV isotherms (Figure II- 1), characteristic of mesoporous solids, with average pore diameter around 20 nm (determined by the BJH method). Likewise, the BET surface of the sample treated with HNO_3 increased, in comparison with the original carbon xerogel. The mesopore surface area and micropore volume of the original CX is not affected by the HNO_3 treatment, varying less than 8 %.

In order to identify and quantify the amount of oxygenated groups incorporated by the applied treatment, the surface chemistry of the samples was analysed by TPD. The total amount of O-containing surface groups released as CO and CO_2 was determined from the areas under the corresponding TPD profiles of the samples (Table II- 2Table II- 1). A negligible amount of oxygen-containing surface groups was found on the pristine material (CNT-O), while the highest amount of these groups was recorded for CNT-Nc. Nevertheless, the CX sample treated with HNO_3 revealed the largest incorporation of O-surface groups (2414 and 1715 μmol g^{-1}, for CO and CO_2, respectively).

Table II- 2. Surface chemistry characterization of oxidized CNT and CX samples with nitric acid at boiling temperature.

Sample	CO (μmol g^{-1})	CO_2 (μmol g^{-1})	$Volatiles_{TGA}$ (% wt.)
CNT-O	299	105	2.3
CNT-N7	1453	1008	9.3
CNT-Nc	1592	1422	15.7
CX-N7	2414	1715	35.1

Volatiles released during TGA analyses of the samples show similar trend as the amounts of CO and CO_2 released during TPD; however, large amounts of surface groups would be expected considering the percentage of volatiles, due to the non-selective nature of the method, which does not distinguish the O-containing groups. All groups thermally decomposed until 900 °C are released during TGA.

The nature of the distinct functional groups can be determined by deconvolution of the CO and CO_2 TPD profiles following the procedure previously developed for activated carbons [19, 20]. A multi gaussian function ca be used for modelling the TPD profiles, taking into account the temperature ranges corresponding to the evolution of CO and CO_2 upon decomposition of the various types of oxygen functional groups.

The CO and CO_2 profiles of CNT and CX samples treated with a 7 mol L^{-1} HNO_3 solution (Figure II- 2) indicate that phenols were the main groups released as CO at moderate to high temperatures and carboxylic acids those released as CO_2 between 200 and 450 °C, for both carbon materials. Carbonyls/quinones and lactones were also identified, in less extent, by the release of CO and CO_2, respectively, at higher temperatures, while carboxylic anhydrides were identified on both CO and CO_2 profiles at middle temperature range [19, 20, 23].

For illustration purposes, Figure II- 3 shows the TPD profiles for CNTs treated with HNO_3 7 mol L^{-1} and their deconvolution into individual components. The CO_2 evolved at lower temperatures is due to the higher amount of carboxylic acids in this sample, allowing the differentiation of two different types of carboxylic acids by the deconvolution of the CO_2 TPD profile, namely strongly acidic (SA) and weakly acidic (WA) carboxylic acids, which have been established to evolve at lower and higher

temperatures, respectively [20]. The carboxylic anhydrides decompose between 350 and 600 °C by releasing one CO and one CO_2 molecule [38], thus same shape and equal magnitude of the group appears in CO_2 and CO profiles. At temperatures above 600 °C, the CO_2 profile shows the presence of a small amount of lactones. A shoulder in the low temperature range of the CO profile was ascribed to carboxylic acids since they appear at the same temperatures where the carboxylic acids evolve in the CO_2 profile (identified as CAc), whose origin, however, is not fully understood at present [20]. In addition to the carboxylic anhydrides, the CO profile includes contributions of phenol groups in a middle temperature range (500-750 °C) followed by carbonyl/quinone groups (above 700 °C), which are more thermally stable than the previous ones and are only released at higher temperatures.

In the case of CNTs, HNO_3 treatment is also frequently used to remove amorphous carbon and metal impurities from the material [39]. Although a non-selective functionalization is achieved, the O-containing groups can be anchored onto the defect sites of sidewalls and open caps of the CNTs or on the edges [25]. Bulk and surface composition of CNT-N treated with a 7 mol L^{-1} HNO_3 solution determined by Elemental Analysis and XPS revealed, as expected, a very large increase of the oxygen content due to the formation of oxygen-containing functional groups in the CNTs surface. A significant decrease of the pH_{PZC} (from neutral to around 2) was achieved after treatment showing a strong acidification of the pristine material.

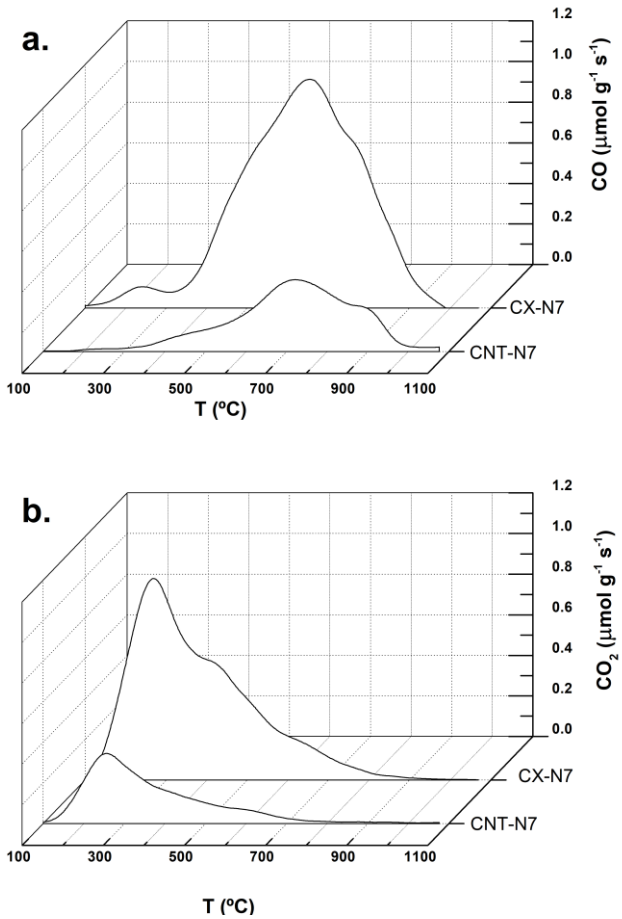

Figure II- 2. TPD profiles of CX and CNT samples treated with a 7 mol L^{-1} nitric acid at boiling temperature: (a) CO release; (b) CO_2 release[3].

[3] Adapted from Catalysis Today 218-219 (2013) 51-56.

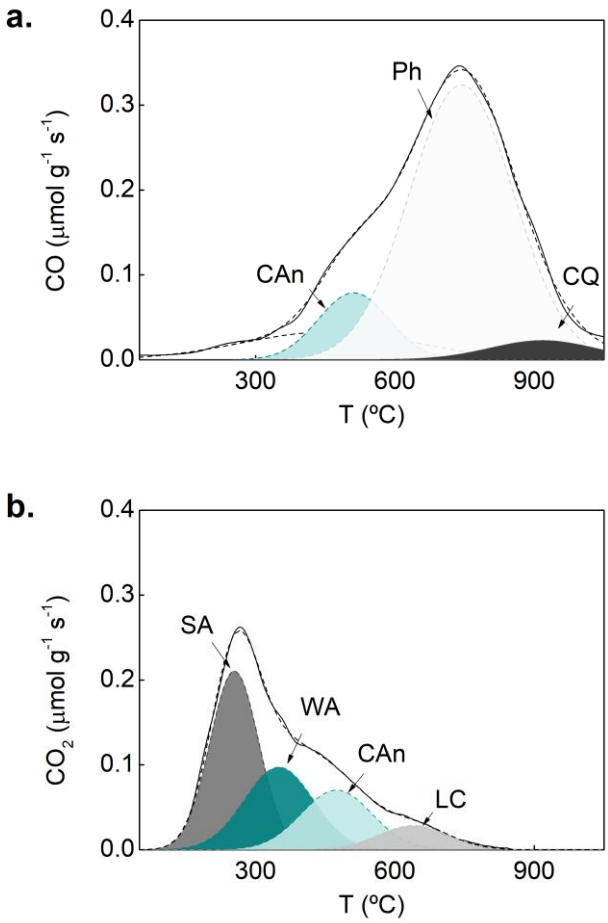

Figure II- 3. Deconvolution of TPD profiles for CNTs treated with a 7 mol L^{-1} nitric acid solution at boiling temperature: groups released as (a) CO and (b) CO_2 (PH phenols; CAn - carboxylic anhydrides; CQ - carbonyl quinones; LC - lactones; CAc - carboxylic acids; SA - strongly acidic CAc; WA - weakly acidic CAc)[4].

[4] Adapted from Journal of Carbon Research C, 2 (2016) 17.

3.2.2.Selective removal of O-surface Groups

An alternative way to induce a basic or neutral surface consists in performing thermal treatments under inert atmosphere at specific temperatures after oxidation with HNO_3, in order to selectively remove some of the groups previously introduced during oxidation. The large amounts of oxygen containing groups incorporated on the CNTs by HNO_3 oxidation [carboxylic acid groups (released below 450 °C) and carboxylic anhydrides (evolved between 350 and 600 °C) and lactones (released above 600 °C) as CO_2 during the TPD experiments, and phenol (500–750 °C) and carbonyl/quinone groups (700–950 °C) released as CO, can be successively removed with the thermal treatments [26]. Thus, samples with different amounts of oxygen groups can be obtained, starting from the oxidized sample (CNT- N).

Table II- 3 summarises the textural and surface chemical modifications observed with the applied treatments. Regarding the textural properties, oxidation with HNO_3 results in an increase of 30 $m^2\ g^{-1}$ for S_{BET} and a decrease of V_P to 0.64 $cm^3\ g^{-1}$, when CNT-O and CNT-N are compared, respectively. The subsequent thermal treatments applied to the oxidized CNTs did not promote additional changes on S_{BET} (the differences between the surface areas of the treated samples were lower than 20 $m^2\ g^{-1}$, which is within the experimental error). Nonetheless, a slight increase of V_P, up to 0.8 $cm^3\ g^{-1}$, is observed suggesting that the removal of the oxygen functionalities improves the accessibility to the tubes.

Table II- 3. Chemical and textural characterization of pre-oxidized and thermally treated CNT samples.

Sample	S_{BET}	V_p	CO	CO_2	pH_{PZC}
	($m^2\ g^{-1}$)	($cm^3\ g^{-1}$)	($\mu mol\ g^{-1}$)	($\mu mol\ g^{-1}$)	(unitless)
CNT-N	324	0.64	1340	841	2.7
CNT-N200	322	0.70	1300	807	2.8
CNT-N400	350	0.72	1145	322	4.3
CNT-N600	391	0.79	650	256	7.0
CNT-N900	376	0.80	108	62	8.3

In contrast with the minor alterations of the textural properties, a drastic change of the surface chemistry is observed after oxidation. The HNO_3 treatment strongly acidifies the original material (pH_{PZC} decreases from neutral character in the pristine CNTs to 2.7 in the oxidized sample without any thermal treatment), which is due to the incorporation of a large amount of oxygen containing groups, including carboxylic acids, carboxylic anhydrides, lactones and phenols, that directly contribute to the acidic character of the surface, and some carbonyl/quinone groups which are neutral or may form basic structures. By the subsequent thermal treatments those groups are selectively removed, leading to a reduction of the acidic character of the surfaces (pH_{PZC} increases from 2.7 to 8.3). Thus, the CNT-N200 sample presents a slightly lower amount of carboxylic acids than CNT-N. The remaining carboxylic acids were almost completely removed, as well as a part of the anhydrides, when the treatment was performed at 400 °C (CNT-N400). After treatment at 600 °C (CNT-N600), the surface only contains phenol and carbonyl/quinone groups, and a small amount of lactones, while the sample treated at 900 °C only presents

residual amounts of carbonyl/quinone groups. Those changes are confirmed by TPD analysis of the samples. The decrease of CO and CO_2 amounts (released during the TPD experiments) depends on the increase of the final temperature of the thermal treatment (Table II- 3). Figure II- 4 schematically illustrates the removal of the functional groups according to the final temperature applied in the thermal treatment.

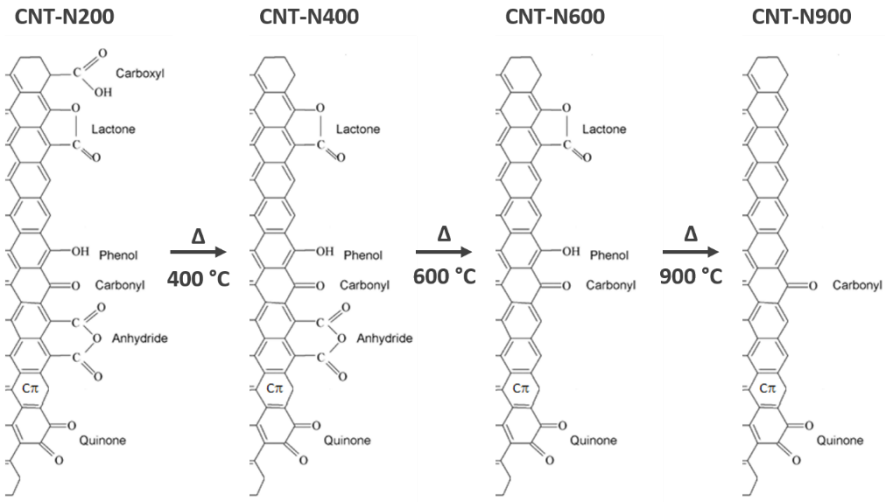

Figure II- 4. Schematic illustration of O-containing groups released at the surface of CNTs during thermal treatment under inert atmosphere.

The removal of the O-containing groups shown in Figure II- 4 was accompanied by the successive removal of the bulk oxygen, determined by EA (by pyrolysis of the samples at 1450 °C), and by the decrease of the surface oxygen determined by XPS. The functionalization degree under the applied treatments normalized by the carbon content (EA) is shown in Figure II- 5. In addition to the good agreement between the results obtained, this shows that the availability of suitable characterization

techniques affords a better understanding of the modifications promoted and consequently a more systematic characterization.

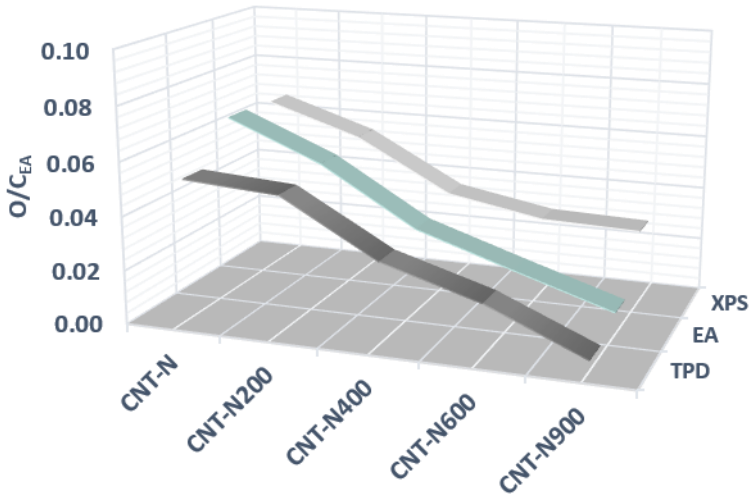

Figure II- 5. Functionalization degree of pre-oxidized and thermally treated CNT samples by different characterization techniques.

3.2.3.Hydrothermal Oxidation

In spite of being frequently performed to functionalize carbon nanotubes, the boiling HNO_3 treatment induces severe degradation effects; in particular, loss of material, tube shortening as well as the formation of structural defects are usually reported [36, 37]. Furthermore, concentrated oxidants are needed and an accurate control of the total amount of groups that are produced on the CNT surface is difficult to achieve. An alternative to the chemical functionalization of CNTs by refluxing with concentrated oxidants can be achieved using hydrothermal oxidation. This methodology, which was first developed for carbon xerogels [28] and later extended to single walled carbon nanotubes [29, 40], uses diluted concentrations of HNO_3 to control the amount of oxygenated functionalities created on the surface of CNTs. The method, which is extremely effective, has shown a strong dependency between the amount of oxygenated-surface groups (carboxylic acids, carboxylic anhydrides, phenols, carbonyl/quinones and lactones) and the HNO_3 concentration. In the present work, the same methodology was extended to commercial multiwalled CNTs.

Figure II- 6 shows the N_2 adsorption-desorption isotherms of pristine and hydrothermally functionalized CNTs. The isotherm obtained for the pristine material can be classified as type II, according to IUPAC. The main difference between the isotherms of pristine and treated materials is related to the hysteresis loop and to the pore volume that decreases by increasing the HNO_3 concentration. The total pore volume (determined from the N_2 uptake at p/p_0=0.99) was 2.71 $cm^3\ g^{-1}$ for pristine CNTs and 1.80, 1.47, 1.14 and 0.97 $cm^3\ g^{-1}$ for materials treated with HNO_3

concentrations of 0.05, 0.10, 0.20 and 0.30 mol L^{-1}, respectively. The BET surface area increased by 27 % (from 311 to 395 $m^2 g^{-1}$) when pristine CNTs were treated with 0.05 mol L^{-1} HNO_3, while only a slight increment of 9 % was observed between the BET surface areas of CNTs treated with the lowest and highest HNO_3 concentrations, 395 and 433 $m^2 g^{-1}$ for 0.05 and 0.30 mol L^{-1} HNO_3, respectively.

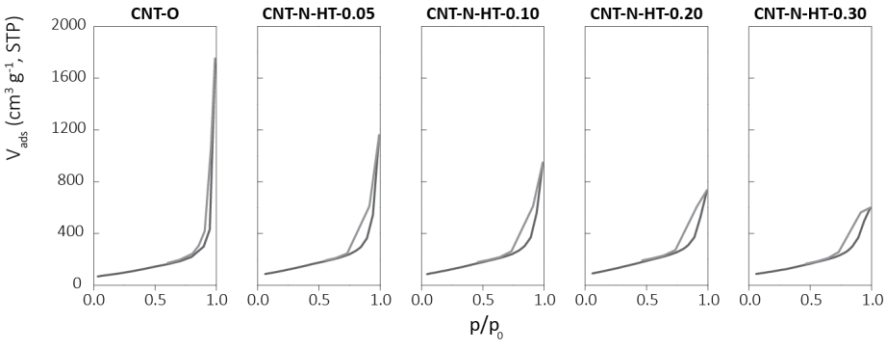

Figure II- 6. N_2 adsorption-desorption isotherms at -196 °C for pristine and hydrothermally functionalized CNTs with different nitric acid concentrations[5].

It is important to note that the pore volume for CNTs is mainly associated to the free space occurring in CNT bundles [29]. Therefore, the isotherms suggest that the HNO_3 treatment has a significant effect on the disentanglement of CNTs, because some pore volume is lost upon hydrothermal oxidation.

The identification and quantification of oxygenated groups was determined from the TPD profiles obtained (Figure II- 7). The TPD profiles measured for the pristine material are also included for comparison.

[5] Adapted from Materials Letters 66 (2012) 64-67.

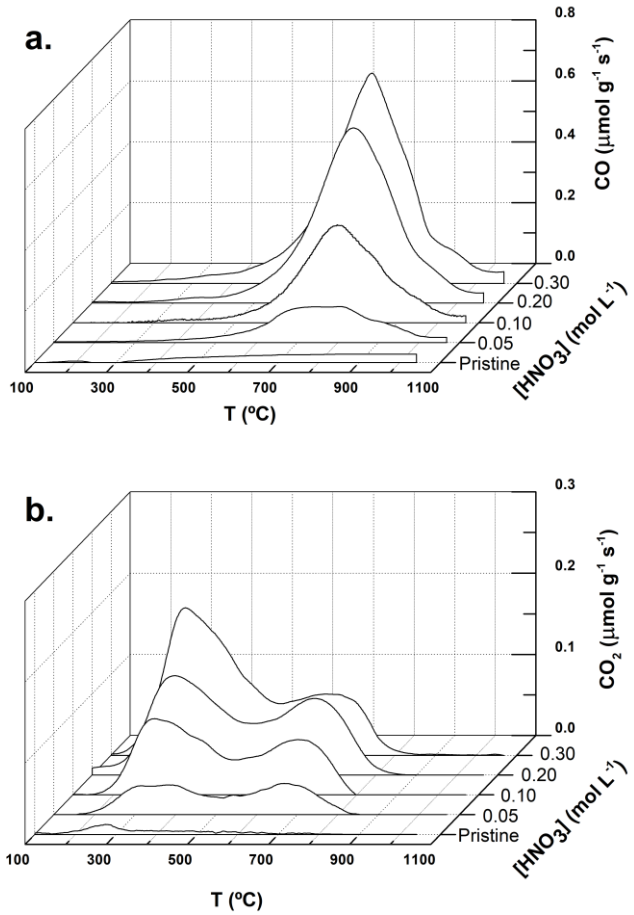

Figure II- 7. TPD profiles for the pristine and hydrothermally treated CNT samples with different HNO_3 concentrations: (a) CO and (b) CO_2 release[6].

The total amounts of surface groups released as CO and CO_2 were determined from the areas under the corresponding TPD profiles and are presented in Table II- 4. The total amount of molecular oxygen released as CO and CO_2 (O_2, % wt.), which is representative of the total amount of

[6] Adapted from Carbon 69 (2014) 311-326.

oxygenated groups introduced on the CNT surface, was calculated based on the amounts determined by the TPD analysis. Additionally, the CO/CO_2 ratio was evaluated to determine the functionalization degree achieved. The CO/CO_2 ratio increases with the increase of the concentration of the oxidizing agent due to the introduction of more acidic groups on the CNT surface that are released as CO_2 and CO. This implies the formation of relatively more acidic groups, in comparison to basic groups, on the surface of carbon material.

Pristine CNTs comprised low amounts of surface groups and a low amount of released O_2 (% wt.). Hydrothermal treatment in the presence of HNO_3 resulted in a marked increase of the release of both CO and CO_2 that depended strongly on the HNO_3 concentration (Figure II- 7).

Table II- 4. Total amounts of CO, CO_2 and O_2 (% wt.) calculated from the TPD profiles obtained for the hydrothermally functionalized CNTs with nitric acid.

Sample	CO	CO_2	O_2	CO/CO_2
	(μmol g^{-1})	(μmol g^{-1})	(% wt.)	(unitless)
CNT-O	178	33	0.4	5.32
CNT-N-HT-0.05	489	195	1.4	2.51
CNT-N-HT-0.10	973	388	2.8	2.51
CNT-N-HT-0.20	1742	588	4.7	2.96
CNT-N-HT-0.30	2015	680	5.4	2.96
CNT-N-BT-7	1511	767	4.9	1.97

A single exponential function was found to describe analytically the evolution of CO and CO_2 amounts and the total amount of molecular oxygen released from the materials' surface (O_2, % wt.) with the HNO_3

concentration (Figure II- 8), in qualitative agreement with the results obtained for hydrothermally treated singe walled CNTs [29, 40], and carbon xerogels [28].

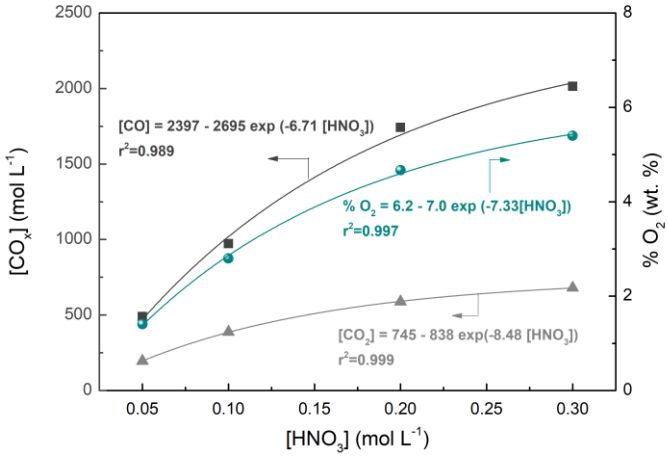

Figure II- 8. Evolution of the amount of CO, CO_2 and molecular O_2 released at the surface of the hydrothermally treated CNTs with HNO_3 concentration[7].

This shows that oxygen surface functionalization of these carbon materials can be accurately controlled through the hydrothermal methodology regardless of the structural differences between them and the different amounts of surface groups introduced on the CNT's surface.

To explore further the modification of the multiwalled CNT's surface chemistry by hydrothermal oxidation, the nature of the distinct functional groups and their amounts were determined as function of the HNO_3 concentration by deconvolution of the CO and CO_2 TPD profiles following

[7] Adapted from Carbon 69 (2014) 311-326.

the procedure previously developed for activated carbons [19, 20]. All profiles were deconvoluted and the amount of each group (determined by calculating the area under the correspondent peak) is presented as a function of the HNO_3 concentration in Figure II- 9. Phenols were the main groups released as CO and carboxylic acids those released as CO_2. Carbonyls/quinones and lactones were also identified by the deconvolution of the CO and CO_2 profiles, respectively, while carboxylic anhydrides were identified on both CO and CO_2 profiles. In addition, an exponential analytic function was found to fit well the HNO_3 concentration dependence of the amount of each single oxygenated moiety (not shown), as found for the total amount of groups on the surface of multiwalled CNTs (Figure II- 8). The amount of all identified surface groups increased with the HNO_3 concentration except for carbonyl/quinone functionalities. The proposed mechanism for the creation/evolution of oxygenated surface groups on CNTs is based on a progressive pathway where the carbonyl/quinone groups (C=O) are formed and further transformed into phenolic (-OH) and carboxylic (-COOH) functionalities [37, 39, 41]. The amount of carbonyl/quinone functionalities decreased with the increase of the HNO_3 concentration, suggesting that the development of phenolic and carboxylic surface groups could in fact result from the conversion of carbonyl/quinones initially created on the CNTs' surface.

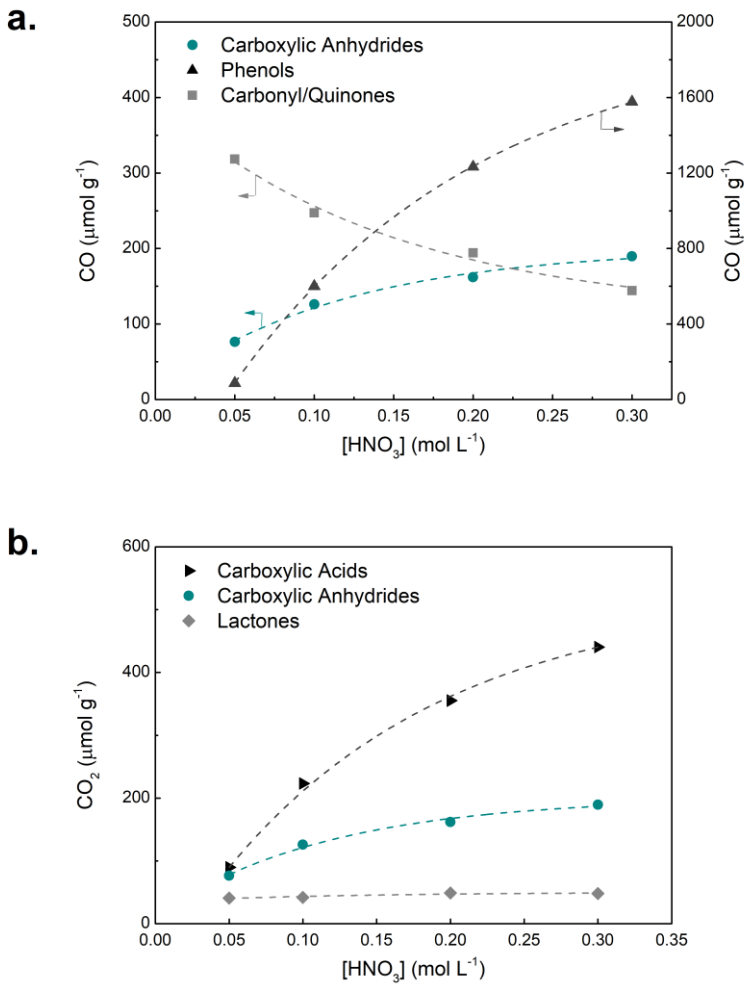

Figure II- 9. Evolution of the amount of specific oxygenated groups created at the surface of the hydrothermally treated CNTs with the HNO_3 concentration and released as CO (a) and CO_2 (b)[8].

[8] Adapted from Carbon 69 (2014) 311-326.

Comparing with the traditional oxidation with HNO_3 at boiling temperature, the hydrothermal functionalization of CNTs using a 0.3 M solution of HNO_3 at 200 °C can achieve similar degree of functionalization, with the amount of oxygen-containing surface groups being even higher when compared with the traditional refluxing with HNO_3. The corresponding amount of surface groups released as CO and CO_2 as well as O_2 (% wt.) are included in Table II- 4.

These results indicate that apart from being a controllable functionalization process that consumes a lower amount of oxidizing agent, hydrothermal oxidation competes well with the harsh boiling HNO_3 treatment in terms of the generation of sufficient quantities of oxygen functionalities on the CNT surface. Nevertheless, the CO_2 amount was relatively higher (by 13 %) in the CNTs oxidized under boiling acid compared to the hydrothermally treated ones (Table II- 4). Specifically, the amounts of carboxylic acids for the CNT-N-BT-7 sample treated by the boiling method (7.0 mol L^{-1}) and for the hydrothermally treated sample at the highest HNO_3 concentration (0.3 mol L^{-1}) reached 331 and 222 μmol g^{-1}, respectively, indicating that more acidic surface groups were produced on the CNT surface not only due to the aggressive oxidizing conditions of the boiling acid method but also because hydrothermal oxidation is performed at 200 °C, a temperature where a fraction of carboxylic acids can be partially released.

In any case, the HNO_3 hydrothermal oxidation methodology can be successfully applied to control the amount of oxygenated functionalities created on the surface of CNTs, by setting with precision the HNO_3 concentration at a given temperature. In addition, a larger amount of oxygen-surface groups was produced on the surface of multiwalled CNTs

than on the surface of single-walled CNTs [29], e.g. 25 % more groups were evolved as CO and 50 % more groups as CO_2, in comparison to single-walled CNTs under the same conditions (0.30 mol L^{-1} HNO_3 at 200 ^{o}C).

Regarding other methodologies to incorporate O-containing surface groups, oxidative treatments in the liquid-phase with H_2O_2 have also been reported, but the degree of functionalization is lower [26]. While treatments with HNO_3 originate materials with large amounts of surface acidic groups, mainly carboxylic acids and, to a smaller extent, lactones, anhydrides and phenol groups [19], H_2O_2 oxidation generates less acidic materials [42] (Table II- 5). Treatment using diluted oxygen (5 % O_2 in N_2 at 500 °C) introduces mainly basic, neutral and slightly acidic oxygenated groups on CNTs surface (mainly phenol and carbonyl/quinone groups). In this case, it should be taken into consideration that O_2 leads to a significant increase of the specific surface area, while the oxidation with H_2O_2 does not promote drastic changes of the textural properties of the CNTs [26]. In general, these functionalization approaches lead to a lower degree of O-incorporation as can be confirmed by the total amount of molecular oxygen released as CO and CO_2 presented in Table II- 5. Only the treatment of CNTs with oxygen plasma reported by Clément et al. [43] shows an oxygen concentration of 17.2 % evaluated by XPS.

Table II- 5. Chemical properties of functionalized commercial CNT samples from the same supplier (Nanocyl NC3100).

Sample	CO (μmol g^{-1})	CO_2 (μmol g^{-1})	O_2 (% wt.)	Ref.
CNT-H_2O_2	466	150	1.2	[26]
CNT-O_2 dil	1339	91	2.4	
CNT-O_2 plasma	---------- n.p. ----------		17.2[a]	[43]
CNT-N-HT-0.30	2015	680	5.4	This work
CNT-N-BT-7	1511	767	4.9	

n.p. – not performed; a) Concentration of atomic oxygen evaluated by XPS.

3.3. Partial Conclusions

The typical functionalization of carbon materials using HNO_3 in liquid-phase phase was performed to incorporate oxygenated surface groups in the surface of CNTs and CXs. The extent of oxidation depends on the concentration of the acid used, in addition to the ratio carbon material/oxidant. The treatment incorporates high amounts of O-containing groups: acidic oxygen groups include carboxylic acids, anhydrides, lactones and phenols, and carbonyls and quinones, as basic or neutral oxygen functional groups, which can be identified by deconvolution of the profiles of CO and CO_2 released during TPD analysis.

Selective removal of some groups introduced during HNO_3 oxidation by thermal treatments under inert atmosphere is an alternative way to obtain basic or neutral carbon materials. This approach has the advantage that the thermal treatments do not promote significant additional changes on the specific surface area of the CNTs.

Although liquid-phase functionalization is frequently performed using HNO_3 as reagent, it is a non-selective functionalization method. Furthermore, severe degradation effects, especially loss of material, tube shortening as well as the formation of structural defects, usually occur during boiling in HNO_3. The hydrothermal methodology can be an alternative to the chemical functionalization by refluxing with concentrated oxidants. The method is quite effective, and the amount of oxygenated-surface groups (carboxylic acids, carboxylic anhydrides, phenols, carbonyl/quinones and lactones) can be correlated with the HNO_3 concentration, with similar degrees of functionalization being achieved.

4. Nitrogen-containing surface groups

The presence of surface nitrogen groups is also extremely important for the catalytic applications of carbon materials and is attracting much interest [1, 22, 23, 25, 44-47]. Doping carbon materials with N was shown to improve the catalytic performance in oxidation reactions [48-51], and in oxygen reduction reactions (ORR) in proton-exchange fuel cells [52-54] as catalysts or as catalyst supports.

The electron rich nitrogen atoms provide additional electrons for the graphitic lattice, increasing surface basicity [44]. In the case of N-doped CNTs they can even give rise to metallic or semi-conductive features with a narrow energy gap [55]. Graphitic nitrogen also plays a determining role in decreasing the overall activation energy, therefore speeding up the activation of oxygen in oxidative dehydrogenation reactions [49]. The main advantage of using N-doped carbons when compared to traditional catalysts is that the nitrogen species are well anchored onto the catalyst structure and, consequently, the drawbacks related to active phase sintering are unlikely to occur even under severe reaction conditions, particularly in liquid-phase reactions [56].

The incorporation of nitrogen atoms onto the carbon structure is relatively easy due to the similar sizes of the nitrogen and carbon atoms [49, 57]. Doping of carbon materials with nitrogen can be achieved in-situ during synthesis or ex-situ using appropriate post-treatments [52], such as arc-discharge, laser ablation, chemical vapor deposition or thermal treatment [58]. Regarding post-treatments, the incorporation of nitrogen can be achieved either by treating the carbon materials with NH_3 gas/air

or using pyrolysis of nitrogen-containing carbon precursors, such as urea, melamine, polyacrylonitriles, polyvinylpyridine, and quinoline-containing pitch [44, 59-61]. Ex-situ functionalization of CNTs via aryl diazonium salt may present an alternative for the incorporation of pyridine- and pyrrole containing dangling groups on CNTs [62]. However, in some cases, the nature of the N-groups presents some limitations as stability at high temperatures or in acidic/alkaline media. In the case of N-doping, the nitrogen atoms are usually in three different sites of the carbon structure substituting the carbon atoms to form graphitic (quaternary), pyridinic and pyrrolic structures [23, 44, 60, 63] that present high thermal stability. The selection of the N-doping method is highly dependent on the availability of synthesis equipment, N sources and operation cost [60].

In this chapter, two methodologies are presented for doping nanocarbon materials (CNT and rGO samples) with nitrogen: hydrothermal treatment with urea (applied to CNTs) and a novel method involving ~~a~~ mechanical treatment under ball milling followed by thermal treatment (applied to CNTs and rGOs). The influence of N-doping on the carbon materials properties (texture, morphology, structure, surface chemistry) was investigated by several characterization techniques.

In addition to the post-treatments, N-doped CXs can be synthesised from resorcinol, formaldehyde and melamine or urea as nitrogen sources. This is an interesting material, since it offers the possibility of tuning their textural properties by adequate selection of the synthesis parameters [64], and can be easily doped with nitrogen by incorporation of a nitrogen precursor during the synthesis [63, 65]. Moreover, the synthesis does not involve contact with any transition metals, therefore carbon materials free from metal contamination and with different nitrogen contents can be

obtained in this way. Although this procedure was not developed in this thesis (and therefore will not be shown in this section), the reader will find its application in liquid-phase oxidation reaction in *Part IV*.

The results presented in this section have been already reported in the following papers:

Catalytic activity and stability of multiwalled carbon nanotubes in catalytic wet air oxidation of oxalic acid: The role of the basic nature induced by the surface chemistry, authored by Raquel P. Rocha, Juliana P.S. Sousa, Adrián M.T. Silva, Manuel F.R. Pereira and José L. Figueiredo, and published in the journal Applied Catalysis B: Environmental Volume 104 pages 330–336 (2011). Author Contributions: Raquel Rocha was responsible for the modification and characterization of carbon nanotube samples. Manuscript was written by R.P. Rocha with substantial supervision of all authors.

Easy method to prepare N-doped carbon nanotubes by ball milling, authored by O.S.G.P. Soares, R.P. Rocha, A.G. Gonçalves, J.L. Figueiredo, J.J.M. Órfão, M.F.R. Pereira, and published in the journal Carbon Volume 91 pages 114–121 (2015). Author Contributions: R.P. Rocha and O.S.G.P. Soares designed the surface chemistry of the ball milled carbon nanotube samples, kindly prepared by O.S.G.P. Soares and characterized by R.P. Rocha, helped by A.G. Gonçalves. Manuscript was written by O.S.G.P. Soares, R.P. Rocha and A.G. Gonçalves with substantial supervision of all authors.

Highly active N-doped carbon nanotubes prepared by an easy ball milling method for advanced oxidation processes, authored by O.S.G.P. Soares, R.P. Rocha, A.G. Gonçalves, J.L. Figueiredo, J.J.M. Órfão and M.F.R. Pereira, and published in the journal Applied Catalysis B: Environmental Volume 192 pages 296-303 (2016). Author Contributions: R.P. Rocha and O.S.G.P. Soares designed the surface chemistry of the ball milled carbon nanotube samples, kindly prepared by O.S.G.P. Soares and characterized by R.P. Rocha, helped by A.G. Gonçalves. Manuscript was written by O.S.G.P. Soares, R.P. Rocha and A.G. Gonçalves with substantial supervision of all authors.

Different methodologies for synthesis of nitrogen doped carbon nanotubes and their use in catalytic wet air oxidation, authored by Raquel P. Rocha, O. Salomé G.P. Soares, Alexandra G. Gonçalves, José J.M. Órfão, M. Fernando R. Pereira and José L. Figueiredo, and published in the journal Applied Catalysis A, General Volume 548 pages 62–70 (2017). Author Contributions: R.P. Rocha and O.S.G.P. Soares designed the surface chemistry of the ball milled carbon nanotube samples, kindly prepared by O.S.G.P. Soares. Samples characterization was kindly assisted by Alexandra G. Gonçalves. Manuscript was written by Raquel P. Rocha with contributions from O. Salomé G.P. Soares and Alexandra G. Gonçalves and with substantial supervision of all authors.

Nitrogen-doped graphene-based materials for advanced oxidation processes, authored by R.P. Rocha, A.G. Gonçalves, L.M. Pastrana-Martínez, B.C. Bordoni, O.S.G.P. Soares, J.J.M. Órfão, J.L. Faria, J.L.

Figueiredo, A.M.T. Silva and M.F.R. Pereira, and published in the journal Catalysis Today Volume 249 pages 192–198 (2015). Author Contributions: Raquel Rocha and B.C. Bordoni performed the characterization of N-doped graphene-based samples, kindly prepared by L.M. Pastrana-Martínez and O.S.G.P. Soares. Manuscript was written by R.P. Rocha with contributions and substantial supervision of all authors.

4.1. Hydrothermal Treatment

Several works report on the growth of N-CNT using chemical vapour deposition (CVD) approaches [47, 55, 66], showing that the incorporation of nitrogen in carbon nanotubes is strongly influenced by the synthesis conditions used (precursor, catalyst, reaction temperature and gas flow rate). Nxumalo et al. [60] showed that the effects of N concentration are more important than the nature of the N source in determining the morphology and the yields of the synthesized N-CNT. High temperature synthesis methods such as arc-discharge and laser ablation have also been reported to dope CNTs [66]. However, due to the easy availability of undoped commercial CNTs, post-treatment methods for the incorporation of N-functionalities have been explored [67]. N-doping of activated carbons was reported a long time ago by Rideal and Wright [68] involving the impregnation with an urea solution, followed by heating under an inert gas to high temperatures. More recently, urea has been used with good success by other authors [69, 70]. Here, a similar methodology is proposed using urea as N-precursor for the N-doping of CNTs. The procedure involves a hydrothermal treatment of CNTs with urea solution followed by a thermal treatment under inert gas.

4.1.1.Methodology

Hydrothermal treatment was conducted at high temperature and pressure over CNTs using urea as nitrogen precursor. In order to increase the yield of nitrogen-containing groups on the surface [71], the pristine CNTs were first treated with concentrated HNO_3 at boiling temperature during 3 h (ratio of 4 g of carbon material to 300 mL of acid). Then, the oxidized material was washed several times with distilled water until the neutral pH was reached. The recovered solid was dried at 110 °C for 24 h in an oven (sample CNT-N). The treatment with urea was carried out in a 160 mL 316-stainless steel high pressure batch reactor (Parr Instruments, USA Mod. 4564. 2 g of the CNTs oxidized with HNO_3 (CNT-N) were added to 70 mL of urea solution (1 M), and stirred at 200 °C during 2 h under N_2 atmosphere. The material was washed several times and dried in the oven (sample CNT-NU). Then, a gas-phase thermal treatment was applied to this sample: 1 g of CNT-NU was heated at 10 °C min^{-1} until 600 °C under a N_2 flow of 100 cm^3 min^{-1} and kept at 600 °C during 60 min (sample CNT-NUT). Figure II- 10 illustrates the methodology adopted for the modification of carbon nanotubes with nitrogen surface groups following the hydrothermal approach.

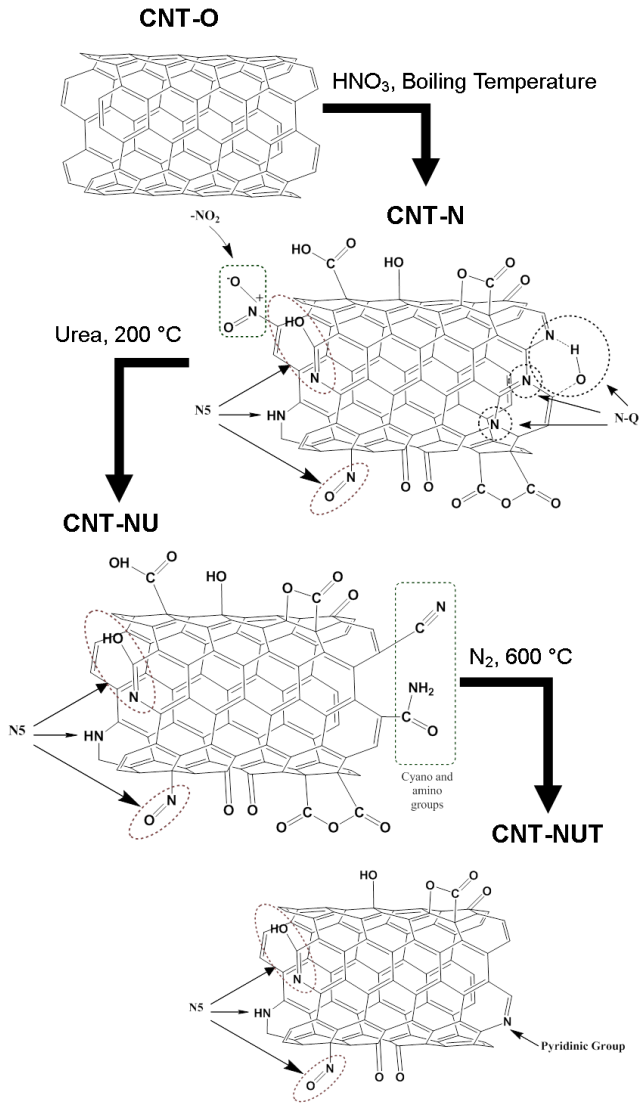

Figure II- 10. Hydrothermal route for incorporation of N-functionalities on CNTs[9].

[9] Reprint from Applied Catalysis B: Environmental 104 (2011) 330–336, with permission from Elsevier.

4.1.2.Induced Properties

The different chemical and thermal treatments (HNO_3 at boiling temperature, liquid-phase urea treatment at 200 °C, and gas-phase thermal treatment with N_2 at 600 °C) were applied to carbon nanotubes to introduce N-functionalities. During each step of the synthesis, textural and chemical properties of the samples were determined by several techniques including N_2 adsorption-desorption isotherms, TPD, pH_{PZC}, EA and XPS.

Regarding the textural characterization, Table II- 6 shows the BET surface areas (S_{BET}) determined from the N_2 adsorption isotherms of CNT samples (Appendix, Figure A. 1). The differences between these surface areas are lower than 100 $m^2\ g^{-1}$, and they could occur by changes in the nanotubes length and perfection as a result of the applied treatments [34] or by opening the tips of the tubes [35]. In particular, the S_{BET} increase from CNT-O to CNT-N can be due to the opening of the tips of some tubes, while the subsequent S_{BET} increase observed after thermal treatment at 600 °C (CNT-NUT) may be related to the removal of oxygen-containing groups from the surface of the carbon nanotubes, thereby increasing the accessible carbon surface area for N_2 adsorption.

The N_2 adsorption isotherms are very similar for all materials (type II according to IUPAC). Therefore, the controlled liquid- and gas-phase treatments applied do not significantly affect the textural properties of CNTs. In addition to the opening of the end caps of some tubes previously mentioned for CNT-N, some differences were detected between the pore volumes determined from the N_2 uptakes at p/p_0 = 0.99 for CNT-O (2.90 $cm^3\ g^{-1}$) and all other samples, respectively 1.49, 1.51 and

1.65 $cm^3\ g^{-1}$ for CNT-N, CNT-NU and CNT-NUT (Table II- 6). Considering that most of the pore volume results from the free space in the CNT bundles, the significantly lower pore volume found for CNT-N when compared with CNT-O can be due to the introduction of oxygen surface groups by the HNO_3 treatment and may indicate a better alignment of the tubes, which are known effects of HNO_3 on multiwalled CNTs [33].

Table II- 6. Evolution of textural and chemical characterization of CNT samples during the hydrothermal treatment steps.

Sample	S_{BET}	V_p	CO	CO_2	pH_{PZC}
	($m^2\ g^{-1}$)	($cm^3\ g^{-1}$)	($\mu mol\ g^{-1}$)	($\mu mol\ g^{-1}$)	(unitless)
CNT-O	302	2.90	200	26	6.8
CNT-N	351	1.49	1710	909	2.8
CNT-NU	351	1.51	1172	607	5.4
CNT-NUT	386	1.65	703	76	7.3

According to the respective pH_{PZC} shown in Table II- 6, the HNO_3 treatment (CNT-N) acidifies the original material (pH_{PZC} decreases from 6.8 to 2.8), the urea treatment (CNT-NU) reduces the acidic character of the sample (pH_{PZC} increases from 2.8 to 5.4), while CNT-NUT is the most basic sample (pH_{PZC} = 7.3). The total amounts of CO and CO_2 released for each sample are presented in Table II- 6. A negligible amount of oxygen-containing surface groups was found on the original material (CNT-O), while the highest amount of these groups was recorded for CNT-N, in agreement with elemental analysis (Table II- 7).

Table II- 7 shows the evolution of the CNTs bulk and surface composition obtained by elemental (C, N, H and O contents) and XPS

analyses, respectively, during the hydrothermal treatment steps. A slight increase of the H and N contents is observed after the treatment with HNO_3 (CNT-N), possibly due to the incorporation of acid and nitrogen groups during the treatment. As expected, a very large increase of the oxygen content was observed due to the formation of oxygen-containing functional groups in the CNTs surface. The liquid phase treatment with urea (CNT-NU) originates an additional increase in the nitrogen content and a decrease of the oxygen content, suggesting the loss of some carboxylic acid groups by the incorporation of nitrogen functional groups on the carbon material, as shown in Table II- 7.

Table II- 7. Evolution of carbon nanotubes bulk and surface composition of CNT samples, determined by elemental and XPS analyses, respectively, during the hydrothermal treatment steps.

Sample	Elemental Analysis				XPS		
	C	H	N	O*	C	N	O
	(% wt.)	(% wt.)	(% wt.)	(% wt.)	(% wt.)	(% wt.)	(% wt.)
CNT-O	98.99	0.10	0.15	0.76	98.62	0.08	1.30
CNT-N	92.38	0.16	0.30	7.16	92.14	0.17	7.69
CNT-NU	93.22	0.07	1.12	5.59	93.35	1.40	5.25
CNT-NUT	95.77	0.13	0.91	3.19	95.78	0.69	3.53

* Oxygen determined by difference.

The N1s spectra of CNT-N, CNT-NU and CNT-NUT samples (Figure II-11) were decomposed based on previous literature [51, 63], in order to establish the nature of the N bonding. A common peak at 400.0–400.2 eV was identified in all samples, corresponding to nitrogen atoms bound to carbon as pyrrolic-N groups (N5). Other peaks were also generated

depending on the applied treatment. For the CNT-N sample, a quaternary nitrogen bond (NQ) at 401.8 eV as well as a N–O species (0.08 %) at a higher binding energy (406.0 eV) were identified. Regarding the CNT-NU sample, cyano and amino groups were detected at 399.1 eV. Pyridinic-N groups (N6) were observed at 398.7 eV for CNT-NUT. These results from XPS analysis were taken as reference for the representation of nitrogen-containing groups in Figure II- 11. Nitrogen groups are poorly detected (less than 0.1 %) in the original carbon nanotubes (Table II- 7) and, thus, these groups were not represented for CNT-O. The HNO_3 treatment introduces a small amount of nitrogen-containing groups on the surface of the carbon material, N–Q (0.06 %), –NO_2 groups (0.08 %) and N5 (0.03 %). The treatment carried out with urea induces the formation of cyano or amino groups (representing 0.88 %), an increase of N5 groups (0.52 %) and the disappearance of the –NO_2 and N–Q groups. Since cyano and amine groups are thermally decomposed, the final thermal treatment eliminates these species, suggesting that some N5 groups are converted to N6 groups (0.36 %) [59, 63].

The CO (Figure II- 12.a) and CO_2 TPD profiles (Figure II- 12.b) indicate that carboxylic acids and phenol groups, as well as some anhydrides, lactones and carbonyl-quinones, are incorporated on the surface of the original CNTs upon HNO_3 treatment (CNT-N), and successively removed by the additional treatments (CNT-NU and CNT-NUT), specially the carboxylic acid groups [19, 20, 23]. In fact, most of the carboxylic acid groups created by the HNO_3 treatment (evolved as CO_2 at 100–450 °C) disappear with the urea treatment (CNT-NU). Because the amount of CO_2 released from CNT-N at 100–450 °C is higher than that evolved from CNT-NU (Figure II- 12.b), one can infer that nitrogen-containing groups were created by the urea

treatment on the CNTs surface, decreasing the amount of carboxylic acid groups, as also indicated by the increase of N content in Table II- 7, from 0.30 to 1.12 % wt. A fraction of the carboxylic acids can also disappear just by the effect of the temperature used in the urea treatment, but only those which evolve as CO_2 below 200 °C in Figure II- 12.b. Since the CNT-NUT sample was treated at 600 °C, its basic nature can be explained by the removal of most of the acidic groups (carboxylic acids, some anhydrides and phenols) while the neutral and basic groups (carbonyl groups evolved as CO at temperatures higher than 600 °C) still remain on the carbon surface after the thermal treatment. Therefore, the pH_{PZC} increases with the sequential treatments not only due to the influence of nitrogen groups but also due to the decrease of the oxygenated acidic groups detected by TPD.

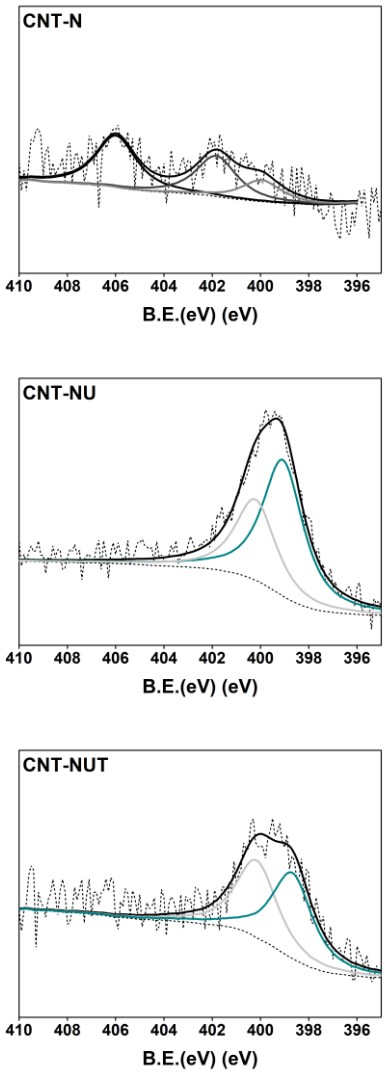

Figure II- 11. N1s spectra for CNT samples during the hydrothermal treatment steps[10].

[10] Adapted from Applied Catalysis B: Environmental 104 (2011) 330–336.

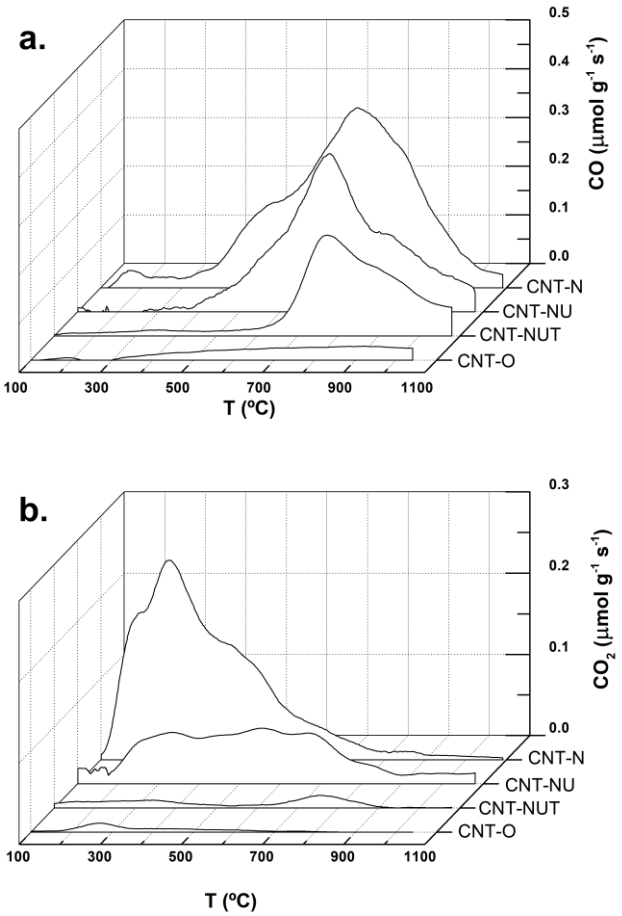

Figure II- 12. CO (a) and CO_2 (b) evolutions in TPD profiles of pristine (CNT-O) and modified CNTs, using consecutive treatments with nitric acid (CNT-N), urea (CNT-NU) and a gas-phase thermal treatment (CNT-NUT)[11].

[11] Adapted from Applied Catalysis B: Environmental 104 (2011) 330–336.

In conclusion, the hydrothermal route allows the incorporation of N-functionalities on carbon nanotubes. The controlled chemical and thermal treatments have little influence on the textural properties of CNTs, which are known as very stable materials. On the contrary, regarding the chemical properties, the pH_{PZC} of the materials decreases upon the HNO_3 treatment and increases after the urea or gas-phase thermal treatments. The CNTs modified with HNO_3, urea and gas-phase thermal treatments present pyridinic and pyrrole nitrogen surface groups and show the highest basic character, being suitable for applications where basic sites are required.

4.2. Mechanical and Thermal Treatments

The hydrothermal treatment presented previously allows the incorporation of N-functionalities onto the carbon surface. However, the procedure involves a complex multistep process, expensive specific equipment (high pressure reactor) is required, as well as severe operating conditions. One-step techniques have been developed in order to synthesize N-doped carbons, such as that reported by Chen et al. using radio frequency magnetron sputtering at relatively low temperatures [72]. In any case, expensive specific equipment is still required. Some of these disadvantages can be overcome by novel strategies. Ball milling has attracted much attention as a promising method for modifying CNTs, namely to adjust their lengths and to open the closed ends [73-75], increasing their specific surface areas [75], or to insert lithium [76]. By ball milling, CNTs can be transformed into curved nanotubes [77], nanoparticles [78], short and open-tipped nanotubes [75], but also in amorphous as well as disrupted tubular structures when prolonged ball milling is applied [73, 79].

This section presents a novel method to obtain carbon materials doped with nitrogen by combining a mechanical ball milling step with a thermal treatment. This approach for N-doping of carbon materials was extensively studied using CNTs, evaluating different ball milling parameters, N-precursors and operating conditions. Later, the same methodology was applied to prepare N-doped rGO materials. Therefore, all procedures explored using CNTs will be presented first, followed by the work done with rGOs.

4.2.1.N-doping of Carbon Nanotubes

4.2.1.1. Methodology

All milled samples were prepared in grinding jars using zirconium oxide balls in a Retsch MM200 equipment without any gas flow. A constant vibration frequency of 15 vibrations/s during 4 h was applied for all ball milled materials. Milling conditions were selected according to the optimization reported by Soares et al. in a previous work [80].

Due to the high number of CNT samples prepared, the presentation will be divided according to the ball milling parameter in study: wet, dry or external N-doping methodology; effect of N-precursor and C/N-precursor ratio; effect of thermal treatment; and effect of the O-surface groups. Commercial CNTs (CNT-O) from Nanocyl 3100 were used as the starting material in all prepared samples. An undoped sample (CNT-BM) was prepared under ball milling using 0.6 g of CNT-O.

Wet, dry or external N-doping methodologies

For the preparation of the N-doped samples, 0.6 g of CNT-O was mixed with 0.26 g of N using melamine or urea as nitrogen precursors, and the mixture was ball milled during 4 h at a constant vibration frequency of 15 vibrations/s. Then, the resulting materials were subjected to a thermal treatment under N_2 flow until 600 ºC (at 10 ℃ min^{-1}) and kept at this temperature during 1 h. The following identification of the samples was used: CNT-BM-X-Y, where BM means ball milled, X is the type of nitrogen precursor used, M for melamine and U for urea, Y is the type of functionalization, DT is the dry treatment (without solvent), WT is the wet

treatment (with solvent) and E means external treatment, i.e., the N-precursor was mixed with CNT-BM outside the ball milling equipment. In the wet treatment, the CNT-O and the N-precursor were mixed in the ball mill in the presence of 3 mL of water or ethanol in the case of urea or melamine, respectively. When the external treatment was applied, 0.6 g of CNT-BM was dipped into an aqueous solution with 0.26 g of N using urea or melamine as nitrogen precursor and water or ethanol as solvent, respectively, and the mixture was stirred for 24 h. Then, the samples were filtered, dried and subjected to the thermal treatment under N_2 flow at 600 ^{o}C for 1 h.

This group evaluates the effect of the solvent in the melamine and urea prepared samples during the ball milling step as well the effect of performing the N-doping outside the ball mill apparatus.

Effect of N-precursor and C/N-precursor ratio

Melamine, urea and NH_3 were selected as N-precursors. In the case of melamine and urea, 0.6 g of pristine CNTs were ball milled with a defined amount of N-precursor. Then, the resulting materials were subjected to a thermal treatment under N_2 flow (100 cm^3 min^{-1}) until 600 °C and kept at this temperature during 1 h. Three CNTs/N-precursor ratios were tested, using 0.2, 0.4 and 0.6 g of melamine, or 0.3, 0.5 and 0.8 g of urea. Samples were labelled according to the precursor employed (M for melamine, U for urea), followed by the N-precursor mass in grams (e.g.: CNT-BM-M0.4). In the case of NH_3, ball milled CNTs (CNT-BM) were thermally treated under gaseous NH_3 until 600 ^{o}C using 100 cm^3 min^{-1} of pure NH_3 (sample CNT-

BM-NH_3) or 100 cm^3 min^{-1} of NH_3 diluted with N_2 (50/50) (v/v) (sample CNT-BM-NH_3-N_2).

With this group of samples, the ratio between the carbon material and the amount of N-precursor is evaluated and compared with gas thermal treatment using NH_3 as N-source.

Effect of the thermal treatment

Regarding the study of the effect of the thermal treatment, 0.6 g of the commercial CNTs were ball milled with melamine (0.4 g) using the same milling conditions (4 h, 15 vibrations/s), and subjected to a thermal treatment under N_2 flow (100 cm^3 min^{-1}) until 200, 400, 600 and 900 °C and kept at this temperature during 1 h (samples CNT-BM-M200, CNT-BM-M400, CNT-BM-M600 and CNT-BM-M900, respectively).

Effect of the O-surface groups

To study the effect of the presence of oxygen surface groups, the commercial CNTs were subjected to a HNO_3 oxidation treatment at boiling temperature in order to incorporate O-containing groups. 4 g of CNTs were treated with 300 mL of a 7 mol L^{-1} HNO_3 solution at boiling temperature for 3 h. Then, the oxidized material was washed several times with distilled water until the neutral pH was reached. The recovered solid was dried at 110 °C for 24 h in an oven. In order to remove selectively the O-groups, the samples were then thermally treated under inert atmosphere (100 cm^3 min^{-1} of N_2) at 10 °C min^{-1} until different final temperatures (200, 400, 600 and 900 ºC), where they were kept during 1 h (samples CNT-N200, CNT-N400, CNT-N600, CNT-N900). Then, the obtained samples were ball

milled with melamine (0.4 g) during 4 h at 15 vibrations/s, and finally thermally treated under N_2 flow (100 cm^3 min^{-1}) until 600 °C and kept at this temperature during 1 h. Samples were denominated according to the temperature used to selectively remove the O-containing groups, ie, CNT-N200-BM-M, CNT-N400-BM-M, CNT-N600-BM-M and CNT-N900-BM-M.

4.2.1.2. Induced Properties

Wet, dry or external N-doping methodologies

Textural properties of the ball milled CNT samples were evaluated by the corresponding N_2 adsorption-desorption isotherms performed at -196 ^oC, in order to assess the modifications promoted by the different mechanical and thermal treatments. Table II- 8 presents the specific surface area, S_{BET}. Differences between the S_{BET} values are lower than 100 m^2 g^{-1}; however, they suggest that during the treatments some changes in the nanotubes structure could occur, leading to the increase/decrease of the accessible surface area for N_2 adsorption. After ball milling, the S_{BET} of the original CNTs (in the absence of melamine or urea) increased from 291 to 391 m^2 g^{-1}. The mechanical treatment markedly reduced the entanglement of the CNTs [80], also leading to shorter CNTs by breaking up the tubes [81, 82], without affecting the tube diameters. The addition of the nitrogen precursors during the dry ball milling treatment (CNT-BM-M-DT and CNT-BM-U-DT samples) leads to a small increase of the surface area comparing to the original sample, but produces samples with lower S_{BET} than the ball milled carbon nanotubes (CNT-BM). Considering that most of the surface area results from the

geometrical area of the CNTs, the presence of surface groups may play an attractive effect between the tubes, leading to higher agglomeration of the material. The addition of the solvent (ethanol/water) during the ball milling treatment (wet treatment - WT) practically does not change the specific surface area of CNTs (CNT-BM-M-WT and CNT-BM-U-WT samples) when compared to the original CNT sample. Materials functionalized after ball milling (CNT-BM-M-E and CNT-BM-U-E samples) present specific surface areas similar to those obtained with the samples submitted to the dry treatment.

Table II- 8. Chemical and textural characterization of pristine and ball milled CNT samples prepared by wet, dry or external methodologies.

Sample	S_{BET}	V_p	CO	CO_2	pH_{PZC}
	($m^2\ g^{-1}$)	($cm^3\ g^{-1}$)	($\mu mol\ g^{-1}$)	($\mu mol\ g^{-1}$)	(unitless)
CNT-O	291	1.1	200	23	6.8
CNT-BM	391	0.67	173	44	6.6
CNT-BM-M-DT	355	0.87	338	214	6.4
CNT-BM-M-WT	285	0.90	352	144	n.p.
CNT-BM-U-DT	353	0.70	273	112	6.5
CNT-BM-U-WT	291	1.1	405	205	n.p.
CNT-BM-M-E	349	0.76	394	223	6.8
CNT-BM-U-E	364	0.70	347	317	6.8

n.d. – not performed.

The N_2 adsorption isotherms at low relative pressure are very similar, in agreement with the small differences in the surface areas of the ball milled samples; however, some differences were observed in the amount of N_2 adsorbed at higher relative pressures, as well as in the desorption

branches (Appendix, Figure A. 2). N_2 adsorption isotherms of CNT-O, CNT-BM-M-WT and CNT-BM-U-WT samples are typically type II, accordingly to IUPAC classification [32], which are characteristic of non-porous materials and represent unrestricted monolayer-multilayer adsorption [83]. In contrast, the remaining samples presented isotherms closer to type IV. They are characteristic of carbons with some mesoporosity. On the other hand, the adsorption and desorption branches are not coincident (hysteresis loop is observed). The broadening of the hysteresis may be due to two contributions in the mesoporous character: the entanglement of nanotubes and the access to the inner cavity [83]. The NLDFT results (Appendix, Figure A. 3) corroborate the previous observations. The wet ball milling treatment (WT) practically does not change the pore size distribution compared to the commercial sample (CNT-O), suggesting that this treatment has no relevant influence in the textural properties of CNTs, i.e. the presence of solvent does not allow the breaking of the carbon nanotubes. Furthermore, the isotherm type of these samples (CNT-BM-U-WT and CNT-BM-M-WT) also does not change (type II); only a small decrease in the adsorption volume at high pressures is noticeable (Appendix, Figure A. 3), mainly in the case of the sample treated with melamine (CNT-BM-M-WT). For the remaining ball milled samples, the number of larger pores (radius higher than 100 Å) is low. However, two significant contributions are observed in the pore size distribution for pore radii in the range of 13 - 28 Å and 35 - 60 Å, which may be explained by the opening of the CNT tips during ball milling, which does not occur in the wet treated samples. Concerning samples submitted to dry or external treatments (DT or E, respectively), a decrease in the number of pores with

radii between 15 and 18 Å is observed, when compared with the ball milled CNTs (CNT-BM).

The mechanical treatment by itself does not promote any functionalization of the carbon nanotube surfaces, as already reported in a previous work [80]. Therefore, the amounts of CO and CO_2 released by TPD (Appendix, Figure A. 4) for the original and the ball milled samples are quite similar (samples CNT-O and CNT-BM). Even the incorporation of O-containing groups that are released as CO_2 was not achieved with the addition of the nitrogen precursor during the mechanical treatment. Actually, the amount of CO released was always significantly higher than that of CO_2, as can be seen in Table II- 8. Accordingly, the largest difference in the N-doped samples was observed for the surface groups decomposed as CO, where a slight increase was observed, especially at temperatures higher than 600 °C. The presence of groups released as CO is related to the thermal treatment applied; i.e. carbonyl/quinone groups were not removed from the surface since they are stable at temperatures above 600 ^{o}C [19]. However, the thermal treatments should have removed the carboxylic acid and anhydride groups, since they are released at temperatures below 600 ^{o}C. Phenols and lactones were partially removed since they are decomposed in the range of 500 to 700 ^{o}C. In general, the TPD results suggest that the prepared ball milled samples are poor in O-containing surface groups. Furthermore, the samples present a neutral character, with pH_{PZC} values around 7 (Table II- 8).

On the other hand, treatments with N precursors result in the incorporation of a significant amount of nitrogen (between 0.2 and 4.8 %) on the surface of the CNTs, as determined by XPS analysis (Table II- 9). The N-doped samples prepared with melamine present higher N content than

the urea treated samples, showing that the use of melamine as N-source allows the incorporation of more N-functionalities. The use of solvent during ball milling revealed a negative effect on the attachment of the N–functionalities, regardless of the precursor used. The dissolution of the nitrogen precursors in the solvents (ethanol or water for melamine and urea, respectively) may restrict contact between the precursor and the carbon material leading to lower final N contents. Furthermore, since this step is performed inside the ball mill, the result is a paste-like material without a homogeneous appearance, suggesting also that the presence of solvent can prevent the breaking of the CNTs. The external treatments allow incorporating a large amount of N-groups, but only in the case of melamine.

The same evidences and tendencies were also observed in the N content determined by elemental analysis (Table II- 9). Regarding the O content determined by XPS (results not shown), samples treated with urea present higher values, probably due to the interaction of the O present in the precursor and the carbon surface; this does not occur in the case of melamine, which does not contain any oxygen.

In addition to the total N content, XPS can provide information on the nature of the N-functionalities. The peak positions of each element were corrected by using that of C1s (285.0 eV). For a better interpretation of the N1s spectra of the prepared samples and the differences obtained with the thermal treatments, samples CNT-BM-M-DT and CNT-BM-U-DT without thermal treatment were also analysed by XPS. The N1s deconvolution spectra were obtained by comparison with the spectra of the corresponding model compounds (melamine or urea). In these two

cases, the N-precursor is physically mixed with the CNT and therefore, it is acceptable that N1s spectra should correspond to the model compounds. The N1s spectrum of the CNT-BM-M-DT sample without thermal treatment (Figure II-13) shows a symmetric peak with a π-excitation between 404 - 406 eV [84]. Deconvolution of the spectrum was based on the N-C bonds present in melamine (C=N-C and C-NH_2), to which correspond two distinct peaks at 399.1 and 400.0 eV, respectively. Since in melamine the N atoms have two chemical states C-NH_2 and C=N-C with a ratio of 1:1, deconvolution was carried out assuming an intensity ratio between the first and the second peak of 1:1 [84]. The N1s spectrum of the sample treated with urea and not submitted to the thermal treatment (CNT-BM-U-DT without TT600) (Figure II-13) was also compared with the reported N1s XPS urea spectrum [85]. A single peak was found, corresponding to the C-NH_2 bond. Furthermore, the urea treated sample revealed a clear C-O interaction in the C1s XPS peak (not shown), which is not noticeable in the melamine sample. After the thermal treatments at 600 °C, the shape and the peaks identified on the N1s spectra drastically changed (Figure II-13). The N1s spectra are asymmetric and suggest overlapping of the peaks. Some hypotheses were taken into account for curve-fitting: treatment of carbonaceous surfaces with N-containing precursors at low temperatures (below 550 °C) leads to the formation of lactams, imides, and amines; on the other hand, treatment at high temperatures results in an increase of quaternary nitrogen (N atoms incorporated in the graphitic layer in substitution of C atoms), pyridinic, and pyrrole-type structures [44]. Since the samples were all thermally treated at 600 °C, the deconvolutions were based in three peaks assuming the presence of quaternary nitrogen (NQ), pyrrole (N5) and pyridinic (N6)

structures. The corresponding binding energies and percentages of the N-functionalities are presented in Table II- 9.

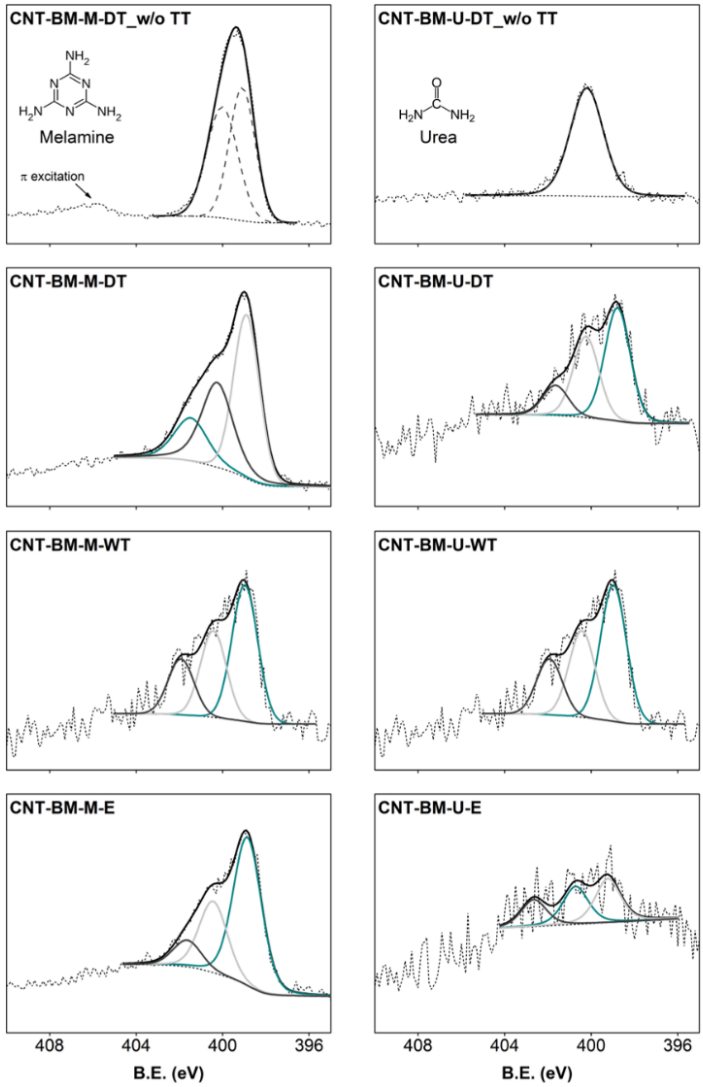

Figure II- 13. N1s XPS spectra recorded from ball milled CNT samples prepared by wet, dry or external methodologies and corresponding fittings[12].

[12] Adapted from Carbon 91 (2015) 114-121.

Table II- 9. N contents determined by XPS and Elemental Analysis (EA) and relative peak contents and positions obtained by N1s spectra fitting of the ball milled CNT samples prepared by wet, dry or external methodologies.

Sample	N content		N_{XPS} deconvolution					
	XPS	EA	N6		N5		NQ	
	(% wt.)	(% wt.)	B.E. (eV)	(% wt.)	B.E. (eV)	(% wt.)	B.E. (eV)	(% wt.)
CNT-BM-M-DT-without TT600	9.6	n.p.	---	---	---	---	---	---
CNT-BM-U-DT-without TT600	1.6	n.p.	---	---	---	---	---	---
CNT-BM-M-DT	4.8	7.6	398.9	2.24	400.3	1.66	401.5	0.87
CNT-BM-U-DT	0.8	0.6	398.8	0.39	400.2	0.28	401.7	0.10
CNT-BM-M-WT	1.1	0.9	399.0	0.56	400.4	0.35	401.9	0.23
CNT-BM-U-WT	0.3	0.2	398.8	0.11	400.1	0.10	401.3	0.07
CNT-BM-M-E	3.1	2.7	398.9	1.86	400.4	0.89	401.6	0.33
CNT-BM-U-E	0.2	0.2	399.2	0.07	400.7	0.06	402.7	0.04

n.d. – not performed.

Regardless of the N-precursor used, the pyridinic group (N6, B.E. = 399.0 ± 0.2 eV) is the most abundant species in all samples, representing between 40 a 60 % of the total N content, followed by the pyrrole group (N5, B.E. = 400.4 ± 0.3 eV) with a relative percentage around 30 %. The NQ groups were also present in all samples, but in lower amount (between 10 and 25 %). The presence of the three types of N-functionalities and the proportion of the groups are in agreement with those commonly accepted in the literature. The final temperature of the thermal treatment (600 °C) is high enough to prevent the presence of lactams, imides, and amines, but sufficiently moderate for some N5 groups to be converted into N6 and to increase the NQ nitrogen content [44]. The identified nitrogen species (NQ, N5 and N6) are, generally, thermally stable on carbons.

Considerations on the N-doping method

The innovative procedure developed in the present work consists in the simple mixing of the carbon material and the N-precursor by ball milling, followed by a thermal treatment. During the last step, the decomposition of the finely mixed N-precursor with the CNT leads to a rich N-doped CNT sample. In spite of the thorough characterization performed, the mechanism of N-incorporation was not well understood. Therefore, additional TGA analyses were performed in order to clarify the functionalization path.

In Figure II- 14.a the TGA profiles of the ball milled CNT (CNT-BM) and of the N-doped samples (using melamine as N precursor by the dry treatment) with and without the thermal treatment under nitrogen at

600 ^{o}C are shown. A significant weight loss (34 %) is observed for the sample CNT-BM-M-DT without thermal treatment in the temperature range of 250 to 350 °C, followed by a minor degradation until 900 °C (7 % of weight loss). The thermal decomposition of pure melamine under inert atmosphere is accomplished in two degradation steps [86]: the generation of nitrogen-containing volatile side groups in a first stage (between 315 and 381 °C) and the decomposition of main chain and nitrogen volatiles from the first stage (in the temperature range of 416 to 748 °C). The presence of these two decomposition stages is clearly observed in the thermogram of the thermally untreated sample, revealing the presence of melamine mixed with carbon nanotubes. In fact, the total weight loss (41 %) observed at the final temperature of the TGA (900 °C) is close to the amount of melamine added to the CNTs (39 %) in the ball milling equipment. However, in the CNT-BM-M sample without thermal treatment melamine decomposition temperatures are shifted to lower temperatures (the first significant weight loss is observed between 250 and 350 ^{o}C, instead of 315 and 381 ^{o}C [86], when using the same heating ramp of 10 ^{o}C min^{-1}), suggesting that the presence of CNTs may accelerate the melamine decomposition process.

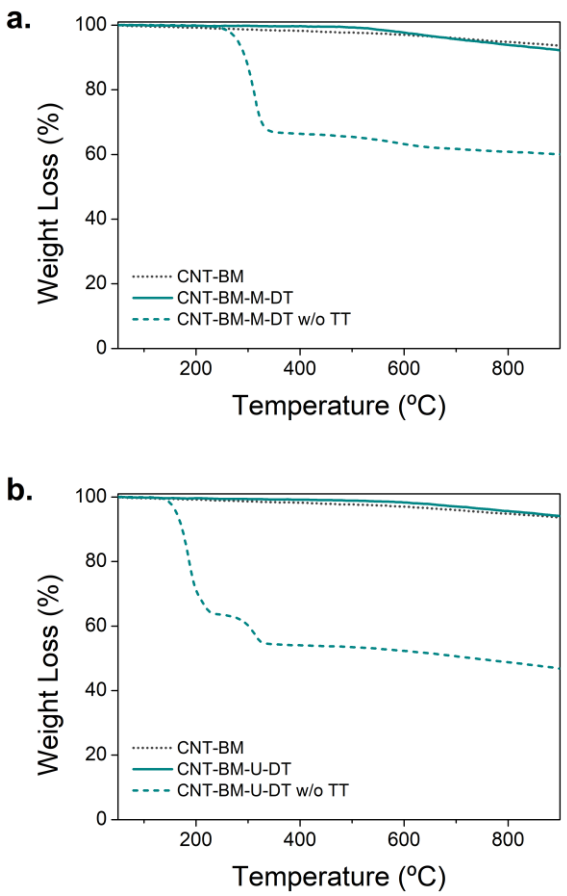

Figure II- 14. TGA profiles of undoped CNTs and N-doped CNTs by the dry treatment with and without thermal treatment using (a) melamine and (b) urea as N-precursors[13].

[13] Adapted from Carbon 91 (2015) 114-121.

In contrast, the thermogram of the thermally treated CNT-BM-M-DT sample revealed a weight loss lower than 1 % below 500 °C and 8 % between 500 and 900 °C. Since the first step of the melamine decomposition had already occurred during the thermal treatment of the sample, this slight weight loss can be due to the decomposition of the main chain and nitrogen volatiles (resulting from the first step of melamine decomposition) or to the release of the remaining oxygen-containing groups present on the CNT surface, which were not released during the thermal treatment. This last hypothesis is well corroborated by the TGA profile of the CNT-BM sample where a slight weight loss is also observed at high temperatures (7 % in total). In this case, the mass decay is only related to the release of oxygen functionalities since no nitrogen compounds are present. As previously discussed, the ball milled CNT samples presented small amounts of oxygen-containing surface groups that are also released during TGA, contributing to the weight loss observed. Regarding the TGA profiles of the other melamine treated CNT samples, the first decomposition step of melamine was also not observed in any of the thermally treated samples and only a slight weight loss (lower than 6 %) at the end of the TGA was obtained for the samples prepared by ball milling or by external treatment with solvent (ethanol) (CNT-BM-M-WT and CNT-BM-M-E).

Concerning the samples treated with urea (Figure II- 14.b), the TGA profile of the sample CNT-BM-U-DT without thermal treatment revealed a significant weight loss below 500 °C, whereas the TGA profile of the sample after the thermal treatment only shows a slight weight loss at high temperatures (about 3 %). Thermal decomposition of neat urea is characterized by a continuous weight loss between 133 °C (melting point)

and 500 °C. About 50 % of urea decomposes into gaseous products (CO_2, NH_3, HNCO and H_2O) until 270 °C, with predominance of NH_3 formation at around 200 °C, whereas the other 50 % remain as solid products. At 500 °C, almost complete thermolysis is achieved, remaining 5 % of the initial mass that can be decomposed until 750 °C [87]. The presence of the solid products (white or yellow) was observed during the thermal treatments at the outlet of the oven reactor. However, in the recovered material there is no evidence of those solids, which suggests that all had been decomposed. N-doping of CNTs by the wet treatments during ball milling or by the external treatments (using as solvent ethanol in the case of melamine and water in the case of urea) did not reveal differences in the TGA profiles Nevertheless, a smaller weight loss is obtained when comparing with the dry treated samples. In any case, those small differences observed at the end of the TGA profiles of different samples can be neglected, taking into consideration the instrumental error. The TGA profiles of the N-precursor/CNT mixtures with and without thermal treatment suggest that the products from the thermal decomposition of the N-precursor are responsible for the incorporation of the N-functionalities onto the carbon surface.

The introduction of high N contents, especially in the case of melamine, may be related to the close contact between the precursor and the CNT due to the previous mechanical mixture performed by ball milling. In contrast to traditional methods, the described procedure is an easy-to-handle option to produce N-doped CNTs.

The procedure developed also allows doping of commercial CNTs without significant loss of the carbon material, i.e., starting the procedure with 0.6 g of pristine CNTs it is possible to produce around 0.6 g of CNT-

BM-M-DT, in the case of the melamine doping dry treatment. Therefore, a yield of almost 100 %, regarding the carbon material, can be obtained by using this method. Other functionalization methods, using liquid or gas-phase reactions at high temperatures, normally induce a significant loss of carbon material, either during the multiple transfer processes, like washing and filtration steps, or even by the deterioration of the carbon material by the oxidizing agents used or the drastic operating conditions applied. In the developed method, no severe operating conditions are used; even the thermal treatment performed at 600 °C under inert gas does not damage the carbon material.

Effect of N-precursor and C/N-precursor ratio

Melamine, urea and NH_3 were used as N-precursors in a solvent-free post-doping method to incorporate N-groups onto the CNTs surface. The first step involves a mechanical treatment under ball milling promoting the breaking of the tubes and the intimate mixture of the N-precursor with the CNTs. There is no chemical functionalization during this first step, as previously reported. The subsequent thermal treatment under inert atmosphere promotes the thermal decomposition of the N-precursors, which are in intimate contact with the CNTs, the release of products being responsible for the incorporation of the N-functionalities onto the carbon surface. Three ratios between CNTs and the amount of N-precursor (melamine or urea) were tested. Regarding the samples prepared with urea, there are no significant differences in the specific surface area (S_{BET}) independently of the CNT/N-precursor ratio applied (341-353 $m^2\ g^{-1}$) (Table II- 10). On the other hand, the proportion between the carbon material and melamine used in the ball milling step affects directly the S_{BET},

especially for high amounts of melamine used. Samples CNT-BM-M0.2 and CNT-BM-M0.4 present similar surface areas (347 and 355 m^2 g^{-1}, respectively), while sample CNT-BM-M0.6 revealed a decrease of around 100 m^2 g^{-1}, which can be explained by the aggregation of the carbon material due to the presence of a large amount of melamine. Regarding the samples prepared with NH_3, the first stage under ball milling (in the absence of any N-precursor) reduces the entanglement of the CNTs, leading to shorter CNTs by breaking up the tubes (S_{BET} increases from 291 (pristine CNTs, CNT-O) to 391 m^2 g^{-1} (ball milled CNTs, CNT-BM)), without promoting changes in the surface chemistry. After the thermal treatment under NH_3 or NH_3/N_2, S_{BET} returns to the original value (276 – 286 m^2 g^{-1}). In addition to the changes observed in the S_{BET}, some differences were detected in the pore volumes determined from the N_2 uptakes at p/p_0 = 0.95. Considering that most of the pore volume results from the free space in the CNT bundles, ball milling and the introduction of nitrogen functionalities lead to a significant decrease of the pore volume. The ball milling treatment by itself is responsible for a decrease of the N_2 uptakes at p/p_0 = 0.95 of about 40 %, while the addition of the N-precursors slight enhances this reduction up to 57 % (samples CNT-BM-M0.6). Ball milling leads to a higher agglomeration of the material, reducing the space between the tubes, while the introduction of N-groups on the CNT surface may favour the interaction between the tubes, resulting also in a higher level of agglomeration of the material.

Concerning the effect of the functionalization degree on the incorporation of N-containing groups onto the carbon surface, the highest efficiency of N-doping was obtained using melamine. Melamine based samples present between 1.9 and 7.6 % wt. of N on their bulk composition

(determined by EA, Table II- 10), while samples prepared with urea present less than 1 % wt. of N in their composition.

Table II- 10. Chemical and textural characterization of ball milled CNT samples using different N-precursors and C/N-precursor ratios.

Sample	S_{BET}	V_p	N_{EA}	N_{XPS}	O_{XPS}	$Volatiles_{TGA}$	Ash_{TGA}
	($m^2\ g^{-1}$)	($cm^3\ g^{-1}$)	(% wt.)	(% wt.)	(% wt.)	(% wt.)	(% wt.)
CNT-BM-M0.2	347	0.59	1.9	2.0	1.3	4.2	1.7
CNT-BM-M0.4	355	0.87	7.6	4.8	0.9	8.6	0.6
CNT-BM-M0.6	241	0.47	7.5	7.0	0.9	11.8	2.0
CNT-BM-U0.3	344	0.57	0.5	n.p.	n.p.	4.6	2.8
CNT-BM-U0.5	353	0.70	0.8	0.8	0.8	6.5	2.6
CNT-BM-U0.8	341	0.65	0.9	n.p.	n.p.	3.1	2.5
CNT-BM-NH_3	286	0.62	0.4	0.7	1.0	3.2	2.1
CNT-BM-NH_3-N_2	276	0.58	0.4	0.5	1.0	3.2	1.7

n.p. – not performed.

Neither in the case of melamine nor in the case of urea, the use of a larger amount of precursor proved to be successful in obtaining a N-richer carbon material. In fact, samples prepared with the largest amount of the N-precursor (CNT-BM-M0.6 and CNT-BM-U0.8) presented similar N-contents as the samples prepared in the middle range of CNT/N-precursor ratio (CNT-BM-M0.4 and CNT-BM-U-0.5). With respect to the gas-phase thermal treatment using pure or diluted NH_3 no differences were observed in the N-content of the samples, suggesting that, under the operating conditions tested, the functionalization degree was not dependent on the gas concentration. Comparing with melamine, considerably less nitrogen is retained in the carbons using urea or NH_3 for N-doping. All samples exhibited a poor surface content in oxygen (assessed by XPS), with values below 1.3 % wt., independently of the precursor/approach used.

The nature of the N-functionalities incorporated on the CNTs were also investigated using the N1s XPS spectra obtained (Figure II- 15). The corresponding binding energies and relative percentages of the N-functionalities are presented in Table II- 11. The asymmetric N1s spectra were deconvoluted in three or four peaks taking into account different assumptions: for samples prepared with melamine and urea, since the samples were thermally treated at 600 °C, the deconvolutions were based in three peaks assuming the presence of quaternary nitrogen (NQ), pyrrole (N5) and pyridinic (N6) structures, which are the typical structures formed in carbon samples prepared above 550 °C; in the case of NH_3 treated samples, the presence of an additional peak located at higher binding energies (B.E.) (around 404.4 – 404.8 eV) was evident, which is assumed to be generated by nitrogen–oxygen complexes (NX), but not much is known about them. The relative quantity of these oxidized nitrogen

species is usually much smaller than that of the other types of nitrogen [44], as observed in the samples CNT-BM-NH_3 and CNT-BM-NH_3-N_2, where NX represents less than 8.8 % of the total nitrogen. In spite of the different N-loads obtained using melamine or urea as precursor, the resulting N-functionalities are similar, including their proportions: thus, the pyridinic group (N6, B.E. = 398.6 $\pm$ 0.3 eV) represents between 45 % and 64 % of the total N content, followed by the pyrrole group (N5, B.E. = 400.1 $\pm$ 0.2 eV) with a relative percentage between 24 and 38 %, and the quaternary groups (NQ, B.E. = 401.4 $\pm$ 0.3 eV) with a lower amount (between 12 % and 19 %). On the contrary, samples treated with NH_3 showed an identical N6/N5 ratio, and a slightly higher content of NQ groups. It is accepted in the literature that the evolution of the types of nitrogen-bonding during heating proceeds with N5 groups being converted into N6 at moderate temperatures, and N6 decreasing with an increase of the NQ content at high temperatures [44]. From the point of view of the proportion of the groups, at first sight, the use of melamine and urea as N-precursors allows to form directly more N6 than the NH_3 treatment, for the same operating temperature, which can be convenient for applications requiring this specific N-functionality.

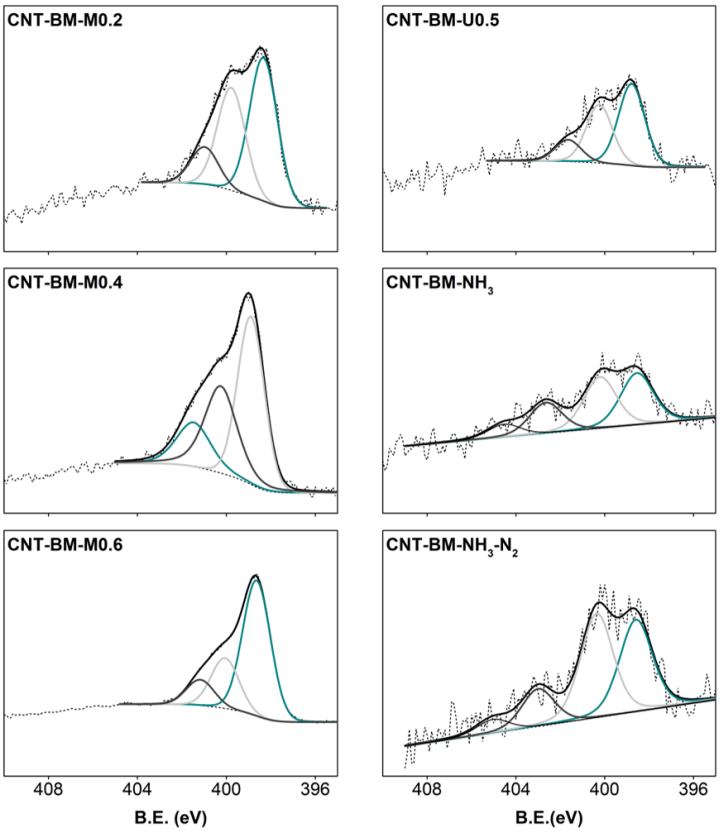

Figure II- 15. N1s spectra recorded for ball milled N-doped CNT samples prepared using different N-precursors[14].

[14] Adapted from Applied Catalysis A, General 548 (2017) 62–70.

Table II- 11. Relative peak contents and positions obtained by N1s spectra fitting of the ball milled CNT samples prepared using different N-precursors.

Sample	Peak #1 (N6)		Peak #2 (N5)		Peak #3 (NQ)		Peak #4 (NX)	
	B.E. (eV)	% Rel.	B.E. (eV)	% Rel.	B.E. (eV)	% Rel.	B.E. (eV)	% Rel.
CNT-BM-M0.2	398.3	50.6	399.8	36.2	401.0	13.2	---	---
CNT-BM-M0.4	398.9	45.8	400.3	35.4	401.5	18.8	---	---
CNT-BM-M0.6	398.6	64.0	400.1	23.8	401.2	12.2	---	---
CNT-BM-U0.5	398.8	50.0	400.2	37.5	401.7	12.5	---	---
CNT-BM-NH_3	398.4	35.3	400.1	35.0	402.6	20.9	404.4	8.8
CNT-BM-NH_3-N_2	398.4	37.2	400.2	42.1	402.8	15.2	404.8	5.5

TGA analyses were performed in order to clarify the functionalization degree of the samples and further complete the samples characterization. The proximate analysis results are presented in Table II- 10. In agreement with the elemental analysis and XPS results, samples treated with NH_3 and urea present a lower amount of volatiles in comparison with the melamine treated samples. TGA profiles (not shown) are identical for all samples: there is almost no weight loss until 600 °C (due to the thermal treatment applied previously until the same temperature) and, therefore, the volatile amounts correspond to the release of components between 600 and 900 °C. In the case of melamine treated samples, the increase of melamine proportion during the samples preparation leads to a proportional increase of the volatiles content (from 4.2 to 11.8 %).

Summing up the influence of the N-precursor used we are able to conclude that the use of melamine leads to the incorporation of a larger amounts of N-functionalities when compared with urea or even NH_3, for the same operating temperature, with the formation of more N6 groups and fewer N5 groups. The ratio between the carbon material and melamine should be carefully chosen in order to avoid compromising the textural properties of the material.

Effect of the thermal treatment

Regarding the use of melamine as N-precursor and considering the observations discussed in the previous section, three additional samples were prepared. Keeping the same methodology and CNTs/melamine ratio used to prepare the sample CNT-BM-M0.4, different final temperatures were tested in the thermal treatment step (200, 400 and 900 °C). The new samples were named accordingly to the temperature applied as CNT-BM-

M200, CNT-BM-M400 and CNT-BM-M900. In this section, sample CNT-BM-M0.4 will be designated as CNT-BM-M600 in order to facilitate discussion between samples. As previously concluded, in the absence of any thermal treatment there was no functionalization of the CNT surface, and only a physical mixture of the carbon material and melamine was obtained, but the effect of the temperature applied was not explored. Therefore, the thermal treatment step is mandatory to achieve the functionalization of the materials.

Regarding the textural properties, there are considerable differences between the samples subjected to thermal treatments at 200 and 400 °C and the samples treated at 600 and 900 °C (Table II- 12). The available surface area for the samples treated at the lower temperatures is quite low (< 100 m^2 g^{-1}) indicating that at these temperatures a simple agglomeration of the precursor and the material is present. However, the increase of the temperature of the thermal treatment allows to recover the accessible surface area characteristic of the CNTs (around 350 m^2 g^{-1}), as well as, albeit discreetly, to recover some space between the tubes (V_P). These observations suggest that samples treated at 200 and 400 °C may still contain a large amount of melamine on their composition. In fact, according to the EA results, sample CNT-BM-M200 presents a N-content of 32.2 % wt., which corresponds more or less to the amount of melamine used in the ball milling, suggesting that almost none of the nitrogen (in the melamine form) has been decomposed. The increase of the final temperature to 400 °C leads to the decrease of the bulk nitrogen to 19.2 % wt., suggesting that the thermal decomposition of melamine starts to occur in this temperature range, continuing until 600 °C (once again, a significant decrease of the N-amount to 7.6 % was observed). However, a

further increase of the temperature to 900 °C removes almost completely all nitrogen from the sample, showing that at such high temperatures the nitrogen retention is compromised.

XPS surface composition revealed a similar trend to EA. Once again, the difference between the bulk composition (EA) and surface composition (XPS) indicates that probably there is a fraction of nitrogen that is not so accessible on the surface of the CNT bundles. Regarding the O content, all samples present a low surface concentration of this element; however, a slight rise of oxygen is observed for the sample treated at 900 °C. At this temperature and with the removal of the N-groups, the CNT surface becomes more reactive, probably due to the presence of more defects in their structure. Those defects may easily be oxidized by simple exposure to air leading to the appearance of oxygen-containing groups on the sample.

To well understand the modifications promoted by the different thermal treatments, TGA analyses were performed and N1s XPS spectra were studied (Figure II-16). Based on the TGA weight loss profiles of the samples, it can be generally concluded that thermal decomposition of melamine proceeds in two defined steps: the first step until 350 °C with the generation of nitrogen-containing volatile groups and a second step with the decomposition of the main chain and nitrogen volatiles until around 700 °C, according to the literature [86], being the first step the main reason for the mass loss observed in the sample CNT-BM-M200. With the thermal treatment at 400 °C, this first step is overtaken and the weight loss is observed at higher temperatures but in lower quantity. In contrast, thermograms of the CNT-BM-M600 and CNT-BM-900 samples present a mass decay lower than 1 % until 500 °C.

The N1s spectrum of sample CNT-BM-M200 revealed that melamine did not decompose during the applied thermal treatment: N–C bonds present a symmetric peak with a maximum at 398.7 eV with a π-excitation between 404 and 408 eV. This spectrum is similar to the untreated mixture of melamine and carbon nanotubes already reported in Figure II-13, evidencing that until 200 °C melamine does not suffer any modifications observed by TGA or XPS analyses. The N1s spectrum of sample CNT-BM-M200 keeps the two-characteristic melamine N–C bonds: the bond C=N–C at around 399.1 eV, and the bond C–NH_2 at around 400.0 eV. On the contrary, the thermal treatment at 400 °C promotes a slight modification of the mixture detected by a change in the symmetry of the N1s spectrum of sample CNT-BM-M400, indicating a decrease of the C–NH_2 bond and the coexistence of other transient species due to the intermediate state of decomposition of melamine and perhaps the initial formation of N-carbon functionalities. After treating the mixture CNTs-melamine at 600 °C, TGA revealed a mass decay lower than 1 % below 500 °C, and, in total around 8 % (at 900 °C). In this case, the N1s spectrum shows unambiguously some new N species, namely the appearance of the pyridinic, pyrrolic and quaternary groups. The nature of these groups does not seem to be affected by the increase of the temperature of the thermal treatment up to 900 °C; however, the amount of the N-functionalities is. Regarding the obtained results, thermal treatment at 600 °C allows the incorporation of an appreciable amount of N-functionalities onto the carbon nanotubes surface, being the most suitable temperature to dope CNTs by the present methodology.

Table II- 12. Chemical and textural characterization of ball milled CNT samples treated with melamine under different thermal treatments.

Sample	S_{BET}	V_p	N_{EA}	N_{XPS}	O_{XPS}	$Volatiles_{TGA}$	Ash_{TGA}
	($m^2\ g^{-1}$)	($cm^3\ g^{-1}$)	(% wt.)	(% wt.)	(% wt.)	(% wt.)	(% wt.)
CNT-BM-M200	79	0.25	32.2	14.4	1.4	40.9	2.9
CNT-BM-M400	75	0.26	19.2	10.8	1.6	25.6	1.1
CNT-BM-M600	355	0.87	7.6	4.8	0.9	8.6	0.6
CNT-BM-M900	330	0.56	0.8	0.4	2.9	5.4	1.3

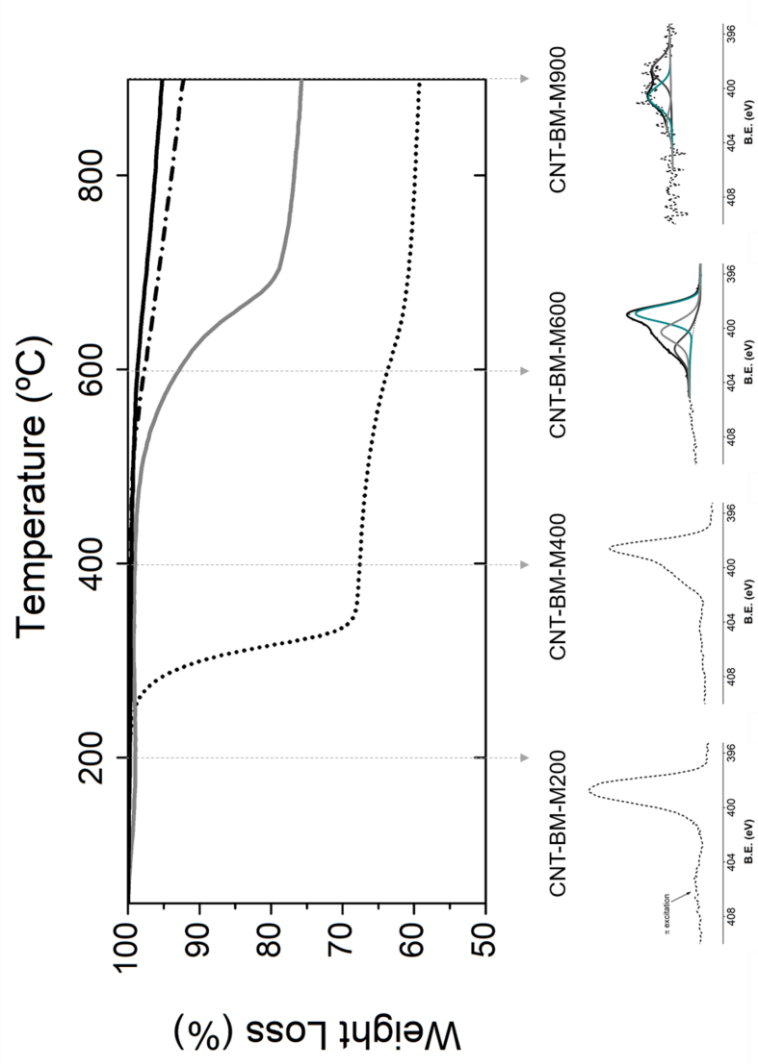

Figure II- 16. TGA profiles and N1s spectra recorded for melamine-doped CNT samples subjected to different thermal treatments.

[15] Adapted from Applied Catalysis A, General 548 (2017) 62–70.

Effect of the O-surface groups

The presence of oxygen-containing functionalities may enhance the yield of nitrogen-containing groups on the surface; therefore, it can be interpreted as a prerequisite for introducing a high amount of nitrogen [71]. In order to investigate this issue, the pristine material was first treated with HNO_3 at boiling temperature and then different thermal treatments were applied to selectively remove the O-containing groups, and therefore to evaluate if there is any specific functionality that contributes to increase the N-content. Table II- 13 summarises the changes in the textural and surface properties observed. Regarding the textural properties, oxidation with HNO_3 results in an increase of 30 $m^2 g^{-1}$ for S_{BET} and a decrease of V_p (from 1.10 to 0.74 $cm^3 g^{-1}$, when CNT-O and CNT-N are compared, respectively). The subsequent thermal treatments applied to the oxidized CNTs did not promote additional changes in S_{BET}. Nonetheless, a slight increase of V_p is observed (from 0.7 to 0.8 $cm^3 g^{-1}$), suggesting that the removal of the oxygen functionalities improves the accessibility to the tubes.

Table II- 13. Chemical and textural characterization of pre-oxidized and thermally treated CNT samples used to study the effect of O-containing groups on the N-doping.

Sample	S_{BET}	V_p	CO	CO_2	pH_{PZC}
	($m^2\ g^{-1}$)	($cm^3\ g^{-1}$)	($\mu mol\ g^{-1}$)	($\mu mol\ g^{-1}$)	(unitless)
CNT-O	291	1.10	200	23	6.8
CNT-N200	322	0.70	1300	807	2.8
CNT-N400	350	0.72	1145	322	4.3
CNT-N600	391	0.78	650	256	7.0
CNT-N900	376	0.80	108	62	8.3

In contrast with the minor alterations of the textural properties, a drastic change of the surface chemistry is observed after oxidation. The HNO_3 treatment strongly acidifies the original material (pH_{PZC} decreases from 6.8 in the pristine CNTs to 2.2 in the oxidized sample not subjected to any thermal treatment), which is due to the incorporation of a large amount of oxygen containing groups, including carboxylic acids, carboxylic anhydrides, lactones and phenols, that directly contribute to the acidic character of the surface, and some carbonyl/quinone groups which are neutral or may form basic structures. With the subsequent thermal treatments those groups are selectively removed [19], leading to a reduction of the acidic character of the surfaces (pH_{PZC} increases from 2.7 to 8.3). Thus, the CNT-N200 sample presents a slightly lower amount of carboxylic acids than CNT-N. The remaining carboxylic acids were practically all removed as well as a part of the anhydrides when the treatment was performed at 400 °C (CNT-N400).

After treatment at 600 °C (CNT-N600), the surface only contains phenol and carbonyl/quinone groups, and a small amount of lactones, while the sample treated at 900 °C only presents residual amounts of carbonyl/quinone groups. Those changes are confirmed by TPD analysis of the samples. The decrease of CO and CO_2 amounts (released during the TPD experiments) depends on the increase of the final temperature of the thermal treatment (Table II- 13). These results are in agreement with the O-bulk composition determined by Elemental Analysis (by pyrolysis of the samples at 1450 °C).

The different oxidized samples were then ball milled with melamine, using the same CNT/melamine ratio used to prepared sample CNT-BM-M0.4, and subsequently thermally treated until 600 °C. Textural properties and surface chemistry characterization after N-doping are presented in Table II-14. The incorporation of the N atoms using pre-oxidized samples results in a decrease of the surface area (S_{BET}) and of the free space in the CNT bundles (V_p). In the case of S_{BET}, the reductions observed range from 69 to 137 $m^2\ g^{-1}$, while the volume of pores decreases to about a half (around 0.40 $cm^3\ g^{-1}$). Despite the damage to the textural properties, the pre-functionalization of the carbon surface improves the extent of N-doping, being possible to achieve higher amounts of nitrogen in the CNTs, regardless of the pre-treatment. Comparing with the un-pre-treated sample CNT-BM-M600 (7.6 %), it is possible to reach even higher N-incorporation using the pre-oxidation followed by thermal treatment until 600 °C (sample CNT-N600-BM-M, 8.4 % of N by EA). Apparently, there is no clear correlation between the nature of the O-functional groups present on the surface and the N-content obtained. The presence of carboxylic acids on the sample CNT-N200 or the absence of any O-

functionalities in sample CNT-N900 lead to similar N amount incorporation at the end (6.2 and 6.9 %, respectively). In contrast, if only the carboxylic acids are removed (sample CNT-N400), a slight decrease of the incorporated nitrogen is observed, suggesting a positive effect of the carboxylic acids. Moreover, in sample CNT-N600, where anhydrides have also been removed, an improvement of the N-content was achieved.

According to these results, we are not able to conclude that the presence of O-functionalities enhances the incorporation of nitrogen. Regarding XPS results, a distinct bulk/surface composition was noticed. From the N-content available on the CNTs (XPS values), different conclusions may be inferred. Apparently, the presence of carboxylic acids showed a positive effect on the attachment of N-groups, the sample CNT-N200-BM-M presenting the highest N surface content (6.7 %). This is corroborated by the reduction of the N surface content to 3.1 % in samples CNT-N400-BM-M and CNT-N600-BM-M. Regarding the CNT-N900-BM-M sample, the increase of the N-functionalities to 4.8 % could be explained by the presence of more defects on the CNT structure promoted by the removal of all O-containing groups until 900 °C; more defects are available on this sample and therefore nitrogen can be more easily incorporated than in any other sample.

Table II- 14. Chemical and textural characterization of pre-oxidized and melamine ball milled CNT samples.

Sample	S_{BET} ($m^2\ g^{-1}$)	V_p ($cm^3\ g^{-1}$)	N_{EA} (% wt.)	N_{XPS} (% wt.)	O_{XPS} (% wt.)	$Volatiles_{TGA}$ (% wt.)	Ash_{TGA} (% wt.)
CNT-N200-BM-M	253	0.399	6.2	6.7	2.9	11.8	2.00
CNT-N400-BM-M	331	0.432	5.5	3.1	3.2	4.2	1.70
CNT-N600-BM-M	254	0.371	8.4	3.1	4.1	4.6	2.80
CNT-N900-BM-M	274	0.429	6.9	4.8	3.2	3.1	2.50

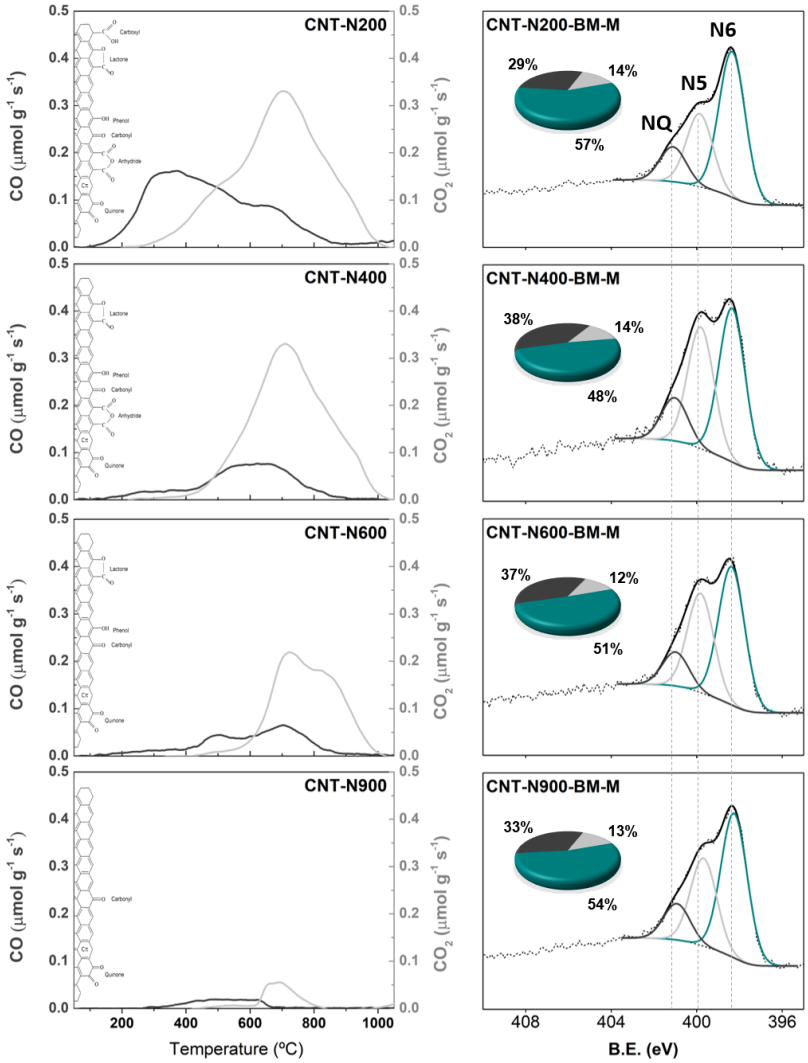

Figure II- 17. At left, CO and CO_2 evolutions in TPD profiles of oxidized CNT samples after the different thermal treatments, illustrating the O-containing groups present; at right, N1s spectra recorded for melamine-doped CNT samples subjected to different thermal treatments[16].

[16] Adapted from Applied Catalysis A, General 548 (2017) 62–70.

Table II- 15. Relative peak contents and positions obtained by N1s spectra fitting of the pre-oxidized and melamine treated CNT samples.

Sample	Peak #1 (N6)		Peak #2 (N5)		Peak #3 (NQ)	
	B.E. (eV)	% Rel.	B.E. (eV)	% Rel.	B.E. (eV)	% Rel.
CNT-N200-BM-M	398.3	57.5	399.9	28.8	401.1	13.7
CNT-N400-BM-M	398.3	48.3	399.8	38.1	401.0	13.6
CNT-N600-BM-M	398.4	50.9	399.8	36.6	401.0	12.5
CNT-N900-BM-M	398.2	53.8	399.7	32.7	400.9	13.5

To go further into the study, N1s XPS spectra of the samples were deconvoluted following the same already enunciated assumptions. Figure II- 17 illustrates the deconvoluted N1s spectra of the samples and the respective N6, N5 and NQ relative composition of each one in pie charts. Ratios between N6/N5/NQ groups are close to those previously obtained for the samples treated with melamine: pyridinic groups correspond to half or more of the total N-content (from 48 to 57 %), while pyrrole groups represent around one-third (29-38 %), N-quaternary being, once again, the less expressive group (around 12% and 14 %). From these deconvolutions, no additional information related to the influence of the pre-treatment could be obtained since samples are similar with respect to the amount and nature of the N-functionalities.

In spite of some inconclusive results, the developed methodology can be interpreted as a solution for the preparation of CNT samples when N and O functionalities are required. In fact, it does not seem that there is a negative impact or competition between both surface groups, which can be interesting for applications where both heteroatoms play a role, as for example in oxidative dehydrogenation of isobutane [48], where N-functionalities and carbonyl groups (O-surface groups) were shown to have a synergic effect.

4.2.2.N-doping of graphene-based materials

4.2.2.1. Methodology

The procedure developed for CNTs was extended to the incorporation of N-functionalities onto the structure of rGOs. The GO material was used as starting material. Briefly, 0.6 g of GO was mixed with 0.26 g of N using urea or melamine as nitrogen precursor (without any solvent) and the mixture was ball milled during 4 h at a constant frequency of 15 vibrations/s. Then, the resulting materials were subjected to a thermal treatment under N_2 flow (100 cm^3 min^{-1}) until 600 °C (at 2 °C min^{-1}) and kept at the maximum temperature during 1 h. Partial reduction of GO occurs during the thermal treatment. The reduced GO materials are denoted as rGO-U (prepared with urea) or rGO-M (prepared with melamine). Reduced GO was also prepared by using the same procedure (mechanical and thermal treatment), but without addition of a nitrogen source (rGO). The GO material was subjected to mechanical treatments using the same experimental conditions.

4.2.2.2. Induced Properties

The ball milling and thermal treatments applied to the GO material promoted several modifications in its textural and chemical properties, as can be seen in Table II- 16. Regarding the textural properties, the apparent surface area (S_{BET}) increased when GO was subjected to the mechanical and thermal treatments without addition of a nitrogen source, i.e. from 23 m^2 g^{-1} (GO) to 263 m^2 g^{-1} (rGO). This effect could be due to the thermal treatment until 600 °C since an increase of GO exfoliation with partial

reduction to rGO occurs during this step, in addition to the mechanical treatment that can also exfoliate GO and cut the graphene sheets during milling. Nevertheless, this value was significantly lower than the theoretical surface area around 2600 m^2 g^{-1} for individual isolated graphene sheets [88] mostly due to the partial exfoliation of the graphene sheets, the defective graphene structure formed during the synthesis of GO, and the O-functional groups remaining on rGO. The N-doping of GO using melamine and urea resulted in a decrease of the surface area in comparison with the rGO material (102, 47 and 263 m^2 g^{-1}, for rGO-M, rGO-U and rGO, respectively, Table II- 16), which suggests that the addition of the N-precursor contributes to a higher aggregation of the graphene sheets, more pronounced when urea is used. Nevertheless, these surface areas are higher than that obtained for the original GO sample (23 m^2 g^{-1}). This effect could be due to the cutting of the graphene sheets that increases the surface area during the ball milling treatment and also due to nitrogen incorporation into the graphene layers. In addition, some agglomeration of the graphene sheets can occur due to the vibration frequency and duration of the milling used in this work, which are higher than the values normally reported for graphene exfoliation [89]. The N_2 adsorption-desorption isotherms for rGO, rGO-U and rGO-M materials (Figure II- 18) can be classified as type II, accordingly to IUPAC [32]. In spite of the similar shape of the isotherms, the amounts of N_2 adsorbed at the relative pressure p/p_0 = 0.95 are much lower in the case of N-doped samples (rGO-U and rGO-M); these differences may reflect different degrees of agglomeration of the graphene sheets, a result of the different nitrogen precursors used.

Table II- 16. Chemical and textural characterization of the graphene-based materials.

Sample	S_{BET}	CO	CO_2	O_2^{TPD}	CO/CO_2	N_{XPS}		pH_{PZC}
	($m^2\ g^{-1}$)	($\mu mol\ g^{-1}$)	($\mu mol\ g^{-1}$)	(% wt.)	(unitless)	(% wt.)	N5/N6	(unitless)
GO	23	4156	5305	23.6	0.8	n.a.	n.a.	2.8
rGO	263	2481	494	5.6	5.0	n.a.	n.a.	6.2
rGO-M	102	1378	405	3.5	3.4	9.3	0.6	7.3
rGO-U	47	1626	262	3.4	6.2	7.5	0.5	8.1

n.a. – not applicable; N5 – pyrrolic N groups; N6 – Pyridinic N groups.

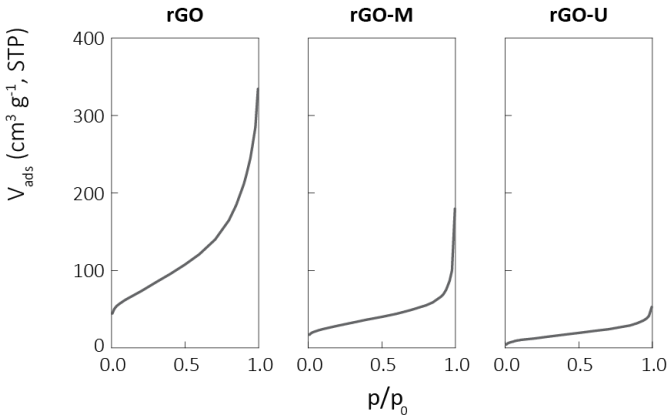

Figure II- 18. N_2 adsorption–desorption isotherms at -196 °C for graphene-based materials[17].

Figure II- 19 represents the TPD profiles corresponding to the groups evolved as CO_2 and CO from the surface of GO, rGO, rGO-U and rGO-M. The total amounts of CO_2 and CO released, the oxygen contents, as well as the pH_{PZC} for GO, rGO and N-doped materials are presented in Table II- 16. CO_2 and CO profiles of GO sample are significantly different from TPD

[17] Adapted from Catalysis Today 249 (2015) 192-198.

profiles of the carbon materials shown until now. The GO TPD profiles show that chemical composition of GO contains mainly epoxy and hydroxyl groups released as CO and CO_2 at low temperatures (< 200 °C) [90-92], in addition to the carboxylic acids, anhydrides groups, lactones (released as CO_2) and anhydrides, phenols and carbonyls/quinones (released as CO) [93]. The TPD analysis of the graphene-based materials after the thermal treatment reveals a decrease of the oxygen content in the case of rGO (5.6 % wt.) compared to GO (23.6 % wt.), which is related to the release of the oxygen-surface groups during the heating until 600 °C, mainly epoxy and hydroxyl groups. After N-doping (both with melamine or urea), a decrease of the oxygen content was also observed, indicating the loss of some oxygenated groups by the incorporation of nitrogen functional groups on the GO material (3.5 and 3.4 % wt. for rGO-M and rGO-U, respectively). For the rGO and N-doped graphene samples (Figure II- 19), there is not a different contribution of the type of groups released as CO and/or CO_2 during TPD. In fact, most of the surface groups of the samples decomposed as CO (the amount of CO released was always significantly higher than that of CO_2, Table II- 16), namely as phenol and carbonyl/quinone groups. The presence of these particular groups is linked with the thermal treatment applied; i.e. carbonyl/quinone groups were not removed from the surface since their release occurs at temperatures above 600 °C [19]. On the other hand, the thermal treatments should have removed the most labile oxygen functional groups, namely epoxy and hydroxyl groups located on the basal planes of GO [93], and carboxylic acid and anhydride groups, since they are released at temperatures below 600 °C.

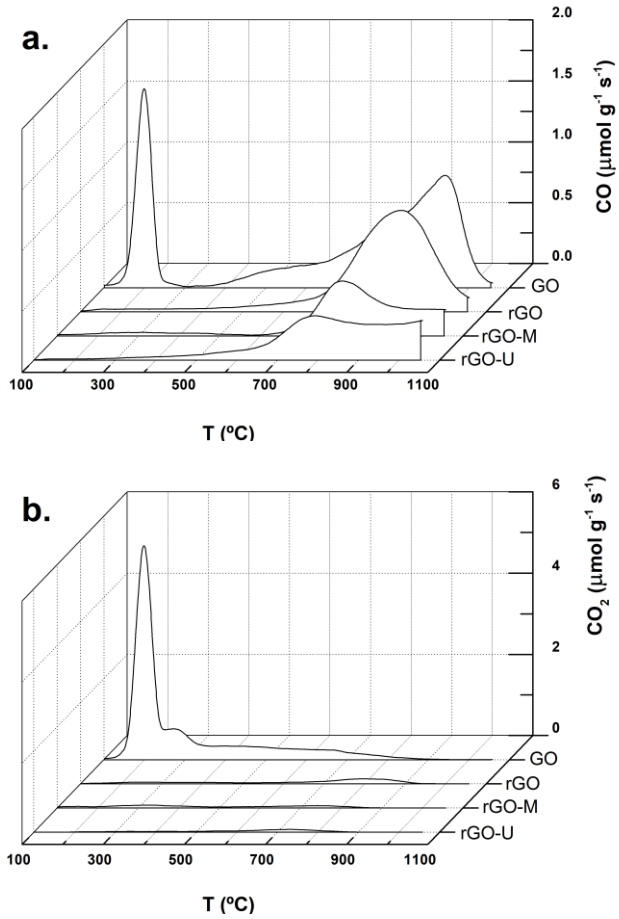

Figure II- 19. CO_2 (a) and CO (b) evolutions in TPD profiles of graphene oxide (GO) and thermally treated graphene-based samples (rGO, rGO-M and rGO-U)[18].

Phenols and lactones were partially removed since they are decomposed in the range of 500–700 °C. The absence (or low content) of acidic surface groups (carboxylic acids, phenol, anhydrides) contributes to the neutral/basic nature of the surface of the graphene-based materials with the samples presenting pH_{PZC} values higher than 6. The incorporation

[18] Adapted from Catalysis Today 249 (2015) 192-198.

of the surface nitrogen groups (rGO-M and rGO-U samples) contributes with additional electrons, increasing the surface basicity (higher values of pH_{PZC}) [44].Significant amounts of N (Table II- 16) were introduced on the surface of the graphene-based materials after the milling treatments (determined by XPS analysis). The sample milled with melamine presents the largest amount of N (9.3 % and 7.5 % for rGO-M and rGO-U, respectively). The XPS N1s spectra of the rGO-M and rGO-U samples were decomposed into three peaks (Figure II- 20). The first peak identified at around 398 eV, designated as N6, is attributed to pyridinic-N. The second peak, situated ca. 400.0 eV, is ascribed to pyrrolic-N, and will be referred as N5. The next peak identified at around 400.9 eV is attributed to quaternary nitrogen (NQ) [94, 95]. However, similar proportions of the different types of nitrogen species were observed in these samples. For instance, the ratio between pyrrolic and pyridinic groups (N5/N6 ratio) is 0.6 in rGO-M and 0.5 in rGO-U. N-quaternary species are also present with similar proportions, corresponding to 17 % in rGO-M and 25 % in rGO-U.

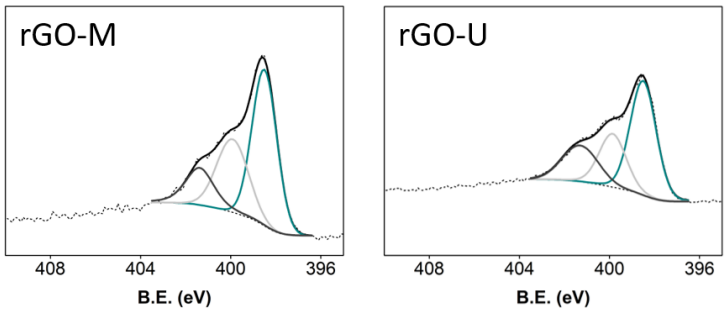

Figure II- 20. N1s XPS spectra for the N-doped graphene-based samples treated with melamine (rGO-M) and urea (rGO-U)[19].

[19] Adapted from Catalysis Today 249 (2015) 192-198.

4.3. Additional Notes

Mechanochemical treatments have gained notable attention in the nanomaterials research community in the last decade [96]. In-situ amino functionalization of CNTs in the presence of ammonium bicarbonate (NH_4HCO_3) allowed introduction of functional groups like amine, amide on the surface of CNTs [97]. Using melamine, Zhao et al. also proposed an efficient two-step method for the preparation of nitrogen-doped CNTs: after washing the CNTs with H_2SO_4/HNO_3, the material was air activated and then mixed under ball milling with melamine, and subsequently pyrolyzed [98]. However, the resulting material subjected to air activation presented lower N retention than air-untreated sample. N-doped graphene has been prepared by ball milling of graphite with melamine, facilitating the exfoliation of the resultant small particles into few-layer N-doped graphene nanosheets under ultrasonication [99]. Authors did not report any thermal treatment after ball milling step; in alternative, a washing step with hot water was performed before ultrasonication. The N-doped graphene nanoplatelets exhibited a high nitrogen content (11.4 % at.) and the presence of pyridinic- N, pyrrolic- and graphitic- N. Under similar procedure, Léon et al. [89] reported an easy and practical method for exfoliation of graphite using melamine, avoiding structural changes of graphene. In this case, they reported the disappearance of C-N bonds after washing with hot water, suggesting that no covalent bonds are formed during the milling treatment. A synthesis route of N-doped nanoparticles have been proposed by Xing et al. involving a ball milling step of graphite under N_2 gas followed by annealing at 700 °C using a N_2–15 % H_2 gas mixture [100]. The ball milling approach has also been

extended to the preparation of N-doped OMCs. The N-enriched OMCs (the highest N content of 31.7 %) was obtained maintaining the ordered mesoporous structure using melamine, Pluronic F127 and phenolic resin (as N-source, template and carbon-source, respectively) via a solvent-free ball milling method followed by pyrolysis under inert atmosphere until 600 °C [101].

In addition to the N-incorporation onto carbon materials, the ball milling approach has been also investigated to incorporate other heteroatoms. Edge-selectively functionalized graphene nanoplatelets with different functional groups were efficiently prepared by dry ball milling of graphite in the presence of hydrogen, carbon dioxide, sulphur trioxide, or carbon dioxide/sulphur trioxide mixture, leading to hydrogen-, carboxylic acid-, sulphonic acid- and carboxylic acid/sulphonic acid-functionalized graphene nanoplatelets [102]. Edge-selectively sulphurized graphene nanoplatelets have been produced by simple dry ball milling of graphite in the presence of sulphur (S_8) [103, 104]. Carbon nanotubes have been also mixed with boron carbide powder by a dry ball milling technique [105]. Ball milling towards doping of carbon materials can become a potential route to produce materials in a cheapest away, avoiding the use of solvents and the consequent production of wastes.

Before the end of this section, a brief comparison between the developed N-doped carbon materials is presented in Table II- 17. Significant amounts of nitrogen can be introduced on the surface of CNTs, especially when melamine is used as N-source. The procedure developed using melamine under ball milling (CNT-BM-M) allows a larger incorporation of nitrogen than the conventional hydrothermal treatment using urea (CNT-NUT) or even under ball milling method (CNT-BM-U).

However, the method is not so efficient for the incorporation of N-groups onto graphene-based materials (rGO-M). The nature of the N-functionalities, identified by XPS, included pyridine-like N atoms (N6), pyrrole-like N atoms (N5), and quaternary nitrogen (NQ), which are usually thermally stable on carbons, but the formation of N-oxidized groups was reported by Zhao et al. using a similar ball milling approach [98].

Table II- 17. Comparison of the degree of N-functionalization over carbon materials by ball milling (BM) approaches or hydrothermal treatment (HT).

Sample	Method	N_{XPS} (% wt.)	N-groups	Ref.
CNT-air-M	BM/Melamine	0.9	N5/N6/NQ/N-O	[98]
CNT-NUT	HT/Urea	0.9	N5/N6	This work
CNT-BM-U	BM/Urea	0.8	N5/N6/NQ	
CNT-BM-M	BM/Melamine	4.8	N5/N6/NQ	
rGO-M	BM/Melamine	0.6	N5/N6/NQ	

4.4. Partial Conclusions

The incorporation of nitrogen atoms onto the carbon structures was successfully carried out using two methodologies: hydrothermal treatment and ball milling approach. The hydrothermal treatment applied to carbon nanotubes using urea as N-precursor involves a complex multi-procedure route (HNO_3 at boiling temperature, liquid-phase urea treatment at 200 °C, and gas-phase thermal treatment with N_2 at 600 °C). In contrast, the ball billing approach consists of a two-step easy to handle method combining a mechanical treatment under ball milling followed by a thermal treatment under inert atmosphere. Several parameters have

been analysed for the novel method: melamine, urea and NH_3 can be successfully used as nitrogen precursor for the N-doping of CNTs and rGO samples by ball milling; nevertheless, the samples doped with melamine present larger N content. The use of a solvent during ball milling revealed a negative effect for the introduction of N-functionalities, regardless of the precursor used. High loading of solid N-precursors does not improve the extension of N-doping, and, on the contrary, it damages the textural properties of the resulting material, in the particular case of melamine prepared samples. During the thermal treatment step, the thermal decomposition of the N-precursor is responsible for the incorporation of the N-functionalities onto the carbon surface due to the close contact between the precursor and the carbon material attained during the ball milling step; 600 °C was found to be the best temperature to perform the thermal treatment using melamine, to reach a cost benefit regarding the amount of N content and the nature of N-functionalities. Pre-oxidation of the CNTs with HNO_3 is an interesting methodology to prepare new samples co-doped with O and N-functionalities, for applications where both heteroatoms may play a role. This promising post-doping method allows the incorporation of large amounts of N-groups, namely, quaternary nitrogen (NQ), pyrrolic (N5) and pyridinic (N6) groups, avoiding the use of solvents and production of wastes. Furthermore, the method is easily scalable for practical applications, since the procedure does not require highly specialized and expensive equipment.

5. Sulphur-containing surface groups

While the N-surface groups enhance the basicity of the carbon surface, strongly acidic properties may be promoted by the incorporation of sulphonic acid groups (-SO_3H) [3, 106, 107]. Although concentrated H_2SO_4 is routinely used for this purpose [107], acidic active carbons can be prepared by the sulphonation of various carbonaceous materials such as sulphonation of incompletely carbonized D-glucose [108] or by using other sulphonating agents as vapour-phase transfer sulphonation with fuming H_2SO_4, benzenesulphonic acid, *p*-toluenesulphonic acid, and "piranha" solution [30, 107, 109, 110].

This chapter is dedicated to the presentation of methodologies used for the introduction of -SO_3H groups onto the surface of CNTs and CXs with the aim of studying their application as environment-friendly solid acid catalysts for acid catalysed reactions. Concentrated H_2SO_4 was used as sulphonation agent in the liquid-phase treatments, and the modification of textural and surface properties was analysed.

The results presented in this section have been already reported in the following papers:

Carbon as a catalyst: Esterification of acetic acid with ethanol, authored by Raquel P. Rocha, Manuel F.R. Pereira and José L. Figueiredo, and published in the journal Catalysis Today Volume 218– 219 pages 51-56 (2013). Author Contributions: Raquel Rocha carried out the experimental work described and wrote the manuscript, with substantial supervision of the other authors.

The role of O- and S-containing surface groups on carbon nanotubes for the elimination of organic pollutants by catalytic wet air oxidation, authored by Raquel P. Rocha, Adrián M.T. Silva, Saudi M.M. Romero, Manuel F.R. Pereira and José L. Figueiredo, and published in the journal Applied Catalysis B: Environmental Volume 147 pages 314-321 (2014). Author Contributions: Raquel P. Rocha and Saudi M.M. Romero carried out the experimental work described. Raquel P. Rocha wrote the manuscript. The work was supervised of by the remaining authors.

Catalytic performance of heteroatom-modified carbon nanotubes in advanced oxidation processes, authored by João Restivo, Raquel P. Rocha, Adrián M. T. Silva, José J. M. Órfão, Manuel F. R. Pereira and José L. Figueiredo, and published in the journal Chinese Journal of Catalysis Volume 35 pages 896–905 (2014). Author Contributions: Raquel P. Rocha performed the modification and characterization of the carbon samples, and tested them in CWAO. João Restivo tested the materials as catalysts for ozonation. The manuscript was jointly written by João Restivo and R.P. Rocha, with substantial supervision of all authors.

5.1. Liquid-Phase Oxidation Treatments

5.1.1.Methodologies

Regarding CXs, the liquid-phase chemical treatment with concentrated H_2SO_4 was performed in a round-bottom flask immersed in a paraffin bath at 150 °C during 6 h. Using the CX-O sample (synthesis described previously in *Chapter* 1) two treatments were done using different ratios of catalyst weight/acid volume: 1 g/150 mL H_2SO_4 (sample CX-S1) and 1 g/20 mL H_2SO_4 (sample CX-S2). The samples were washed with distilled water until neutral pH, and finally dried at 110 °C in an oven during the night. Lastly, one portion of the CX-S1 sample was subjected to a final thermal treatment up to 250 °C using He as inert gas (heated at 10 °C min^{-1}; He flow of 25 cm^3 min^{-1}) with the aim of removing part of the surface groups incorporated during the sulphonation treatment, sample CX-S1-250.

For comparison, a H_2SO_4 treatment was also employed using pristine CNTs NC3100 from Nanocyl™ at the same operating conditions (1 g/150 mL H_2SO_4; 150 °C during 6 h, sample CNT-S^{150}). Under a lower operating temperature, two additional CNT samples were prepared. The sample CNT-S was prepared in a round-bottom flask immersed in a paraffin bath at 50 °C during 4 h using 2 g of CNTs per 150 mL of H_2SO_4. A mixture of HNO_3/H_2SO_4 (1:3 v/v) was used to prepare the sample CNT-NS by refluxing the pristine CNTs with the acidic solution (2 g of CNTs per 150 mL of HNO_3/H_2SO_4) at 50 °C during 4 h. The samples were washed with distilled water until neutral pH was reached, and finally dried at 110 °C in an oven during the night.

5.1.2.Induced Properties

Figure II- 21 shows the N_2 adsorption-desorption isotherms of original and modified CX samples. Isotherms of the CX samples are characteristic of mesoporous solids (isotherms type IV), according to the IUPAC classification [16, 32], presenting a hysteresis loop, which is associated with capillary condensation taking place in mesopores. Table II-18 summarizes the textural properties of the original and H_2SO_4 treated carbon samples at 150 °C, determined from the N_2 adsorption-desorption isotherms. The H_2SO_4 treatment performed over the CX-O samples promoted a decrease of the BET surface area of the sample; the reduction is about 250 $m^2\ g^{-1}$ when a higher ratio of carbon/acid is applied (sample CX-S1). Likewise, this decrease is observed concerning the V_p determined at p/p_0=0.99, the mesoporous surface area (S_{meso}) and the micro-pore volume (V_{micro}). The average mesopore diameter (d_p) was not affected by the treatment, remaining around 17 nm (determined by the BJH method) for both H_2SO_4-treated CX samples. These results indicate that the H_2SO_4 treatment contributes to reduce the microporosity of the material, contrary to what happens with HNO_3 [28]. A decrease of S_{BET} and V_p is also observed for the CNT-S^{150} sample, treated with H_2SO_4 under the same conditions as sample CX-S1. However, the N_2 adsorption isotherm of the CNT-S^{150} sample is a typical type II, characteristic of non-porous materials (not shown).

Table II- 18. Textural properties of pristine and sulphuric acid treated carbon samples at 150 °C.

Sample	S_{BET}	V_p	S_{Meso}	V_{Micro}	d_p
	$m^2\ g^{-1}$	$(cm^3\ g^{-1})$	$(m^2\ g^{-1})$	$(cm^3\ g^{-1})$	(nm)
CX-O	672	1.16	244	0.173	17.4
CX-S1	416	0.95	213	0.084	17.3
CX-S2	528	1.04	222	0.125	17.4
CNT-O	302	2.90	---------- n.a. ----------		
CNT-S^{150}	231	2.31	---------- n.a. ----------		

n.a. – not applicable.

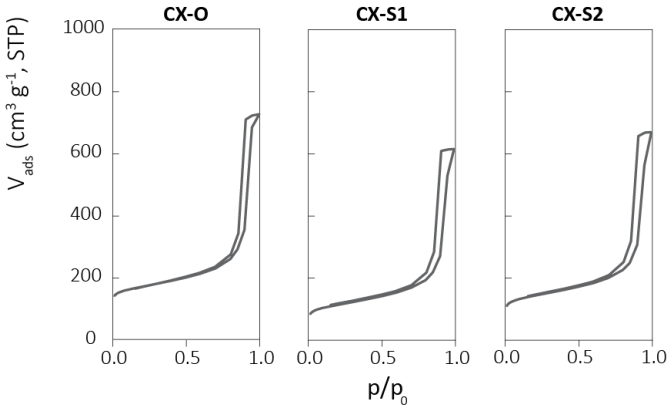

Figure II- 21. N_2 adsorption–desorption isotherms at -196 °C for pristine and sulphuric acid treated CX samples[20].

Elemental, XPS, TPD and TGA analyses were done in order to identify the amount and the nature of the surface groups introduced during the H_2SO_4 treatment. Table II- 19 shows the results obtained. Regarding the CX

[20] Adapted from Catalysis Today 218–219 (2013) 51–56.

materials, the CX-S1 sample presented the highest bulk and surface sulphur contents (2.1 and 3.2 %, determined by EA and XPS, respectively), as expected, since it was prepared with a higher ratio of H_2SO_4 (1:150). On the contrary, the CX-S2 sample prepared with a ratio 1:20 has only 1.6 and 1.9 % (EA and XPS, respectively). The thermally treated sample, CX-S1-250, presents a residual amount of bulk sulphur (only 0.2 %), which shows that most of the incorporated S-containing groups are released from the surface of the carbon structure at low temperatures (below 250 °C). The H_2SO_4 treatment is not so effective for the incorporation of S-surface groups onto CNTs as in CXs. Sample CNT-S^{150} prepared in the same way as CX-S1 presents one third of the S content reached in CXs, only 0.7 %. The S2p spectra of S-doped CX and CNT samples (Figure II- 22) show a common peak around 169 eV, which is the binding energy typically attributed to -SO_3H groups [111-113]. The absence of other peaks, especially at lower BE, allows to conclude that other S-containing groups (such as the thiol groups that traditionally appears at 163 eV [114] and sulphides at 164 eV) are not incorporated during the treatment applied.

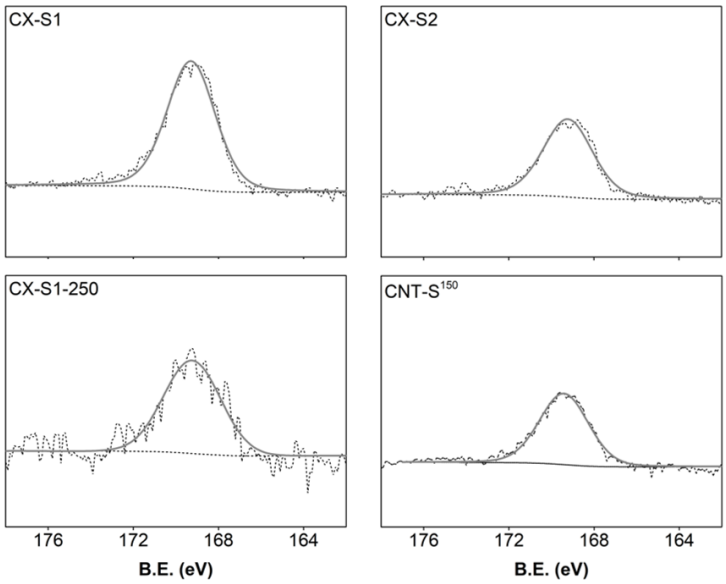

Figure II- 22. S2p XPS spectra for the sulphuric acid treated carbon samples at 150 °C[21].

In addition to the S-incorporation, H_2SO_4 treatment embodies a large amount of O-containing groups, identified by EA and XPS, independently of the nature of the carbon material. However, the amounts of CO and CO_2 released during the TPD analyses (Table II- 19) are very low, suggesting that the typical carboxylic acids, anhydrides, phenols, lactones and carbonyl-quinone groups easily incorporated upon HNO_3 treatment are poorly incorporated by the H_2SO_4 treatment. In fact, sample CX-S1 presented the highest amounts of CO and CO_2 (only 732 and 330 μmol g^{-1}, respectively) and these amounts of CO and CO_2 groups desorbed represent only 2.2 % of oxygen (determined by TPD) which is strongly inferior to the amounts estimated by EA and XPS (21.7 and 16.2 %). Those

[21] Adapted from Catalysis Today 218-219 (2013) 51-56.

results show that, in spite of the smaller amounts of CO and CO_2 releasing groups incorporated with the H_2SO_4 treatment, the $-SO_3H$ groups represent a large percentage (by weight) of the total surface groups, which is corroborate by the amount of volatiles released during the TGA analyses (Table II- 19).

The MS signal of SO_2 (m/z = 64) was followed during the TPD analysis of selected S-doped samples (Figure II- 23). The TPD profiles reveal desorption of S-containing groups from the surface in a specific temperature range (200–400 °C) mainly due to the decomposition of $-SO_3H$ groups into SO_2 species [29]. In agreement with the previous results of EA and XPS analyses, the amounts of SO_2 released decrease in the same order as the S content, as follows: CX-S1, CX-S2 and CNT-S^{150}.

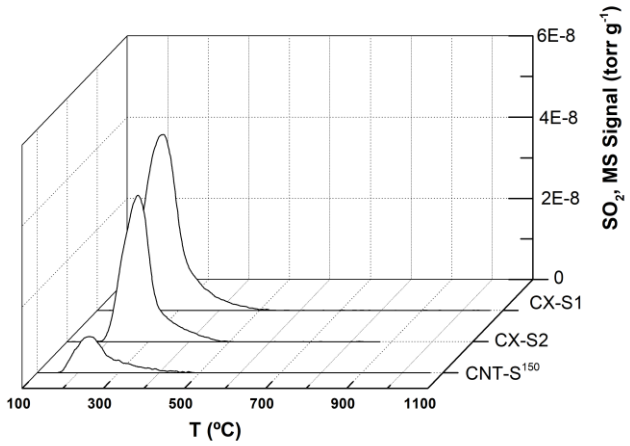

Figure II- 23. MS signal of groups released as SO_2 (m/z = 64) during TPD analysis of sulphuric acid treated carbon samples at 150 °C[22].

[22] Adapted from Catalysis Today 218-219 (2013) 51-56.

Table II- 19. Bulk surface characterization by elemental analysis and surface chemistry characterization by XPS, TPD and TGA analyses of pristine and sulphuric acid treated carbon samples at 150 °C.

Sample	Elemental Analysis					XPS				TPD			TGA
	C	N	H	S	O*	C	N	O	S	CO	CO_2	O_2^{TPD}	Volatiles
	(% wt.)					(% wt.)				($\mu mol\ g^{-1}$)	($\mu mol\ g^{-1}$)	(% wt.)	(% wt.)
CX-O	92.4	0.7	0.4	---	6.5	n.p.				n.p.			n.p.
CX-S1	74.7	0.2	1.3	2.1	21.7	79.9	0.7	16.2	3.2	732	330	2.2	16.4
CX-S2	75.5	0.1	0.9	1.6	21.9	81.0	0.5	16.6	1.9	657	191	1.7	15.0
CX-S1-250	74.6	0.1	0.3	0.2	24.8	89.4	0.3	9.7	0.6	n.p.			n.p.
CNT-O	93.2	0.9	0.2	---	5.7	n.d.				299	105	0.8	2.3
CNT-S150	84.7	0.2	0.5	0.7	13.9	94.2	0.2	4.4	1.2	395	238	1.4	11.9

Oxygen determined by difference; n.p. – not performed.

Regarding CNTs prepared under a lower operating temperature (samples CNT-S and CNT-NS, prepared at 50 instead of 150 °C) no significant changes in the shape of the N_2 adsorption isotherms were observed between the pristine CNTs and the treated samples (not shown). Isotherms present a typical shape characteristic of non-porous materials and can be classified as type II, according to IUPAC [16, 32]. In spite of the similar shape of the isotherms, it is possible to observe some specific differences in the amounts of N_2 adsorbed at high relative pressure (as shown by the V_p determined at p/p_0=0.95) and in the S_{BET} values presented in Table II- 20.

Table II- 20. Textural properties and surface chemistry of the pristine and sulphuric acid treated CNT samples at 50 °C.

Sample	S_{BET}	V_p	CO	CO_2	$Volatiles_{TGA}$
	($m^2\ g^{-1}$)	($cm^3\ g^{-1}$)	($\mu mol\ g^{-1}$)	($\mu mol\ g^{-1}$)	(% wt.)
CNT-O	326	0.67	187	33	1.8
CNT-S	293	0.71	381	195	7.3
CNT-NS	394	0.89	2035	1397	16.0

While the treatment with H_2SO_4 (CNT-S) promotes a slight decrease in S_{BET} and V_p (to 293 $m^2\ g^{-1}$ and 0.71 $cm^3\ g^{-1}$, respectively), the CNT-NS sample (treated with H_2SO_4/HNO_3 mixture) presents slight higher values of S_{BET} and V_p in comparison with pristine CNTs (however, lower than HNO_3 treated sample CNT-N from *Chapter* 3). The changes in V_p may reflect different degrees of agglomeration of the CNTs, as a result of different surface chemistries induced by functionalization. This may indicate that

the treatment with H_2SO_4/HNO_3 mixture might partially open some of the nanotube tips.

In order to identify and quantify the amounts of oxygenated groups incorporated by the applied treatment, the surface chemistry was analysed by TPD. The CO and CO_2 profiles of samples CNT-S and CNT-NS are shown in Figure II- 24. Large amounts of different types of oxygen containing groups were successfully incorporated using the H_2SO_4/HNO_3 mixture (CNT-NS sample), despite the low temperature employed in this treatment (50 °C). A release of 2035 μmol g^{-1} of anhydrides, phenols and carbonyl/quinone groups as observed in the CO desorbed during TPD, and 1397 μmol g^{-1} as carboxylic acids, anhydrides and lactones in the case of CO_2 [19, 20, 23]. In contrast, the amounts of CO and CO_2 released during TPD were insignificant in the case of the H_2SO_4 treatment (CNT-S), CO and CO_2 increasing less than 200 μmol g^{-1} when compared with the pristine sample. For these two treated samples (CNT-NS and CNT-S), the MS signal of m/z=64 was also followed during the TPD analysis (Figure II- 24.c). These profiles reveal that the desorption of S-containing groups occurs in the same temperature range observed previously (200-400 °C). In agreement with the H_2SO_4 concentration used in each treatment, the CNT-S sample showed a richer surface than CNT-NS, with respect to S-containing groups, with nearly the triple amount of SO_2 released (579 and 203 μmol g^{-1} for CNT-S and CNT-NS, respectively). The S2p spectrum of CNT-S (Figure II- 25) shows again a single peak at 169 eV, which is attributed to $-SO_3H$ groups [113].

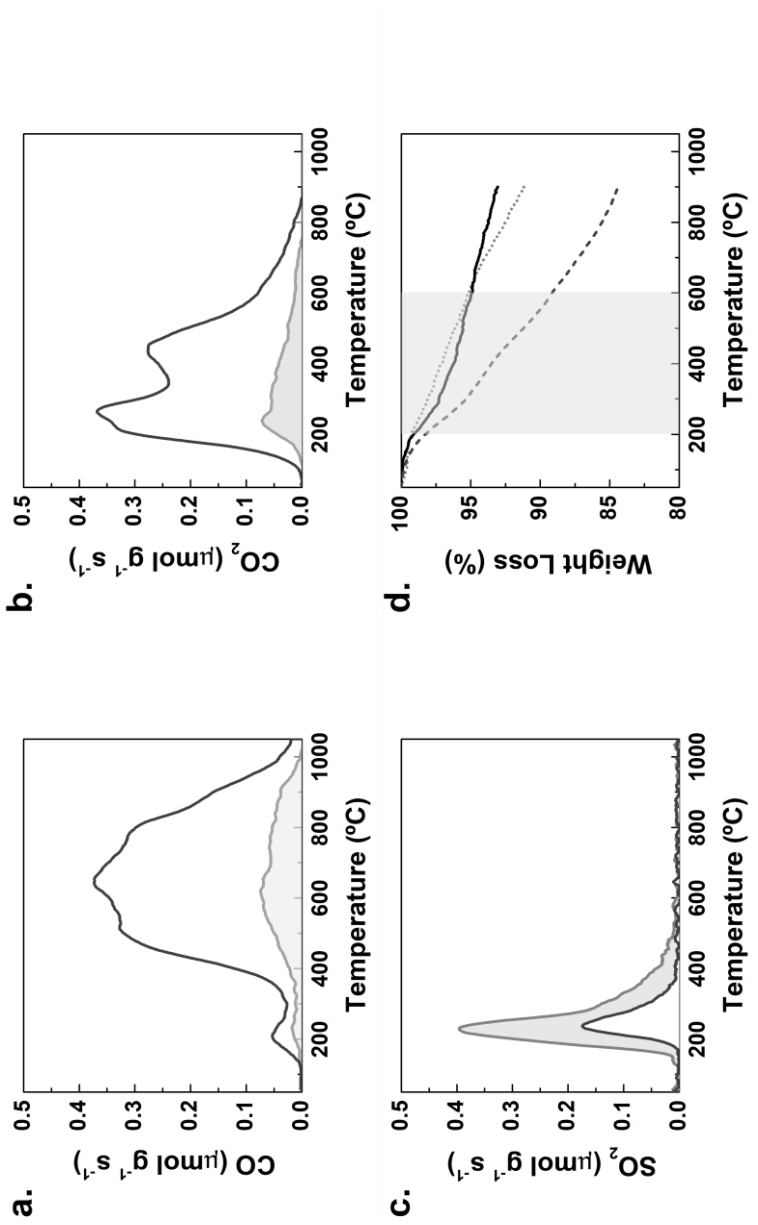

Figure II- 24. Profiles of (a) CO, (b) CO_2 and (c) SO_2 evolved in TPD of samples treated with sulphuric acid (CNT-S as dark grey) and with a mixture of sulphuric and nitric acid (CNT-NS as light grey) at 50 °C; (d) Weight loss of CNT-S and CNT-NS samples determined by TGA.

[23] Adapted from Applied Catalysis B Environmental 147 (2014) 314–321.

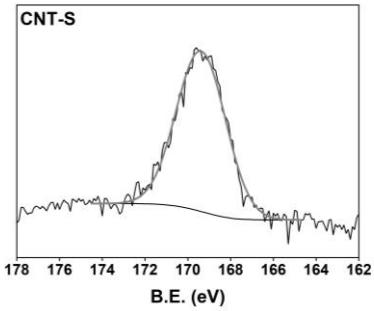

Figure II- 25. S2p XPS spectrum for the sulphuric acid treated CNT sample at 50 °C[24].

An overall estimation of the amount of volatiles was also obtained by thermogravimetric analysis up to 900 °C under N_2 atmosphere (Table II-20). In agreement with TPD analysis, the amount of volatiles is higher in the sample treated with the H_2SO_4/HNO_3 mixture. Figure II- 24.d shows the results of thermogravimetric analysis under He for CNT-NS and CNT-S samples. Here, it is possible to observe that the weight loss of CNT-S is high between 200-400 °C, precisely in the range of temperature where SO_2 is released, becoming less pronounced above 600 °C. The weight loss for CNT-NS is more notorious during the whole TGA temperature range due to its significantly higher content of surface groups, including both O- and S-containing groups (Table II- 20). In spite of the higher O- and S- content, sample CNT-NS presents a lower acid character than CNT-S. The pH_{PZC} of CNT-S was 2.5 against 4.8 of the CNT-NS sample.

Incorporation of $-SO_3H$ groups onto carbon materials has been reported in literature using similar liquid-phase treatments. Activated carbon Norit ROX 0.8, for instance, was treated with H_2SO_4 at different

[24] Adapted from Applied Catalysis B Environmental 147 (2014) 314–321.

concentrations (5, 10 and 18 mol L^{-1}) and temperatures (80 and 150 °C) [2, 115, 116]. The concentration of acidic surface groups, mainly thiol (-SH) and -SO_3H groups determined by XPS, increased with the H_2SO_4 concentration and with the treatment temperature [2]. Single and multiwalled carbon nanotubes can be sulphonated easily to attach -SO_3H groups with a high density of acid sites [3, 106]; however, activated carbon can hardly be sulphonated under the same conditions. In addition to the use of H_2SO_4 as S-source, some authors reported also the H_2SO_4/HNO_3 mixture for sulphonation of single walled and multiwalled carbon nanotubes [30, 109], or performed a pre-oxidation treatment with HNO_3 before sulphonation with H_2SO_4 [106]. Following the controlled hydrothermal functionalization (as that reported in *Chapter* 3 for HNO_3 oxidation), Morales-Torres et al. [7] proposed the same methodology for the hydrothermal oxidation with H_2SO_4 of single and multiwalled CNTs. A solution of H_2SO_4 (containing ammonium persulphate $(NH_4)_2S_2O_8$) was used as oxidizing agent and the synthesis carried out in autoclave at 200 °C. Still regarding nanostructured materials, sulphonated graphene has been also prepared by covalent attachment of -SO_3H-containing aryl radicals produced by homogeneous reduction of 4-benzene-diazoniumsulphonate using H_3PO_2 on the carbon surface [117]; by in situ formation of benzene sulphonic acid by treatment with sodium nitrite and sulphanilic acid [118] or obtained by sulphonation of GO using chlorosulphonic acid in chloroform [119], for instance. However, it can be also synthesized by the facile hydrothermal sulphonation of reduced graphene oxide with fuming H_2SO_4 at 180 °C [120].

Table II- 21 compares selected sulphonated carbon materials from the literature with those prepared in this work. Direct functionalization with

H_2SO_4 originates high incorporation of S-containing groups at low temperature or even at high temperature (250 °C [3]); however, in the last case the authors determined the SO_2 amount based on the uptake of NH_3 during NH_3 adsorption experiments. Regarding the hydrothermal methodology (CNT- H_2SO_4 HT samples), contrary to what was observed with HNO_3 (low acid concentration allowing similar functionalization as the conventional HNO_3 boiling approach), the hydrothermal treatment of CNT with H_2SO_4 revealed a weak incorporation of S-containing groups on the surface [120], but a considerable increase of surface functional groups that can be released as CO and CO_2. The simultaneous use of H_2SO_4/HNO_3 led to higher incorporation of -SO_3H; however, in this case a large amount of O-functionalities was also incorporated. Comparing the functionalization of the different carbon materials (ACs, CXs and CNTs), the sample CX-S1 presents the highest surface composition of -SO_3H groups, in spite of the moderate temperature used in the treatment.

Porous carbons functionalized with -SO_3H have been presented as environmental-friendly solid acid catalysts, and they are particularly important in reactions where typically liquid acids are used. Selected samples of this chapter will be tested as catalysts in the subsequent parts dedicated to evaluate the potential use of the carbon materials in acid catalysed reactions and in Catalytic Wet Air Oxidation.

Table II- 21. Chemical properties of SO_3H-doped carbon samples from the literature and comparison with prepared CX and CNT samples.

Sample	CO	CO_2	SO_2	Nature of S-groups	Ref.
	($\mu mol\ g^{-1}$)	($\mu mol\ g^{-1}$)	($\mu mol\ g^{-1}$)		
AC-H_2SO_4, conc (T=150 °C)	1560	260	680	$-SO_3H/-SH$[1]	[2]
CNT-H_2SO_4, conc (T=250 °C)	---	---	1900[2]	$-SO_3H$[3]	[3]
CNT- H_2SO_4, 0.3 M HT (T=200 °C)[a]	1312	471	81	$-SO_3H$	[7]
CNT- H_2SO_4, 0.3 M HT (T=200 °C)[b]	625	164	53		
CX-S1 (T=150 °C)	732	330	1623		
CNT-S (T=50 °C)	381	195	579	$-SO_3H$[1]	This work
CNT- NS (T=50 °C)	2035	1394	203		

[a] With and [b] without ammonium persulphate during the sulphonation; [1] Confirmed by XPS; [2] Based on the uptake of ammonia during ammonia adsorption experiments; [3] Identified by FTIR.

5.2. Partial Conclusions

The introduction of -SO_3H groups onto the carbon surface of CNTs and CXs has been successfully carried out using concentrated H_2SO_4 as sulphonation agent in a liquid-phase treatment, resulting materials with a strong acidic character. Without significant damage of the textural properties of the carbon materials, the incorporation of the -SO_3H groups on CX samples was found to be easier than in CNTs. The ratio between the mass of carbon material and the acid volume is crucial to reach a higher -SO_3H content. These groups also revealed low thermal stability, a large fraction being removed by thermal treatment until 250 °C. The -SO_3H groups were the only S-species identified by XPS analysis of the samples. In spite of that, small amounts of other O-containing groups are incorporated during the H_2SO_4 sulphonation treatment. In contrast, the treatment carried out with the H_2SO_4/HNO_3 mixture incorporates a large amount of carboxylic acids, anhydrides, phenols, carbonyl/quinone and lactone groups; however, a lower degree of S-functionalization was achieved.

(This page intentionally left blank)

6. Section Conclusions

Tuning carbon materials surface chemistry properties play an important role for the development of new carbon materials and their potential use as catalysts in different applications. Different heteroatoms can be successively attached to the carbon material surface like O, N, S, depending on the treatment performed.

An overview of the different possibilities for tuning the surface chemistry of carbon materials has been proposed with emphasis on their application in liquid-phase reactions, either as metal-free catalysts for environmental processes or as acid catalysts for acid catalysed reactions. The fine tuning allows a good distribution and arrangement of the heteroatoms in the graphitic lattice which is of a paramount importance concerning the catalytic behaviour of the materials.

Liquid-phase functionalization routes explored to incorporate different O, N and S heteroatoms onto the surface of carbon materials are schematically represented in Figure II- 26. Chemical treatments with HNO_3, H_2SO_4 and with a mixture of HNO_3/H_2SO_4 incorporate different O-containing groups (carboxylic acids, anhydrides, phenols, carbonyl/quinones, lactones) onto the surface of carbon materials or, when H_2SO_4 is employed, S-containing groups (such as -SO_3H groups). All these chemical treatments increase the acidic character of the CNTs, while thermal treatments remove the surface groups, simultaneously increasing the pH_{PZC} of the surface.

An alternative method to the chemical functionalization of CNTs by refluxing with concentrated HNO_3 can be achieved using hydrothermal oxidation. This methodology uses diluted concentrations of HNO_3 to

control the amount of oxygenated functionalities created on the surface. The method is quite effective, and the amount of oxygenated-surface groups can be correlated with the HNO_3 concentration.

Regarding liquid-phase functionalization, an ex-situ approach to incorporate nitrogen onto the carbon structure of carbon nanotubes has been proposed using urea as N-precursor. However, the method implicates multi-step procedures, like pre-oxidation of the surface, and does not allow high incorporation of N-functional groups. Alternatively, an easy to handle method to prepare N-doped carbon materials (CNTs and rGOs) was developed, involving a mechanical treatment under ball milling, followed by thermal treatment under inert atmosphere until 600 °C. In addition, the method avoids the use of solvents and production of wastes, and the incorporation of large amounts of N-groups (pyridine, pyrrole and quaternary nitrogen) is especially obtained using melamine as N-precursor. Furthermore, this method is easily scalable for practical applications, since the procedure does not require highly specialized and expensive equipment. Figure II- 27 schematically illustrates the novel easy method to prepare N-doped carbon nanotubes by ball milling.

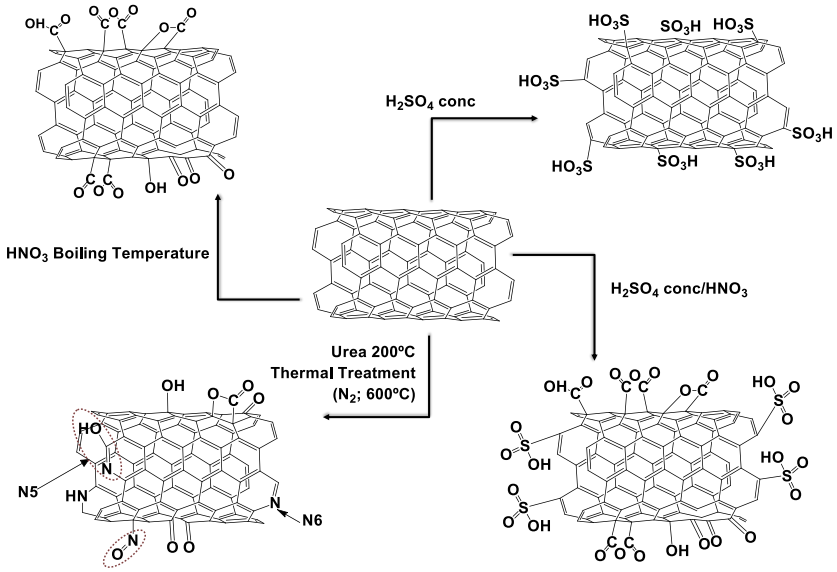

Figure II- 26. Schematic liquid-phase functionalization routes to incorporate different O, N, and S heteroatoms onto the surface of carbon nanotubes[25].

[25] Adapted from Chinese Journal of Catalysis 35 (2014) 896–905.

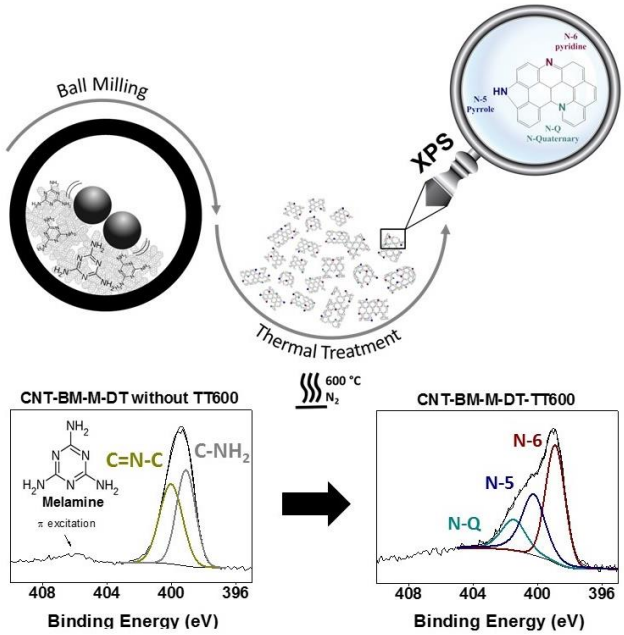

Figure II- 27. Illustration of the novel easy method to prepare N-doped carbon nanotubes by ball milling, with detailed N1s spectra evolution[26].

[26] Adapted from Journal of Carbon Research C, 2 (2016) 17.

References

[1] J.L. Figueiredo, M.F.R. Pereira, Carbon as Catalyst, Carbon Materials for Catalysis, John Wiley & Sons, Inc.2009, pp. 177-217.
[2] H.T. Gomes, S.M. Miranda, M.J. Sampaio, J.L. Figueiredo, A.M.T. Silva, J.L. Faria, The role of activated carbons functionalized with thiol and sulfonic acid groups in catalytic wet peroxide oxidation, Applied Catalysis B: Environmental, 106 (2011) 390-397.
[3] F. Peng, L. Zhang, H. Wang, P. Lv, H. Yu, Sulfonated carbon nanotubes as a strong protonic acid catalyst, Carbon, 43 (2005) 2405-2408.
[4] Nanocyl S.A. NANOCYLTM NC3100 series - Technical-Data-Sheet-NC3100-V05 (25 January 2016).
[5] C.M. White, R. Banks, I. Hamerton, J.F. Watts, Characterisation of commercially CVD grown multi-walled carbon nanotubes for paint applications, Progress in Organic Coatings, 90 (2016) 44-53.
[6] V. Stefov, M. Najdoski, G. Bogoeva-Gaceva, A. Buzarovska, Properties assessment of multiwalled carbon nanotubes: A comparative study, Synthetic Metals, 197 (2014) 159-167.
[7] S. Morales-Torres, T.L.S. Silva, L.M. Pastrana-Martinez, A.T.S.C. Brandao, J.L. Figueiredo, A.M.T. Silva, Modification of the surface chemistry of single- and multi-walled carbon nanotubes by HNO3 and H2SO4 hydrothermal oxidation for application in direct contact membrane distillation, Physical Chemistry Chemical Physics, 16 (2014) 12237-12250.
[8] J.-P. Tessonnier, D. Rosenthal, T.W. Hansen, C. Hess, M.E. Schuster, R. Blume, F. Girgsdies, N. Pfänder, O. Timpe, D.S. Su, R. Schlögl, Analysis of the structure and chemical properties of some commercial carbon nanostructures, Carbon, 47 (2009) 1779-1798.
[9] N. Mahata, A.R. Silva, M.F.R. Pereira, C. Freire, B. de Castro, J.L. Figueiredo, Anchoring of a [Mn(salen)Cl] complex onto mesoporous carbon xerogels, Journal of Colloid and Interface Science, 311 (2007) 152-158.
[10] N. Mahata, M.F.R. Pereira, F. Suárez-García, A. Martínez-Alonso, J.M.D. Tascón, J.L. Figueiredo, Tuning of texture and surface chemistry of carbon xerogels, Journal of Colloid and Interface Science, 324 (2008) 150-155.
[11] N. Job, R. Pirard, J. Marien, J.-P. Pirard, Porous carbon xerogels with texture tailored by pH control during sol–gel process, Carbon, 42 (2004) 619-628.
[12] P.V. Samant, F. Gonçalves, M.M.A. Freitas, M.F.R. Pereira, J.L. Figueiredo, Surface activation of a polymer based carbon, Carbon, 42 (2004) 1321-1325.
[13] L.M. Pastrana-Martínez, S. Morales-Torres, V. Likodimos, J.L. Figueiredo, J.L. Faria, P. Falaras, A.M.T. Silva, Advanced nanostructured photocatalysts based on reduced graphene oxide–TiO2 composites for degradation of diphenhydramine pharmaceutical and methyl orange dye, Applied Catalysis B: Environmental, 123-124 (2012) 241-256.

[14] W.S. Hummers, R.E. Offeman, Preparation of Graphitic Oxide, Journal of the American Chemical Society, 80 (1958) 1339-1339.
[15] S. Stankovich, D.A. Dikin, R.D. Piner, K.A. Kohlhaas, A. Kleinhammes, Y. Jia, Y. Wu, S.T. Nguyen, R.S. Ruoff, Synthesis of graphene-based nanosheets via chemical reduction of exfoliated graphite oxide, Carbon, 45 (2007) 1558-1565.
[16] M. Thommes, K. Kaneko, V. Neimark Alexander, P. Olivier James, F. Rodriguez-Reinoso, J. Rouquerol, S.W. Sing Kenneth, Physisorption of gases, with special reference to the evaluation of surface area and pore size distribution (IUPAC Technical Report), Pure and Applied Chemistry, 2015, pp. 1051.
[17] M. Ottaway, Use of thermogravimetry for proximate analysis of coals and cokes, Fuel, 61 (1982) 713-716.
[18] J. Rivera-Utrilla, I. Bautista-Toledo, M. Ferro-García, C. Moreno-Castilla, Activated carbon surface modifications by adsorption of bacteria and their effect on aqueous lead adsorption, Journal of Chemical Technology & Biotechnology, 76 (2001) 1209-1215.
[19] J.L. Figueiredo, M.F.R. Pereira, M.M.A. Freitas, J.J.M. Órfão, Modification of the surface chemistry of activated carbons, Carbon, 37 (1999) 1379-1389.
[20] J.L. Figueiredo, M.F.R. Pereira, M.M.A. Freitas, J.J.M. Órfão, Characterization of active sites on carbon catalysts, Industrial and Engineering Chemistry Research, 46 (2007) 4110-4115.
[21] P. Serp, J.L. Figueiredo, Carbon materials for catalysis, John Wiley & Sons, Hoboken, N.J., 2009.
[22] J.L. Figueiredo, Functionalization of porous carbons for catalytic applications, Journal of Materials Chemistry A, 1 (2013) 9351-9364.
[23] J.L. Figueiredo, M.F.R. Pereira, The role of surface chemistry in catalysis with carbons, Catalysis Today, 150 (2010) 2-7.
[24] T.J. Bandosz, Surface Chemistry of Carbon Materials, Carbon Materials for Catalysis, John Wiley & Sons, Inc.2008, pp. 45-92.
[25] D.S. Su, S. Perathoner, G. Centi, Nanocarbons for the Development of Advanced Catalysts, Chemical Reviews, 113 (2013) 5782-5816.
[26] A.G. Gonçalves, J.L. Figueiredo, J.J.M. Órfão, M.F.R. Pereira, Influence of the surface chemistry of multi-walled carbon nanotubes on their activity as ozonation catalysts, Carbon, 48 (2010) 4369-4381.
[27] O. Byl, J. Liu, J.T. Yates, Etching of Carbon Nanotubes by OzoneA Surface Area Study, Langmuir, 21 (2005) 4200-4204.
[28] A.M.T. Silva, B.F. Machado, J.L. Figueiredo, J.L. Faria, Controlling the surface chemistry of carbon xerogels using HNO3-hydrothermal oxidation, Carbon, 47 (2009) 1670-1679.
[29] R.R.N. Marques, B.F. Machado, J.L. Faria, A.M.T. Silva, Controlled generation of oxygen functionalities on the surface of Single-Walled Carbon Nanotubes by HNO3 hydrothermal oxidation, Carbon, 48 (2010) 1515-1523.
[30] F. Avilés, J.V. Cauich-Rodríguez, L. Moo-Tah, A. May-Pat, R. Vargas-Coronado, Evaluation of mild acid oxidation treatments for MWCNT functionalization, Carbon, 47 (2009) 2970-2975.

[31] V. Datsyuk, M. Kalyva, K. Papagelis, J. Parthenios, D. Tasis, A. Siokou, I. Kallitsis, C. Galiotis, Chemical oxidation of multiwalled carbon nanotubes, Carbon, 46 (2008) 833-840.
[32] K.S.W. Sing, Reporting physisorption data for gas/solid systems with special reference to the determination of surface area and porosity (Recommendations 1984), Pure and Applied Chemistry, 1985, pp. 603.
[33] I.D. Rosca, F. Watari, M. Uo, T. Akasaka, Oxidation of multiwalled carbon nanotubes by nitric acid, Carbon, 43 (2005) 3124-3131.
[34] G. Ovejero, J.L. Sotelo, M.D. Romero, A. Rodríguez, M.A. Ocaña, G. Rodríguez, J. García, Multiwalled carbon nanotubes for liquid-phase oxidation. Functionalization, characterization, and catalytic activity, Industrial and Engineering Chemistry Research, 45 (2006) 2206-2212.
[35] M. Monthioux, B.W. Smith, B. Burteaux, A. Claye, J.E. Fischer, D.E. Luzzi, Sensitivity of single-wall carbon nanotubes to chemical processing: an electron microscopy investigation, Carbon, 39 (2001) 1251-1272.
[36] H. Hu, B. Zhao, M.E. Itkis, R.C. Haddon, Nitric Acid Purification of Single-Walled Carbon Nanotubes, The Journal of Physical Chemistry B, 107 (2003) 13838-13842.
[37] J. Zhang, H. Zou, Q. Qing, Y. Yang, Q. Li, Z. Liu, X. Guo, Z. Du, Effect of Chemical Oxidation on the Structure of Single-Walled Carbon Nanotubes, The Journal of Physical Chemistry B, 107 (2003) 3712-3718.
[38] J.M. Calo, D. Cazorla-Amorós, A. Linares-Solano, M.C. Román-Martínez, C.S.-M. De Lecea, The effects of hydrogen on thermal desorption of oxygen surface complexes, Carbon, 35 (1997) 543-554.
[39] I. Gerber, M. Oubenali, R. Bacsa, J. Durand, A. Gonçalves, M.F.R. Pereira, F. Jolibois, L. Perrin, R. Poteau, P. Serp, Theoretical and Experimental Studies on the Carbon-Nanotube Surface Oxidation by Nitric Acid: Interplay between Functionalization and Vacancy Enlargement, Chemistry – A European Journal, 17 (2011) 11467-11477.
[40] G.E. Romanos, V. Likodimos, R.R.N. Marques, T.A. Steriotis, S.K. Papageorgiou, J.L. Faria, J.L. Figueiredo, A.n.M.T. Silva, P. Falaras, Controlling and Quantifying Oxygen Functionalities on Hydrothermally and Thermally Treated Single-Wall Carbon Nanotubes, The Journal of Physical Chemistry C, 115 (2011) 8534-8546.
[41] D.-Q. Yang, J.-F. Rochette, E. Sacher, Functionalization of Multiwalled Carbon Nanotubes by Mild Aqueous Sonication, The Journal of Physical Chemistry B, 109 (2005) 7788-7794.
[42] C. Moreno-Castilla, M.A. Ferro-Garcia, J.P. Joly, I. Bautista-Toledo, F. Carrasco-Marin, J. Rivera-Utrilla, Activated Carbon Surface Modifications by Nitric Acid, Hydrogen Peroxide, and Ammonium Peroxydisulfate Treatments, Langmuir, 11 (1995) 4386-4392.
[43] P. Clément, A. Ramos, A. Lazaro, L. Molina-Luna, C. Bittencourt, D. Girbau, E. Llobet, Oxygen plasma treated carbon nanotubes for the wireless monitoring of nitrogen dioxide levels, Sensors and Actuators B: Chemical, 208 (2015) 444-449.

[44] H.-P. Boehm, Catalytic Properties of Nitrogen-Containing Carbons, in: P. Serp,J.L. Figueiredo (Eds.), Carbon Materials for Catalysis, pp. 219-265, John Wiley & Sons, Inc. Hoboken, NJ 2009.
[45] H. Wang, T. Maiyalagan, X. Wang, Review on Recent Progress in Nitrogen-Doped Graphene: Synthesis, Characterization, and Its Potential Applications, ACS Catalysis, 2 (2012) 781-794.
[46] D. Yu, E. Nagelli, F. Du, L. Dai, Metal-Free Carbon Nanomaterials Become More Active than Metal Catalysts and Last Longer, Journal of Physical Chemistry Letters, 1 (2010) 2165-2173.
[47] B.M. Philippe Serp, CHAPTER 6 Doped Nanostructured Carbon Materials as Catalysts, Nanostructured Carbon Materials for Catalysis, The Royal Society of Chemistry2015, pp. 268-311.
[48] I. Pelech, O.S.G.P. Soares, M.F.R. Pereira, J.L. Figueiredo, Oxidative dehydrogenation of isobutane on carbon xerogel catalysts, Catalysis Today, 249 (2015) 176-183.
[49] C. Chen, J. Zhang, B. Zhang, C. Yu, F. Peng, D. Su, Revealing the enhanced catalytic activity of nitrogen-doped carbon nanotubes for oxidative dehydrogenation of propane, Chemical Communications, 49 (2013) 8151-8153.
[50] J.P.S. Sousa, M.F.R. Pereira, J.L. Figueiredo, NO oxidation over nitrogen doped carbon xerogels, Applied Catalysis B: Environmental, 125 (2012) 398-408.
[51] J.P.S. Sousa, A.M.T. Silva, M.F.R. Pereira, J.L. Figueiredo, Wet Air Oxidation of Aniline Using Carbon Foams and Fibers Enriched with Nitrogen, Separation Science and Technology, 45 (2010) 1546 - 1554.
[52] Y. Zhou, K. Neyerlin, T.S. Olson, S. Pylypenko, J. Bult, H.N. Dinh, T. Gennett, Z. Shao, R. O'Hayre, Enhancement of Pt and Pt-alloy fuel cell catalyst activity and durability via nitrogen-modified carbon supports, Energy & Environmental Science, 3 (2010) 1437-1446.
[53] L. Tao, Q. Wang, S. Dou, Z. Ma, J. Huo, S. Wang, L. Dai, Edge-rich and dopant-free graphene as a highly efficient metal-free electrocatalyst for the oxygen reduction reaction, Chemical Communications, 52 (2016) 2764-2767.
[54] S. Wang, L. Zhang, Z. Xia, A. Roy, D.W. Chang, J.B. Baek, L. Dai, Angew. Chem. Int. Ed., 51 (2012) 4209 - 4212.
[55] P. Ayala, R. Arenal, M. Ruemmeli, A. Rubio, T. Pichler, The doping of carbon nanotubes with nitrogen and their potential applications, Carbon, 48 (2010) 575-586.
[56] D.-V. Cuong, H. Ba, Y. Liu, T.-P. Lai, J.-M. Nhut, P.-H. Cuong, Nitrogen-doped carbon nanotubes on silicon carbide as a metal-free catalyst, Chinese Journal of Catalysis, 35 (2014) 906-913.
[57] S. Peng, K.J. Cho, Ab initio study of doped carbon nanotube sensors, Nano Letters, 3 (2003) 513-517.
[58] A. Zahoor, M. Christy, Y.J. Hwang, Y.R. Lim, P. Kim, K.S. Nahm, Improved electrocatalytic activity of carbon materials by nitrogen doping, Applied Catalysis B-Environmental, 147 (2014) 633-641.

[59] S. Kundu, W. Xia, W. Busser, M. Becker, D.A. Schmidt, M. Havenith, M. Muhler, The formation of nitrogen-containing functional groups on carbon nanotube surfaces: a quantitative XPS and TPD study, Physical Chemistry Chemical Physics, 12 (2010) 4351-4359.
[60] E.N. Nxumalo, P.J. Letsoalo, L.M. Cele, N.J. Coville, The influence of nitrogen sources on nitrogen doped multi-walled carbon nanotubes, Journal of Organometallic Chemistry, 695 (2010) 2596-2602.
[61] L. Zhao, L.-Z. Fan, M.-Q. Zhou, H. Guan, S. Qiao, M. Antonietti, M.-M. Titirici, Nitrogen-Containing Hydrothermal Carbons with Superior Performance in Supercapacitors, Advanced Materials, 22 (2010) 5202-+.
[62] G. Tuci, C. Zafferoni, P. D'Ambrosio, S. Caporali, M. Ceppatelli, A. Rossin, T. Tsoufis, M. Innocenti, G. Giambastiani, Tailoring Carbon Nanotube N-Dopants while Designing Metal-Free Electrocatalysts for the Oxygen Reduction Reaction in Alkaline Medium, ACS Catalysis, 3 (2013) 2108-2111.
[63] H.F. Gorgulho, F. Gonçalves, M.F.R. Pereira, J.L. Figueiredo, Synthesis and characterization of nitrogen-doped carbon xerogels, Carbon, 47 (2009) 2032-2039.
[64] N. Job, A. Théry, R. Pirard, J. Marien, L. Kocon, J.-N. Rouzaud, F. Béguin, J.-P. Pirard, Carbon aerogels, cryogels and xerogels: Influence of the drying method on the textural properties of porous carbon materials, Carbon, 43 (2005) 2481-2494.
[65] M. Pérez-Cadenas, C. Moreno-Castilla, F. Carrasco-Marín, A.F. Pérez-Cadenas, Surface Chemistry, Porous Texture, and Morphology of N-Doped Carbon Xerogels, Langmuir, 25 (2008) 466-470.
[66] C.P. Ewels, M. Glerup, Nitrogen doping in carbon nanotubes, Journal of Nanoscience and Nanotechnology, 5 (2005) 1345-1363.
[67] K.N. Wood, R. O'Hayre, S. Pylypenko, Recent progress on nitrogen/carbon structures designed for use in energy and sustainability applications, Energy & Environmental Science, 7 (2014) 1212-1249.
[68] E.K. Rideal, W.M. Wright, CLXXXIV.-Low temperature oxidation at charcoal surfaces. Part I. The behaviour of charcoal in the absence of promoters, Journal of the Chemical Society, Transactions, 127 (1925) 1347-1357.
[69] F. Adib, A. Bagreev, T.J. Bandosz, Adsorption/Oxidation of Hydrogen Sulfide on Nitrogen-Containing Activated Carbons, Langmuir, 16 (2000) 1980-1986.
[70] A. Bagreev, J. Angel Menendez, I. Dukhno, Y. Tarasenko, T.J. Bandosz, Bituminous coal-based activated carbons modified with nitrogen as adsorbents of hydrogen sulfide, Carbon, 42 (2004) 469-476.
[71] R. Arrigo, M. Hävecker, S. Wrabetz, R. Blume, M. Lerch, J. McGregor, E.P.J. Parrott, J.A. Zeitler, L.F. Gladden, A. Knop-Gericke, R. Schlögl, D.S. Su, Tuning the Acid/Base Properties of Nanocarbons by Functionalization via Amination, Journal of the American Chemical Society, 132 (2010) 9616-9630.
[72] J. Chen, X. Wang, X. Cui, G. Yang, W. Zheng, One-step synthesis of N-doped amorphous carbon at relatively low temperature as excellent metal-free electrocatalyst for oxygen reduction, Catalysis Communications, 46 (2014) 161-164.

[73] J.H. Ahn, H.S. Shin, Y.J. Kim, H. Chung, Structural modification of carbon nanotubes by various ball milling, Journal of Alloys and Compounds, 434 (2007) 428-432.
[74] W.M. Tucho, H. Mauroy, J.C. Walmsley, S. Deledda, R. Holmestad, B.C. Hauback, The effects of ball milling intensity on morphology of multiwall carbon nanotubes, Scripta Materialia, 63 (2010) 637-640.
[75] N. Pierard, A. Fonseca, J.F. Colomer, C. Bossuot, J.M. Benoit, G. Van Tendeloo, J.P. Pirard, J.B. Nagy, Ball milling effect on the structure of single-wall carbon nanotubes, Carbon, 42 (2004) 1691-1697.
[76] C.S. Wang, G.T. Wu, W.Z. Li, Lithium insertion in ball-milled graphite, Journal of Power Sources, 76 (1998) 1-10.
[77] J.Y. Huang, H. Yasuda, H. Mori, Highly curved carbon nanostructures produced by ball-milling, Chemical Physics Letters, 303 (1999) 130-134.
[78] Y.B. Li, B.Q. Wei, J. Liang, Q. Yu, D.H. Wu, Transformation of carbon nanotubes to nanoparticles by ball milling process, Carbon, 37 (1999) 493-497.
[79] Y. Oh, J. Choi, Y. Kim, K. Kim, S. Baik, The effects of ball milling process on the diameter dependent fracture of single walled carbon nanotubes, Scripta Materialia, 56 (2007) 741-744.
[80] O.S.G.P. Soares, A.G. Goncalves, J.J. Delgado, J.J.M. Órfão, M.F.R. Pereira, Modification of carbon nanotubes by ball-milling to be used as ozonation catalysts, Catalysis Today, 249 (2015) 199-203.
[81] F. Li, Y. Lu, L. Liu, L. Zhang, J. Dai, J. Ma, Relations between carbon nanotubes' length and their composites' mechanical and functional performance, Polymer, 54 (2013) 2158-2165.
[82] Á. Kukovecz, T. Kanyó, Z. Kónya, I. Kiricsi, Long-time low-impact ball milling of multi-wall carbon nanotubes, Carbon, 43 (2005) 994-1000.
[83] F. Béguin, E. Flahaut, A. Linares-Solano, J. Pinson, Surface Properties, Porosity, Chemical and Electrochemical Applications, in: A. Loiseau, P. Launois, P. Petit, S. Roche, J.-P. Salvetat (Eds.) Understanding Carbon Nanotubes: From Basics to Applications, Springer Berlin Heidelberg, Berlin, Heidelberg, 2006, pp. 495-549.
[84] A.P. Dementjev, A.d. Graaf, M.C.M.v.d. Sanden, K.I. Maslakov, A.V. Naumkin, A.A. Serov, X-Ray photoelectron spectroscopy reference data for identification of the C N phase in carbon-nitrogen films, Diamonds and Related Materials, (2000) 1904-1907.
[85] Journal of the Ceramic Society of Japan, Supplement 112-1, PacRim5 Special Issue 112 [5] (2010) S1408-S14010.
[86] N. Seetapan, N. Limparyoon, S. Kiatkamjornwong, Effect of fire retardant on flammability of acrylamide and 2-acrylamido-2-methylpropane sodium sulfonate copolymer composites, Polymer Degradation and Stability, 96 (2011) 1927-1933.
[87] M. Eichelbaum, R.J. Farrauto, M.J. Castaldi, The impact of urea on the performance of metal exchanged zeolites for the selective catalytic reduction of NOx: Part I. Pyrolysis and hydrolysis of urea over zeolite catalysts, Applied Catalysis B: Environmental, 97 (2010) 90-97.

[88] M.D. Stoller, S. Park, Y. Zhu, J. An, R.S. Ruoff, Graphene-Based Ultracapacitors, Nano Letters, 8 (2008) 3498-3502.
[89] V. Leon, M. Quintana, M.A. Herrero, J.L.G. Fierro, A.d.l. Hoz, M. Prato, E. Vazquez, Few-layer graphenes from ball-milling of graphite with melamine, Chemical Communications, 47 (2011) 10936-10938.
[90] S. Liu, Z. Chen, N. Zhang, Z.-R. Tang, Y.-J. Xu, An Efficient Self-Assembly of CdS Nanowires–Reduced Graphene Oxide Nanocomposites for Selective Reduction of Nitro Organics under Visible Light Irradiation, The Journal of Physical Chemistry C, 117 (2013) 8251-8261.
[91] P. Solís-Fernández, R. Rozada, J.I. Paredes, S. Villar-Rodil, M.J. Fernández-Merino, L. Guardia, A. Martínez-Alonso, J.M.D. Tascón, Chemical and microscopic analysis of graphene prepared by different reduction degrees of graphene oxide, Journal of Alloys and Compounds, 536 (2012) S532-S537.
[92] A. Lerf, H. He, M. Forster, J. Klinowski, Structure of Graphite Oxide Revisited, The Journal of Physical Chemistry B, 102 (1998) 4477-4482.
[93] L.M. Pastrana-Martínez, S. Morales-Torres, V. Likodimos, P. Falaras, J.L. Figueiredo, J.L. Faria, A.M.T. Silva, Role of oxygen functionalities on the synthesis of photocatalytically active graphene–TiO2 composites, Applied Catalysis B: Environmental, 158–159 (2014) 329-340.
[94] R.J.J. Jansen, H. van Bekkum, XPS of nitrogen-containing functional groups on activated carbon, Carbon, 33 (1995) 1021-1027.
[95] J.P.S. Sousa, M.F.R. Pereira, J.L. Figueiredo, Catalytic oxidation of NO to NO2 on N-doped activated carbons, Catalysis Today, 176 (2011) 383-387.
[96] K.S. Suslick, Mechanochemistry and sonochemistry: concluding remarks, Faraday Discussions, 170 (2014) 411-422.
[97] P.C. Ma, S.Q. Wang, J.-K. Kim, B.Z. Tang, In-Situ Amino Functionalization of Carbon Nanotubes Using Ball Milling, Journal of Nanoscience and Nanotechnology, 9 (2009) 749-753.
[98] Z. Zhao, Y. Dai, G. Ge, X. Guo, G. Wang, Nitrogen-doped carbon nanotubes via a facile two-step approach as an efficient catalyst for the direct dehydrogenation of ethylbenzene, Physical Chemistry Chemical Physics, 17 (2015) 18895-18899.
[99] X. Yuhua, C. Hao, Q. Jia, D. Liming, Nitrogen-doped graphene by ball-milling graphite with melamine for energy conversion and storage, 2D Materials, 2 (2015) 044001.
[100] T. Xing, J. Sunarso, W. Yang, Y. Yin, A.M. Glushenkov, L.H. Li, P.C. Howlett, Y. Chen, Ball milling: a green mechanochemical approach for synthesis of nitrogen doped carbon nanoparticles, Nanoscale, 5 (2013) 7970-7976.
[101] J. Zhu, J. Yang, R. Miao, Z. Yao, X. Zhuang, X. Feng, Nitrogen-enriched, ordered mesoporous carbons for potential electrochemical energy storage, Journal of Materials Chemistry A, 4 (2016) 2286-2292.
[102] I.-Y. Jeon, H.-J. Choi, S.-M. Jung, J.-M. Seo, M.-J. Kim, L. Dai, J.-B. Baek, Large-Scale Production of Edge-Selectively Functionalized Graphene Nanoplatelets via Ball Milling and Their Use as Metal-Free Electrocatalysts for Oxygen Reduction Reaction, Journal of the American Chemical Society, 135 (2013) 1386-1393.

[103] I.-Y. Jeon, S. Zhang, L. Zhang, H.-J. Choi, J.-M. Seo, Z. Xia, L. Dai, J.-B. Baek, Edge-Selectively Sulfurized Graphene Nanoplatelets as Efficient Metal-Free Electrocatalysts for Oxygen Reduction Reaction: The Electron Spin Effect, Advanced Materials, 25 (2013) 6138-6145.
[104] J. Xu, J. Shui, J. Wang, M. Wang, H.-K. Liu, S.X. Dou, I.-Y. Jeon, J.-M. Seo, J.-B. Baek, L. Dai, Sulfur–Graphene Nanostructured Cathodes via Ball-Milling for High-Performance Lithium–Sulfur Batteries, ACS Nano, 8 (2014) 10920-10930.
[105] R.H. Woodman, B.R. Klotz, R.J. Dowding, Evaluation of a dry ball-milling technique as a method for mixing boron carbide and carbon nanotube powders, Ceramics International, 31 (2005) 765-768.
[106] H. Yu, Y. Jin, Z. Li, F. Peng, H. Wang, Synthesis and characterization of sulfonated single-walled carbon nanotubes and their performance as solid acid catalyst, Journal of Solid State Chemistry, 181 (2008) 432-438.
[107] W. Kiciński, M. Szala, M. Bystrzejewski, Sulfur-doped porous carbons: Synthesis and applications, Carbon, 68 (2014) 1-32.
[108] M. Okamura, A. Takagaki, M. Toda, J.N. Kondo, K. Domen, T. Tatsumi, M. Hara, S. Hayashi, Acid-Catalyzed Reactions on Flexible Polycyclic Aromatic Carbon in Amorphous Carbon, Chemistry of Materials, 18 (2006) 3039-3045.
[109] S. Hanelt, G. Orts-Gil, J.F. Friedrich, A. Meyer-Plath, Differentiation and quantification of surface acidities on MWCNTs by indirect potentiometric titration, Carbon, 49 (2011) 2978-2988.
[110] R. Xing, Y. Liu, Y. Wang, L. Chen, H. Wu, Y. Jiang, M. He, P. Wu, Active solid acid catalysts prepared by sulfonation of carbonization-controlled mesoporous carbon materials, Microporous and Mesoporous Materials, 105 (2007) 41-48.
[111] E. Cano-Serrano, G. Blanco-Brieva, J.M. Campos-Martin, J.L.G. Fierro, Acid-Functionalized Amorphous Silica by Chemical Grafting−Quantitative Oxidation of Thiol Groups, Langmuir, 19 (2003) 7621-7627.
[112] J.G.C. Shen, R.G. Herman, K. Klier, Sulfonic Acid-Functionalized Mesoporous Silica: Synthesis, Characterization, and Catalytic Reaction of Alcohol Coupling to Ethers, The Journal of Physical Chemistry B, 106 (2002) 9975-9978.
[113] A.P. Terzyk, The influence of activated carbon surface chemical composition on the adsorption of acetaminophen (paracetamol) in vitro: Part II. TG, FTIR, and XPS analysis of carbons and the temperature dependence of adsorption kinetics at the neutral pH, Colloids and Surfaces A: Physicochemical and Engineering Aspects, 177 (2001) 23-45.
[114] Q. Yang, J. Liu, J. Yang, M.P. Kapoor, S. Inagaki, C. Li, Synthesis, characterization, and catalytic activity of sulfonic acid-functionalized periodic mesoporous organosilicas, Journal of Catalysis, 228 (2004) 265-272.
[115] H.T. Gomes, S.M. Miranda, M.J. Sampaio, A.M.T. Silva, J.L. Faria, Activated carbons treated with sulphuric acid: Catalysts for catalytic wet peroxide oxidation, Catalysis Today, 151 (2010) 153-158.
[116] A. Katsoni, H.T. Gomes, L.M. Pastrana-Martínez, J.L. Faria, J.L. Figueiredo, D. Mantzavinos, A.M.T. Silva, Degradation of trinitrophenol by sequential catalytic

wet air oxidation and solar TiO2 photocatalysis, Chemical Engineering Journal, 172 (2011) 634-640.
[117] J. Ji, G. Zhang, H. Chen, S. Wang, G. Zhang, F. Zhang, X. Fan, Sulfonated graphene as water-tolerant solid acid catalyst, Chemical Science, 2 (2011) 484-487.
[118] N. Oger, Y.F. Lin, E. Le Grognec, F. Rataboul, F.-X. Felpin, Graphene-promoted acetalisation of glycerol under acid-free conditions, Green Chemistry, 18 (2016) 1531-1537.
[119] P.P. Upare, J.-W. Yoon, M.Y. Kim, H.-Y. Kang, D.W. Hwang, Y.K. Hwang, H.H. Kung, J.-S. Chang, Chemical conversion of biomass-derived hexose sugars to levulinic acid over sulfonic acid-functionalized graphene oxide catalysts, Green Chemistry, 15 (2013) 2935-2943.
[120] F. Liu, J. Sun, L. Zhu, X. Meng, C. Qi, F.-S. Xiao, Sulfated graphene as an efficient solid catalyst for acid-catalyzed liquid reactions, Journal of Materials Chemistry, 22 (2012) 5495-5502.

(This page intentionally left blank)

PART III

Acid Catalysed Reactions

CONTENT

(This page intentionally left blank)

Introductory note

Esterification, etherification, hydration, hydrolysis, alkylation and isomerisation are well-known acid catalysed reactions [1]. In the absence of a catalyst, these reactions are too slow, therefore, they must be performed in the presence of a heterogeneous or homogeneous catalyst [2]. Esters are used in a wide range of chemical industries and are obtained from carboxylic acids or their derivatives. Ethyl acetate is one of the most important esters, and can be produced by the esterification of acetic acid with ethanol [3]. This reaction is also frequently used as a model reaction for acid catalysed reaction studies [4, 5]. Direct reaction between alcohol and carboxylic acid can be conducted under acid or base catalysis conditions; however, the first is the most popular method for esterification. Acid catalysts include Brønsted acids (such as HCl, HBr, H_2SO_4, $NaHSO_4$, H_3PO_4, HBF_4, etc.) and Lewis acids ($BF_3{\cdot}OEt_2$, $BlCl_3$, $AlCl_3$, 3,4,5-trifluorobenzeneboronic acid, etc.) as homogeneous catalysts [6], sulphuric acid being the most commonly employed catalyst. However, it is strongly corrosive, leaves sulphate residues [3] and its separation from the product is difficult and involves high energy consumption. Such drawbacks can be avoided by using a heterogeneous acid catalyst. Solid acids have a great advantage; they can be removed from the reaction mixture by filtration and thus applied to large-scale production [6]. Solids acids used as catalysts for esterification reactions include: Nafion-H, Amberlyst 15, zeolites, mesoporous silicas, phosphorus oxides, inorganic Sn- or Ti-based solid acids, heteropolyacids, acid catalysts supported in zirconia, silica gel, neutral alumina, activated carbon or ion-exchange resins [6].

In addition, carbon-based materials have been also reported in esterification reactions. Concerning non-porous carbons, sulphonation of incompletely carbonized naphthalene [7, 8] and carbonization of D-glucose followed by sulphonation with sulphuric acid [9] provide strong protonic carbon materials for the formation of ethyl acetate. The materials resulting from the thermal treatment of *p*-toluenesulphonic acid with D-glucose proved to be highly efficient solid-acid catalysts in reactions such as esterification of succinic acid with ethanol [10]. In addition, sulphonated carbonaceous materials prepared from lignosulphonate were shown to be comparable to the ion-exchange resin Amberlyst-15 in the esterification of cyclohexane carboxylic acid with anhydrous ethanol [11]. High catalytic activity in the esterification of acetic acid has been obtained using non-ordered mesoporous carbons using a sulphonated (SO_3H-bearing) carbon catalyst prepared by impregnating the cellulosic precursor (wood powder) with $ZnCl_2$ prior to activation and sulphonation in the work of Kitano et al. [12]. Sulphonated mesoporous carbonaceous material (Starbons-SO_3H) was reported by Budarin et al. [13] for the esterification of different organic acids with ethanol. Roldán et al. [14, 15] reported the use of sulphonated hydrothermal carbons (HTCs) as solid acid catalysts in esterification of palmitic acid with methanol, and even found that they benchmarked with a commercial activated carbon sulphonated by the same method. As an alternative to the non-ordered [7, 8] or nonporous carbons [12], Wang et al. reported the high catalytic activity of sulphonated ordered mesoporous carbon CMK-5 in ethyl acetate formation, with a better performance than Nafion in the same operating conditions [16]. On the esterification of oleic acid with ethanol, also Rui Lui and his collaborators tested sulphonated ordered mesoporous carbons

(OMC) synthesized by covalent attachment of sulphonic acid-containing aryl radicals [17].

Nanostructured carbon-based materials, as CNTs and graphene, are also catalyst candidates for acid-catalysed reactions. Functionalization with acidic sites with suitable hydrophobicity and controllable wettability can greatly improve reactants adsorption and hydrophilic products desorption, enhancing activity, stability and reusability in a variety of organic substrates [18].

Some carbon nanostructures have been already tested: sulphonated single walled CNTs were found a strong protonic acid catalyst for the production of ethyl acetate [19] and methyl acetate [20]. Poly (*p*-styrenesulphonate acid)-grafted multi-walled CNTs showed high catalytic activity in the esterification of lauric acid with methanol [21] and hydrothermal sulphating of reduced graphene oxide with fuming sulphuric acid provided a catalyst for the esterification of acetic acid with cyclohexanol [22].

In the present part, the effect of the different surface chemistry of CNTs and CXs prepared in Part II was evaluated in the esterification reaction of acetic acid with ethanol, as a model acid-catalysed reaction and their performances as solid acid catalysts compared with other reported carbon materials with sulphonic acid groups ($-SO_3H$).

Outline

The third part of this thesis starts with a description of the experimental system used to perform the catalytic studies and the analytical techniques adopted to assess the catalytic performance of strong acid carbon materials in the ethyl acetate formation by esterification of acetic acid with ethanol. Thereafter, catalytic activity and stability results are presented, and the obtained performances compared with reported results from the literature. The section ends with the more relevant conclusions concerning the use of strong acid carbon materials in acid catalysed reactions.

Most of the results presented in this section have been already reported in the paper *Carbon as a catalyst: Esterification of acetic acid with ethanol*, authored by Raquel P. Rocha, Manuel F.R. Pereira and José L. Figueiredo, and published in the journal Catalysis Today Volume 218-219 pages 51-56 (2013). Author Contributions: Raquel Rocha performed the synthesis, modification and characterization of the carbon samples and tested them in the esterification reaction. The manuscript was written by Raquel P. Rocha with substantial supervision of M.F.R. Pereira and J.L. Figueiredo.

1. Esterification of Acetic Acid with Ethanol

Carbon materials prepared and/or modified in *Part* II were selected for catalytic tests in the esterification of acetic acid with ethanol. The materials were chosen according to their textural and surface chemical properties with the aim to clarify their potential use as solid acid catalyst in acid catalysed reactions, using the esterification of acetic acid with ethanol as model reaction This is considered as a prototype for esterification reactions, and the reactants are small enough to minimize mass transfer limitations (the kinetic diameter of acetic acid is reported to be 0.436 nm [23]). Ethanol was chosen for the reaction due to the lower toxicity compared with methanol which is also a common short carbon chain alcohol used in the reaction.

Equation 1

$$CH_3COOH + CH_3CH_2OH \leftrightarrow CH_3COOCH_2CH_3 + H_2O$$

1.1. Experimental

1.1.1. Experimental Set-Up

The catalytic assessments of the acidic carbon materials in the esterification of acetic acid with ethanol (simplified non-catalytic chemical reaction given in Equation 1) were carried in a round-bottom flask with necks for sample extraction and for coupling a condenser, immersed in a paraffin thermostatic bath. Reactor heating and stirring are controlled by a stirrer hotplate, with integrated temperature and stirring control (Figure III- 1). A cylindrical Teflon coated magnetic stirrer bar was used to promote the continuous stirring inside the flask. The reactor was charged with 0.1 mol of acetic acid, 1 mol of ethanol and 0.20 g of catalyst and finally the temperature was set as 70 °C. The carbon material was recovered at the end of each run by filtration and washed several times with distilled water for further characterization, or for reutilization in cyclic experiments. A blank experiment without catalyst was also performed in the same conditions. For comparison, homogeneous catalysis using H_2SO_4 as catalyst was also studied.

In cyclic experiments, the same procedure was followed. After each experiment, the solution was filtered and the carbon sample washed with distilled water and dried, in order to be used in another run. This procedure was repeated two times (totalizing three consecutive runs). Reproducibility tests showed relative errors lower than $\pm$ 6 %.

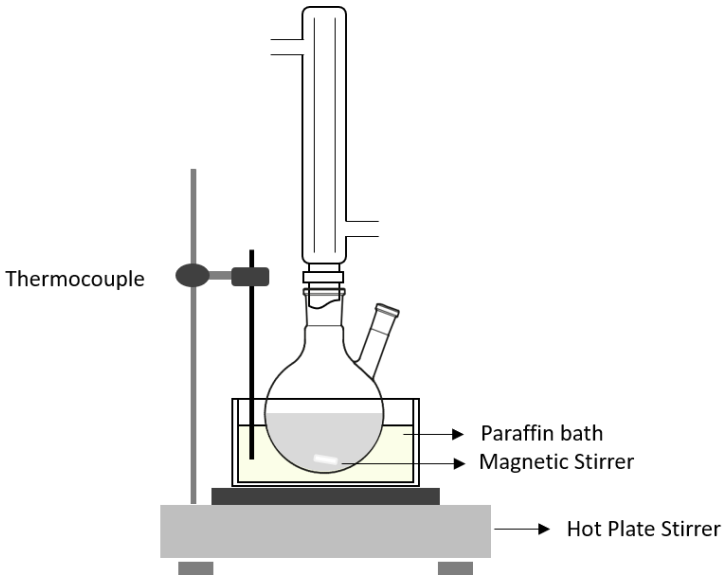

Figure III- 1. Scheme of the experimental set-up used.

1.1.2.Chemicals

Acetic acid (CH_3COOH, AcAc) at 99.7 %, ethyl acetate anhydrous 99.8 % ($CH_3CH_2COOCH_2CH_3$, EtAc) and sulphuric acid (H_2SO_4) with a nominal 95-98 % concentration used were purchased from Sigma Aldrich. Absolute ethanol (CH_3CH_2OH, EtOH) from Carlo Erba was used in the experiments.

1.1.3.Analytical Techniques

Samples periodically withdrawn from the reactor were analysed by high performance liquid chromatography (HPLC) with a HitachiElite LaChrom system equipped with ultraviolet (UV) and refractive index (RI) detectors in series. A Bio-Rad Aminex HPX-87Hcolumn (300 mm × 7.8 mm) working at room temperature and a 4 mmol L^{-1} H_2SO_4 solution as mobile phase (flow rate of 0.8 mL min^{-1}) were used. Acetic acid consumption was followed using the UV detector (λ = 210 nm), while ethyl acetate formation was followed by RI. Analyses were made using an injection volume of 15 μL. Calibration curves (2–0.1 mol L^{-1}) were made and linear responses were obtained in this range (R^2 of calibration lines higher than 0.99). The retention times for acetic acid and ethyl acetate were 11.8 and 22.3 min, respectively. All solutions and standard compounds were prepared with ultrapure water with a resistivity of 18.2 mΩ at room temperature, obtained from a Milllipore Mili-Q system.

1.2. Catalysts Evaluation

1.2.1.Catalysts

CNTs from NANOCYL™ NC3100 series and CXs prepared by the sol–gel process were modified by different chemical and thermal treatments with H_2SO_4 and HNO_3 in order to produce materials with different textural properties and acidic nature.

Liquid-phase oxidations were performed using a carbon material/HNO_3 ratio of 1:75 (w/v), at boiling temperature during 3 h, using different acid concentrations (7, 10 mol L^{-1} and concentrated). The resulting samples were designated in terms of the HNO_3 concentration as CNT-N7, CNT-N10 and CNT-Nc. A CXs oxidized with a 7 mol L^{-1} HNO_3 solution was also tested (CX-N). H_2SO_4-CX treated samples were obtained by liquid-phase chemical treatment at 150 °C during 6 h, using two carbon material/ H_2SO_4 solution ratios: 1:150 (w/v) (sample CX-S1) and 1:20 (sample CX-S2). An additional sample CX-S1-250 was prepared from sample CX-S1 subjected to an inert thermal treatment up to 250 °C. Detailed information about the methodologies used and thorough characterization of the samples have been presented in *Part II*. Table III- 1 briefly summarizes the more relevant properties of this group of samples to support the discussion of their catalytic performance.

Table III- 1. Relevant textural and chemical properties of the original and treated carbon materials tested in the esterification of acetic acid with ethanol.

Sample	S_{BET}	CO	CO_2	S_{XPS}
	($m^2\ g^{-1}$)	($\mu mol\ g^{-1}$)	($\mu mol\ g^{-1}$)	(% wt.)
CNT-N7	358	1453	1008	--------
CNT-Nc	312	1592	1422	-------
CX-N7	697	2414	1715	-------
CX-S1	416	732	330	3.18
CX-S2	528	657	191	1.89

The presence of sulphonic acid groups was identified by X-ray photoelectron spectroscopy on the H_2SO_4-treated samples. Carboxylic acids and anhydrides, phenols, some lactones and carbonyl-quinone groups were incorporated during the HNO_3 treatment, as shown by temperature programmed desorption. Oxidation with HNO_3 affects more the textural properties (the effect is more pronounced in the case of CNTs than in CXs) promoting an increase of surface area, while a decrease of surface area was observed with the H_2SO_4 treatment.

1.2.2.Catalytic Performance

The catalytic activity of the samples was evaluated in the esterification of acetic acid with ethanol as describe above. Catalyst evaluation is discussed in terms of ethyl acetate formation during the reaction time.

Figure III- 2 shows the yields of ethyl acetate achieved using selected samples. Under the operating conditions employed, the non-catalytic reaction can be neglected (Blank curve). Homogeneous catalytic reaction using the traditional Brønsted acid catalyst H_2SO_4 shows an extremely fast formation of ethyl acetate in one hour of reaction (more than 70 % of yield). From the solid catalysts tested, the sample functionalized with H_2SO_4 (CX-S1) was the most active, with a yield of 52 % after 6 h, followed by the CX-S2 and CNT-Nc samples. HNO_3-treated CX (CX-N7) revealed the worst performance.

However, it should be noted that the homogeneous reaction using H_2SO_4 was performed using an amount of acid density equivalent to that of the CX-S1 sample (1.80 mmol g^{-1}, determined by titration), but the acid density in the case of CX-S1 represents all acidic groups (including carboxylic acids, that are measurable by the titration technique) reason why the ethyl acetate rate formation using the CX-S1 sample is lower than the homogeneous catalyst.

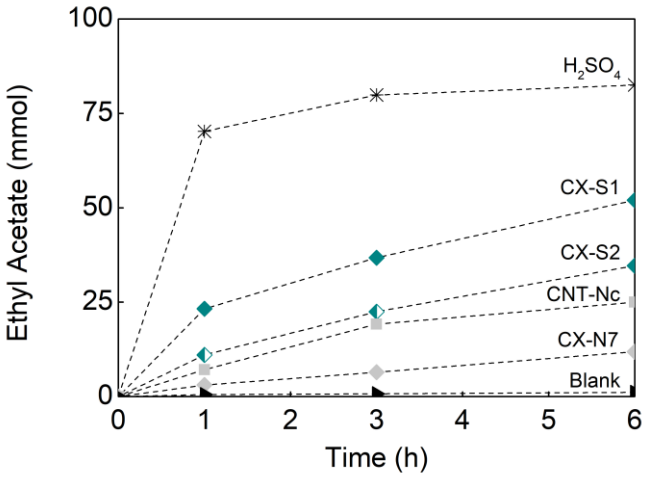

Figure III- 2. Ethyl acetate formation during the reaction time in non-catalytic experiment (Blank), using H_2SO_4 as homogeneous catalyst, and heterogeneous carbon materials as catalysts[27].

As shown in Figure III- 2, S-doped samples are highly active solid catalysts, whereas HNO_3 treated samples do not present appreciable catalytic activity. One possible explanation is the difference in the acidity (i.e., acid strength) of the samples. Since acidic groups of different nature were incorporated into two different types of carbon structures, the samples were divided in two groups for a better understanding of their catalytic performance: S containing samples (S-samples) (CX-S1, CX-S2, and CX-S1-250, in decreasing order of the S content) and HNO_3 functionalized samples (CNT-Nc, CX-N7, CNT-N10 and CNT-N7, in decreasing order of the carboxylic acid groups, released as CO_2). Regarding the S-samples, a good correlation is obtained between the rate of formation of ethyl acetate after 1 h and the concentration of SO_3H groups determined from XPS data (Figure III-3), showing that the catalytic activity is

[27] Adapted from Catalysis Today 218-219 (2013) 51-56.

proportional to the acid amount on the carbon surface. This means that it is possible to correlate the catalytic properties of the carbon materials with their surface chemistry. For the same reaction (esterification of ethyl acetate), Okamura et al. [9] reported a similar linear correlation between the catalytic activities and SO_3H densities over carbon materials obtained by sulphonation of carbonized D-glucose. However, reporting such correlations is not the general rule in the published literature.

With respect to the HNO_3-treated samples, the lower rates observed can be partially explained by the low acidity of the incorporated groups. In any case, it demonstrates that the HNO_3 treatment generates enough acidity in the material to be used as an acid catalyst, in spite of the low activity. The catalytic activity relates well to the amount of carboxylic acids determined by deconvolution of CO_2 profiles during the TPD analysis, as also shown in Figure III- 3. HNO_3-oxidized activated carbons were also found to be able to promote esterification of phenylacetic and benzoic acids with alcohols (ethanol, 1-butanol, 1-octanol). However, the increase in the alcohol chain length had a negative influence on the conversion [24]. Although the carboxylic acid groups underperform compared with $-SO_3H$ groups, the presence of functional groups such as -COOH and -OH has been reported to facilitate the reaction of levulinic acid with ethanol [25], presumably through hydrogen-bonding interaction between these surface functional groups and the γ-keto group of levulinic acid.

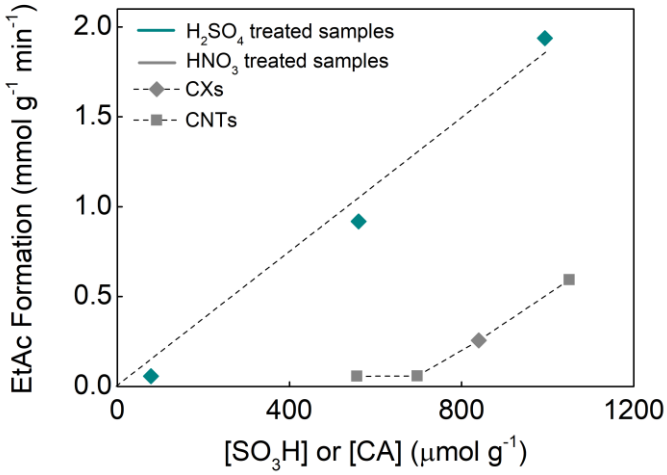

Figure III- 3. Ethyl acetate (EtAc) formation rate after 1 h using treated CX and CNT samples as function of the respective surface concentration of sulphonic (SO_3H)/carboxylic acid (CA) groups[28].

The catalytic stability of the sample CX-S1 was studied in three consecutive runs, which is an important factor when a new catalyst is being tested. Figure III- 4 shows the consecutive runs with fresh acetic acid and with the materials recovered after each run, as well as the rate of ethyl acetate formation for the first hour of reaction. In spite of the high activity shown in the first run, the catalytic performance of CX-S1 markedly decreases when reused in consecutive runs, more pronounced from the first to the second runs.

[28] Adapted from Catalysis Today 218-219 (2013) 51-56.

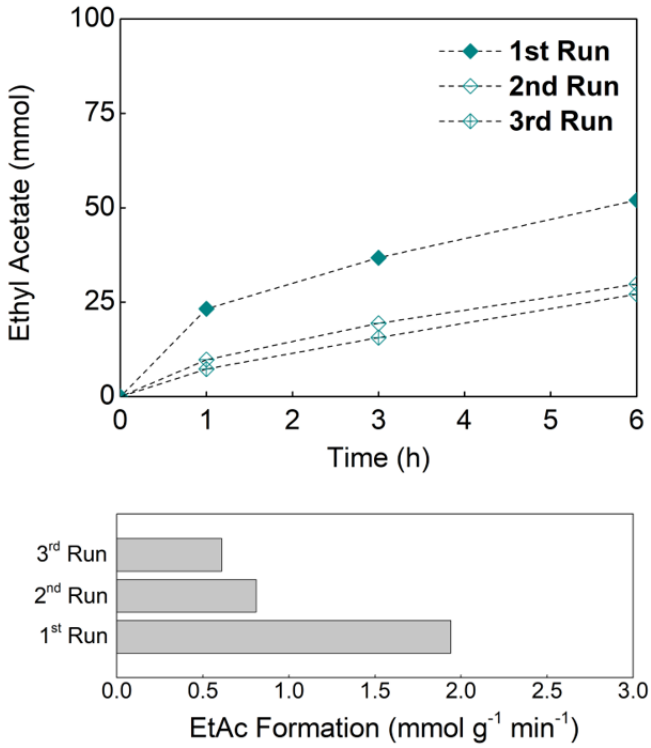

Figure III- 4. Ethyl acetate (EtAc) formation during the reaction time and rate of formation of ethyl acetate using the CX-S1 sample in the cyclic experiments[29].

After the third cycle, the material was characterized by TPD. The amount of SO_2 released, corresponding to the desorption of sulphonic groups, had decreased from 1623 to 1024 μmol g^{-1}, which could explain the decrease in catalytic activity.

Deactivation of sulphonated catalysts has been attributed to leaching of sulphonic/sulphated species [26, 27] or of soluble polycyclic aromatics with sulphonic groups [8, 21], hydrolysis of sulphonic groups [28], water and esters adsorption or even reaction of alcohol used with surface groups [26, 29]. On

[29] Adapted from Catalysis Today 218-219 (2013) 51-56.

the other hand, the decrease in catalytic performance can also be explained by formation of sulphonic esters, as reported by Fraile et al. [15]. According to their work, the formation of sulphonate esters accounts for the deactivation behaviour in reactions taking place in alcohol solvents, particularly using methanol, while leaching of sulphonated species has only a minor role in the deactivation. In the case of CX-S1 sample the decrease of around 37 % of the SO_2 groups evolved in TPD after reaction suggests that leaching of the sulphonic groups may be the reason for the observed deactivation.

Literature Overview

Although the esterification of acetic acid was performed with the aim of evaluating the acid strength of the prepared carbon materials, the obtained results can be compared with other reported carbon materials with sulphonic acid groups (-SO_3H). The turnover frequency (TOF) offers a straightforward way to compare data obtained in different laboratories [30]. A brief comparison with published results using similar operating conditions is shown in Table III- 2. Experiments had been carried out at 70 °C, using 0.1 mol of acetic acid to 1.0 mol of ethanol, and 0.2 g of catalyst.

Although the acidity of the samples was determined using different techniques, TOF of the CX-S1 sample prepared in this work (1.9 min^{-1}) is competitive with similar catalytic performances published in the literature, as single walled CNTs treated with H_2SO_4 (SWCNTs, TOF = 1.9 min^{-1}) [19], and with conventional strong solid acid catalysts, such as the protonated Nafion resin NR50, TOF = 1.5 min^{-1} [9]). It also performs better than carbon-based materials (CBM) prepared from glucose or naphthalene incomplete

carbonization. Thus, CXs with a strong acid character can be used as catalysts for the esterification of acetic acid, and the catalytic activity can be correlated with the amount of the strong acid sites. This methodology can be extended to other types of acid-catalysed reactions.

Table III- 2. Literature overview of TOF values obtained in esterification of acetic acid with ethanol using conventional strong acid catalysts and carbon-based materials and comparison with CX-S1 sample.

Catalyst	Acidity (mmol g^{-1})	TOF (min^{-1})	Ref.
Amberlyst 15	3.8[a,1]	0.2	[19]
SWCNT	0.67[c]	1.9	[19]
Nafion NR50	0.9[b]	1.5	[9]
Glucose CBM	1.3[b]	1.6	[9]
Naphtlene CBM	4.9[a]	1.4	[7]
CX-S	1.0[d]	1.9	This work

a) Determined by titration; b) Estimated from the S content in sample compositions determined by elemental analysis; c) related with the amount of adsorbed NH_3; d) based on the S content determined by XPS; 1 - taken from reference [31].

1.3. Section Conclusions

Oxidation of CNTs and xerogels with HNO_3 and H_2SO_4 increases their surface acidity, mainly as a result of the carboxylic acid and sulphonic acid groups formed, respectively. Due to the strong acidic character of S-doped carbon materials, they exhibit excellent performances as solid acid catalysts in the esterification of acetic acid with ethanol. The uncatalysed reaction can be neglected under the operating conditions employed; while the sample functionalized with H_2SO_4 (CX-S1) leads to an ethyl acetate yield of 52 % in 6 h of reaction. The sulphonic acid groups seem to be more adequate for this reaction than the acidic oxygen containing groups incorporated by oxidation with HNO_3. A good correlation was obtained between the rate of formation of ethyl acetate and the concentration of sulphonic acid groups in the case of H_2SO_4 treated samples. The turn-over frequency determined (1.9 min^{-1}) is competitive with other carbon-based materials reported in the literature, including with the conventional strong solid acid catalyst Nafion resin NR50 (TOF = 1.5 min^{-1}). As a result, H_2SO_4 treated CX can be an alternative to replace the strongly corrosive H_2SO_4, despite its lower rate of ethyl acetate formation compared with H_2SO_4, due to the great advantage of being easily separated from the reaction mixture by filtration. The potential of these carbon materials can be extended to other typically acid catalysed reactions such as etherification, hydration, hydrolysis, alkylation, acetalization and isomerisation reactions.

References

[1] J. Helminen, M. Leppamaki, E. Paatero, P. Minkkinen, Monitoring the kinetics of the ion-exchange resin catalysed esterification of acetic acid with ethanol using near infrared spectroscopy with partial least squares (PLS) model, Chemometrics and Intelligent Laboratory Systems, 44 (1998) 341-352.
[2] H.J. Arnikar, T.S. Rao, A.A. Bodhe, A gas chromatographic study of the kinetics of the uncatalysed esterification of acetic acid by ethanol, Journal of Chromatography A, 47 (1970) 265-268.
[3] J. Otera, J. Nishikido, Industrial Uses, Esterification, Wiley-VCH Verlag GmbH & Co. KGaA2010, pp. 293-322.
[4] J. Giménez, J. Costa, S. Cervera-March, Catalysis by ion-exchange sulfonated resins: Comparative study of gel and macroporous types and influence of divinylbenzene concentration, Applied Catalysis, 31 (1987) 221-234.
[5] J. Gimenez, J. Costa, S. Cervera, Vapor-phase esterification of acetic acid with ethanol catalyzed by a macroporous sulfonated styrene-divinylbenzene (20%) resin, Industrial & Engineering Chemistry Research, 26 (1987) 198-202.
[6] J. Otera, J. Nishikido, Reaction of Alcohols with Carboxylic Acids and their Derivatives, Esterification, Wiley-VCH Verlag GmbH & Co. KGaA2010, pp. 3-157.
[7] M. Hara, T. Yoshida, A. Takagaki, T. Takata, J.N. Kondo, S. Hayashi, K. Domen, A Carbon Material as a Strong Protonic Acid, Angewandte Chemie International Edition, 43 (2004) 2955-2958.
[8] X. Mo, D.E. Lopez, K. Suwannakarn, Y. Liu, E. Lotero, J.G. Goodwin, Jr., C. Lu, Activation and deactivation characteristics of sulfonated carbon catalysts, Journal of Catalysis, 254 (2008) 332-338.
[9] M. Okamura, A. Takagaki, M. Toda, J.N. Kondo, K. Domen, T. Tatsumi, M. Hara, S. Hayashi, Acid-Catalyzed Reactions on Flexible Polycyclic Aromatic Carbon in Amorphous Carbon, Chemistry of Materials, 18 (2006) 3039-3045.
[10] B. Zhang, J. Ren, X. Liu, Y. Guo, Y. Guo, G. Lu, Y. Wang, Novel sulfonated carbonaceous materials from p-toluenesulfonic acid/glucose as a high-performance solid-acid catalyst, Catalysis Communications, 11 (2010) 629-632.
[11] D. Lee, Preparation of a sulfonated carbonaceous material from lignosulfonate and its usefulness as an esterification catalyst, Molecules, 18 (2013) 8168-8180.
[12] M. Kitano, K. Arai, A. Kodama, T. Kousaka, K. Nakajima, S. Hayashi, M. Hara, Preparation of a Sulfonated Porous Carbon Catalyst with High Specific Surface Area, Catalysis Letters, 131 (2009) 242-249.
[13] V.L. Budarin, J.H. Clark, R. Luque, D.J. Macquarrie, Versatile mesoporous carbonaceous materials for acid catalysis, Chemical Communications, (2007) 634-636.
[14] L. Roldán, E. Pires, J.M. Fraile, E. García-Bordejé, Impact of sulfonated hydrothermal carbon texture and surface chemistry on its catalytic performance in esterification reaction, Catalysis Today, 249 (2015) 153-160.

[15] J.M. Fraile, E. García-Bordejé, L. Roldán, Deactivation of sulfonated hydrothermal carbons in the presence of alcohols: Evidences for sulfonic esters formation, Journal of Catalysis, 289 (2012) 73-79.
[16] X. Wang, R. Liu, M.M. Waje, Z. Chen, Y. Yan, K.N. Bozhilov, P. Feng, Sulfonated Ordered Mesoporous Carbon as a Stable and Highly Active Protonic Acid Catalyst, Chemistry of Materials, 19 (2007) 2395-2397.
[17] R. Liu, X. Wang, X. Zhao, P. Feng, Sulfonated ordered mesoporous carbon for catalytic preparation of biodiesel, Carbon, 46 (2008) 1664-1669.
[18] F. Liu, K. Huang, A. Zheng, F.-S. Xiao, S. Dai, Hydrophobic Solid Acids and Their Catalytic Applications in Green and Sustainable Chemistry, ACS Catalysis, (2017).
[19] H. Yu, Y. Jin, Z. Li, F. Peng, H. Wang, Synthesis and characterization of sulfonated single-walled carbon nanotubes and their performance as solid acid catalyst, Journal of Solid State Chemistry, 181 (2008) 432-438.
[20] F. Peng, L. Zhang, H. Wang, P. Lv, H. Yu, Sulfonated carbon nanotubes as a strong protonic acid catalyst, Carbon, 43 (2005) 2405-2408.
[21] X.-H. Zhang, Q.-Q. Tang, D. Yang, W.-M. Hua, Y.-H. Yue, B.-D. Wang, X.-H. Zhang, J.-H. Hu, Preparation of poly(p-styrenesulfonic acid) grafted multi-walled carbon nanotubes and their application as a solid-acid catalyst, Materials Chemistry and Physics, 126 (2011) 310-313.
[22] F. Liu, J. Sun, L. Zhu, X. Meng, C. Qi, F.-S. Xiao, Sulfated graphene as an efficient solid catalyst for acid-catalyzed liquid reactions, Journal of Materials Chemistry, 22 (2012) 5495-5502.
[23] T.C. Bowen, R.D. Noble, J.L. Falconer, Fundamentals and applications of pervaporation through zeolite membranes, Journal of Membrane Science, 245 (2004) 1-33.
[24] D.M. Nevskaia, R.M. Martín-Aranda, Nitric Acid-Oxidized Carbon for the Preparation of Esters Under Ultrasonic Activation, Catalysis Letters, 87 (2003) 143-147.
[25] I. Ogino, Y. Suzuki, S.R. Mukai, Esterification of levulinic acid with ethanol catalyzed by sulfonated carbon catalysts: Promotional effects of additional functional groups, Catalysis Today, (2017).
[26] J.A. Melero, L.F. Bautista, G. Morales, J. Iglesias, D. Briones, Biodiesel Production with Heterogeneous Sulfonic Acid-Functionalized Mesostructured Catalysts, Energy & Fuels, 23 (2009) 539-547.
[27] K. Suwannakarn, E. Lotero, J.G. Goodwin, C. Lu, Stability of sulfated zirconia and the nature of the catalytically active species in the transesterification of triglycerides, Journal of Catalysis, 255 (2008) 279-286.
[28] X. Tian, L.L. Zhang, P. Bai, X.S. Zhao, Sulfonic-acid-functionalized porous benzene phenol polymer and carbon for catalytic esterification of methanol with acetic acid, Catalysis Today, 166 (2011) 53-59.
[29] J.A. Melero, L.F. Bautista, G. Morales, J. Iglesias, R. Sánchez-Vázquez, Biodiesel production from crude palm oil using sulfonic acid-modified mesostructured catalysts, Chemical Engineering Journal, 161 (2010) 323-331.

[30] M. Boudart, Turnover Rates in Heterogeneous Catalysis, Chemical Reviews, 95 (1995) 661-666.
[31] R. Jia, J. Ren, X. Liu, G. Lu, Y. Wang, Design and synthesis of sulfonated carbons with amphiphilic properties, Journal of Materials Chemistry A, 2 (2014) 11195-11201.

(This page intentionally left blank)

PART IV

Catalytic Wet Air Oxidation

CONTENT

(This page intentionally left blank)

Introductory note

Wet air oxidation (WAO) is an advanced oxidation process (AOP) developed to remove organic contaminants from water and to treat highly polluted wastewater by oxidation [1, 2]. Under non-catalytic conditions, WAO requires high temperatures (200-320 °C) and pressures (20-200 bar) to operate [3-5]. However, the introduction of a homogeneous or heterogeneous catalyst can increase the process efficiency under less severe conditions (130-250 °C; 5-50 bar) [6, 7]. Although noble metals or metal oxides can be used as catalysts in catalytic wet air oxidation (CWAO), they are prone to leaching and deactivation phenomena, which affect the design of a clean technology [7, 8]. In this context, metal-free carbon materials provide an alternative to replace metal-based catalysts. The catalytic activity of carbon materials in oxidation processes can be enhanced by modification of their textural and chemical properties [9]. While the effect of the textural properties (such as pore size and surface area) in the catalytic activity in CWAO is well understood [10], the role of surface chemistry is still not completely established. A systematic study was performed to assess the influence of O, S, and N heteroatoms on the surface of carbon materials in CWAO. For this goal, carbon materials with different surface chemical properties prepared/modified in *Part* II, including carbon nanotubes (CNTs), carbon xerogels (CXs) and graphene-based materials (rGOs), were tested as catalysts in the oxidation of two model compounds (oxalic acid and phenol) by CWAO. The performance of the catalysts was then related to their chemical properties, and the oxidation mechanisms with different surface groups were discussed.

Outline

The fourth part of this thesis is organized in three main chapters. A description of the experimental system used to perform the studies and the analytical techniques adopted to assess the catalytic performance of the tested carbon materials is presented in *Chapter 1*. The catalytic performance of different metal-free carbon materials is presented in *Chapter* 2. Catalyst evaluation begins with a preliminary assessment using CNTs with different chemical properties (from acidic to basic surface) (*Chapter 2.1*). Based on the conclusions of this first study, two sections follow: the first one dedicated to investigate the influence of acidic surface groups (*Chapter 2.2*) and the second one illustrating the influence of nitrogen-functional groups (*Chapter 2.3*). In the latter, the study is extended to other carbon materials other than CNTs, namely rGOs and CXs. Then, the mechanism of CWAO in the presence of metal-free carbon materials with different functional groups is discussed (*Chapter 2.4*). The section ends with the most relevant conclusions concerning the use of metal-free carbon catalysts in CWAO (*Chapter* 3), including an overview of their opportunity as catalysts, evidencing their strengths and weaknesses for real applications.

1. Experimental

1.1. Experimental Set-Up

The catalytic assessment of metal-free carbon materials was carried out in a 160 mL 316-stainless steel high pressure batch reactor (Parr Instruments, USA Mod. 4564) (Figure IV- 1).

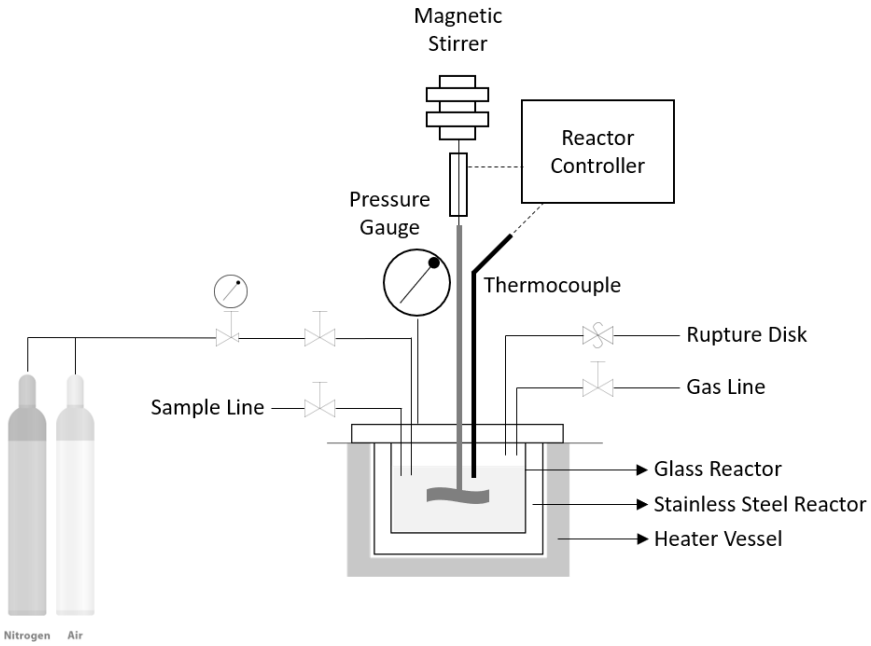

Figure IV- 1. Scheme of the batch experimental set-up used.

A glass cylinder inside the reactor is used to prevent possible catalytic effects due to the reactor building material and in order to minimize corrosion problems [11]. Reactor heating and stirring are controlled by the coupled PARR 4842 controller. A type J thermocouple in direct contact with the liquid solution is used to control the temperature inside the

reactor. Gases are fed to the reactor by a high-pressure line, bubbling directly into the liquid phase. This allows a better dispersion of the gas phase in the liquid phase, reducing the mass transfer limitations at the gas-liquid interface. Liquid aliquots are recovered by a sampling line. The reactor is also equipped with a gas outlet line and a safety rupture disk.

Experiments presented in *Chapter 2.1* were performed by injection of a concentrated solution of the model compound (oxalic acid) into the reactor, while solutions of the model compounds at the desired concentrations were placed into the reactor before heating the system in the case of the experiments described in the remaining chapters. This second approach could be applied because the model pollutants selected (oxalic acid and phenol) are thermally stable during heating, and no thermal decomposition of the organic compounds occurs. By replacing the injection system, a faster dispersion of the gas phase in the liquid phase is achieved, minimizing diffusional limitations at the beginning of the reaction. This is particularly important when a fast degradation of the pollutant in study is observed (in the presence of highly efficient catalysts), ensuring that the initial reaction phase is well characterized.

Experiments of *Chapter* 2.1

In experiments by injection, 70 mL of ultrapure water and 0.2 g of catalyst were placed into the reactor. The reactor was flushed with pure nitrogen until the complete removal of oxygen, and then pressurized with 5 bar of nitrogen and pre-heated up to the desired temperature (T=140 °C) under continuous stirring. When the desired temperature was reached, 5 mL of a concentrated oxalic acid solution was injected with pure air, an oxalic acid concentration of 1000 mg L^{-1} being obtained inside the reactor

at a total pressure of 40 bar (32 bar of air pressure), corresponding to 7 bar of oxygen partial pressure. This was considered as time zero for the reaction (t=0 min).

Experiments of *Chapters* 2.2-2.4

In the remaining experiments, 75 mL of an aqueous solution of the model organic compound and a desired mass of catalyst were placed into the reactor. The reactor was flushed with pure nitrogen until the complete removal of oxygen, and then pressurized with 5 bar of nitrogen and pre-heated up to the desired temperature under continuous stirring. When the desired temperature was reached, pure air was injected to obtain a total pressure of 40 bar inside the reactor (corresponding to 7 bar of O_2 partial pressure), this being considered time zero for the reaction (t=0 min).

The oxidation reaction depends on the concentration of oxygen in the liquid phase [12]. Therefore, the temperatures, pressures and the initial concentrations of model compounds were selected after preliminary experiments and by taking into account the concentration of oxygen that is dissolved in the liquid phase at the selected temperatures and pressures.

CWAO of oxalic acid was performed at 140 °C using an initial solution concentration of 1000 mg L^{-1}. Preliminary non-catalytic experiments showed that thermolysis of the oxalic acid could occur at higher temperatures (above 180 °C), and that at a lower temperature (120 °C) the availability of dissolved oxygen in solution might be compromised. Therefore, 140 °C and a total pressure of 40 bar were chosen to perform the WAO and CWAO studies using oxalic acid. At this temperature, the

oxygen partial pressure corresponds to 7 bar, considering the water vapour pressure at the selected temperature (3.6 bar) and the admission of air as oxidant (excess of oxygen). According to the simplified chemical equations for oxalic acid and phenol oxidation (Equation 1 and Equation 3, respectively), for similar molar contents of oxalic acid and phenol, more oxygen is required for the oxidation of phenol. Therefore, a low phenol concentration (75 mg L^{-1}) was chosen, ensuring that enough dissolved oxygen was available to degrade phenol at the selected temperature (160 °C) and keeping the same total system pressure (P_T= 40 bar).

Equation 2

$$2C_2H_2O_4 + O_2 \rightarrow 4CO_2 + 2H_2O$$

Equation 3

$$C_6H_6O + 7O_2 \rightarrow 6CO_2 + 3H_2O$$

All experiments were performed under continuous stirring at 500 rpm in order to ensure proper mass transfer of air in the liquid phase [13, 14] and at natural pH (around 3 for oxalic acid and around 6 for phenol).

The carbon material was recovered at the end of each run by filtration and washed several times with distilled water for further characterization, or for reutilization in cyclic experiments. When required, cyclic experiments were performed to evaluate the catalyst lifetime using the same operating conditions (T, P, catalyst amount and fresh solutions of the model pollutants). Due to the loss of sample mass occurring in each test, as a result of the aliquots collection or during the filtration at the end of the experiment, duplicate and triplicate experiments were performed to

recover enough catalyst for further utilization. Materials were recovered and mixed after each run, and used in the next cycles. Adsorption experiments (Ads) were also performed in the autoclave under similar experimental conditions, but replacing air by pure nitrogen (40 bar of total pressure). Non-catalytic oxidation runs were carried out with air in the absence of catalyst, experiments denoted as WAO experiments. Reproducibility tests showed relative errors lower than ±5 %.

1.2. Chemicals

Oxalic acid (OxAc) in the form of white crystals (≥ 99 %), phenol (Ph) as transparent crystalline powder (≥ 99 %), hydroquinone (HQ) (≥ 99 %), and sodium persulphate (≥ 99 %) white solids, and *tert*-Butanol (*t*-BuOH) liquid (≥99.5 %) were purchased from Sigma-Aldrich. 1,4-Hydroquinone (≥99.5 %) from ACROS Organics was also used.

All solutions were prepared with ultrapure water with a resistivity of 18.2 mΩ at room temperature, obtained from a Milllipore Mili-Q system.

High-purity synthetic air in a compressed gas cylinder ALPHAGAZ 1 grade with a purity of 99.999 % from Air Liquide was used as oxygen source. Pure nitrogen in a compressed gas cylinder ALPHAGAZ 1 grade with a purity of 99.999 % from Air Liquide was used in the adsorption experiments and for purging.

1.3. Analytical Techniques

Liquid aliquots (around 1 mL) were withdrawn from the reactor during reaction and centrifuged for further analysis. The volume of samples periodically withdrawn was limited to 10 % of the total volume in order to ensure that the total system volume and concentration of the catalyst in solution were kept constant.

The samples were analysed by high performance liquid chromatography (HPLC) with a Hitachi Elite LaChrom system equipped with a Diode Array Detector (L-2450). A Bio-Rad Aminex HPX-87H column (300 mm x 7.8 mm) working at room temperature in isocratic elution mode with a 4 mmol L^{-1} H_2SO_4 solution as mobile phase (flow rate of 0.6 cm^3 min^{-1}) was used for oxalic acid identification and quantification (performed at λ = 210 nm). In selected experiments, the determination of oxalic acid concentration was performed using an Alltech OA-1000 column (300 mm ×6.5 mm) and a H_2SO_4 solution (5 mmol L^{-1}) at a flow rate of 0.6 cm^3 min^{-1} (as mobile phase) at λ = 200 nm. Analyses were made using an injection volume of 15 μL. Calibration curves (5–1200 mg L^{-1}) were made and linear responses were obtained in this range (R^2 of calibration lines higher than 0.999).

In phenol oxidation experiments, the samples were analysed in a Purospher Star RP-18 endcapped column (250 mm × 4.6 mm, 5 μm particles) working at room temperature. The mobile phase was a mixture of water and methanol 40/60 (v/v) (isocratic elution mode) with a flow rate of 1 cm^3 min^{-1}. Phenol was determined at λ = 270 nm. Analyses were made using an injection volume of 50 μL. Calibration curves (2.5 – 100 mg L^{-1}) were made and linear responses were obtained in this range

(R^2 of calibration lines higher than 0.999). For the possible products of phenol degradation, hydroquinone (HQ) and benzoquinone (BQ), analyses were performed using the same method but determined at λ = 290 nm and 245 nm, respectively. Calibration curves (2.5–75 mg L^{-1}) were made and linear responses were obtained in this range (R^2 of calibration lines higher than 0.999), in both cases.

All solutions and standard compounds were prepared with ultrapure water with a resistivity of 18.2 mΩ at room temperature, obtained from a Milllipore Mili-Q system. A maximum relative standard deviation of 2 % was accepted in the analyses.

The total organic carbon (TOC) was also determined at the end of each experiment, using a Shimadzu TOC-5000A analyser. The pH variation during the experiments was also recorded.

(This page intentionally left blank)

2. Catalyst Evaluation

Carbon materials prepared and/or modified in *Part* II were selected for catalytic tests in the degradation of model pollutants by CWAO. The materials were chosen according to their textural properties and surface chemistry, with the aim to clarify their potential use as metal-free catalysts in the degradation of organic compounds by CWAO. Moreover, catalyst evaluation was outlined with the ambition to clarify the more adequate properties and type of carbon materials and to elucidate the mechanism behind the use of carbon materials in the selected application.

Oxalic acid and phenol (Figure IV- 2) were selected as model compounds to perform the studies and to evaluate the process efficiency. Oxalic acid is representative of short chain carboxylic acids, which are typical refractory compounds appearing as end-products in advanced oxidation processes, while phenol is a more complex aromatic organic compound, commonly found in industrial effluents, but also an extensively studied molecule in the literature.

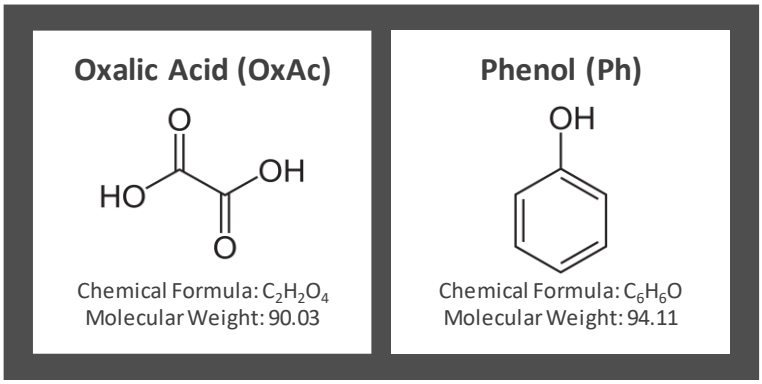

Figure IV- 2. Selected model compounds for degradation by CWAO.

2.1. Preliminary Assessment

Organic pollutants can diffuse easily through meso- and macropores, where the degradation takes place at a faster rate than in the micropores [15]. Therefore, mesoporous carbons with high external surface area are usually more efficient for CWAO processes than carbon materials that are essentially microporous. In this context, CNTs are very attractive materials for CWAO, where the accessibility of the solution and, consequently, of the dissolved pollutants to the carbon surface is expected to be easier than when using activated carbons (ACs), which are typical microporous materials [16]. An exploratory study was carried out to assess the role of the basic nature induced by the surface chemistry on the catalytic activity and stability of commercial multiwalled CNTs in CWAO of oxalic acid. CNTs modified by chemical and thermal treatments, presenting different surface chemical properties, from acidic to neutral character, were used in the survey. They were directly applied as catalysts in CWAO, without any impregnated metal.

Most of the results presented in this section have been already reported in the paper *Catalytic activity and stability of multiwalled carbon nanotubes in catalytic wet air oxidation of oxalic acid: The role of the basic nature induced by the surface chemistry*, authored by Raquel P. Rocha, Juliana P.S. Sousa, Adrián M.T. Silva, Manuel F.R. Pereira and José L. Figueiredo, and published in the journal Applied Catalysis B: Environmental Volume 104 pages 330–336 (2011). Author Contributions: Raquel Rocha performed the modification and CWAO catalytic tests of CNT samples, kindly assisted by J.P.S. Sousa. The manuscript was written by

R.P. Rocha under the supervision of Adrián M.T. Silva, M.F.R. Pereira and J.L. Figueiredo.

2.1.1.Catalysts

CNTs from NANOCYL^{TM} NC3100 series were used as catalysts with and without different oxidation and/or thermal treatments. Four samples were selected: CNT-O, CNT-N, CNT-NU, CNT-NUT. The original material (CNT-O) was first treated with HNO_3 (CNT-N) at boiling temperature. A subsequent hydrothermal treatment with urea was carried out at 200 °C (sample CNT-NU). Then, a gas-phase thermal treatment until 600 °C was applied to this sample (sample CNT-NUT). Detailed information about the methodologies used and thorough characterization of the samples were presented in *Part II*. Table IV- 1 briefly summarizes the most relevant properties of this group of samples to support the discussion of their catalytic performance.

Table IV- 1. Relevant textural and chemical properties of the pristine and treated CNTs for the preliminary assessment.

Sample	S_{BET}	CO	CO_2	N_{EA}	pH_{PZC}
	($m^2\ g^{-1}$)	($\mu mol\ g^{-1}$)	($\mu mol\ g^{-1}$)	(% wt.)	(unitless)
CNT-O	302	200	26	0.15	6.8
CNT-N	351	1710	909	0.30	2.8
CNT-NU	351	1172	607	1.12	5.4
CNT-NUT	386	703	76	0.91	7.3

Texturally, the CNT samples do not present significant differences regarding the BET surface areas (lower than 100 m^2 g^{-1}). On the other hand, they revealed strong different chemical properties regarding oxygen and nitrogen contents, and, consequently, different surface character, ranging from acidic to neutral/basic.

2.1.2.Catalytic Performance

The catalytic activity of the CNT samples was evaluated in the oxidation of oxalic acid by CWAO. Non-catalytic (WAO) and catalytic experiments were conducted at 140 °C and 40 bar of total pressure, corresponding to 32 bar of air pressure. Adsorption (Ads) experiments were performed under identical experimental conditions (P, T, amount of CNTs), but replacing air by pure nitrogen. A catalyst load of 0.2 g was used in the catalytic and adsorption assessments. Catalyst evaluation is discussed in terms of the normalized model pollutant concentration (C/C_0) as a function of time in the experiments.

From Figure IV- 3 it can be observed that oxalic acid is poorly oxidized under the operating conditions employed in the absence of a catalyst, while the CNT materials show high catalytic activity, with almost complete degradation of oxalic acid after 120 min of reaction, regardless of the sample tested (pristine and treated).

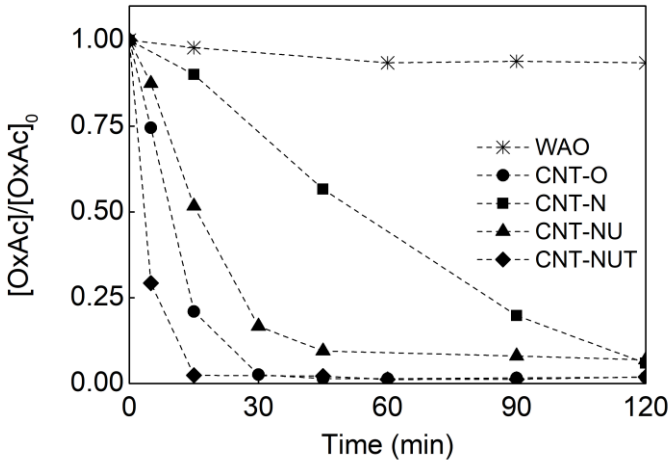

Figure IV- 3. Evolution of normalized oxalic acid concentration at 140 °C and 40 bar of total pressure under non-catalytic conditions (WAO) and preliminary catalytic experiments in CWAO[30].

Oxalic acid is selectively converted into CO_2, because no by-products were detected by HPLC analysis and the TOC removal is equal to the oxalic acid disappearance. The results obtained with all the CNT samples under inert atmosphere (N_2) were similar to those obtained in non-catalytic conditions (adsorption experiments of CNT-O and CNT-NUT illustrated in Figure IV- 5).

These results allow to conclude that:

(i) oxalic acid is thermally stable at 140 °C and 40 bar;

(ii) the homogeneous non-catalytic oxidation of oxalic acid can be neglected at the studied operating conditions;

(iii) there is no contribution from adsorption in the removal of oxalic acid;

[30] Adapted from Applied Catalysis B: Environmental 104 (2011) 330–336.

(iv) CNTs are very active catalysts for CWAO degradation of oxalic acid even without any supported metal.

Among the materials tested, the best performance was obtained with CNT-NUT, oxidizing more than 95 % of the initial oxalic acid concentration in 15 min. For this same period, the original CNTs (CNT-O) also present a high activity with about 80 % of oxalic acid degradation, while only 10 % and 48 % were achieved for CNT-N and CNT-NU, respectively. These results indicate that CNT-O and CNT-NUT were the best catalysts, leading to complete degradation of oxalic acid after 30 min. In contrast CNT-N shows the worst performance among the CNTs tested, with an extremely slow oxidation of oxalic acid in comparison to the other materials.

The textural properties of the tested samples are relatively similar, and no correlation was found between the catalytic activity and the surface area of these materials (Table IV- 1). With respect to the type of N groups, no correlation was found because the type of N groups is very different between the samples. However, it seems that pyridinic groups (N6) may play an important role in the degradation of oxalic acid by CWAO because they were only observed for the most active sample (CNT-NUT). In fact, Sousa et al. [17] found a linear correlation between the total organic carbon removal in aniline degradation by CWAO and the N6 content of carbon fibres, indicating that the presence of these groups increases the catalytic efficiency. This was ascribed to the increased basicity of the carbon surface. These groups are Lewis bases that induce basicity at the carbon surface and, therefore, increase the respective active sites for the removal of organic compounds [17, 18].

In the present case, the sample with the highest amount of nitrogen (CNT-NU) has neither the highest basicity nor the best performance.

However, a significant amount of oxygenated groups (namely CO_2 releasing groups that present acid properties) is also present in this sample, which could explain the worse performance when compared with CNT-NUT and CNT-O samples. The best performance was obtained with the CNT-NUT sample, which has the second highest amount of nitrogen, presents a very low amount of CO_2 releasing groups and is the less acidic sample. The original material (CNT-O), with a negligible amount of nitrogen or oxygen, is the second less acidic sample and has also a good performance in the CWAO of oxalic acid. The good performance of the pristine CNTs (CNT-O) can be explained by the presence of π electrons on the surface, which are known to be active sites for the formation of radicals [19]. The electrons may be transferred from the catalyst to adsorbed oxygen molecules, producing highly reactive radicals in the presence of water [18]. Therefore, it seems that there is a relationship between the catalytic activity and the basic properties of the materials.

Normalized oxalic acid decay profiles using the CNT samples typically describe a first-order reaction with different rate constants. Thus, the apparent rate constant (k) was determined by fitting of the experimental data to Equation 4:

Equation 4

$$r_{OxAc} = -\frac{d[OxAc]}{dt} = k \cdot [OxAc]$$

where r_{OxAc} is the rate of degradation of oxalic acid and $[OxAc]$ is the concentration of oxalic acid at a given time, t.

Integration of Equation 4, taking into consideration that for t=0 min, oxalic acid concentration is $[OxAc]_0$, leads to:

Equation 5

$$ln([OxAc]) = ln([OxAc]_0) - kt$$

The apparent initial reaction rate constants (k) (based in the first 15 min of reaction) were determined from the slopes of the straight lines obtained by plotting $-ln([OxAc]/[OxAc]_0)$ with respect to time.

The values obtained for the apparent initial reaction rate constants were 0.100, 0.012, 0.042 and 0.247 min^{-1}, for CNT-O, CNT-N, CNT-NU and CNT-NUT, respectively ($R^2 \geq 0.97$). According to pH_{pzc} values (Table IV- 1), the basicity decreases as follows: CNT-NUT > CNT-O > CNT-NU > CNT-N, corresponding exactly to the sequence of the initial reaction rate constants, as shown in Figure IV- 4.

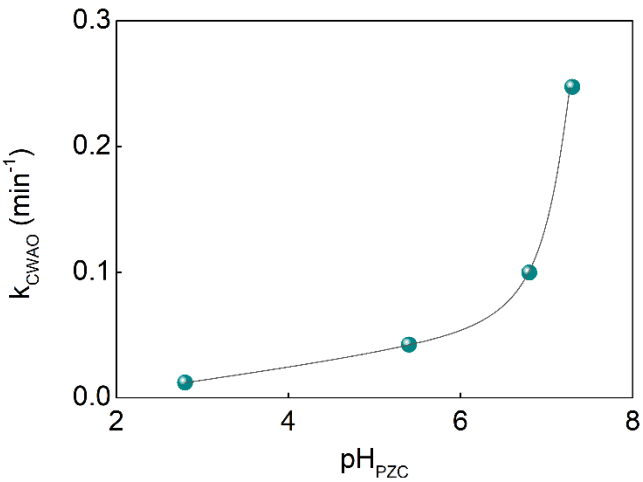

Figure IV- 4. Apparent first-order initial reaction rate constants (k) vs. pH_{PZC} for the pristine and treated CNT samples[31].

[31] Adapted from Applied Catalysis B: Environmental 104 (2011) 330–336.

Therefore, the basic/acid nature of CNTs seems to play the most important role on the performance of these materials in CWAO, the oxidation rate strongly depending on the CNT chemical properties. The weak activity observed for CNT-N (the sample with the second largest surface area) may then be related to the acidic character of this sample, indicating that CNTs with lower acid character are more efficient than those with higher acid character. This observation is in agreement with the relevance that has been attributed to basic sites on carbon materials for liquid-phase reactions [9, 17, 19-21]. The same conclusion was reached in CWAO studies with phenol and ACs and CNTs as catalysts [22-25].

Catalytic stability of CNTs in cyclic experiments

The catalyst lifetime is of paramount importance when a new material is tested. Consecutive CWAO runs, with a fresh oxalic acid solution and with the materials recovered after each run, were performed for the two most efficient catalysts (CNT-O and CNT-NUT) (Figure IV- 5). Although the reaction is very fast in the 1st run with CNT-NUT, the catalytic performance slightly decreases when reused in consecutive runs. A slight loss of catalyst activity is also observed with CNT-O from the 1st to the 2nd run and 3rd run. Even so, both catalysts (CNT-O and CNT-NUT) still present a high efficiency under consecutive runs.

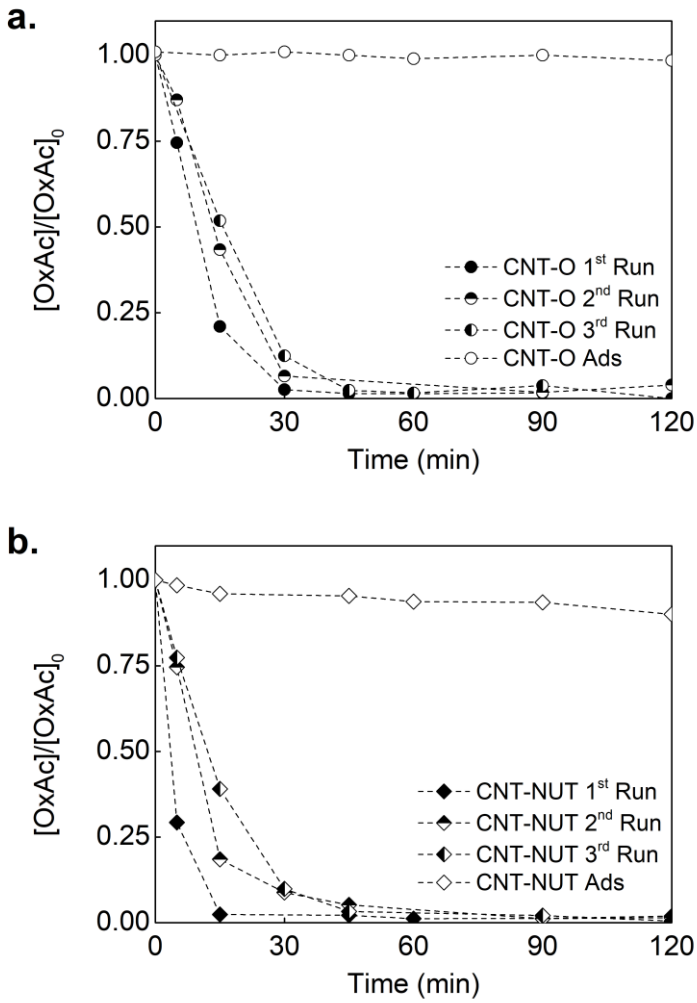

Figure IV- 5. Evolution of normalized oxalic acid concentration in CWAO cyclic runs and adsorption (Ads) experiments with (a) CNT-O and (b) CNT-NUT[32].

[32] Adapted from Applied Catalysis B: Environmental 104 (2011) 330–336.

Thorough characterization of the catalysts after reaction indicates that the presence of oxygen or even the experimental conditions do not induce significant changes in the textural or chemical surface properties (Table IV- 2).

Table IV- 2. Chemical and textural characterization of pristine and treated CNTs before and after the preliminary CWAO assessment.

Sample	S_{BET}	CO	CO_2	pH_{PZC}
	($m^2\ g^{-1}$)	($\mu mol\ g^{-1}$)	($\mu mol\ g^{-1}$)	(unitless)
CNT-O	302	200	26	6.8
CNT-O 1st Run	329	346	58	7.0
CNT-O 2nd Run	327	n.d.	n.d.	6.6
CNT-O 3rd Run	318	n.d.	n.d.	6.6
CNT-N	351	1710	909	2.8
CNT-N 1st Run	n.d.	1806	868	6.1
CNT-NU	351	1172	607	5.4
CNT-NU 1st Run	352	n.d.	n.d.	5.7
CNT-NUT	386	703	76	7.3
CNT-NUT 1st Run	388	1018	116	6.7
CNT-NUT 2nd Run	338	942	122	6.6
CNT-NUT 3rd Run	358	1125	177	6.2

n.d. – not determined.

It was observed that there is not a large change in the pH_{pzc} of the original sample (CNT-O). The pH_{pzc} values of the basic materials decrease slightly after use, while those of the acidic materials increase. After use, there is not much difference in the values of pH_{pzc}, which tend to be

between 6 and 7. The differences in the BET surface areas between samples recovered in consecutive runs were practically negligible. Therefore, the decrease in catalyst activity during consecutive runs, especially for CNT-NUT, is not due to possible blockage of surface area by intermediate compounds. CWAO by-products can induce a partial deactivation of carbon materials, reason why metals have been impregnated to degrade strongly adsorbed intermediates, especially phenolic condensation by-products over active carbons [26]. However, no by-products were expected for the oxalic acid degradation.

2.1.3.Partial Conclusions

Oxalic acid is very stable under non-catalytic conditions at 140 ^{o}C while it can be totally degraded with CNTs in less than 30 min, at the same operating conditions. The apparent initial first-order reaction rate constants found for CWAO of oxalic acid follow exactly the same order as the pH_{pzc} of the materials tested, namely 0.247 > 0.100 > 0.042 > 0.012 min^{-1} for pH_{pzc} of 7.3 > 6.8 > 5.4 > 2.8. Therefore, CNTs with a basic nature are markedly more active catalysts than CNTs with a pronounced acid character, the oxidation reaction rate of oxalic acid depending on the chemical properties of these materials. The CNTs modified with HNO_3, urea and gas-phase thermal treatments (CNT-NUT sample) showed the highest basic character and also the highest catalytic activity. The cyclic CWAO experiments also demonstrate that the CNT textural properties and surface chemistry are quite stable at the investigated operating conditions. Therefore, CNTs without any impregnated metal proved to be promising catalysts for CWAO and their catalytic activity can be enhanced by increasing their basic sites.

2.2. The Role of Acidic Surface Groups

Basic sites (or low acidic character) have been identified by most authors as the most favourable, not only for CWAO [10, 17, 21, 22, 24, 25, 27], but also for other advanced oxidation process [9, 28, 29], for example, catalytic ozonation [19, 20]. However, some authors [30-34] have claimed a positive effect of carboxylic acid surface groups when CNTs were used for the degradation of phenol by CWAO. This is in disagreement with the main findings of the previous section, where it was observed that the apparent initial first-order rate constants were lower for the CNTs with a marked acid character. Therefore, there is a controversy in the literature regarding the active sites on CNTs (i.e. sites of basic or acidic nature) required to achieve the best performance in the CWAO process.

The main purpose of this sub-chapter is to clarify this issue, namely to identify the most suitable surface properties of CNTs when they are used as catalysts (without any impregnated metal) in the CWAO process. For this study, CNTs submitted to chemical and thermal treatments in order to incorporate different heteroatoms on the surface (mainly O-, S- and N-containing groups) were tested as catalysts in CWAO. In addition to oxalic acid oxidation, the catalytic performance of the CNTs samples was also extended to the degradation of phenol.

Part of the results presented in this section has been already reported in the paper *The role of O- and S-containing surface groups on carbon nanotubes for the elimination of organic pollutants by catalytic wet air oxidation*, authored by Raquel P. Rocha, Adrián M.T. Silva, Saudi M.M. Romero, Manuel F.R. Pereira and José L. Figueiredo, and published in the journal Applied Catalysis B: Environmental Volume 147 pages 314-321 (2014). Author Contributions: Raquel P. Rocha and Saudi M.M. Romero carried out the experimental work described. Raquel P. Rocha wrote the manuscript. The work was supervised of by the remaining authors.

Another part of the results has also been reported in the paper *Catalytic performance of heteroatom-modified carbon nanotubes in advanced oxidation processes*, authored by João Restivo, Raquel P. Rocha, Adrián M. T. Silva, José J. M. Órfão, Manuel F. R. Pereira and José L. Figueiredo, and published in the journal Chinese Journal of Catalysis Volume 35 pages 896–905 (2014). Author Contributions: Raquel P. Rocha performed the modification and characterization of the carbon samples, and tested them in CWAO. João Restivo tested the materials as catalysts for ozonation. The manuscript was jointly written by João Restivo and R.P. Rocha, with substantial supervision of all authors.

2.2.1.Catalysts

CNTs subjected to several liquid-phase chemical treatments (using HNO_3, H_2SO_4, a mixture of HNO_3/H_2SO_4) as well as gas-phase thermal treatments under nitrogen atmosphere (at 200, 400 and 600 °C) were used as catalysts on this study. The sample CNT-NUT (urea treated sample) was also including in this section. Detailed information about the methodologies used and thorough characterization of the samples may be found in *Part II*. Table IV- 3 and Figure IV- 6 recall the most relevant properties of this group of samples to support the discussion of their catalytic performance.

Table IV- 3. Relevant textural and chemical properties of the pristine and modified CNTs used to study the role of acidic surface groups.

Sample	S_{BET}	V_P	CO	CO_2	SO_2	pH_{PZC}
	($m^2\ g^{-1}$)	($cm^3\ g^{-1}$)	($\mu mol\ g^{-1}$)	($\mu mol\ g^{-1}$)	($\mu mol\ g^{-1}$)	(unitless)
CNT-O	326	0.67	187	33	n.a.	6.8
CNT-N	400	1.02	1852	1233	n.a.	2.2
CNT-N200	408	1.10	1308	727	n.a.	2.5
CNT-N400	408	1.06	1205	113	n.a.	4.8
CNT-N600	389	1.03	826	43	n.a.	7.2
CNT-NS	394	0.89	2035	1394	203	4.8
CNT-S	293	0.71	381	195	579	2.5
CNT-NUT	386	1.65	701	72	n.a.	7.3

n.a. – not aplicable

The HNO_3 and HNO_3/H_2SO_4 treatments induced a pronounced acidic character in the pristine CNTs (originally with a neutral pH_{pzc} of 6.8), creating a large amount of carboxylic acids, anhydrides and phenol surface groups, and also lactones and carbonyl/quinone surface groups (CNT-N and CNT-NS samples) (Figure IV- 6). The treatment with H_2SO_4 alone, or with the HNO_3/H_2SO_4 mixture, led to the additional introduction of S-containing groups (such as sulphonic groups, $-SO_3H$) that are released as SO_2 during TPD (597 μmol g^{-1} and 203 μmol g^{-1}, respectively, for samples CNT-S and CNT-NS). The thermal treatments under N_2 applied to the oxidized CNT-N sample produce samples with successively lower acid character, samples labelled as CNT-N200, CNT-N400 and CNT-N600, in agreement with the temperature of the treatment.

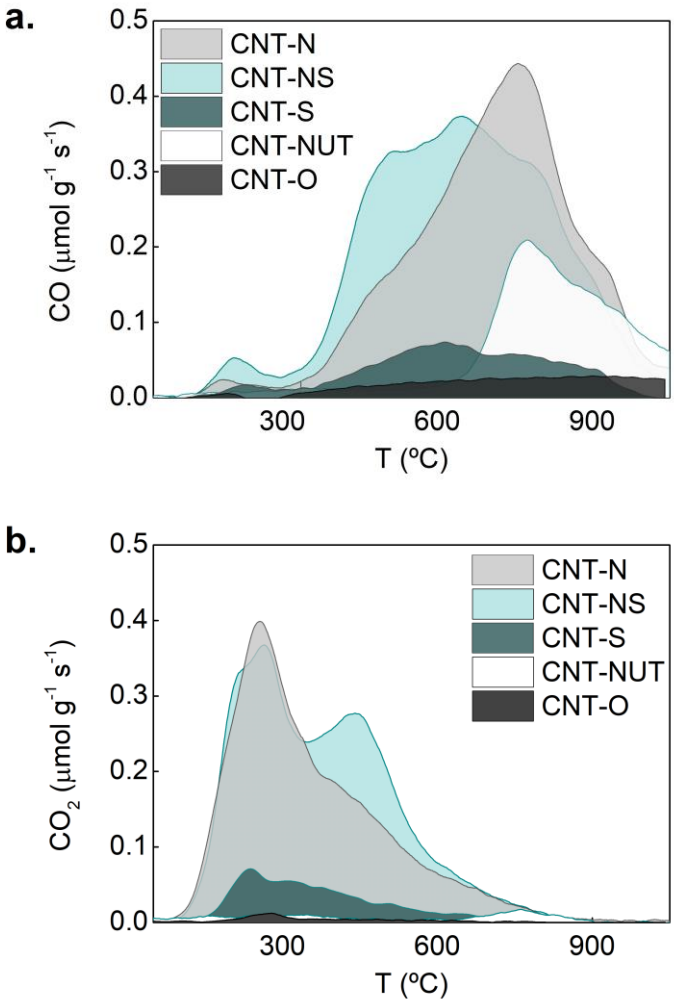

Figure IV- 6. Profiles of CO (a) and CO_2 (b) evolved in TPD of the pristine and nitric, sulphuric acid and urea treated CNT samples[33].

[33] Adapted from Chinese Journal of Catalysis 35 (2014) 896–905.

2.2.2.Catalytic Performance

The catalytic activity of the selected CNT samples was studied using oxalic acid and phenol as model pollutants. It is important to remark that, from now on, the catalytic results presented were carried out by using the solutions of the model compounds at the desired concentrations placed into the reactor before heating the system. For this reason, the catalytic performance of some previously presented samples is repeated and may show a slight deviation from what has been already shown. All non-catalytic, catalytic and adsorption experiments of oxalic acid were conducted at 140 °C, while phenol tests were performed at 160 °C, in both cases at 40 bar of total pressure. Adsorption (Ads) experiments were performed under identical experimental conditions (P, T, amount of CNTs), but replacing air by pure nitrogen. A material load of 0.2 g was used in the catalytic and adsorption assessments. Once again, catalyst evaluation is discussed in terms of the normalized model pollutant concentration (C/C_0) as a function of time in the non-catalytic and catalytic experiments. Adsorption contribution was studied for all prepared materials and for both pollutants. As expected, the adsorption of the model pollutants was negligible regardless the materials tested, due to the non-microporous nature of the CNTs.

Figure IV- 7.a shows that using CNTs treated with HNO_3 (CNT-N) as catalyst, or even after subsequent thermal treatments (CNT-N200, CNT-N400 and CNT-N600), the degradation of oxalic acid is significantly increased, total degradation being achieved in less than 60 min with the CNT-N600 sample, in contrast with the poor oxidation in the absence of a catalyst (WAO), previously observed.

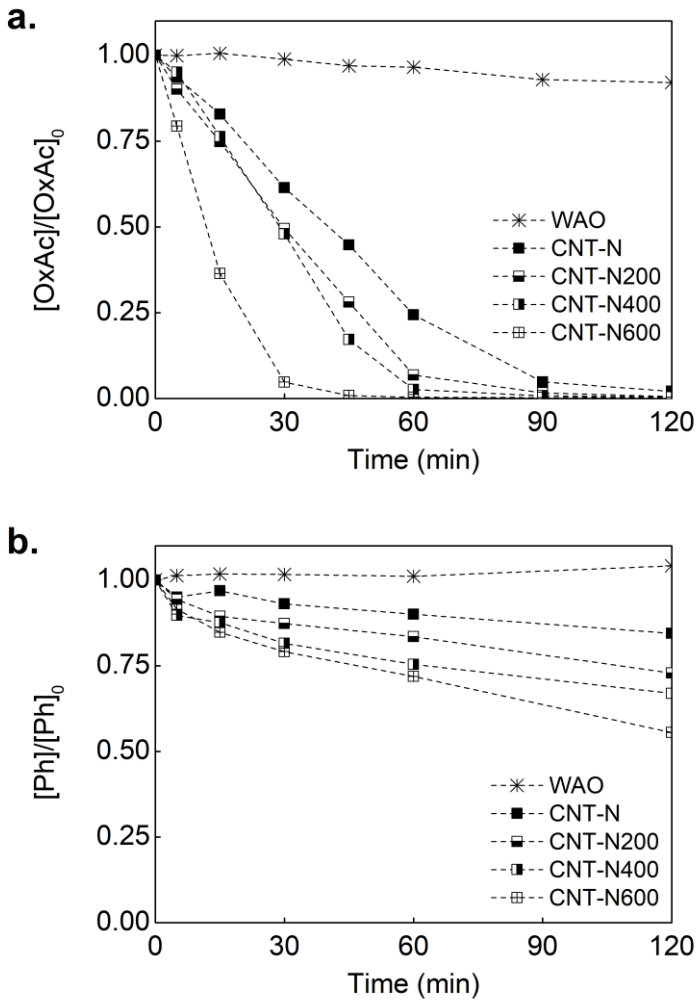

Figure IV- 7. Evolution of the normalized (a) oxalic acid and (b) phenol concentration under non-catalytic conditions (WAO) and using the nitric acid and thermally treated CNT samples as catalysts in CWAO[34].

[34] Adapted from Applied Catalysis B Environmental 147 (2014) 314–321.

The better catalytic performances obtained with the samples treated at higher temperatures can be related to the successive removal of the acidic groups (i.e. decrease in the amount of groups released as CO_2 and corresponding increase of pH_{pzc}). The influence of the CNTs surface chemistry in the degradation of oxalic acid is clearly shown in Figure IV-8.a, where the amount of CO_2 released during the TPD analyses and the pH_{pzc} of these samples were plotted against the oxalic acid conversions obtained after 45 min of reaction. Therefore, in general, the catalytic activity decreases as the acidity of the samples increases.

Figure IV- 7.b shows that phenol is not degraded in the absence of catalyst (WAO) and, once again, the sample treated at 600 ^{o}C (CNT-N600), which is also the less acidic sample of the set of materials shown in Figure IV- 7.b, exhibits the best catalytic performance. The increase of the catalytic activity can be associated to the decrease of the acidic nature of these samples, as evidenced in Figure IV- 8.b for this pollutant and as observed also for oxalic acid. Then, the conversion of phenol at 120 min of reaction increases with the decrease of the CO_2 amount released during the TPD experiments, as well as with the increase of the corresponding pH_{pzc} of these samples. Therefore, the basic/acid nature of the CNTs seems to play an important role on the performance of these materials in CWAO experiments, as was already discussed in a previous section.

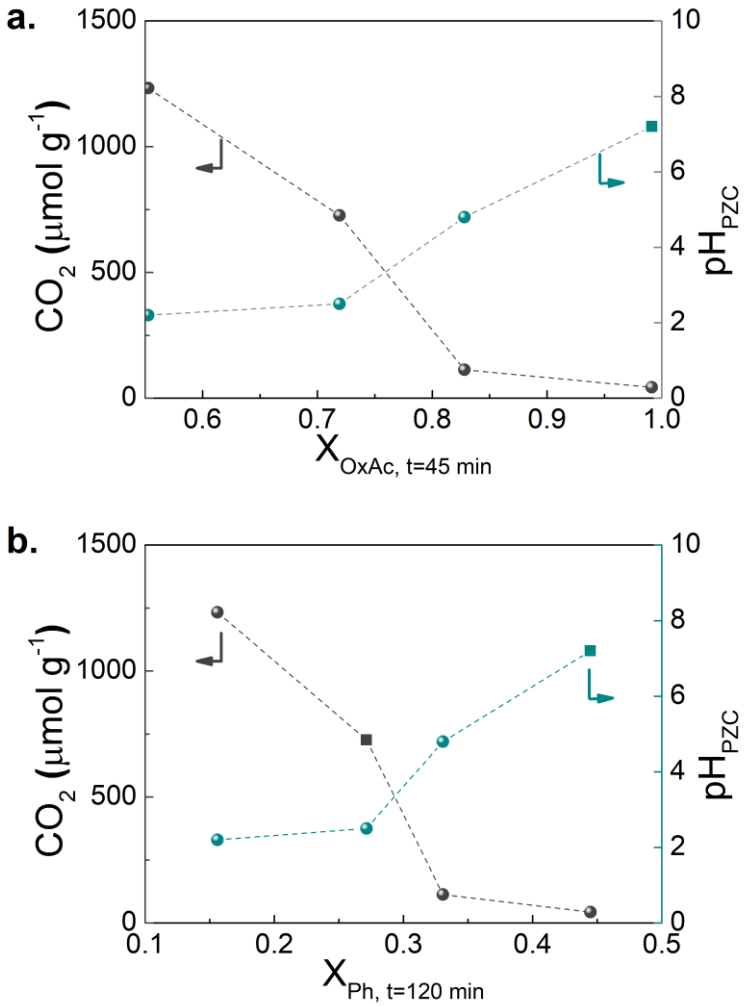

Figure IV- 8. Amount of CO_2 released during the TPD analyses (left) and pH_{PZC} (right) of nitric acid and thermally treated CNT samples, plotted against oxalic acid (a) and phenol (b) conversions obtained after 45 min and 120 min of reaction, respectively[35].

[35] Adapted from Applied Catalysis B Environmental 147 (2014) 314–321.

These results are in agreement with the commonly reported effect of the basicity of carbon materials for liquid-phase oxidation reactions [9, 17, 28] and with other results observed in degradation of phenol by CWAO using AC and/or CNTs, where the treatment with HNO_3 has a negative effect on the catalytic activity of the carbon materials [10, 22, 24].

However, all these results seem to contradict other publications where the carboxylic acid groups attached to the surface of CNTs [30-33], or even at carbon fibres and graphite [33], have been claimed as promoting their catalytic activity for the oxidation of phenol and other model pollutants (as nitrobenzene and aniline [34]) by the CWAO process.

The catalytic performance of the other prepared samples (CNT-S, CNT-NS and CNT-NUT) was also studied with the aim to clarify this issue.

Figure IV- 9 shows the results obtained in the degradation of oxalic acid when samples CNT-S, CNT-NS and CNT-NUT were employed. For comparative purposes, the results obtained with CNT-N are also included. A clear influence of the surface chemistry of the carbon samples in the catalytic performance can be observed. The acidic samples CNT-N, CNT-NS and CNT-S (which present low pH_{pzc}) underperform compared with the samples with neutral or slightly basic nature (CNT-O and CNT-NUT) in oxalic acid oxidation (Figure IV- 9). Complete oxidation occurs in less than 30 min when samples CNT-O and CNT-NUT are used. The absence of acidic groups (O-containing or S-containing) leads to a faster degradation of oxalic acid, as observed with samples CNT-O and CNT-NUT. However, a faster removal of oxalic acid is achieved in the presence of CNT-NUT sample, in agreement with what was observed in the preliminary study. The presence of nitrogen groups could favour the interaction of oxygen

with the carbon surface [35], with oxygen being possibly activated into species that react with the adsorbed organic pollutant [21, 36, 37].

Longer reaction times are required to obtain full conversion of oxalic acid with the acidic samples: at least 60 min with CNT-S, 90 min with CNT-NS and 120 min with CNT-N. Nevertheless, sample CNT-NS performs better than CNT-N in CWAO, in spite of its slightly larger amount of surface groups released as CO_2 in TPD (Table IV- 3). This can be ascribed to the presence of S-groups in CNT-NS; indeed, these groups enhance the catalytic activity of the material, as also observed with CNT-S, which is the best of the acidic samples for oxalic acid degradation by CWAO.

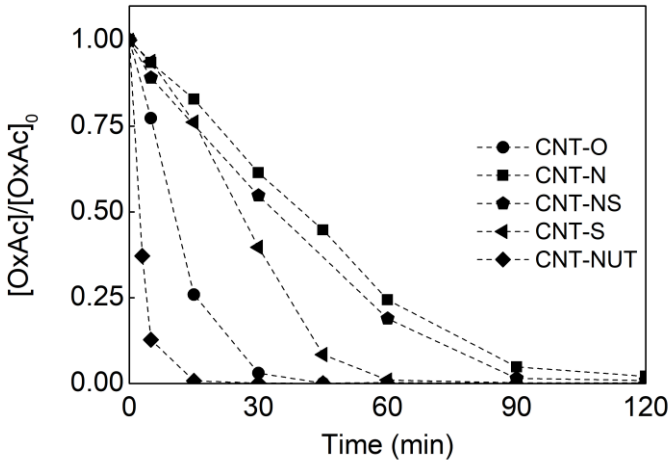

Figure IV- 9. Evolution of the normalized oxalic acid concentration, using the nitric and sulphuric acid and urea treated CNT samples as catalysts in CWAO[36].

Concerning the degradation of phenol (Figure IV- 10.a), CNT-N presents worse catalytic performance compared with CNT-O and CNT-NUT

[36] Adapted from Chinese Journal of Catalysis 35 (2014) 896–905.

samples. Less than 10 % of phenol conversion is obtained using the sample CNT-N after 2 h of reaction. This proves that conversion is faster when the acid character of the carbon samples decreases, suggesting that the absence of strong oxygen-containing acidic groups (such as carboxylic acids and anhydrides) is more favourable for the liquid phase oxidation reactions. However, only 44 % and 64 % of phenol conversion is obtained by CWAO after 120 min of reaction when using the pristine CNT-O sample and the CNT-NUT sample, respectively (Figure IV- 10). Surprisingly the CNT-S sample, enriched with S-containing groups, shows the highest catalytic activity for the oxidation of phenol, 100 % of phenol conversion being achieved after 90 min, in spite of the strong acidic character of this sample (pH_{PZC} = 2.5, Table IV- 3). Notwithstanding the fast phenol conversion achieved with the CNT-S sample, TOC removal was not higher than 57 % after 120 min. While in the CWAO experiments with oxalic acid this pollutant was completely converted into CO_2 (no by-products being detected by HPLC analysis, the TOC removal being equal to the oxalic acid disappearance), in phenol degradation differences between the concentration decay and the TOC removal were different when using the CNT-S and the CNT-NS samples (Figure IV- 10.b). This indicates that reaction by-products are formed and not totally degraded at the end of this experiment with phenol. In fact, several by-products are involved in the possible reaction pathways of phenol oxidation by CWAO [38], hydroquinone and benzoquinone being identified as the most representative intermediates, which were also detected in the present experiments together with oxalic acid. The sample treated with the mixture of HNO_3/H_2SO_4 (CNT-NS) showed better performance than CNT-N

and lower activity than CNT-S for both pollutants, but more notoriously with phenol (Figure IV- 10.a).

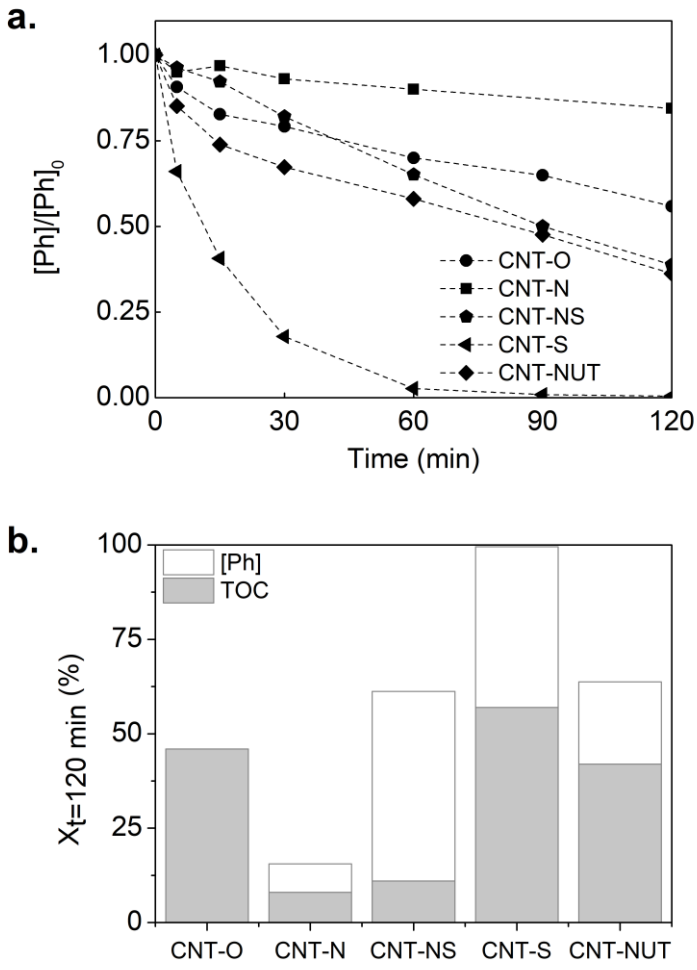

Figure IV- 10. (a) Evolution of the normalized phenol concentration during time and (b) phenol degradation and TOC conversion at 120 min of reaction, using the nitric and sulphuric acid and urea treated CNT samples as catalysts in CWAO (0.2 g of catalyst)[37].

[37] Adapted from Chinese Journal of Catalysis 35 (2014) 896–905.

Due to the high temperature in the CWAO experiments, -SO_3H groups may decompose forming strongly oxidant sulphate radicals, which can be responsible for initiating the degradation of phenol. However, they do not allow high levels of mineralization, suggesting that they can be selective for phenol oxidation but are not able to degrade the various by-products formed (particularly short chain carboxylic acids, as oxalic acid). In fact, the S-modified samples underperformed in the oxalic acid oxidation, in comparison with CNT-O and CNT-NUT. The enhanced activity of ACs containing S-groups has already been demonstrated in the catalytic wet peroxide oxidation of acid dyes [39, 40]. It was suggested that the presence of the S-species promotes a better adsorption of the probe dye molecule and a faster reaction, in spite of the low reaction temperature (50 °C). Other authors have reported good results in the degradation of phenol by CWAO with CNTs oxidized with mixtures of H_2SO_4 and HNO_3. However, these results were ascribed to the presence of carboxylic acid groups, neglecting the S-containing groups which can also be incorporated onto the CNTs by such treatment [30-32].

According to the amounts of CO_2 released during the TPD experiments of the samples CNT-N and CNT-NS (Table IV- 3), large amounts of carboxylic acid groups are released, 1233 and 1397 μmol g^{-1}, respectively. In contrast, CNT-S (Figure IV- 6) presents low amount of O-containing groups released as CO_2 (195 μmol g^{-1}), in the same order of magnitude as the CO_2 amounts released in samples thermally treated above 400 °C (samples CNT-N400 and CNT-600). Therefore, the unexpected high catalytic performance of CNT-S has to be related to the S-containing groups (released as SO_2 in the TPD analyses) that are incorporated in this sample (Table IV- 3).

In order to better understand the results obtained with CNT-S, its catalytic stability was investigated in cyclic experiments with phenol. Figure IV- 11 shows that this sample drastically loses its catalytic activity after the first run, only ca. 10 % of phenol degradation being achieved in 120 min in the second run, and there is no contribution from pure adsorption in the removal of phenol.

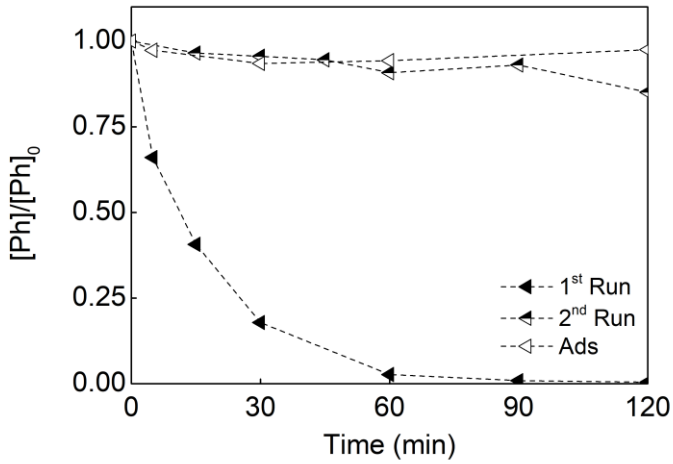

Figure IV- 11. Evolution of the normalized phenol concentration using the sulphuric acid treated sample CNT-S as catalyst in cyclic CWAO runs and adsorption (Ads) experiment[38].

The TPD profiles of this sample before and after the CWAO experiment with phenol are shown in IV- 12. It can be observed that most of the groups released as SO_2 disappear after the CWAO run (IV- 12.a). The marked decrease of the catalytic performance of this sample after the first

[38] Adapted from Chinese Journal of Catalysis 35 (2014) 896–905.

run (Figure IV- 11) seems to be related to the disappearance of the S-containing groups.

In fact, the high temperature and pressure used in the CWAO process could justify the removal of S-containing groups from the carbon surface, since the temperatures employed (140-160 °C) are close to the temperature where SO_2 desorbs (around 200 °C), and the high pressure could also play a role in the process. Therefore, the release of these groups to the liquid medium during the first experiment may lead to the formation of strong oxidant species, such as sulphate radicals, which are well known by their strong oxidizing potential [41]. The detection of lower amount of S-groups by TPD after the first run might be caused by fouling, as a result of deposition of phenol degradation products over the surface, blocking these groups. This possibility has been ruled out, because the TPD results show that only the evolved SO_2 decreases after the 1st run (IV-12.a), while the amounts of evolved CO and CO_2 are similar, as shown in IV- 12.b and c.

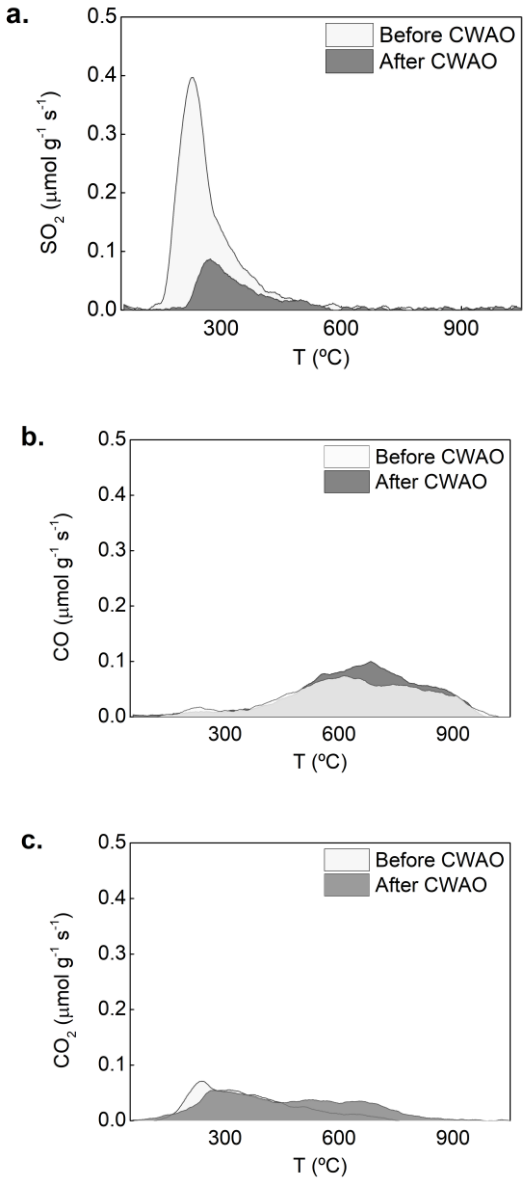

Figure IV- 12. (a) SO_2, (b) CO and (c) CO_2 evolved in TPD of CNT-S catalyst before and after the used in phenol degradation[39].

[39] Adapted from Applied Catalysis B Environmental 147 (2014) 314–321.

The presence of S-containing groups can also justify the higher conversion obtained with CNT-NS after 120 min in comparison to CNT-N (Figure IV- 10.a), both samples presenting quite similar TPD profiles with respect to CO and CO_2 (Figure IV- 12), but CNT-NS having also a certain amount of groups released as SO_2 (203 μmol g^{-1}) due to the use of H_2SO_4 in its treatment. The CNT-NS sample is also slightly more active than CNT-N for the degradation of oxalic acid (Figure IV- 9). Such observations could explain some results reported in literature, where CNTs subjected to oxidative treatments with mixtures of H_2SO_4 and HNO_3 are employed for degradation of phenol by CWAO [30-32], at temperature and pressure conditions similar to those employed in the present work. Besides O-containing groups, such as carboxylic acids, S-containing groups can be also incorporated onto the CNTs after treatments with mixtures of H_2SO_4 and HNO_3, these S-containing groups being responsible for the catalytic activity of the CNTs, instead of the carboxylic acid groups.

Concerning the characterization of the sample CNT-S after being used in the oxalic acid oxidation, the profiles of SO_2 released during TPD experiments with CNT-S samples after CWAO are presented in Figure IV-13. It is clear that a large amount of S-containing surface groups is removed from the material after reaction. The loss of sulphur groups was larger after the catalytic experiments, in comparison to the adsorption or blank (in the absence of organic compound) experiments. TPD analysis of used samples reveals that there is also a slight increase in the concentration of oxygen-containing surface groups, as observed in the case of phenol (IV- 12.b and c). The S2p spectra obtained by XPS (Figure IV- 13.b) show that there are no changes in the nature of the sulphur

groups of sample CNT-S. Nevertheless, a decrease in the concentration of -SO_3H groups was observed, in agreement with the results from TPD.

In order to better elucidate the reaction pathway involved using this peculiar sample (CNT-S) additional results will be presented in section 2.4 *Mechanistic Considerations*.

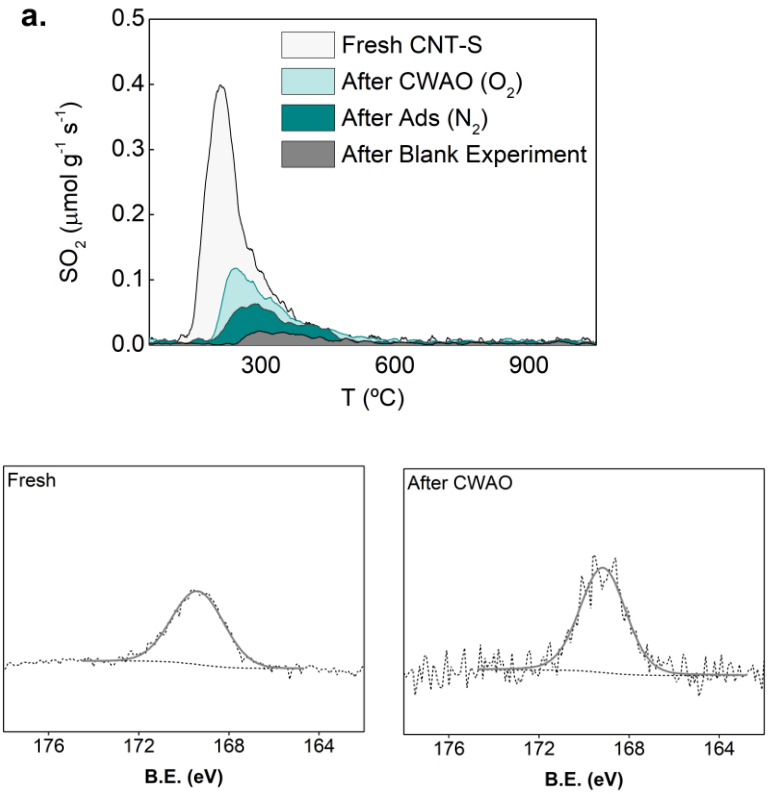

Figure IV- 13. (a) Profiles of SO_2 evolved in TPD and (b) S2p XPS spectra of the CNT-S sample before and after experiments with oxalic acid[40].

[40] Adapted from Chinese Journal of Catalysis 35 (2014) 896–905.

The sample CNT-NUT recovered after oxalic acid oxidation was also analysed by XPS. The N 1s spectra of the CNT-NUT sample, before and after the oxidation process, are presented in Figure IV- 14. Samples recovered after CWAO and adsorption experiments did not show any significant alteration in the N 1s spectrum obtained by XPS. Deconvolution of the spectra showed similar relative amounts of pyridine-like (N6), pyrrole-like (N5), and quaternary nitrogen (NQ) surface groups. The stability of sample CNT-NUT (reported in the preliminary study) can be attributed also to the stability of the N-groups. The formation of surface oxygen acidic groups slightly hinders their performance, but the catalysts retain good activity in this reaction.

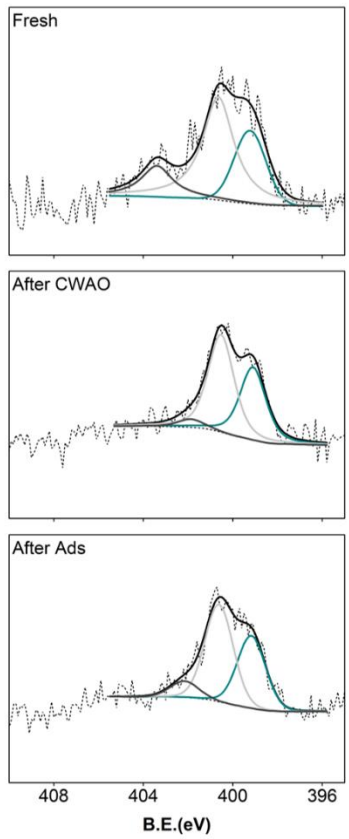

Figure IV- 14. N 1s XPS spectra of the fresh and used CNT-NUT sample after CWAO and adsorption (Ads) experiments using oxalic acid[41].

[41] Adapted from Chinese Journal of Catalysis 35 (2014) 896–905.

2.2.3.Partial Conclusions

Pristine CNTs can promote the total oxalic acid and partial phenol degradation, but the performance can be increase by the incorporation of N-functionalities (sample CNT-NUT).

The incorporation of large amounts of O-containing groups (mainly carboxylic acids and anhydrides, and phenols) on the HNO_3 treated sample (CNT-N) leads to a decrease of the intrinsic CNTs catalytic performance. Therefore, it was demonstrated that these groups are not beneficial for the process under the operating conditions tested. However, the catalytic activity of the CNTs can be recovered by thermal treatments that selectively remove these groups. Indeed, it was observed that the conversion of the pollutants increases as the pH_{PZC} of the materials increases, ie, as the amount of O-containing surface groups released as CO_2 decreases. However, CNTs modified with H_2SO_4 or HNO_3/H_2SO_4, which have a strong acidic character (low pH_{PZC}), showed an unexpected high activity for degradation of both model pollutants, more notable using the sample CNT-S and in phenol degradation. The performance of these materials was explained by the presence of S-containing surface groups. However, the catalytic activity of the CNTs treated with H_2SO_4 is drastically reduced in cyclic experiments due to the decomposition of the S-containing surface groups, as the result of the very high temperatures used in CWAO process.

Therefore, in general, the catalytic activity of pristine CNTs can be enhanced by the incorporation of nitrogen functionalities, which increases CNTs basicity, but some specific groups, such as S-containing groups, can lead to a different behaviour even if they are acidic.

2.3. N-doped Carbon Materials

In addition to increasing the catalytic performance of carbon materials, N-doping provides their increased stability in both acidic and alkaline media [29, 42]. The outstanding performance of N-doped CNTs can be due to the distribution and arrangement of the heteroatoms on the CNT lattice [43]. The results described in the previous sections show that faster removal of the selected model compounds can be obtained by using nitrogen doped CNTs. The nitrogen atoms in the sample CNT-NUT were bound to three different sites of the carbon structure forming graphitic (quaternary), pyridinic and pyrrolic structures. The main objective of the present section is to study in more detail efficient and stable N-doped catalysts, capable of mineralizing (i.e., totally oxidizing) organic pollutants in water and wastewater. The performance of the novel N-doped CNTs and rGOs prepared by ball milling using melamine, urea and ammonia (NH_3) was assessed in the oxidation of oxalic acid and phenol by catalytic wet air oxidation. Regarding the N-doped CNTs, an extensive work was carried out to evaluate the effect of the synthesis parameters in the catalytic performance. Furthermore, N-doped CXs synthesized from resorcinol, formaldehyde and melamine or urea as nitrogen sources were also investigated as potential catalysts for this application.

2.3.1.Carbon Nanotubes

Doping of carbon materials with nitrogen can be achieved in-situ during synthesis or ex-situ using appropriate post-treatments or thermal treatment. Generally, all these methods require high energy consumption and multistep procedures, which increase the cost of manufacturing N-doped catalysts, limiting their practical applications. Preparation of the previously reported sample CNT-NUT is a good example of the complexity and multistep procedures involved in the incorporation of the N-functionalities. Therefore, a novel methodology to dope CNTs with nitrogen using a ball milling step was proposed (and presented in *Part II*) as a simple method of obtaining N-doped CNTs that can be easily prepared and does not depend on highly specialized and expensive equipment. This sub-chapter describes the catalytic performance of these novel materials as metal-free catalysts in CWAO using oxalic acid and phenol as model pollutants.

Part of the results presented in this section has already been reported in the paper *Highly active N-doped carbon nanotubes prepared by an easy ball milling method for advanced oxidation processes*, authored by O.S.G.P. Soares, R.P. Rocha, A.G. Gonçalves, J.L. Figueiredo, J.J.M. Órfão and M.F.R. Pereira, and published in the journal Applied Catalysis B: Environmental Volume 192 pages 296-303 (2016). Author Contributions: R.P. Rocha and O.S.G.P. Soares designed the experiments and prepared the N-doped CNTs. The catalytic tests were performed by R.P. Rocha (CWAO) and A.G. Gonçalves (ozonation). The manuscript was written by

O.S.G.P. Soares, R.P. Rocha and A.G. Gonçalves with substantial supervision of J.L. Figueiredo, J.J.M. Órfão and M.F.R. Pereira.

Another part of the results was reported in the paper *Different methodologies for synthesis of nitrogen doped carbon nanotubes and their use in catalytic wet air oxidation*, authored by Raquel P. Rocha, O. Salomé G.P. Soares, Alexandra G. Gonçalves, José J.M. Órfão, M. Fernando R. Pereira and José L. Figueiredo, and published in the journal Applied Catalysis A, General Volume 548 pages 62–70 (2017). Author Contributions: R.P. Rocha and O.S.G.P. Soares designed the experiments and prepared the N-doped CNTs. R.P. Rocha performed the CWAO catalytic tests and also characterization of the samples, kindly assisted by Alexandra G. Gonçalves. The manuscript was written by Raquel P. Rocha with contributes from O. Salomé G.P. Soares and Alexandra G. Gonçalves and with substantial supervision of José J.M. Órfão, M. Fernando R. Pereira and José L. Figueiredo.

2.3.1.1. Catalysts

N-doped CNTs prepared using the ball milling approach were selected for catalytic test. An undoped ball milled sample (CNT-BM) prepared using the same milling conditions was also investigated for comparison, as well as the pristine carbon material (CNT-O). In general, N-doping under ball milling consists in mixing the carbon material with the N-precursor under ball milling, and then applying a thermal treatment under inert atmosphere. However, some variations were performed and studied.

Due to the high number of samples prepared and tested in CWAO, the results presentation will be divided in terms of the ball milling parameter under study: wet, dry or external N-doping methodology; effect of N-precursor; effect of thermal treatment; and effect of the O-surface groups. Detailed information about the methodologies used and thorough characterization of the samples can be found in *Part* II. Table IV- 4-7 briefly recall the most relevant properties of each group of samples to support the discussion of their catalytic performance.

<u>Wet, dry or external N-doping methodologies</u>

This group evaluates the effect of the solvent in the melamine and urea prepared samples and the effect of performing the N-doping outside the ball mill apparatus. N-doped samples (CNT-BM-M-DT, CNT-BM-M-WT, CNT-BM-U-DT and CNT-BM-U-WT) were prepared in the same apparatus by mixing the pristine CNTs with melamine (M) or urea (U), in the presence or absence of a solvent (wet treatment (WT) or dry treatment (DT) samples, respectively). Thereafter, samples were thermally treated under

inert atmosphere until 600 °C. In the case of melamine, the catalytic performance when no thermal treatment was performed after ball milling was also investigated (samples without thermal treatment, w/o TT). Additionally, two more samples were doped with nitrogen (CNT-BM-M-E and CNT-BM-U-E) by an external treatment (E), i.e., the N-precursor was mixed with CNT-BM outside the ball milling equipment.

Table IV- 4. Relevant textural and chemical properties of the pristine and modified CNTs prepared by the wet, dry and external N-doping methodologies.

Sample	S_{BET}	CO	CO_2	N_{XPS}
	($m^2\ g^{-1}$)	($\mu mol\ g^{-1}$)	($\mu mol\ g^{-1}$)	(% wt.)
CNT-O	291	200	23	n.p.
CNT-BM	391	173	44	n.p.
CNT-BM-M-DT	355	338	214	4.8
CNT-BM-M-WT	285	352	144	1.1
CNT-BM-U-DT	353	273	112	0.8
CNT-BM-U-WT	291	405	205	0.3
CNT-BM-M-E	349	394	223	3.1
CNT-BM-U-E	364	347	317	0.2

n.p. – not performed

In spite of the different treatments applied, the samples show differences in the surface area (S_{BET}) lower than 100 $m^2\ g^{-1}$, even upon the addition of the N-precursors. The ball milling treatment of the pristine CNTs leads to the most significant increase of the surface area (CNT-BM sample, 391 $m^2\ g^{-1}$), while the wet treatments result in samples with the lowest specific surface areas (CNT-BM-M-WT and CNT-BM-U-WT

samples). Regarding the surface chemistry, the TPD results indicate that the ball milled samples are poor in O-containing surface groups, similar amounts of CO and CO_2 being released by all samples. All samples present an almost neutral character (pH_{pzc} between 6.4 and 6.8), due to the incorporation of a significant amount of nitrogen (between 0.2 and 4.8 %) on the surface of the CNTs, as determined by XPS analysis. Samples prepared using melamine as N-precursor present higher N contents than those prepared with urea. The use of a solvent during the milling step had a negative effect on the attachment of the N-functionalities, regardless of the precursor used. The nature of the N-functionalities, identified on the materials surface, included N6, N5 and NQ surface groups.

Effect of N-precursor

Melamine, urea and NH_3 were investigated as N-precursors. Three CNTs/N-precursor ratios were tested, using 0.2, 0.4 and 0.6 g of melamine, or 0.3, 0.5 and 0.8 g of urea. Samples were labelled according to the precursor employed (M for melamine, U for urea), followed by the N-precursor mass in grams (e.g.: CNT-BM-M0.4). In the case of NH_3, 0.6 g of the raw CNTs were ball milled under the milling conditions previously reported (sample CNT-BM) and thereafter thermally treated under gaseous NH_3 until 600 °C, using pure NH_3 (sample CNT-BM-NH_3) or NH_3 diluted with N_2 (50/50) (v/v) (sample CNT-BM-NH_3-N_2).

Table IV- 5. Relevant textural and chemical properties of modified CNTs using different N-precursors and CNT/precursor ratios.

Sample	S_{BET}	N_{EA}	NX_{XPS}	$N6_{XPS}$	$N5_{XPS}$	NQ_{XPS}
	($m^2\ g^{-1}$)	(% wt.)	(% wt.)		(% Rel.)	
CNT-BM-M0.2	347	1.9	2.0	50.6	36.2	13.2
CNT-BM-M0.4	355	7.6	4.8	45.8	35.4	18.8
CNT-BM-M0.6	241	7.5	7.0	64.0	23.8	12.2
CNT-BM-U0.3	344	0.5	n.p.	---	---	---
CNT-BM-U0.5	353	0.8	0.8	50.0	37.5	12.5
CNT-BM-U0.8	341	0.9	n.p.	---	---	---
CNT-BM-NH_3	286	0.4	0.7	35.3	35.0	20.9
CNT-BM-NH_3-N_2	276	0.4	0.5	37.2	42.1	15.2

n.d. – not detected

The specific surface area is preserved independently of the N-precursor or CNT/N-precursor ratios used, the differences being lower than 100 $m^2\ g^{-1}$. In contrast, the extension of N incorporation and the nature of the N-functionalities depend on both parameters. Doping with melamine results in higher N retention, in comparison with urea or NH_3. High CNT/N-precursor ratios do not improve the level of functionalization. The nature of the N-groups incorporated, NQ, N5 and N6 structures, was equal for melamine and urea treated samples, while in samples treated with NH_3 an additional peak was observed (attributed to nitrogen–oxygen complexes, NX).

Effect of the thermal treatment

Regarding the effect of the thermal treatment, 0.6 g of the commercial CNTs was ball milled with melamine (0.4 g) and subjected to a thermal treatment under N_2 flow until 200, 400, 600 and 900 °C and kept at this temperature during 1 h (samples CNT-BM-M200, CNT-BM-M400, CNT-BM-M600 and CNT-BM-M900, respectively).

Table IV- 6. Relevant textural and chemical properties of the melamine CNT samples treated at different temperatures.

Sample	S_{BET}	V_P	N_{EA}	$Volatiles_{TGA}$
	($m^2\ g^{-1}$)	($cm^3\ g^{-1}$)	(% wt.)	(% wt.)
CNT-BM-M200	79	0.25	32.2	40.9
CNT-BM-M400	75	0.26	19.2	25.6
CNT-BM-M600	355	0.87	7.6	8.6
CNT-BM-M900	330	0.56	0.8	5.4

The available surface area of the samples treated at the lower temperatures is quite low (< 100 $m^2\ g^{-1}$) indicating that at these temperatures the simple agglomeration of the precursor and the material occurs. However, the increase of the temperature of the thermal treatment allows to recover the accessible surface area characteristic of the CNTs to around 350 $m^2\ g^{-1}$, as well as, albeit discreetly, to recover some space between the tubes (V_P). A significant decrease of the N-amount to 7.6 % was observed by treating the sample at 600 °C and a further increase of the temperature to 900 °C removes almost completely all nitrogen from the sample, showing that at such high temperatures the nitrogen

retention is compromised. The appearance of pyridinic, pyrrolic and quaternary groups was only observed in the samples CNT-BM-M600 and CNT-BM-M900, suggesting that these groups do not seem to be affected by the increase of the temperature of the thermal treatment up to 900 °C; however, the total amount of the N-functionalities is.

Effect of the O-surface groups

To study the effect of the oxygen surface groups, the commercial CNTs were subjected to a HNO_3 oxidation treatment at boiling temperature in order to incorporate O-containing groups. Then, in order to remove selectively the O-groups, the samples were thermally treated under inert atmosphere until different final temperatures (200, 400, 600 and 900 °C), where they were kept during 1 h (samples CNT-N200, CNT-N400, CNT-N600, CNT-N900). Then, the obtained samples were ball milled with melamine (0.4 g) and finally thermally treated under N_2 until 600 °C and kept at this temperature during 1 h. Samples were denominated according to the temperature used to selectively remove the O-containing groups, ie, CNT-N200-BM-M, CNT-N400-BM-M, CNT-N600-BM-M and CNT-N900-BM-M.

The incorporation of the N atoms using pre-oxidized samples results in a decrease of the surface area (S_{BET}) and of the free space in the CNT bundles (V_P). Apparently, there is no clear correlation between the nature of the O-functional groups present on the surface and the N-content obtained. The presence of carboxylic acids on the sample CNT-N200, or the absence of any O-functionalities in sample CNT-N900 led to similar amounts of nitrogen incorporated at the end (6.2 and 6.9 %, respectively).

According to these results, we are not able to conclude that the presence of O-functionalities enhances the incorporation of nitrogen. The ratios between N6/N5/NQ groups are close to those previously obtained for the samples treated with melamine: pyridinic groups correspond to half or more of the total N-content (from 48 to 57 %), while pyrrole groups represent around one-third (29–38 %), N-quaternary being, once again, the less expressive group (between 12 % and 14 %).

Table IV- 7. Relevant textural and chemical properties of the pre-oxidized and thermally treated CNT samples.

Sample	S_{BET}	N_{EA}	NX_{XPS}	$N6_{XPS}$	$N5_{XPS}$	NQ_{XPS}
	($m^2\ g^{-1}$)	(% wt.)	(% wt.)		(% Rel.)	
CNT-N200-BM-M	253	6.2	6.7	57.5	28.8	13.7
CNT-N400-BM-M	331	5.5	3.1	48.3	38.1	13.6
CNT-N600-BM-M	254	8.4	3.1	50.9	36.6	12.5
CNT-N900-BM-M	274	6.9	4.8	53.8	32.7	13.5

2.3.1.2. Catalytic Performance

The catalytic activity of the selected CNT samples was studied using oxalic acid and phenol as model pollutants. All non-catalytic, catalytic and adsorption experiments of oxalic acid were conducted at 140 °C, while phenol tests were performed at 160 °C, in both cases at 40 bar of total pressure. Adsorption (Ads) experiments were performed under identical experimental conditions (P, T, amount of CNTs), but replacing air by pure nitrogen. Different material loads were used in the catalytic experiments of this section, therefore, the amount of catalyst applied will be indicated in each case. Once again, catalyst evaluation is discussed in terms of the normalized model pollutant concentration (C/C_0) as a function of time in the non-catalytic and catalytic experiments. The adsorption contribution was studied for all prepared materials and for both pollutants. As expected, the adsorption of the model pollutants was negligible, regardless of the materials tested, due to the non-microporous nature of the CNTs.

Wet, dry or external N-doping methodologies

Figure IV- 15 shows the normalized concentrations of oxalic acid during the reaction time. Total conversion of the model compound is achieved in the presence of the original and the modified CNT samples, in contrast with the poor oxidation observed in the absence of catalyst (WAO). Complete oxidation of oxalic acid can be achieved in less than 60 min using the original CNT sample (Figure IV- 15.a), but a faster removal is observed using the sample CNT-BM. The mechanical treatment

performed during ball milling promotes some changes in the nanotubes structure: breaking the tubes leads to shorter CNTs [44, 45], the entanglement of the CNTs decreases, and samples with higher specific surface area and with small particle sizes of agglomerates are obtained [46]. The increase of the available surface area (from 291 to 391 $m^2 g^{-1}$) in the CNT-BM sample allows higher amount of active sites, increasing the reaction rate in comparison with the pristine CNTs. The incorporation of N-groups on the CNTs, using melamine or urea as N-precursors, improves the catalytic activity of the original CNT sample leading to a more rapid degradation of the organic compound.

Figure IV- 15.b shows the effect of the thermal treatment applied after the mechanical mixing of the CNTs with melamine under ball milling in the presence/absence of solvent. Without thermal treatment (CNT-BM-M-DT_w/o TT and CNT-BM-M-WT_w/o TT samples) the catalysts underperform compared with the thermally treated ones, suggesting that the presence of pure melamine mixed with CNTs may impair the diffusion of the reactants to the carbon surface where adsorption and reaction take place. In fact, the samples not thermally treated revealed a worse performance than CNT-BM or even pristine CNTs, confirming that the N-precursor hardly contributes to the catalytic activity. According to the deconvolution of the N1s XPS spectrum of the sample CNT-BM-M-DT-w/o TT (shown in Part II), the only N-C bonds present are those characteristic of melamine; therefore, the ball milling of CNTs with melamine does not promote any chemical functionalization of the carbon surface. Thus, the catalytic activity observed for the samples not thermally treated should be credited to the CNTs.

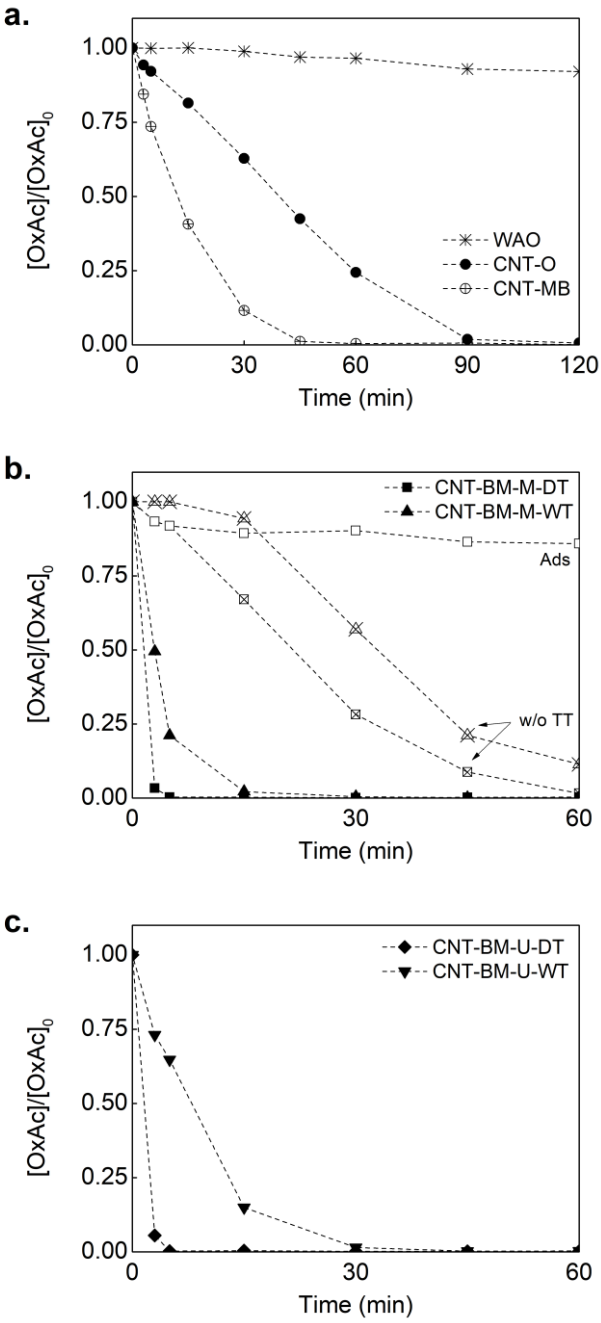
a.
[OxAc]/[OxAc]0
1.00
0.75
0.50
0.25
0.00
0
30
60
90
120
Time (min)
WAO
CNT-O
CNT-MB
b.
[OxAc]/[OxAc]0
1.00
0.75
0.50
0.25
0.00
0
30
60
Time (min)
CNT-BM-M-DT
CNT-BM-M-WT
Ads
w/o TT
c.
[OxAc]/[OxAc]0
1.00
0.75
0.50
0.25
0.00
0
30
60
Time (min)
CNT-BM-U-DT
CNT-BM-U-WT

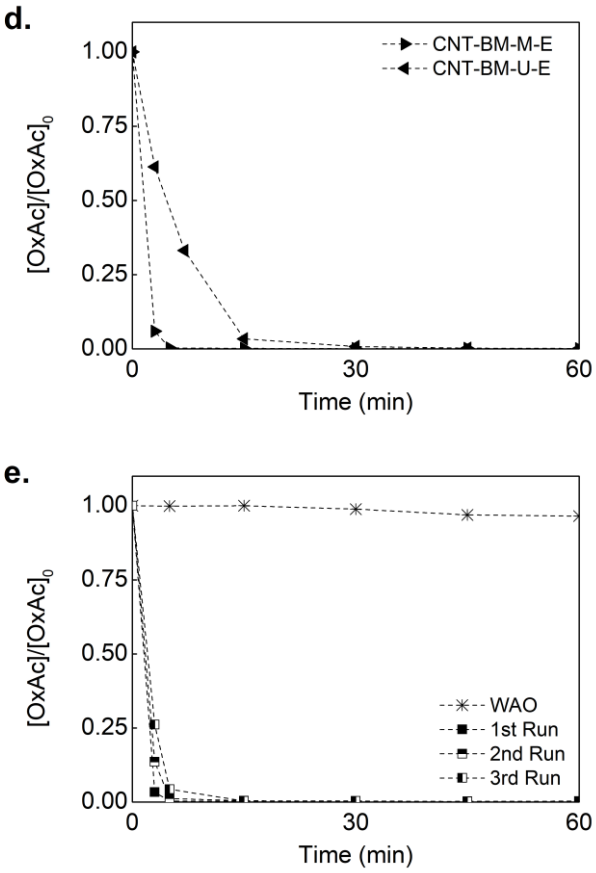

Figure IV- 15. Evolution of the normalized oxalic acid concentration under non-catalytic conditions (WAO), in adsorption experiments (Ads) and by using ball milled CNTs as catalysts in CWAO (0.1 g of catalyst)[42].

Besides the thermal treatment, the use or not of a solvent (dry or wet treatments) during the ball milling step also results in distinct catalytic performances of the samples. Sample CNT-BM-M-DT leads to an extremely fast removal of oxalic acid, total conversion being observed after about 5 min of reaction, with no contribution of adsorption (Ads CNT-

[42] Adapted from Applied Catalysis B Environmental 192 (2016) 296–303.

BM-M-DT curve, Figure IV- 15.b), phenomenon that is negligible during the reaction under the operating conditions used. By using CNT-BM-M-WT sample, the total conversion of oxalic acid is achieved after 15-30 min of reaction. In fact, the samples present significant differences in the amount of N-functionalities (4.8 % for CNT-BM-M-DT and 1.1 % for CNT-BM-M-WT determined by XPS, Table IV- 4). The use of solvent in the samples preparation, which may restrict the contact between the precursor and the carbon material, revealed a negative effect on the incorporation of N-groups. The same was observed when urea was used as N-precursor (Figure IV- 15.c). As observed in the melamine samples, complete conversion of oxalic acid is achieved in 5 min using the CNT-BM-U-DT sample, while around 30 min of reaction are required for full compound mineralization when using the CNT-BM-U-WT sample.

Concerning samples submitted to external treatments, i.e., the N-precursor is mixed with CNT-BM outside the ball milling equipment, the use of melamine as N-source seems to result in a sample with better catalytic performance than urea (Figure IV- 15.d), which may be directly related to the N-content introduced (3.1 % against 0.2 % determined by XPS for CNT-BM-M-E and CNT-BM-U-E samples, respectively). However, in any case, both samples lead to complete oxalic acid removal in less than 30 min of reaction. Besides the good performance of the samples obtained by the external treatment, the preparation method involves a dual-step procedure (ball milling of CNTs plus external contact with the N-precursor and solvent). Sample CNT-BM-M-DT combines an easy and simple preparation method without solvent, leading to high catalytic activity for the oxidation of oxalic acid by CWAO. Therefore, this sample was selected for more detailed studies.

Figure IV- 15.e shows the normalized oxalic acid concentration during 3 consecutive runs using the same catalyst (CNT-BM-M-DT) with fresh solutions of oxalic acid. The cyclic experiments show a slight deactivation of the catalyst during CWAO, but in spite of that full degradation of oxalic acid is observed in less than 15 min. This deactivation is commonly observed during successive runs of CWAO using carbon catalysts, and is ascribed to a slight oxidation of the carbon surface promoted by the operating conditions used.

Figure IV- 16 shows the N1s XPS spectra of CNT-BM-M-DT, CNT-BM-U-DT and CNT-BM-M-E before and after being used in CWAO of oxalic acid. After reaction, the samples kept the original N-functionalities (N6, N5 and NQ groups) with similar proportions; however, a slight increase of the O content was observed in the three cases (from around 0.8 – 1.0 % in the original form to 1.9 – 2.8 % after reaction), which is related to the slight oxidation of the surface as already discussed (Table IV- 8). Nevertheless, the N-groups revealed to be stable and there are no significant changes of the N-functionalities after oxalic acid oxidation by CWAO.

The positive effect of N-groups on the catalytic activity of carbon materials for liquid phase oxidation reactions is reiterated by the present results. All the prepared samples revealed the presence of three types of N-groups (quaternary nitrogen, NQ; pirrole, N5; and pyridinic, N6), according to the deconvolution of their respective N1s spectra (Figure IV-16). However, the three most active samples presented high N contents (between 0.8 and 4.8 %) and also a high relative % of N6 groups (between 47 and 60 %). Due to the high catalytic activity of the samples evaluated in this work, especially CNT-BM-M-DT, CNT-BM-U-DT and CNT-BM-M-E, that revealed similar performances under the operating conditions used, a

correct and clear distinction between the oxalic acid removal rates using these three samples is not feasible. In fact, two additional CWAO experiments were performed using a lower catalyst loading (0.040 mg) and, despite the drastic reduction of catalyst amount, samples CNT-BM-M-DT and CNT-BM-U-DT presented similar high performances for oxalic acid oxidation (total removal in 15 min, results not shown).

Table IV- 8. Oxygen contents determined by XPS and relative peak contents and positions obtained by N1s spectra fitting of selected samples, before and after CWAO experiments.

Sample		O_{XPS}	$N6_{XPS}$	$N5_{XPS}$	NQ_{XPS}
		(% wt.)		(% Rel.)	
CNT-BM-M-DT	**Fresh**	0.9	2.24	1.66	0.87
	Aft. CWAO	1.9	2.91	1.62	0.65
CNT-BM-U-DT	**Fresh**	0.8	0.39	0.28	0.10
	Aft. CWAO	2.8	0.27	0.26	0.06
CNT-BM-M-E	**Fresh**	1.0	1.86	0.89	0.33
	Aft. CWAO	2.5	1.36	0.90	0.37

.

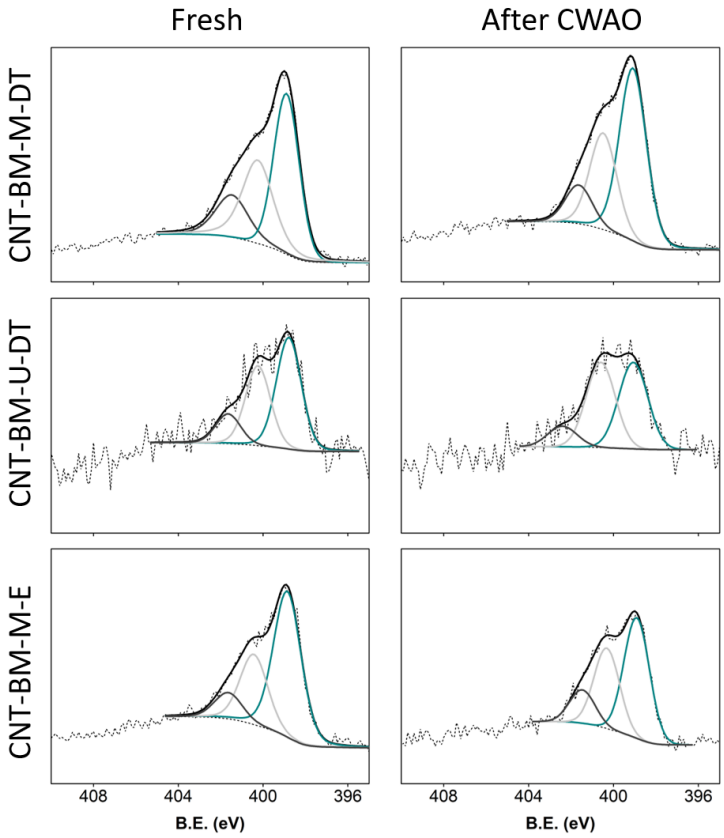

Figure IV- 16. N1s XPS spectra for some fresh ball milled CNT samples and after being used in CWAO of oxalic acid[43].

[43] Adapted from Applied Catalysis B Environmental 192 (2016) 296–303.

Effect of N-precursor

Figure IV- 17.a illustrates the catalytic performance of the CNTs prepared with different N-precursors in oxalic acid oxidation, using 50 mg of catalyst. The undoped CNT sample (CNT-O) achieves around 75 % of oxalic acid degradation in 60 min. However, the incorporation of N leads to a drastic decrease of the time required to fully mineralize the carboxylic acid. Independently of the N-precursor used for N-doping (melamine, urea or NH_3), or the ratio N-precursor/CNTs used, all samples showed a very good catalytic performance, with full oxalic acid conversion in less than 15 min. Comparing the conversion of oxalic acid reached after only 5 min using the different samples (Figure IV- 17.b), slight differences can be found: sample CNT-BM-M0.4 is the most active, followed by CNT-BM-U0.5. Regarding the melamine doped samples, the lower surface area available in CNT-BM-M0.6 seems to harm the performance of this sample comparing with CNT-BM-M0.4 (sample with similar N-content). This clearly recommends to pay special attention to the balance between the amount of N incorporated and the accessible surface area; otherwise, the introduction of functionalities may have a negative effect, decreasing the catalytic potential of the sample. In fact, sample CNT-BM-M0.2 that only presents around 2 % of nitrogen, but with a reasonable specific surface area (around 350 $m^2\ g^{-1}$) leads to similar oxalic acid conversion. A similar trend was observed with the urea doped samples (Figure IV- 17.b); the sample with the highest S_{BET} leads to a faster oxalic acid degradation, despite the fact that sample CNT-BM-U-0.8 had a higher N content. In the NH_3-treated samples, as expected, the sample treated with pure NH_3 leads

to a faster degradation than the other sample that has a lower S_{BET} and lower N-content.

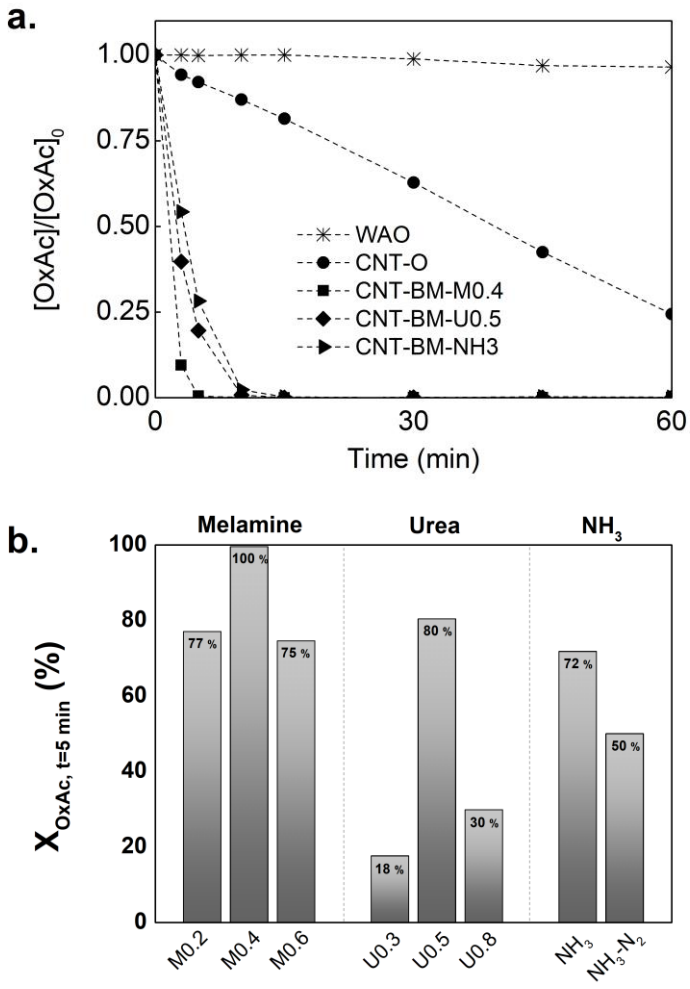

Figure IV- 17. (a) Evolution of the normalized oxalic acid concentration and (b) oxalic acid conversion reached at 5 min of reaction using CNTs prepared with different N-precursors (0.05 g of catalyst)[44].

[44] Adapted from Applied Catalysis A, General 548 (2017) 62–70.

Selected samples were also tested in the CWAO of phenol (Figure IV-18). As expected, phenol is harder to oxidize than oxalic acid, but around 97 % of degradation after 120 min was achieved using sample CNT-BM-M0.4. In the CWAO of phenol, the catalytic differences between the samples become clearer, the following order of performance being observed, which follows the same trend as the N-content of the samples: CNT-O < CNT-BM-NH_3 < CNT-BM-U0.5 < CNT-BM-M0.4.

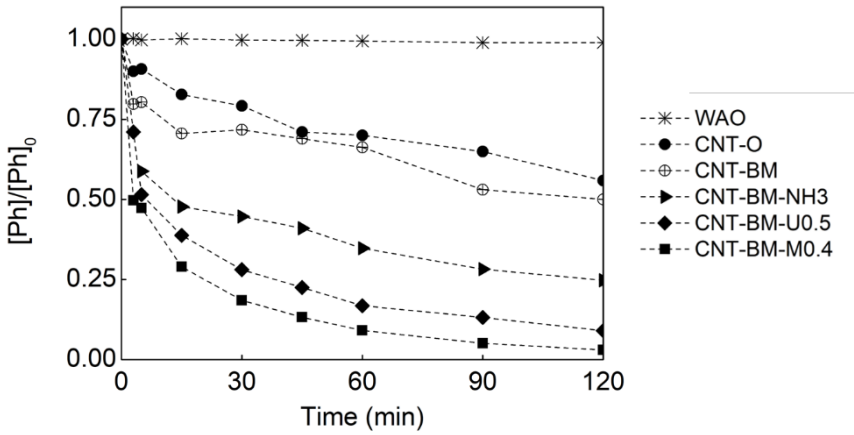

Figure IV- 18. Evolution of the normalized phenol concentration under non-catalytic conditions (WAO) and by using ball milled CNTs as catalysts in CWAO (0.2 g of catalyst)[45].

[45] Adapted from Applied Catalysis A, General 548 (2017) 62–70.

Effect of the thermal treatment

Regarding the performance of samples subjected to different thermal treatments for oxalic acid degradation (Figure IV- 19), important observations can be made: the presence of undecomposed melamine does not contribute to an improvement of the CNT activity (this was previously observed with the sample CNT-BM-M-DT_w/o TT, not thermally treated). Melamine prepared samples at 200 and 400 °C underperform compared with samples 600 and 900 °C. Conversely, after treating the melamine/CNT composite at 600 °C, the formed N-structures show a striking activity, accomplished by an increase of the oxalic acid oxidation rate. This exceptional activity slightly dropped when the material was treated at 900 °C, due to the significant decrease of the N content.

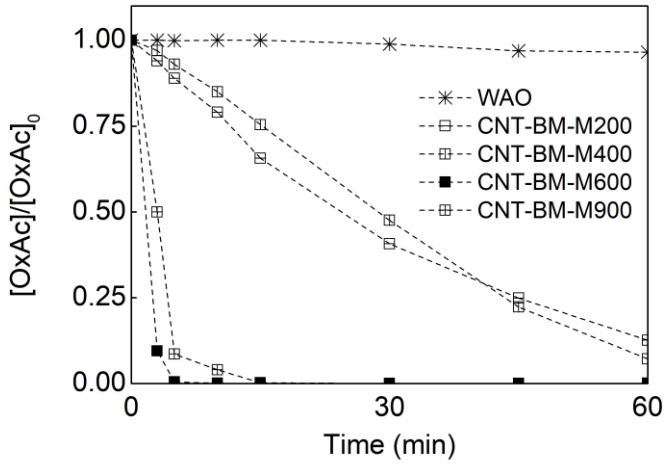

Figure IV- 19. Evolution of the normalized oxalic acid concentration during time using CNTs prepared with melamine and subjected to different thermal treatments (0.05 g of catalyst)[46].

[46] Adapted from Applied Catalysis A, General 548 (2017) 62–70.

Effect of the O-surface groups

The pre-incorporation of O-functionalities before N-doping showed slight modifications of the textural and surface properties of the samples, therefore the catalytic activity of this set of samples is pretty close (Figure IV- 20.a). All samples are able to completely mineralize oxalic acid in 15 min; however, it can be observed that the presence of the remaining O-surface groups has a negative effect on the catalytic activity, with the samples CNT-N200-BM-M and CNT-N400-BM-M being less active for oxalic acid abatement. Sample CNT-N900-BM-M shows the best performance among this set of samples. Regarding phenol experiments, a similar trend was observed, ie, the thermal treatments and subsequent removal of the O-functionalities result in an increase of the catalytic performance of the samples (Figure IV- 20.b). However, in comparison with the sample CNT-BM-M0.4, the lower specific surface area of the pre-oxidized samples seems to negatively influence the catalytic performance, leading to a worse capacity for phenol degradation.

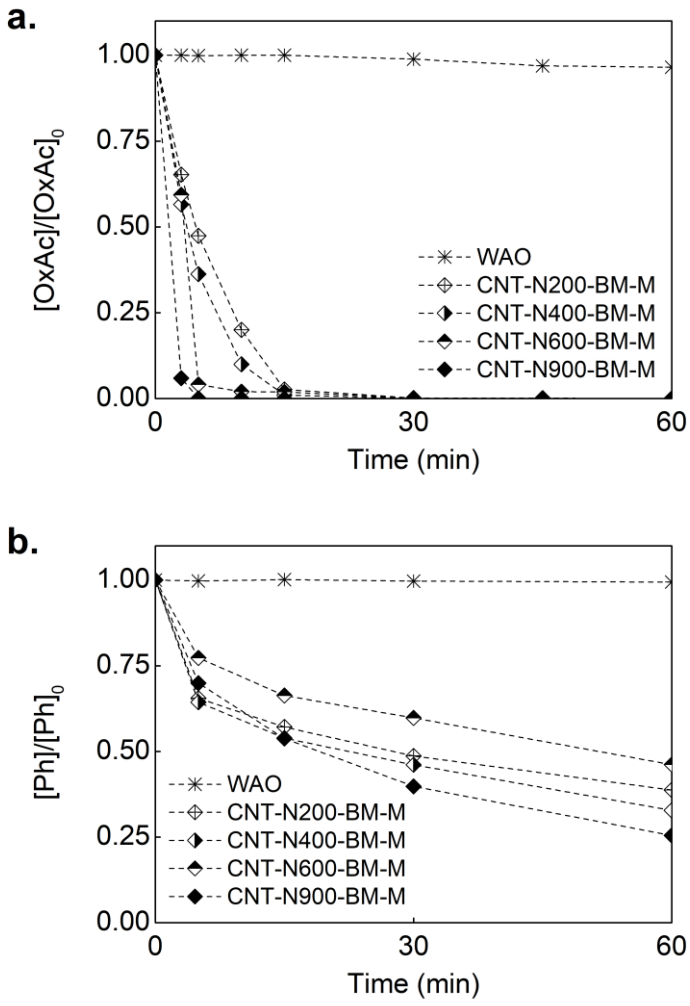

Figure IV- 20. Evolution of the normalized (a) oxalic acid and (b) phenol concentrations during time using pre-oxidized melamine doped CNT samples[47].

Taking into account all the catalytic results of this section, active samples were not necessarily extremely rich in nitrogen, good

[47] Adapted from Applied Catalysis A, General 548 (2017) 62–70.

performances being obtained with samples with low N content (for instance, using samples CNT-BM-U0.5 and CNT-BM-NH_3). So, apart from the N-content, the good catalytic activity of the majority of the samples should be linked to the nature of the N-functionalities, which are mainly, pyridinic and pyrrolic groups and quaternary nitrogen. These species are present in all the prepared N-doped samples, independently of the total N content. However, the more abundant species was always the pyridinic group (N6), whatever the precursor used. Based on this, it is possible to offer a qualitative discussion about the nature of the N-functionalities introduced on the carbon structure and their subsequent effect on the pollutants degradation. Taking into account some considerations taken from the literature, it seems that higher percentage of N6 groups may be more adequate for this application. This species was also the most abundant type of nitrogen found in the sample CNT-NUT, and Sousa et al. [17] also correlated the TOC removal of aniline degradation by CWAO with the pyridinic-N group (N6) content of the carbon fibres tested.

The catalytic activity of N-containing carbon materials is often associated with their basic properties, but other effects, as electron donation, may also enhance the activity of N-doped carbon materials [47]. In fact, it has been reported in the literature that the electronic interaction of oxygen with nitrogen-containing surface groups is high and, consequently, more active oxygen species can be generated [21, 35] to react with the adsorbed organic compounds leading to their oxidation. This may be due to the transfer of electrons from the catalyst to the adsorbed oxygen, originating highly reactive oxygen species [47]. Pyridine-like N groups are electron rich structures [48]: they have six π electrons plus an unshared pair in a nitrogen sp2 orbital; therefore, the unshared

pair can be used to form radical species and, since the unshared pair is not involved in the π system, the aromatic character of the ring is not much affected. This could also explain the stability of the group after the reaction, no significant changes being observed in the N6 group. In the case of NQ functionalities, this group also increases the electron density of the surface, but their electrons are involved in the conjugation of the π system, and therefore, their ability to donate electrons to the oxygen molecules to form the reactive species should be lower than in the case of N6 groups. Similar reasoning occurs in the presence of pyrrolic-like groups, the unshared pair of electrons being involved in the π system. In this case, to act as an electron donor, the aromaticity of the molecule has to be sacrificed. Besides the different contributions, the incorporation of N-functionalities on the carbon surface contributes to increase the electronic density of the π system and to improve the surface basicity, leading to higher catalytic activity, which may follow an electron donation reaction mechanism. In order to better elucidate the reaction pathway involved using N-doped samples, additional results will be presented in section 2.4 *Mechanistic Considerations*.

After testing different N-precursors (melamine, urea or NH_3), CNT/N-precursor ratios, and pre- and post-thermal treatments, sample CNT-BM-M0.4 seems to be the most balanced sample for the application tested. This sample is prepared by an easy and simple handling method, without solvents or any additional pre- or post-treatment. Nevertheless, the other prepared samples may be interesting, particularly the pre-oxidized samples, for other applications where O- and N-functionalities may play an important role in the reaction mechanism

2.3.1.3. Partial Conclusions

The simple post-doping method developed incorporates large amounts of N-groups into the CNT sp2 network, namely, quaternary nitrogen (NQ), pyrrolic (N5) and pyridinic (N6) groups. Different approaches were tested by mixing the CNTs in the ball mill with a N-precursor (in the presence or absence of a solvent) followed by thermal treatments, or alternatively treated under NH_3 flow. The influence of different nitrogen precursors (melamine, urea and NH_3), precursor/ CNTs ratios, O-containing surface groups and final temperatures of the thermal treatment was evaluated in the catalytic performance of the samples in CWAO. The obtained metal-free catalysts are able to effectively decompose oxalic acid and phenol, representing an attractive alternative to replace noble metals and metal oxide catalysts, traditionally used in CWAO. The catalytic oxidation of the model pollutants is faster in the presence of samples rich in nitrogen, and also favoured in the absence of O-containing surface groups on the CNT surface. The material prepared by ball milling with melamine without solvent and thermally treated until 600 °C is the most promising sample, combining an easy preparation with high amount of N-functionalities. Under the operation conditions used, oxalic acid was completely mineralized in 5 min, and around 97 % of phenol degradation was achieved in 2 h. The excellent performance observed for the N-doped samples seems to be related to the high amount of N-functionalities incorporated into the carbon lattice, mainly as N6 groups. Cyclic experiments showed high stability of the N-groups on the CNT surface, maintaining the original N-functionalities upon reutilization.

2.3.2.Graphene Based Materials

Since its isolation and characterization in 2004 [49], graphene and derivatives have emerged as materials of great interest due to their remarkable properties [50, 51]. The unique properties of the two-dimensional structure, active surface area, outstanding electronic properties and promising mechanical and thermal stability, make graphene and its derivatives promising metal-free heterogeneous catalysts [52]. Following the same methodology applied to CNTs, N-functionalities were incorporated onto rGOs using the ball milling approach and tested in the CWAO of oxalic acid and phenol. rGOs synthesis was performed considering the characterization and catalytic results obtained with CNTs prepared using the ball milling approach. Therefore, the procedure adopted for rGOs uses melamine and urea as N-precursor, following the dry treatment methodology (absence of a solvent during the ball milling step) and a final thermal treatment until 600 °C.

Most of the results presented in this section were reported in the paper *Nitrogen-doped graphene-based materials for advanced oxidation processes*, authored by R.P. Rocha, A.G. Gonçalves, L.M. Pastrana-Martínez, B.C. Bordoni, O.S.G.P. Soares, J.J.M. Órfão, J.L. Faria, J.L. Figueiredo, A.M.T. Silva and M.F.R. Pereira, and published in the journal Catalysis Today Volume 249 pages 192–198 (2015). Author Contributions: Raquel Rocha and B.C. Bordoni performed the CWAO catalytic tests and characterization of rGOs kindly prepared by L.M. Pastrana-Martínez and O.S.G.P. Soares. A.G. Gonçalves and B.C. Bordoni performed catalytic ozonation experiments. The manuscript was written by R.P. Rocha with

contributions from all authors and with substantial supervision of J.J.M. Órfão, J.L. Faria, J.L. Figueiredo, A.M.T. Silva and M.F.R. Pereira.

2.3.2.1. Catalysts

Nitrogen-doped rGOs were prepared by the modified Hummers method using natural graphite as primary precursor, followed by chemical and thermal reduction processes, and finally ball milled with melamine or urea (rGO-M and r-GO-U). Reduced GO was also prepared by using the same procedure (mechanical and thermal treatment), but without addition of a nitrogen source (rGO sample). The catalytic activity of the GO sample was not evaluated due to its strong acidic character (pH_{pzc} < 3), which has been proved to have a negative effect on the catalytic performance of carbon materials in the oxidation processes in study. Detailed information about the methodologies used and thorough characterization of the samples were presented in *Part II*. Table IV- 9 briefly summarizes the most relevant properties of this group of samples to support the discussion of their catalytic performance.

Table IV- 9. Relevant textural and chemical properties of the rGO samples.

Sample	S_{BET}	V_P	N_{XPS}
	($m^2\ g^{-1}$)	($cm^3\ g^{-1}$)	(% wt.)
rGO	263	0.40	n.p.
rGO-M	102	0.13	9.3
rGO-U	47	0.06	7.5

n.p.–not performed

The rGO samples present quite different aggregation degree of the graphene sheets, revealed by their widely different apparent surface areas (S_{BET}) and amounts of N_2 adsorbed at the relative pressure p/p_0= 0.95. Significant amounts of N were introduced on the surface of the rGO samples after the milling treatments (determined by XPS analysis), pyridinic-N (N6) being identified as the most abundant species (higher than 50 % wt. of total nitrogen content), followed by pyrrolic-N (N5) (25-35 % wt.) and quaternary nitrogen (NQ) (17-25 % wt.), respectively for rGO-M and rGO-U samples.

2.3.2.2. Catalytic Performance

The rGO samples doped and undoped with nitrogen groups were tested as catalysts in the oxidation of oxalic acid and phenol by CWAO. Oxalic acid experiments were conducted at 140 °C and phenol experiments at 160 °C, both at 40 bar of total pressure. Adsorption (Ads) experiments were performed under identical experimental conditions (P, T, amount of CNTs), but replacing air by pure nitrogen. A catalyst load of 0.1 g was used in the catalytic and adsorption assessments. Catalyst evaluation is discussed in terms of the normalized model pollutant concentration (C/C_0) as a function of time in the non-catalytic and catalytic experiments.

The conversion of the model pollutant significantly increased by using the rGO samples. Figure IV- 21 shows that total removal of oxalic acid can be achieved in less than 60 min using the rGO samples with no by-products being detected by HPLC analysis. Oxalic acid was more quickly removed

from the solution using samples rGO and rGO-M than by rGO-U. However, adsorption contributes to the decay of oxalic acid concentration. Although the adsorption of oxalic acid over the N-doped samples (rGO-M and rGO-U) was lower than 15 % after 60 min, about 30 % of oxalic acid was adsorbed in the case of the rGO sample (reaching about 45 % after 120 min). Therefore, the fast removal of the compound under catalytic conditions using the rGO sample has a significant contribution from adsorption, which cannot be neglected.

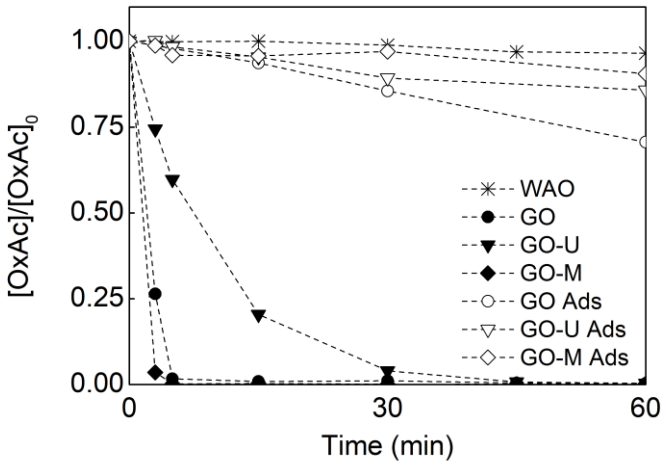

Figure IV- 21. Evolution of the normalized oxalic acid concentration under non-catalytic conditions (WAO), adsorption experiments (Ads) and using rGO samples as catalysts in CWAO (0.1 g of catalyst)[48].

Besides the adsorption contribution, rGO leads to total oxalic acid removal, exhibiting a good catalytic activity for the reaction, probably due to the presence of the π electron system of the reduced graphene oxide

[48] Adapted from Catalysis Today 249 (2015) 192-198.

[53], which contributes to the basicity of the carbon surface [9]. Regarding the rGO-M sample, where the adsorption contribution is much lower, it seems that the introduction of the nitrogen surface groups leads to an increase of the catalytic performance. The worst performance was obtained with the rGO-U sample, more time being required to oxidize oxalic acid completely. This can be due to the lower amount of nitrogen and to the low surface area of the material. In fact, this sample has only 47 m^2 g^{-1} of specific surface area due to the compaction of the layers during the ball milling treatment with urea, which can decrease the outer surface accessible to oxalic acid.

Post-reaction analysis of the rGO-M (CWAO) and rGO-U (CWAO) samples by XPS (Figure IV- 22) showed that the nitrogen functionalities were stable, with no significant changes of the N groups after oxalic acid oxidation by CWAO, as observed with CNTs. Similar proportions of the different types of nitrogen species identified on the fresh samples, pyridinic-N (N6), pyrrolic group (N5) and quaternary nitrogen (NQ), were observed after use in the oxalic acid oxidation.

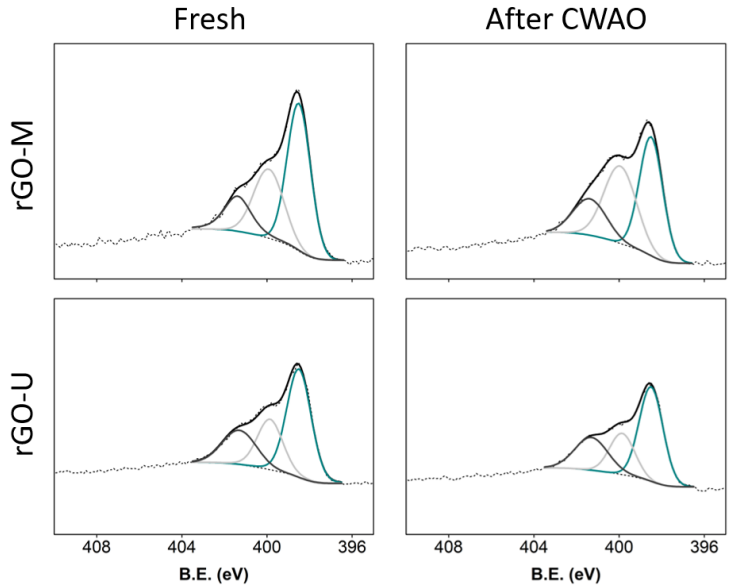

Figure IV- 22. N 1s XPS spectra for the fresh rGO-M and rGO-U samples and after being used in CWAO of oxalic acid[49].

Regarding phenol oxidation experiments (Figure IV- 23), once again, the use of the rGO samples increases the removal of the pollutant from the solution (that is not converted in the absence of catalyst). In this case, the rGO-M sample clearly exhibits the best catalytic performance (50 % of phenol removal after 120 min) followed by the rGO and rGO-U samples, with a small contribution of adsorption using samples rGO-M and rGO-U (less than 8 %). The adsorption experiment using the rGO sample was not performed but it is expected to be higher than this value, as in the oxalic acid case, due to the high surface area of the sample.

[49] Adapted from Catalysis Today 249 (2015) 192-198.

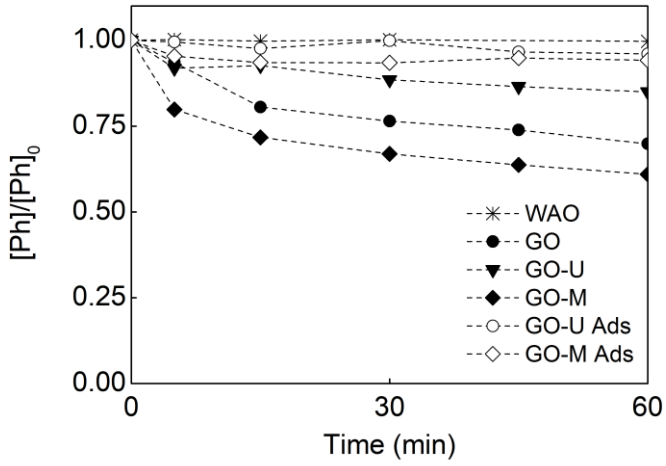

Figure IV- 23. Evolution of the normalized phenol concentration under non-catalytic conditions (WAO), adsorption experiments (Ads) and using rGO samples as catalysts in CWAO (0.1 g of catalyst)[50].

It is important to note that the CWAO experiments do not lead to total oxidation of phenol; several compounds are involved in the possible reaction pathways of phenol oxidation by CWAO [38], such as hydroquinone and benzoquinone, which have been identified as the most representative intermediates in t present work. Furthermore, TOC conversions in the oxidation of phenol were low with the rGO-M and rGO-U samples (only 22 and 11 %, respectively).

The catalytic activity of the rGO samples for oxalic acid and phenol oxidation by CWAO can be related to their surface properties (essentially basic/neutral nature and absence of strong acidic groups). The improved catalytic performance obtained with the rGO-M sample highlights once more the positive effect of the nitrogen groups, as previously reported in

[50] Adapted from Catalysis Today 249 (2015) 192-198.

the case of CNTs. Besides the accessible low surface area (102 m^2 g^{-1}), sample rGO-M presents high N surface content (9.3 % wt.) of which more than 50 % are pyridinic-like groups (N6). Therefore, once again, it seems that the presence of these Lewis base groups (N6) may play an important role by inducing the carbon surface basicity and, therefore, increasing the active sites for the removal of organic compounds [17, 18]. In the case of oxalic acid, comparing with N-doped CNTs prepared by ball milling, small differences were obtained using the rGO-M and the sample doped with melamine by dry treatment (CNT-BM-M, Figure IV- 15.b) using the same amount of catalysts (0.1 g), only around 5 min of reaction being required to reach full oxalic acid degradation. Besides the stability and the relative high catalytic performance under the oxidation of oxalic acid, rGO-M presents low performance in phenol degradation in comparison to the equivalent CNT sample (CNT-BM-M) (Figure IV- 24).

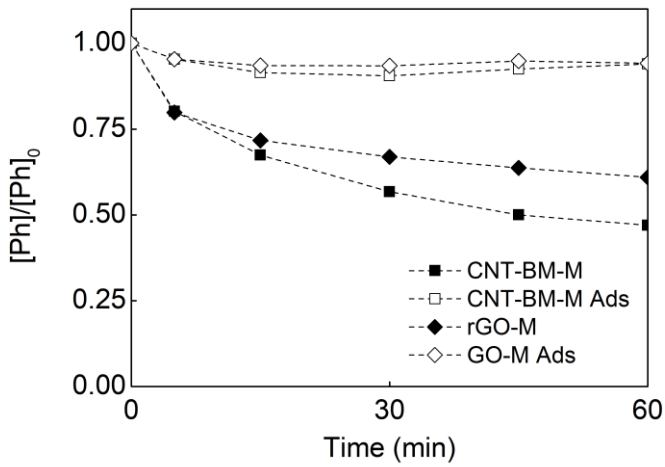

Figure IV- 24. Evolution of the normalized phenol concentration using melamine rGO sample and melamine doped CNTs in adsorption experiments (Ads) and as catalysts in CWAO (0.1 g of catalyst).

In addition, rGO samples present some drawbacks with respect to their application as catalyst in CWAO. Indeed, catalyst handling is problematic, due to the extremely fine nature of the material (thin powder), which will be difficult to recover by filtration at the end of the reaction. While CNTs can be easily recovered using filter paper with a pore size between 5 and 13 μm, rGO samples required, in most cases, a double filtration process using a filter paper with a particle retention greater than 2 μm.

Moreover, synthesis of the rGO and N-doped rGO samples is much more complex than synthesis of N-doped CNTs using the same ball milling approach, specially concerning the synthesis of GO, involving several steps with low yields of material obtained. Therefore, their complex preparation methodology and their use in powder form can be a handicap for their application as catalysts in CWAO.

2.3.2.3. Partial Conclusions

The addition of N-groups to the graphene structure markedly affected the catalytic performance of the synthesized materials in the degradation of oxalic acid and phenol by CWAO. Oxalic acid is efficiently oxidized by CWAO using the N-modified rGO samples. Phenol cannot be fully mineralized by CWAO; however, the use of the N-modified rGO samples significantly improved its degradation. In comparison with the homologous CNT sample, the melamine doped rGO exhibits lower catalytic activity, with additional problems regarding the handling and

recovery of the material, making them, at least as tested in powder form, less suitable for this application.

2.3.3.Carbon Xerogels

In addition to CNTs and rGO samples, CXs can be an interesting catalyst option for CWAO. Their synthesis does not involve contact with any transition metals (avoiding lixiviation of metals during the reaction), their textural properties can be tuned by adequate selection of the synthesis parameters [54], and they can be easily doped with nitrogen by incorporation of a nitrogen precursor during the synthesis [55, 56]. These features make it possible to develop a more systematic approach, consisting in testing carbon materials with similar textural properties and different surface chemistries, in order to assess the effect of nitrogen on the performance of carbon materials in these AOPs.

Most of the results presented in this section have been already reported in the paper *Nitrogen-doped carbon xerogels as catalysts for advanced oxidation processes*, authored by R.P. Rocha, J. Restivo, J.P.S. Sousa, J.J.M. Órfão, M.F.R. Pereira and J.L. Figueiredo, and published in the journal Catalysis Today Volume 241 – Part A, pages 73–79 (2015).

Author Contributions: Raquel Rocha performed the CWAO catalytic tests and post-characterization of carbon-xerogel samples, kindly made available for tests by J.P.S. Sousa. J. Restivo performed catalytic ozonation experiments. The manuscript was written by R.P. Rocha with contributions from all authors and with substantial supervision of J.J.M. Órfão, M.F.R. Pereira and J.L. Figueiredo.

2.3.3.1. Catalysts

A series of nitrogen-doped CXs, kindly made available by Doctor Juliana Sousa, were tested as catalysts. Detailed preparation is described elsewhere [57]. In brief, a gel was prepared using resorcinol and formaldehyde, together with a nitrogen precursor (either urea or melamine). Before gelation, the pH of the solution was adjusted to the desired value (6.9). Afterwards, the gels were carbonized at different temperatures under nitrogen flow (700 or 900 °C). The materials prepared with urea were named CXU, and those prepared with melamine were named CXM, followed by the pH of the solution prior to gelation, and the carbonization temperature. The CX samples selected for the present work were CXM_6.9_700, CXM_6.9_900, and CXU_6.9_700, since they have relatively similar textural properties and different types and amounts of nitrogen surface groups. In addition, a CX sample without nitrogen was prepared from resorcinol and formaldehyde at pH=6.9, and carbonized at 500 °C (CX_6.9_500). Catalysts were used in powder form with a particle size between 0.2 and 0.3 mm. Detailed information about the methodologies used in the synthesis of CXs and thorough characterization of the samples can be found elsewhere [57]. Table IV- 10 briefly summarizes the most relevant properties of this group of samples to support the discussion of their catalytic performance.

Table IV- 10. Relevant textural and chemical properties of the CX samples.

Sample	S_{BET}	CO	CO_2	N_{EA}	pH_{PZC}
	($m^2\ g^{-1}$)	($\mu mol\ g^{-1}$)	($\mu mol\ g^{-1}$)	(% wt.)	(unitless)
CXM_6.9_700	287	454	489	4.0	7.1
CXM_6.9_900	331	395	169	3.6	7.6
CXU_6.9_700	461	1292	579	2.9	7.4
CX_6.9_500	486	1226	444	---	7.0

It is worth noting that the different parameters used in the preparation method (nitrogen precursor, pH, and carbonization temperature) resulted in CXs with different textural and surface chemical properties. The surface oxygenated groups were assessed by the amounts of CO and CO_2 released during the TPD experiments which are shown in Table IV- 10 together with the pH at the point of zero charge. XPS analysis revealed the presence of three nitrogen functionalities on the surface of the selected nitrogen-doped CX samples: pyridine-like N, pyrrole-like N atoms, and quaternary nitrogen, with a bulk concentration between 2.9 and 4.0 determined by Elemental Analysis.

2.3.3.2. Catalytic Performance

Oxalic acid is poorly oxidized with the undoped sample CX_6.9_500, only 10 % could be degraded after 60 min (Figure IV- 25). However, oxalic acid was completely degraded in less than 45 min in the presence of the N-doped CXs. In any case, oxalic acid is directly mineralized, because no by-products are detected by HPLC analysis and the TOC removal corresponds to the oxalic acid disappearance.

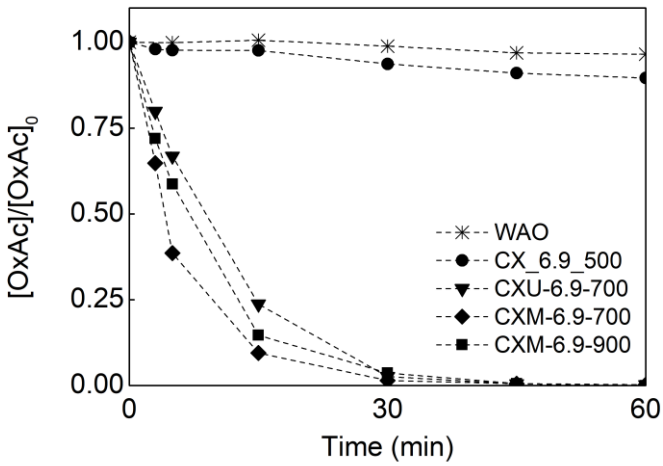

Figure IV- 25. Evolution of the normalized oxalic acid concentration under non-catalytic conditions (WAO) and using the CX samples as catalysts in CWAO (0.05 g of catalyst)[51].

As shown in Table IV- 10, the textural properties of the tested N-doped CX samples are not widely different (ΔS_{BET} < 150 $m^2\ g^{-1}$), and no correlation was found between the catalytic activity and the surface area

[51] Adapted from Catalysis Today 241 (2014) 73–79.

of these materials. The surface of the CX samples is essentially basic/neutral (pH_{pzc} between 7.0 and 7.6), indicating the absence of strong acidic groups. This observation is in agreement with the relevance that has been attributed to basic sites on the surface of carbon materials for CWAO [9], using carbon fibres enriched with nitrogen [17], ACs [22, 24], and also the CNTs and rGO samples tested.

The good catalytic performances obtained in the degradation of oxalic acid by CWAO with the N-doped CXs highlight the positive effect of the nitrogen groups. The amounts of surface nitrogen groups of the CXM and CXU samples, determined by XPS, are in the range of 2.6 to 3.8 % (Table IV- 10). Among the materials tested, the best performance was obtained with CXM_6.9_700, more than 90 % of oxalic acid being converted in 15 min, while the conversions obtained with samples CXM_6.9_900 and CXU_6.9_700 were 85 % and 76 %, respectively.

Normalized oxalic acid decay profiles describe a first-order reaction with different rate constants. Thus, the apparent initial reaction rate constants (k) (based in the first 15 min of reaction) were determined by the slope of the straight line obtained by plotting $-ln([OxAc]/[OxAc]_0)$ with respect to time, following the methodology previously reported. The values obtained for the apparent initial reaction rate constants were 0.160, 0.125, 0.094 and 0.002 min^{-1}, for CXM_6.9_700, CXM_6.9_900, CXU_6.9_700 and CX_6.9_500, respectively ($R^2 \geq 0.99$).

According to the XPS results, the amount of nitrogen groups decreases as follows: CXM_6.9_700 > CXM_6.9_900 > CXU_6.9_700, which is exactly the sequence of the reaction rate constants. A strong positive correlation was observed between the apparent reaction rate constants and the total nitrogen contents determined by XPS, as shown in

Figure IV- 26. Sousa et al. [17] have also found a linear correlation between the total organic carbon removal in aniline degradation by CWAO and the pyridinic-N group (N6) content of carbon fibres, indicating that the presence of these groups increases the catalytic efficiency. In the present CX samples, the fitting of the apparent reaction rate constants against the N6 groups also results in a linear positive correlation, although with a lower correlation coefficient (R^2= 0.98, result not shown) than that observed using the total nitrogen content.

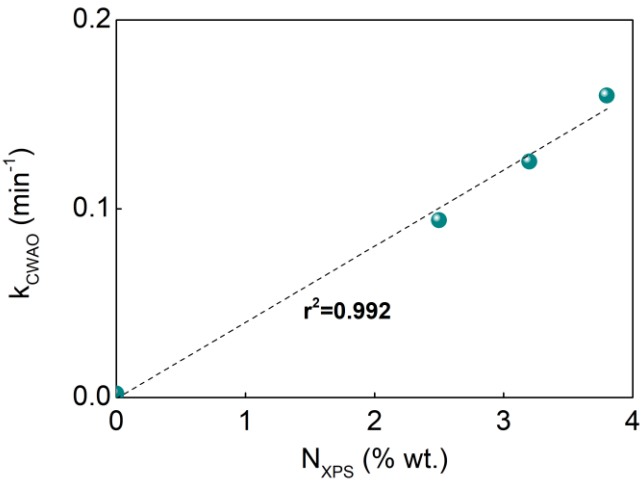

Figure IV- 26. Apparent first-order reaction rate constants (k_{CWAO}) vs. the total amount of nitrogen determined by XPS[52].

In contrast with the CNT and rGO tested samples, it was possible to establish a linear correlation in the case of the CX samples. Pristine CNTs and rGO present a considerable catalytic activity even without nitrogen functionalities, which is explained by the presence of π electrons on the

[52] Adapted from Catalysis Today 241 (2014) 73–79.

surface, that are known to be active sites for the formation of radicals [19]. Therefore, in these cases synergic effects of the π -electron system and the N-surface groups are playing a role. However, in the case of CXs, a low intrinsic catalytic activity was observed for the undoped sample, allowing to evaluate the single effect of nitrogen, without the contribution of the intrinsic surface catalytic activity.

Cyclic experiments using sample CXM_6.9_700 were performed to assess the possible deactivation of the catalyst during CWAO. Figure IV- 27 shows that complete conversion of oxalic acid is obtained after 30 min of reaction in three successive runs. Additionally, adsorption experiments also show that the extent of oxalic acid adsorption on the catalyst is not significant when compared with the removals obtained during the CWAO (adsorption after 60 min is less than 20 %). Very slight differences are observed during the two first runs (about 90 % of oxalic acid degradation in 15 min). However, the oxalic acid abatement in the same time was only 83 % in the third run, which can be explained by changes in the surface chemistry of the carbon catalyst promoted by the oxidative conditions in the reactor. Indeed, in the post-characterization of the different CNT samples previously reported and tested under similar operating conditions (140 °C and 40 bar of total pressure), it was observed that the pH_{pzc} decreased after reaction, while the amount of CO_2 released by TPD increased upon successive reutilization of the catalyst. An increase of the surface O content determined by XPS also indicated the formation of acidic groups on the surface, which have a negative influence on the catalytic activity of carbon materials for oxalic acid oxidation by CWAO. XPS analysis of the CXM_6.9_700 sample after CWAO experiment did not reveal any

significant alteration in the N1s spectrum (Figure IV- 28). Due to the difficulty in distinguishing clearly the N5 and NQ components, we opted to give their total amount.

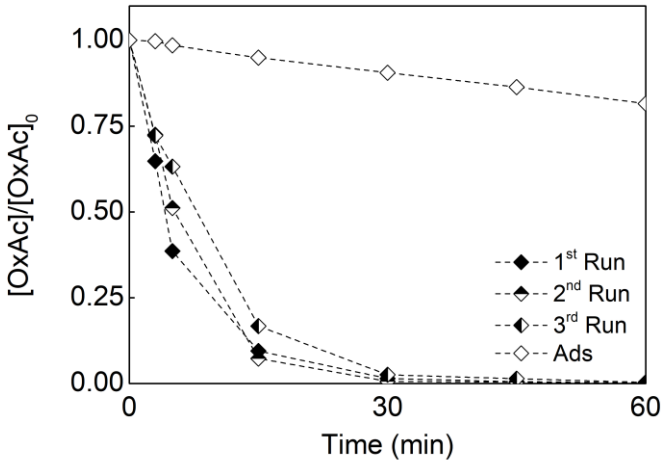

Figure IV- 27. Evolution of the normalized oxalic acid concentration in CWAO cyclic experiments using the CXM_6.9_700 sample as catalyst and in the adsorption experiment under pure nitrogen (Ads) (0.05g of catalyst)[53].

[53] Adapted from Catalysis Today 241 (2014) 73–79.

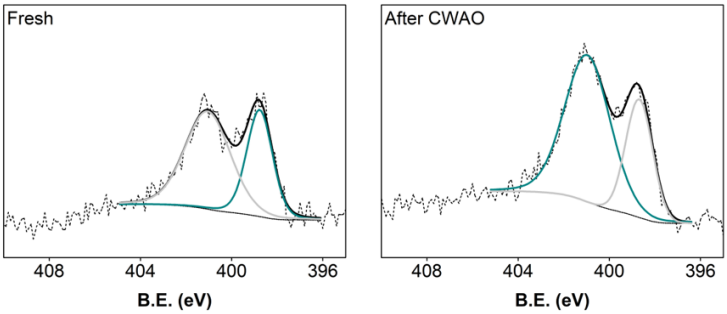

Figure IV- 28. N1s XPS spectra for the CXM_6.9_700 sample before and after used in oxalic acid degradation by CWAO[54].

The nitrogen containing CX samples underperform in the oxalic acid oxidation compared with previously reported results using CNTs and rGOs samples. With the most active CNT sample, oxalic acid full mineralization can be achieved in less than 5 min using the same catalyst loading and operating conditions, while the best CX sample required around 45 min to achieve similar conversion. Furthermore, a more pronounced deactivation of the catalyst was observed during cyclic experiments, demonstrating that CNTs are more resistant to oxidation during the reaction than the CXs. In spite of their lower catalytic activity and higher deactivation, additional results will be presented in section 2.4 *Mechanistic Considerations* to compare the reaction pathway involved using N-doped CNTs and CXs.

[54] Adapted from Catalysis Today 241 (2014) 73–79.

2.3.3.3. Partial Conclusions

CXs prepared by the sol–gel process using melamine and urea as nitrogen precursors were tested as catalysts in the oxalic acid degradation by catalytic wet air oxidation. The selected samples have very small amounts of acidic surface groups (low amounts of CO_2 released in TPD), their pH_{PZC} being neutral or slightly basic, but they present different types and amounts of nitrogen groups. The effect of these properties on the catalytic performance of the materials was evaluated. The N-doped CX samples showed high catalytic activity, oxalic acid being completely degraded in less than 45 min under the conditions tested. A strong positive correlation between the apparent reaction rate constant and the amount of nitrogen determined by XPS was also obtained. Therefore, N-doping improves the catalytic performance of the CXs in the liquid phase oxidation process. The effect of nitrogen is evident, the rate constants increasing by two orders of magnitude in comparison with the nitrogen-free material. Cyclic experiments showed a slight loss of performance, probably due to the oxidation of the carbon surface promoted by the operating conditions.

2.4. Mechanistic Considerations

It is general accepted that the oxidizing power of WAO is based on the high solubility of oxygen at these severe conditions and the high temperature that increases the reaction rates and production of free oxygen radicals [3]. For many years, it has been accepted that the process involves a chain reaction mechanism in which oxygen and hydroxyl ($HO^{\bullet}$), hydroperoxyl ($HO_2^{\bullet}$), organic hydroperoxyl [3, 4] free radicals and oxyradicals [4] actively participate in the reaction. Several free radical reactions consisting of initiation, propagation, and termination of free radical have been proposed to take place during the WAO of various organic compounds [6, 58], in which the induction or initiation step represents the time required to produce a minimum free radical concentration. When catalysts are employed in the WAO system it is postulated that the catalyst performs three roles that enhance the wet oxidation process, these being oxygen activation, radical generation and organic oxidation, and, therefore, the same role of the free-radicals is accepted. Besides the free radical (homolytic) reaction, also ionic (heterolytic) oxidation reaction mechanisms have been proposed for the CWAO of organic compounds [59]. For a catalyst with poor activity, the free radical mechanism may predominate, and thus high catalyst concentration could lead to a longer induction period or lower oxidation rate due to the chain termination caused by interaction between free radicals and catalyst. This might explain the lower pollutant conversion over some catalysts in comparison to the uncatalyzed oxidation. On the other hand, the redox mechanism may predominate in the presence of catalysts with high activity [58]. A simple but generally accepted free

radical chain mechanism pointed out by Pintar and Levec [60] is still being considered in mechanistic studies of CWAO. The catalytic phenol oxidation in aqueous solution involves a heterogeneous-homogeneous free radical mechanism, which postulates a heterogeneous initiation step on the catalyst surface followed by a homogeneous propagation and either heterogeneous or homogeneous termination reactions [64]. Since carbon materials have been introduced as catalysts in CWAO, the most sophisticated CWAO kinetic studies take into account the heterogeneous nature of solid catalysed oxidation reactions involving adsorption of reactants, surface reaction and desorption of products [24]. Some kinetic models ignore the adsorption of dissolved molecular oxygen while others include participation of adsorbed oxygen in the mechanism.

In spite of all the studies already published regarding the use of carbon materials as catalysts in CWAO, the reaction pathways involved in those reactions are still in doubt. Despite of their complexity, it is generally accepted that: a) the reaction mechanisms involve free radicals; b) basic carbons are the best catalysts; c) oxidation of the organic compounds may occur both in the liquid phase (homogeneous reaction) and on the catalyst surface [9].

The difficulty in clarifying the mechanism is strictly related with the difficult identification and quantification of the radicals involved. In addition, it is also difficult to inactivate potential active sites to assess their participation in the reaction pathway. Although numerous researchers have proposed that oxidation occurs mostly via free-radical chemical reactions, only a few have provided direct experimental evidence to support these claims. The severe operating conditions at which they are formed, their instability and the experimental difficulties in determining

the presence of such species in the reaction media are some of the reasons for their unequivocal identification [6]. In a few works reported in the literature, electron spin resonance (ESR) spectroscopy coupled to a spin trapping technique was used to identify the radicals involved. In some of them, hydroxyl radicals ($HO^{\bullet}$) have been identified as intermediates in the reaction [61]. Some studies provided indirect evidence of free radical reactions. Co-oxidation is one of them, which involves the oxidation of an organic compound by free radical intermediates generated from another organic compound [58]. Alternative indirect experimental studies were used to prove the presence of the radicals in the reaction. The indirect method for determining free-radical reactions involves the use of compounds known to inhibit free-radical reactions, *tert*-butanol being the most common radical scavenger used. It has been used with phenol [62] and *p*-toluenesulphonic acid [63], and it was found that the rate of oxidation decreased in the presence of the radical scavenger, indicating that a free-radical reaction was taking place.

Using this indirect method for determining free-radical reactions involved in CWAO, this section presents an attempt to clarify the role of the free radicals on the mechanism of CWAO using carbon materials. Differences in the mechanism taking place when N-doped or S-doped carbon materials are used as catalysts are discussed and highlighted.

Most of the results presented in this section have been already reported in papers dealing with the CWAO studies described in the preceding sections. To allow a better reading, understanding and comparison between the materials and mechanisms involved, a compilation of results shown below was adapted from the published papers.

N-doped carbon materials

Selected N-doped carbon samples were tested in CWAO in the presence of the radical scavenger *tert*-butanol (*t*-BuOH) with a concentration ten times higher than the model pollutant (oxalic acid). *t*-BuOH can scavenge the hydroxyl radicals in competition with other compounds in liquid phase [64, 65], decreasing the removal rate of the other compounds [63, 66]. Therefore, with these reactions the assessment of the hydroxyl radical interaction in the removal of the organic compound was attempted.

Figure IV- 29 shows a CWAO experiment using pristine commercial CNTs (CNT-O) performed in the presence of *t*-BuOH. The obtained results were very similar to those obtained in the absence of the radical scavenger, suggesting that hydroxyl radicals in solution were not the relevant species involved in the oxidation mechanism, and that oxalic acid oxidation should be mainly promoted by active oxygen species on the CNT surface produced from the decomposition of oxygen or by other free radicals in solution. The surface mechanism has been already reported for ACs used in advanced oxidation processes [9, 19, 67]. Similar evidences were observed with N-doped CXs (sample CXM_6.9_700, Figure IV- 29). The results obtained in the presence or absence of *t*-BuOH are identical, suggesting that hydroxyl radicals in the liquid phase are not needed, and that an alternative surface reaction mechanism is available for oxalic acid oxidation. Regarding the N-doped CNT sample, the same fast degradation of oxalic acid in the presence of *t*-BuOH corroborates the independence from hydroxyl radicals in solution.

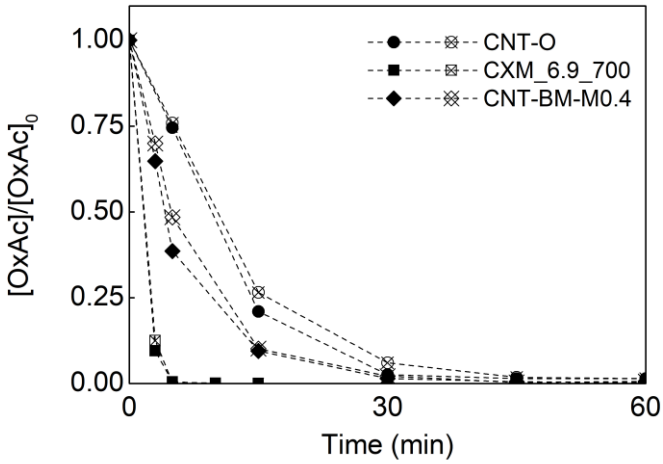

Figure IV- 29. Evolution of the normalized oxalic acid concentration, using as-received commercial CNTs (CNT-O, 0.2 g), melamine doped CNTs (CNT-BM-M0.4, 0.05 g) and N-doped CXs (CXM_6.9_700, 0.05 g) in the presence (filled symbols) and absence (crossed symbol) of *tert*-butanol under CWAO experiments (140 °C; 40 bar of total pressure).

As previously commented, in addition to hydroxyl radicals, other free-radicals may be formed during CWAO. Unfortunately, techniques as electron paramagnetic resonance (ESR) spin-trapping, that allow the identification and/or quantification of the radicals in solution, were not available to ascertain the eventual presence of other radicals in the solution. In fact, Wang et al. [33] used this technique for the detection of the active species produced in the CWAO of phenol using CNTs as catalyst. While in the absence of catalyst no observable ESR signal was detected (suggesting the absence of radicals or very low concentration of radicals), using the CNTs they found the formation of perhydroxyl ($^{\bullet}OOH$) and superoxide ($O_2^{\bullet-}$) radicals during the phenol degradation by CWAO. The

production of these radicals has been attributed to the carboxylic acid groups on the surface of these materials.

However, in the present work, excluding the undoped CX sample (CX_6.9_500), none of the tested carbon materials showed a typically reaction behaviour characteristic of a free-radical mechanism, which is normally described by an initial induction period where none oxidation is observed until a critical free-radical concentration is achieved [12]. The absence of this initial step using the pristine CNTs, the rGO sample and the other N-doped samples tested, suggests that a free-radical mechanism in the liquid phase is not involved in the reaction. Furthermore, in the case of a free-radical mechanism, several by-products are typically found during the degradation of the organic pollutant. This was not observed under the conditions tested and even the formation of hydroquinone and benzoquinone from phenol, observed in batch operation mode, is low. For an initial phenol concentration of 75 mg L^{-1}, the maximum formation of hydroquinone and benzoquinone was lower than 0.2 mg L^{-1} using pristine CNTs and an equivalent CNT-BM-M0.4 sample [68]. Considering all the experiments, a radical reaction in the liquid-phase in the tested carbon materials is not probable.

In the case of the pristine CNT and rGO samples, the oxidation reaction may be promoted by the π electrons on the surface, which are known to be active sites for the formation of radicals [19] in the presence of water [18]. The electrons may be transferred from the catalysts to adsorbed oxygen, producing highly reactive radicals that can react with adsorbed organic compounds leading to the oxidation of the organic pollutants.

Also the enhanced catalytic activity observed in the presence of N-functionalities seems to result from the interaction of oxygen with the carbon surface [35]. The activation of oxygen by nitrogen groups to generate active oxygen species was reported in the case of an NH_3-treated AC [21]. N-groups with delocalized extra electrons were identified as the possible species responsible for the enhanced chemisorption [35] and activation of oxygen molecules [37]. Such active oxygen species can react with adsorbed organic compounds leading to the oxidation of the organic pollutants. Therefore, in the presence of N-functionalities on the carbon surface, hydroxyl radicals in the liquid phase may not be required, suggesting that the oxidation reaction can occur by an alternative surface reaction mechanism, possibly as described above. This could also justify the clear catalytic improvement observed when N-doped CX samples were tested in CWAO of oxalic acid, since the homologous undoped sample (CX_6.9_500) revealed a poor catalytic performance.

Although the catalytic results presented do not allow to establish clearly which is the best N-functionality to improve oxygen chemisorption and activation, all the extremely active catalysts tested presented high relative amounts of the pyridinic group (N6). Pyridine-like N groups are electron rich structures [48]: they have six π electrons plus an unshared pair in a nitrogen sp2 orbital; therefore, the unshared pair can be used to adsorb oxygen species and, since the unshared pair is not involved in the π system, the aromatic character of the ring is not much affected. This can be interpreted as an electron donation, where electrons from the catalyst are used to adsorb oxygen originating highly reactive oxygen species [47], without sacrificing the aromaticity of the molecule or the basal plane. In contrast, in N5 and NQ functionalities, their electrons are involved in the

conjugation of the π system and, consequently, their ability to donate electrons to oxygen molecules to form the reactive species is expected to be lower.

According to the results, the proposed reaction pathway for oxalic acid degradation by CWAO involves the adsorption of oxygen and oxalic acid on the carbon surface, oxygen being activated into reactive species that react with the adsorbed oxalic acid. The results suggest that surface oxidation is the main mechanism for oxalic acid degradation in the presence of nitrogen-doped carbons. Figure IV- 30 schematically illustrates these possible reaction pathways.

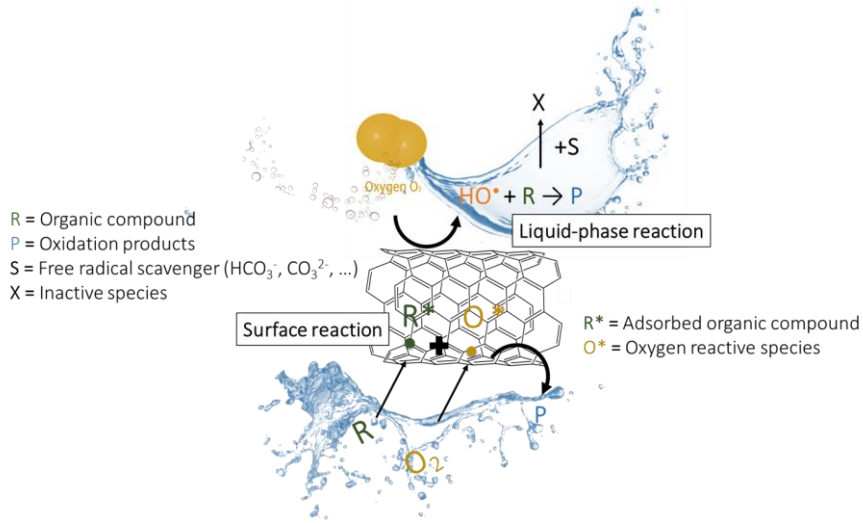

Figure IV- 30. Scheme of the reactions that might occur between the surface of CNTs and oxygen as oxidative agent during CWAO experiments[55].

[55] Adapted from Journal of Carbon Research C, 2 (2016) 17.

S-doped carbon materials

A different reaction pathway may be involved in the case of S-doped CNTs. Sodium persulphate and potassium persulphate are strong oxidizing agents often used to form sulphate radicals for several applications where strong oxidant radicals are required. They are frequently used for in-situ chemical oxidation [41, 69] and some advanced oxidation technologies [70-74], with the sulphate radical ($SO_4^{\bullet-}$) being produced by thermal activation, reaction with ozone-derived species or photolysis of persulphate anions [75].

In a first attempt to clarify the reaction mechanism involved in CWAO with the S-modified samples, experiments were done by adding *t*-BuOH in a concentration ten times higher than that of the model pollutant (Figure IV- 31). Surprisingly, major differences were observed: while oxalic acid removal using the CNT-S sample does not seem to be affected by the presence of the radical scavenger, phenol degradation strongly decreases upon addition of *t*-BuOH, reaching a maximum conversion of around 70 %. This suggests that the radicals formed in the presence of the CNT-S sample may be selective for pollutants degradation, and, in particular, for phenol.

In order to go deeper into this matter, CWAO experiments were done with the pristine CNTs by adding sodium persulphate as a source of sulphate radicals. The amount of sodium persulphate added to each system was determined by considering the mass of catalyst used in the CWAO experiments (200 mg) and the amount of SO_2 released by sample CNT-S in TPD (579 μmol g^{-1}). Therefore, the reactions were performed using equivalent S molar concentrations of the carbon samples as a source of sulphate radicals.

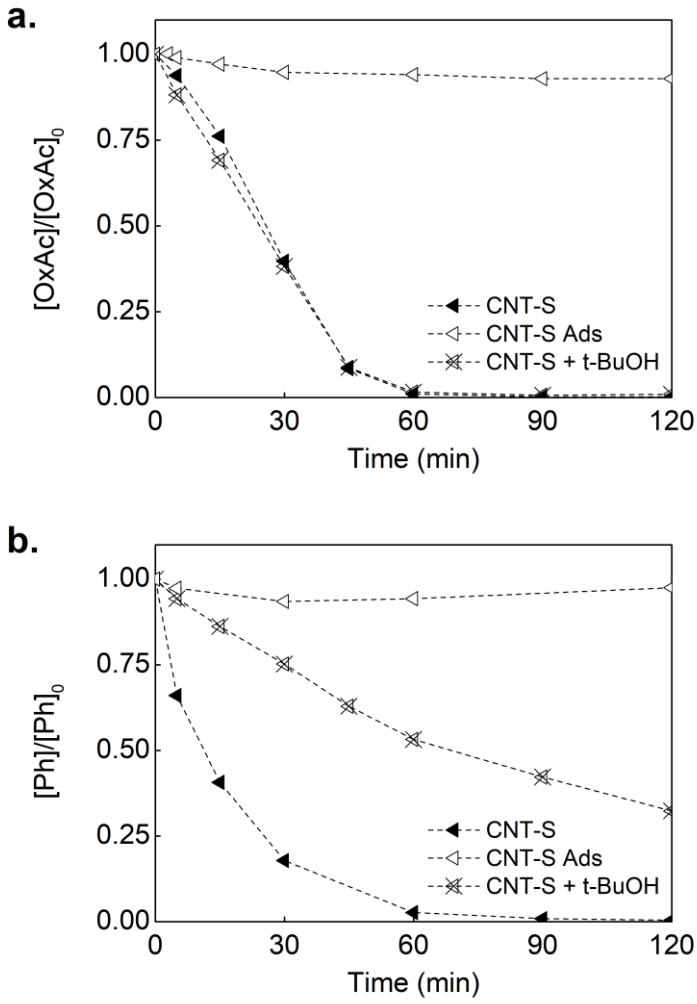

Figure IV- 31. Evolution of the normalized (a) oxalic acid and (b) phenol concentration under CWAO experiments with or without the radical scavenger *tert*-butanol, and respective adsorption experiments (Ads)[56].

[56] Adapted from Chinese Journal of Catalysis 35 (2014) 896–905.

The thermal activation of sulphate radicals occurs (by decomposition of the S-containing surface groups, $-SO_3H$) and the reaction mechanism involves sulphate radicals in solution. In the CWAO process, it was expected that the addition of sodium persulphate could lead to the thermal activation of the sulphate radicals due to the high operating temperatures.

Figure IV- 32 shows the oxalic acid and phenol degradation under identical operating conditions tested in CWAO, in the presence or absence of sodium persulphate ($Na_2S_2O_8$). The addition of $Na_2S_2O_8$ to the system does not promote any degradation of oxalic acid, neither improve the catalytic activity of the pristine CNT-O sample (curve CNT-O + $Na_2S_2O_8$). These results demonstrate that radicals formed from the thermal activation of the persulphate are not selective for oxalic acid degradation. On the other hand, Figure IV- 32.b shows that phenol is quickly converted when sodium persulphate is added to the reaction system in the absence of any catalyst ($Na_2S_2O_8$ curve). Since phenol is refractory in non-catalytic conditions (WAO), phenol abatement in such experiment should be related to the presence of the sulphate radicals formed by the chemical activation of persulphate ions. In addition, in the case of phenol, an improvement of the catalytic performance of the pristine CNTs was observed when $Na_2S_2O_8$ was added to the system. However, comparing with the CNT-S sample, where a lower rate of phenol conversion was observed, the liquid phase reaction with persulphate leads to a lower mineralization of phenol (37 % of TOC removal after 2 h of reaction at 160 °C with $Na_2S_2O_8$ vs. 57 % in the CWAO experiment with sample CNT-S).

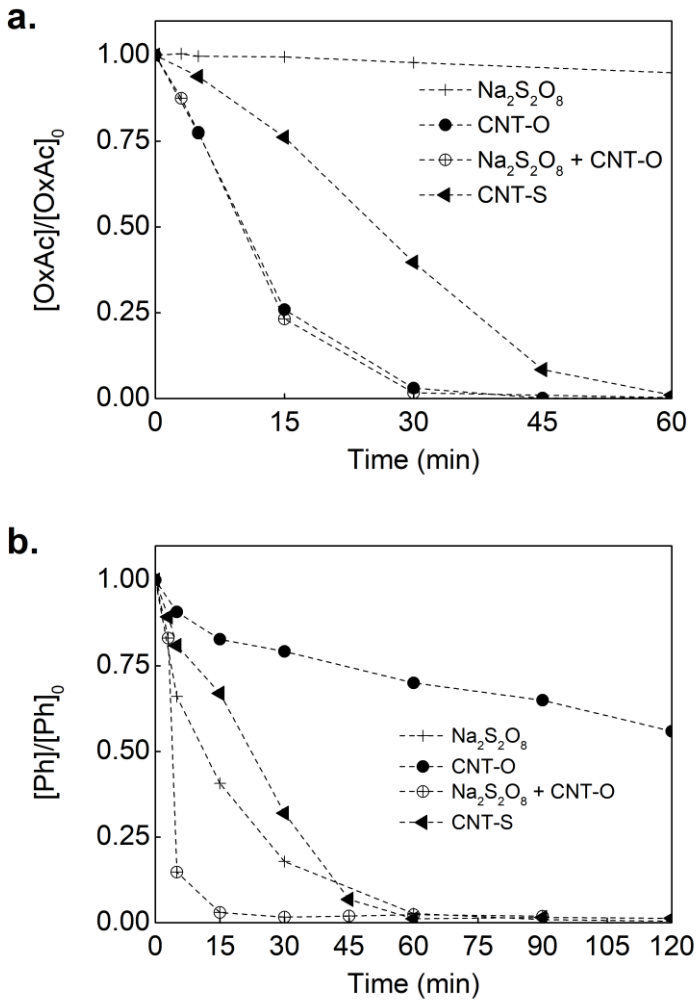

Figure IV- 32. Evolution of the normalized (a) oxalic acid and (b) phenol concentration under CWAO experiments in the presence or absence of persulphate ($Na_2S_2O_8$)[57].

[57] Adapted from Chinese Journal of Catalysis 35 (2014) 896–905.

It is important to mention that the activity of $Na_2S_2O_8$ in phenol oxidation was also observed when the operating temperature was decreased to 140 °C, similar catalytic activity being achieved as that observed in the reaction performed at 160 °C (phenol concentration decay of 97 % in 15 min of reaction). This also eliminates eventual concerns about the temperature being enough to promote the thermal activation of sulphate radicals in the oxalic acid experiments. A supplementary experiment using $Na_2S_2O_8$ without any carbon material was performed in the absence of oxygen, ie, replacing oxygen by pure nitrogen at 40 bar of total pressure (result not shown). From this experiment, an additional conclusion was reached: in the absence of oxygen, the phenol concentration decay was only 25 % in the first 5 min of reaction; after this period, a plateau is reached, and the concentration remains constant until the end of the reaction (120 min). This indicates that oxygen plays an important role in the activation of $Na_2S_2O_8$. In fact, in other oxidation processes [72, 74], hydroxyl radicals (generated in the presence of oxygen) were reported to be responsible for the generation of sulphate radicals in the presence of persulphate ions.

So, in summary, these results lead to the conclusion that, in the case of phenol, the reaction mechanism involves free radicals in solution. In the absence of persulphate ions (with which *t*-BuOH can also react [41]), the radical scavenger can react with hydroxyl radicals. Therefore, the decrease in the phenol degradation rate in the experiment with the CNT-S sample and *t*-BuOH (Figure IV- 31) can be due to: (1) hydroxyl radicals in solution that play a role in the phenol oxidation mechanism being quenched by *t*-BuOH; (2) sulphate radicals formed upon release of the S-groups from the CNT surface being scavenged by *t*-BuOH (it should be remembered that S-

surface groups originally present in the fresh sample are lost during the reaction); or (3) a synergistic effect of both radicals. In fact, it has been reported that the active species taking part in the oxidation of organic compounds in the carbon/persulphate combined system are both $SO_4^{\bullet-}$ and $OH^{\bullet}$ radicals [71, 74, 76].

The strongly different selectivity for model pollutants degradation and the loss of activity observed after reaction, makes it possible to conclude that this sample is not recommended as a potential catalyst for the CWAO process, since under real conditions it will be selective towards the pollutants, not ensuring effectiveness in the destruction of all the compounds.

2.5. Final Remarks and Literature Overview

Many organic compounds undergoing WAO gradually degrade to low molecular weight compounds and, finally, to highly refractory lower carboxylic acids. For instance, Devlin and Harris [77] have studied wet air oxidation of phenol and listed various oxidation products. These include monobasic and dibasic acids, such as acetic acid, formic acid, glyoxalic acid, oxalic acid, etc. Oxidation of these low molecular weight compounds is often the rate-controlling step during wet air oxidation (WAO) of an aqueous waste stream exhibiting very high chemical oxygen demand (COD) [78]. In particular the wet oxidation of oxalic acid was found to require more severe conditions as compared to glyoxalic acid [79]. The results reported in literature for non-catalytic WAO of oxalic acid show that high temperatures (above 220 °C at 8 bar of pure O_2) are required in the absence of a catalyst to obtain 35 % oxidation of this pollutant (500 mgL^{-1}) after 30 min [78]. The chemical oxygen demand reduction of oxalic acid in aqueous solutions is also low (4 %) in non-catalytic conditions at 245 °C or even in the presence of a homogeneous $CuSO_4$ catalyst at a lower temperature (6 % for 140 °C, 7 bar O_2) after 30 min [79]. Higher activities were found with a Pt/charcoal catalyst (30–60 %, initial oxalic concentration of 5000 mg L^{-1}) for the same period of time under less severe conditions, 53 °C at atmospheric pressure, [80], and ca. 90 % of oxidation with a Pt/Al_2O_3 catalyst at 80 °C [81]. At 90 °C and at atmospheric pressure, 75 % of oxalic acid degradation (for an initial concentration of 2000 mg L^{-1}) was obtained after 5 h of reaction with a Pt/ceria promoted alumina [82]. Regarding the use of carbon materials as catalysts in oxalic acid conversion by CWAO, no studies were found in the

literature where oxalic acid was considered as the main pollutant. However, in works related to phenol degradation using carbon materials, some publications report the formation of oxalic acid during the phenol degradation [10, 31-33]. In those works, the carbon materials tested were reported to be able to degrade the oxalic acid formed. In the work of Wang et al. [33], 2000 mg L^{-1} of oxalic acid was degraded at 160 °C in less than 30 min but using a larger amount of catalyst (0.4 g of CNTs) and a much higher pressure of oxygen (25 bar of pure oxygen). This was from the literature the most competitive sample from the literature, in comparison to the here tested samples, particularly the sample CNT-BM-M.

The oxidation of aqueous phenol by oxygen was studied many years ago under severe temperatures and pressures (up to 300 °C and 170 bar of pressure) [59, 77, 83, 84]. Phenols and its derivates are the most common model pollutants studied, representing around 50 % of the studies performed under catalytic wet air oxidation accordingly to the ISI Web of Knowledge in 2012 [85]. Under non-catalytic conditions, a phenol degradation of 90 % was reached after 120 min of reaction at 265 °C and 9 bar of oxygen partial pressure in semi-batch experiments [86]. Due to the difficulty in achieving high phenol mineralization under less severe conditions, researchers dedicated several studies first to the development of homogeneous catalysts and later to heterogeneous materials, including supported noble metals, supported and unsupported metal oxides, metal salts and carbon materials. A comprehensive survey of investigations on catalysts for CWAO processes is provided in several reviews of Matatov-Meytal and Sheintuch [87], Imamura [88], Bhargava et al. [6], Levec and Pintar [7] and Cybulski [8]. In addition Stüber et al. [24] reviewed the use of carbon materials, such as ACs, graphites and carbon blacks in CWAO

processes, including phenol degradation. The diverse batch and continuous phenol degradation studies by CWAO over carbon catalyst reported almost 100 % phenol conversion and 85 % TOC or COD destruction at 160 °C, 2-45 bar O_2 and space times or reaction times of about 0.3 h or 3–6 h, respectively [24]. In comparison with supported catalysts, using carbon catalysts no deactivation and/or metal leaching is observed in the oxidation process. However, almost all the carbon catalysts exhibited accumulation of refractory compounds on the surface after phenol degradation. Furthermore, oxygen attacks the carbon surface, continuously producing new surface oxide groups and changing the original activity of the carbon catalyst. In this context, novel nanocarbon materials have been tested. Yang et al. [30] reported full phenol degradation and a TOC conversion of 76 % using MWCNT treated with a mixture of HNO_3/H_2SO_4 as catalyst at 160 °C and 20 bar of pure oxygen pressure. This result was obtained with a starting solution of 1000 mg L^{-1}, using 0.8 g of catalyst in a 500 mL of solution. In subsequent works of the authors [31-34], they tested carbon fibres and graphite, but only a small improvement was obtained with ozone treated CNTs: full phenol degradation was achieved in 90 min (155 °C; 25 bar of pure oxygen; 0.4 g of catalyst), but TOC conversion reached 80 % in 120 min. Soria-Sánchez et al. [10] tested different carbon nanostructured materials, nanofibres (CNFs), CNTs and high surface area graphite. Oxidized-CNFs were the most active catalyst tested, reaching 90 % of phenol conversion (mineralization of 50 %) in 3 h under the conditions tested (phenol initial concentration of 2000 mg L^{-1}; catalyst loading of 4 g L^{-1}; 140 °C, 20 bar of total pressure). Ruthenium nanoparticles supported on nitrogen-doped CNFs have been also tested by Ayusheev et al. [89], but required 5 h of reaction to full

phenol conversion (initial phenol concentration of 2000 mg L^{-1}; 1.67 g L^{-1} of catalyst, 180 °C, 50 bar total pressure). Removal of 97 % of phenol with 94.2 % selectivity to CO_2 and H_2O was observed using 0.95 % wt. Pt-containing nanoparticles (NPs) [38]. They highlighted that the conversions obtained were significantly higher than those for the conventional Pt/Al_2O_3 catalyst with similar amount of the active metal or for Pt(5 %)/ AC. The results were obtained at 95 °C and 10 bar of pure oxygen pressure in 5 h of reaction. Most of the results published in the literature report good performance of carbon material under phenol oxidation, but direct comparison with the results reported in this thesis is difficult because different reaction parameters were tested, particularly the initial phenol concentration and the catalyst loading. A closer evaluation within the reported catalytic achievements may be found in the work of Santos et al. [68]. Under similar operation conditions (phenol initial concentration of 75 mg L^{-1}; 160 °C, 8 bar of pure oxygen), a poor phenol conversion is achieved using CeO_2 as catalyst (<20 % in 2 h of reaction), but 1 % Pt (wt.) supported on pristine CNTs promoted full phenol degradation in 60 min and a TOC conversion of 80 % in 2 h. However, the concentration of intermediate compounds, as hydroquinone and benzoquinone, was much higher when platinum was used as catalyst, compared with pristine CNTs or N-doped CNTs.

The best catalytic performances for oxalic acid and phenol oxidation by CWAO in each class of carbon materials tested using N-doped carbon materials were obtained with samples CNT-BM-M, rGO-M and CXM_6.9_700 samples. Regardless of the already highlighted problems associated with the application of each material as catalyst in CWAO, namely the fine powder form of rGO-M and the complex synthesis of

CXM_6.9_700, CNT-BM-M seems to be the most adequate catalyst for the reaction. High catalytic efficiency for oxalic acid and phenol degradation was obtained with this sample, lower deactivation was observed and, furthermore, it can be prepared by an easy to handle method that avoids the use of solvents and waste production.

From batch to continuous mode

CWAO experiments under batch operation result in a lower investment cost compared with the continuous mode. However, high labour costs are involved in reactor filling and cleaning step. Furthermore, batch processing is difficult to apply to a large-scale production. In this context and for large-scale wastewater and water treatments, reactors under continuous operation may be preferred. In spite of this, in most cases, the CWAO experiments using carbon materials as catalysts are performed in batch mode (including the presented results) and only a few papers describe tests in continuous mode, mostly using carbon as catalyst [22, 25, 68, 90-93]. In cases where authors compared the performance of batch and continuous operation, different initial rates of phenol oxidation were observed, being much higher in a slurry reactor when compared to a trickle bed reactor, for instance [92]. Those differences were explained by different factors including mass transfer limitations, ineffective catalyst wetting and preferential flow. Therefore, since different phenomena can affect the observed reaction rates when the reaction is performed in a batch or in a continuous reactor, running the experiments in both types of reactor is important to understand the reaction mechanisms and to select the most appropriate catalyst and operating conditions to enable a viable

application of the technology [68]. Santos et al. reported a comparison between batch and continuous operation of CWAO of oxalic acid and phenol over N-doped CNTs as well as the influence of several reaction parameters (temperature, dissolved oxygen concentration and initial phenol concentration) [68]. The N-doped CNT sample tested by Santos et al. was prepared by the methodology developed and reported here, using the ball milling approach and melamine as N-source. Therefore, their results can provide an extension to the use of the CNT-BM-M sample in CWAO under continuous operation. Regarding the tested parameters, it was found that the dissolved oxygen concentration, controlled by the oxygen partial pressure, had only a small effect on the phenol and TOC removals, considering the range under study. In contrast, the temperature had a more significant effect, an optimal temperature of 160 °C being determined. In the continuous mode operation, phenol and TOC removals of 80 and 50 %, respectively, were achieved in steady state at 160 °C and 12 bar of oxygen partial pressure, with an initial phenol concentration of 500 mg L^{-1}. However, catalyst deactivation was observed, probably due to the formation of phenolic polymers that deposit on the surface of the catalyst, blocking the access to the functional groups. Nevertheless, a significant regeneration of the N-doped catalyst could be achieved by thermal treatment at 600 °C under nitrogen atmosphere.

From lab-scale to real applications

Reported works in the literature and the work developed in this thesis support the potential of carbon materials as catalysts in CWAO. Nevertheless, further studies may be conducted to get conclusive results on the application with real wastewaters, deactivation vulnerability and biodegradability of the effluents in order to emphasise their cost efficiency [85].

Bearing in mind a real scale application, the use of carbon materials in powder form in trickle-bed reactors can be a problem. Some drawbacks are associated with potential channelling, high-pressure drop, and decrease of the catalyst efficiency. Macrostructured supports can provide better control of the contact time of reactants and products with the catalyst, leading to a potential increase in selectivity. Honeycomb monoliths and SiC foams can be an alternative to powder, granules or extrudates of carbon materials to be used in a real application. Both are suitable for applying thin-coated layers of various materials, for instance, by dipcoating [94]. Hierarchical structures, with controlled macroscopic shapes and coated with metal-free carbon materials have been extensively developed over the last few decades for numerous relevant catalytic processes, where mass and heat transfer can be easily optimized for better catalytic performance and stability [95]. Coating of macroscopic supports with carbon materials for catalytic applications has been developed as an industrial key-process [96]. These advances provide new opportunities for the development of macrostructured catalysts, more adequate for real applications than conventional catalysts in powder form.

(This page intentionally left blank)

3. Section Conclusions

Looking for alternatives to replace noble metals and metal oxide catalysts, traditionally used in the CWAO process, the present work discloses the potentialities of carbon materials as metal-free catalysts in liquid phase oxidation reactions for wastewater and water treatment by CWAO. Commercial CNTs, rGO samples and CXs were studied as potential catalysts for oxalic acid and phenol degradation, as model compounds for CWAO. It was found that the performance of carbon materials can be substantially enhanced by tailoring the textural and chemical properties by appropriate thermal or chemical post-treatments.

Oxalic acid is very stable under non-catalytic conditions at 140 °C, but it can be totally degraded with pristine commercial CNTs from Nanocyl^{TM} in less than 30 min, at the same operating conditions. Phenol is not degraded in the absence of a catalyst at 160 °C, and is more difficult to convert using pristine CNTs, only 40 % conversion being obtained in 120 min. Even without any functionalization, the performance of pristine CNTs can be improved by mechanical treatments such as ball milling, resulting in higher oxalic acid and phenol conversions.

It was found that the apparent initial first order reaction rate constants for CWAO of oxalic acid correlate with the point of zero charge of the CNT samples, CNTs with a basic nature being markedly more active catalysts than CNTs with a pronounced acid character.

Using the CNT samples treated with HNO_3 and subjected to thermal treatments as catalysts for degradation of oxalic acid and phenol by CWAO, it was observed that the conversion of these pollutants increases

also as the amount of O-containing surface groups present on the catalyst surface released as CO_2 decreases.

However, CNTs modified with H_2SO_4 or HNO_3/H_2SO_4, which have a strong acidic character (low pH_{pzc}), showed an unexpected high activity for degradation of both model pollutants. The performance of these materials was explained by the presence of S-containing surface groups that may originate strong oxidant species in the liquid-phase, such as sulphate radicals. Nevertheless, the catalytic activity of the CNTs treated with H_2SO_4 is drastically reduced in cyclic experiments due to the decomposition of the S-containing surface groups, as the result of the high temperatures used in the CWAO process. Therefore, in general, the catalytic activity of CNTs increases with their basicity, but some specific groups, such as S-containing groups, can lead to a different behaviour even if they are acidic.

The presence of nitrogen groups on the carbon surface leads to a faster removal of both model compounds. Several metal-free N-doped CNT catalysts have been prepared using a ball milling approach. Different approaches were tested by mixing the CNTs in a ball mill with a N-precursor (with and without a solvent) followed by thermal treatments, or alternatively treated under NH_3 flow. Different nitrogen precursors (melamine, urea and NH_3), precursor/ CNTs ratios, O-containing surface groups and final temperatures of the thermal treatment were evaluated towards the generation of active and stable N-species. Using an easy to handle, solvent-free post-doping method it was possible to incorporate N-groups into the CNT sp2 network, namely, quaternary nitrogen, pyrrolic and pyridinic groups. All prepared samples showed high catalytic performance during the oxidation of oxalic acid and phenol. So far, those samples are the best metal-free carbon catalysts tested in both processes.

Compared to traditional catalysts (noble metals or metal oxides), the N-species are well anchored onto the catalyst structure and, as a result, the drawbacks related to loss of active phase are improbable to occur even under severe reaction conditions; in addition, the stability and electron transfer rate are improved, leading to a higher durability of the catalysts during the catalytic processes.

The methodology was extended to the incorporation of N-groups into the graphene structure, revealing that N-doping affected the catalytic performance of the synthesized materials in the degradation of oxalic acid and phenol by CWAO. However, due to the thin powder form of the rGO samples, handling may be a problem for their application.

The tested CX samples allow to clarify the role of the N-functionalities. A strong positive correlation between the apparent reaction rate constant and the amount of nitrogen determined by XPS was also obtained. Therefore, N-doping improves the catalytic performance of the CXs in the liquid phase oxidation. The rate constants increased by two orders of magnitude in comparison with the nitrogen-free material.

Clarification of the mechanism involved in the CWAO has been attempted by using the radical scavenger *tert*-butanol. Excluding S-doped samples, the results obtained in the presence of *t*-BuOH were very similar to those obtained in the absence of the radical scavenger, suggesting that hydroxyl radicals in solution were not the relevant species involved in the oxidation mechanism. When other N-doped carbon materials were tested in CWAO (CXs) similar evidences were observed. Therefore, it was proposed that the conversion of pollutants by CWAO can occur by means of surface active species produced from the decomposition of oxygen. The enhanced catalytic activity observed in the presence of N-functionalities

seems to result from the interaction of oxygen with the carbon surface. N-groups with delocalized extra electrons were identified as the possible species responsible for the enhanced chemisorption and activation of oxygen molecules. Such active oxygen species can react with adsorbed organic compounds leading to the oxidation of the organic pollutants.

References

[1] V.S. Mishra, V.V. Mahajani, J.B. Joshi, Wet Air Oxidation, Industrial & Engineering Chemistry Research, 34 (1995) 2-48.
[2] D. Mantzavinos, M. Sahibzada, A.G. Livingston, I.S. Metcalfe, K. Hellgardt, Wastewater treatment: wet air oxidation as a precursor to biological treatment, Catalysis Today, 53 (1999) 93-106.
[3] S.T. Kolaczkowski, P. Plucinski, F.J. Beltran, F.J. Rivas, D.B. McLurgh, Wet air oxidation: a review of process technologies and aspects in reactor design, Chemical Engineering Journal, 73 (1999) 143-160.
[4] F. Luck, Wet air oxidation: past, present and future, Catalysis Today, 53 (1999) 81-91.
[5] H. Debellefontaine, J.N. Foussard, Wet air oxidation for the treatment of industrial wastes. Chemical aspects, reactor design and industrial applications in Europe, Waste Management, 20 (2000) 15-25.
[6] S.K. Bhargava, J. Tardio, J. Prasad, K. Foger, D.B. Akolekar, S.C. Grocott, Wet Oxidation and Catalytic Wet Oxidation, Industrial & Engineering Chemistry Research, 45 (2006) 1221-1258.
[7] J. Levec, A. Pintar, Catalytic wet-air oxidation processes: A review, Catalysis Today, 124 (2007) 172-184.
[8] A. Cybulski, Catalytic Wet Air Oxidation: Are Monolithic Catalysts and Reactors Feasible?, Industrial & Engineering Chemistry Research, 46 (2007) 4007-4033.
[9] J.L. Figueiredo, M.F.R. Pereira, The role of surface chemistry in catalysis with carbons, Catalysis Today, 150 (2010) 2-7.
[10] M. Soria-Sánchez, A. Maroto-Valiente, J. Álvarez-Rodríguez, V. Muñoz-Andrés, I. Rodríguez-Ramos, A. Guerrero-Ruíz, Carbon nanostrutured materials as direct catalysts for phenol oxidation in aqueous phase, Applied Catalysis B: Environmental, 104 (2011) 101-109.
[11] H.T. Gomes, Oxidação Catalítica por Via Húmida de Poluentes Orgânicos, Faculdade de Engenharia da Universidade do Porto, 2002, pp. 242.
[12] A.M.T. Silva, R.M. Quinta-Ferreira, J. Levec, Catalytic and Noncatalytic Wet Oxidation of Formaldehyde. A Novel Kinetic Model, Industrial & Engineering Chemistry Research, 42 (2003) 5099-5108.
[13] Â.C. Apolinário, A.M.T. Silva, B.F. Machado, H.T. Gomes, P.P. Araújo, J.L. Figueiredo, J.L. Faria, Wet air oxidation of nitro-aromatic compounds: Reactivity on single- and multi-component systems and surface chemistry studies with a carbon xerogel, Applied Catalysis B: Environmental, 84 (2008) 75-86.
[14] H.T. Gomes, B.F. Machado, A. Ribeiro, I. Moreira, M. Rosário, A.M.T. Silva, J.L. Figueiredo, J.L. Faria, Catalytic properties of carbon materials for wet oxidation of aniline, Journal of Hazardous Materials, 159 (2008) 420-426.
[15] S. Morales-Torres, A.M.T. Silva, A.F. Pérez-Cadenas, J.L. Faria, F.J. Maldonado-Hódar, J.L. Figueiredo, F. Carrasco-Marín, Wet air oxidation of trinitrophenol with

activated carbon catalysts: Effect of textural properties on the mechanism of degradation, Applied Catalysis B: Environmental, 100 (2010) 310-317.
[16] G. Ovejero, J.L. Sotelo, M.D. Romero, A. Rodríguez, M.A. Ocaña, G. Rodríguez, J. García, Multiwalled carbon nanotubes for liquid-phase oxidation. Functionalization, characterization, and catalytic activity, Industrial and Engineering Chemistry Research, 45 (2006) 2206-2212.
[17] J.P.S. Sousa, A.M.T. Silva, M.F.R. Pereira, J.L. Figueiredo, Wet Air Oxidation of Aniline Using Carbon Foams and Fibers Enriched with Nitrogen, Separation Science and Technology, 45 (2010) 1546 - 1554.
[18] H.-P. Boehm, Catalytic Properties of Nitrogen-Containing Carbons, in: P. Serp,J.L. Figueiredo (Eds.), Carbon Materials for Catalysis, pp. 219-265, John Wiley & Sons, Inc. Hoboken, NJ 2009.
[19] P.C.C. Faria, J.J.M. Órfão, M.F.R. Pereira, Activated carbon catalytic ozonation of oxamic and oxalic acids, Applied Catalysis B: Environmental, 79 (2008) 237-243.
[20] A.G. Gonçalves, J.L. Figueiredo, J.J.M. Órfão, M.F.R. Pereira, Influence of the surface chemistry of multi-walled carbon nanotubes on their activity as ozonation catalysts, Carbon, 48 (2010) 4369-4381.
[21] H. Chen, G. Yang, Y. Feng, C. Shi, S. Xu, W. Cao, X. Zhang, Biodegradability enhancement of coking wastewater by catalytic wet air oxidation using aminated activated carbon as catalyst, Chemical Engineering Journal, 198–199 (2012) 45-51.
[22] M. Santiago, F. Stüber, A. Fortuny, A. Fabregat, J. Font, Modified activated carbons for catalytic wet air oxidation of phenol, Carbon, 43 (2005) 2134-2145.
[23] M. Soria-Sánchez, E. Castillejos-López, A. Maroto-Valiente, M.F.R. Pereira, J.J.M. Órfão, A. Guerrero-Ruiz, High efficiency of the cylindrical mesopores of MWCNTs for the catalytic wet peroxide oxidation of C.I. Reactive Red 241 dissolved in water, Applied Catalysis B: Environmental, 121–122 (2012) 182-189.
[24] F. Stüber, J. Font, A. Fortuny, C. Bengoa, A. Eftaxias, A. Fabregat, Carbon materials and catalytic wet air oxidation of organic pollutants in wastewater, Topics in Catalysis, 33 (2005) 3-50.
[25] M.E. Suarez-Ojeda, F. Stüber, A. Fortuny, A. Fabregat, J. Carrera, J. Font, Catalytic wet air oxidation of substituted phenols using activated carbon as catalyst, Applied Catalysis B: Environmental, 58 (2005) 105-114.
[26] A. Quintanilla, N. Menéndez, J. Tornero, J.A. Casas, J.J. Rodríguez, Surface modification of carbon-supported iron catalyst during the wet air oxidation of phenol: Influence on activity, selectivity and stability, Applied Catalysis B: Environmental, 81 (2008) 105-114.
[27] G. Yang, H. Chen, H. Qin, Y. Feng, Amination of activated carbon for enhancing phenol adsorption: Effect of nitrogen-containing functional groups, Applied Surface Science, 293 (2014) 299-305.
[28] J.L. Figueiredo, Functionalization of porous carbons for catalytic applications, Journal of Materials Chemistry A, 1 (2013) 9351-9364.
[29] J.L. Figueiredo, M.F.R. Pereira, Carbon as Catalyst, Carbon Materials for Catalysis, John Wiley & Sons, Inc.2009, pp. 177-217.

[30] S. Yang, W. Zhu, X. Li, J. Wang, Y. Zhou, Multi-walled carbon nanotubes (MWNTs) as an efficient catalyst for catalytic wet air oxidation of phenol, Catalysis Communications, 8 (2007) 2059-2063.
[31] S. Yang, X. Li, W. Zhu, J. Wang, C. Descorme, Catalytic activity, stability and structure of multi-walled carbon nanotubes in the wet air oxidation of phenol, Carbon, 46 (2008) 445-452.
[32] S. Yang, X. Wang, H. Yang, Y. Sun, Y. Liu, Influence of the different oxidation treatment on the performance of multi-walled carbon nanotubes in the catalytic wet air oxidation of phenol, Journal of Hazardous Materials, 233–234 (2012) 18-24.
[33] J. Wang, W. Fu, X. He, S. Yang, W. Zhu, Catalytic wet air oxidation of phenol with functionalized carbon materials as catalysts: Reaction mechanism and pathway, Journal of Environmental Sciences (China), 26 (2014) 1741-1749.
[34] S. Yang, Y. Sun, H. Yang, J. Wan, Catalytic wet air oxidation of phenol, nitrobenzene and aniline over the multi-walled carbon nanotubes (MWCNTs) as catalysts, Frontiers of Environmental Science & Engineering, (2014).
[35] E. Pollak, G. Salitra, A. Soffer, D. Aurbach, On the reaction of oxygen with nitrogen-containing and nitrogen-free carbons, Carbon, 44 (2006) 3302-3307.
[36] H. Cao, L. Xing, G. Wu, Y. Xie, S. Shi, Y. Zhang, D. Minakata, J.C. Crittenden, Promoting effect of nitration modification on activated carbon in the catalytic ozonation of oxalic acid, Applied Catalysis B: Environmental, 146 (2014) 169-176.
[37] G.S. Szymański, T. Grzybek, H. Papp, Influence of nitrogen surface functionalities on the catalytic activity of activated carbon in low temperature SCR of NOx with NH3, Catalysis Today, 90 (2004) 51-59.
[38] E.M. Sulman, V.G. Matveeva, V.Y. Doluda, A.I. Sidorov, N.V. Lakina, A.V. Bykov, M.G. Sulman, P.M. Valetsky, L.M. Kustov, O.P. Tkachenko, B.D. Stein, L.M. Bronstein, Efficient polymer-based nanocatalysts with enhanced catalytic performance in wet air oxidation of phenol, Applied Catalysis B: Environmental, 94 (2010) 200-210.
[39] H.T. Gomes, S.M. Miranda, M.J. Sampaio, A.M.T. Silva, J.L. Faria, Activated carbons treated with sulphuric acid: Catalysts for catalytic wet peroxide oxidation, Catalysis Today, 151 (2010) 153-158.
[40] H.T. Gomes, S.M. Miranda, M.J. Sampaio, J.L. Figueiredo, A.M.T. Silva, J.L. Faria, The role of activated carbons functionalized with thiol and sulfonic acid groups in catalytic wet peroxide oxidation, Applied Catalysis B: Environmental, 106 (2011) 390-397.
[41] C. Liang, H.-W. Su, Identification of Sulfate and Hydroxyl Radicals in Thermally Activated Persulfate, Industrial & Engineering Chemistry Research, 48 (2009) 5558-5562.
[42] F. Rodríguez-Reinoso, The role of carbon materials in heterogeneous catalysis, Carbon, 36 (1998) 159-175.
[43] Y. Zhang, J. Zhang, D.S. Su, Substitutional Doping of Carbon Nanotubes with Heteroatoms and Their Chemical Applications, Chemsuschem, 7 (2014) 1240-1250.

[44] Á. Kukovecz, T. Kanyó, Z. Kónya, I. Kiricsi, Long-time low-impact ball milling of multi-wall carbon nanotubes, Carbon, 43 (2005) 994-1000.
[45] F. Li, Y. Lu, L. Liu, L. Zhang, J. Dai, J. Ma, Relations between carbon nanotubes' length and their composites' mechanical and functional performance, Polymer, 54 (2013) 2158-2165.
[46] O.S.G.P. Soares, A.G. Goncalves, J.J. Delgado, J.J.M. Órfão, M.F.R. Pereira, Modification of carbon nanotubes by ball-milling to be used as ozonation catalysts, Catalysis Today, 249 (2015) 199-203.
[47] H.-P. Boehm, Catalytic Properties of Nitrogen-Containing Carbons, in: P. Serp,J.L. Figueiredo (Eds.), Carbon Materials for Catalysis, John Wiley & Sons, Inc. Hoboken, NJ2009.
[48] R. Czerw, M. Terrones, J.C. Charlier, X. Blase, B. Foley, R. Kamalakaran, N. Grobert, H. Terrones, D. Tekleab, P.M. Ajayan, W. Blau, M. Ruhle, D.L. Carroll, Identification of electron donor states in N-doped carbon nanotubes, Nano Letters, 1 (2001) 457-460.
[49] K.S. Novoselov, A.K. Geim, S.V. Morozov, D. Jiang, Y. Zhang, S.V. Dubonos, I.V. Grigorieva, A.A. Firsov, Electric Field Effect in Atomically Thin Carbon Films, Science, 306 (2004) 666-669.
[50] A.K. Geim, K.S. Novoselov, The rise of graphene, Nature Materials, 6 (2007) 183.
[51] A.K. Geim, Graphene: Status and Prospects, Science, 324 (2009) 1530-1534.
[52] N.M. Julkapli, S. Bagheri, Graphene supported heterogeneous catalysts: An overview, International Journal of Hydrogen Energy, 40 (2015) 948-979.
[53] S. Pei, H.-M. Cheng, The reduction of graphene oxide, Carbon, 50 (2012) 3210-3228.
[54] N. Job, R. Pirard, J. Marien, J.-P. Pirard, Porous carbon xerogels with texture tailored by pH control during sol–gel process, Carbon, 42 (2004) 619-628.
[55] H.F. Gorgulho, F. Gonçalves, M.F.R. Pereira, J.L. Figueiredo, Synthesis and characterization of nitrogen-doped carbon xerogels, Carbon, 47 (2009) 2032-2039.
[56] M. Pérez-Cadenas, C. Moreno-Castilla, F. Carrasco-Marín, A.F. Pérez-Cadenas, Surface Chemistry, Porous Texture, and Morphology of N-Doped Carbon Xerogels, Langmuir, 25 (2008) 466-470.
[57] J.P.S. Sousa, M.F.R. Pereira, J.L. Figueiredo, NO oxidation over nitrogen doped carbon xerogels, Applied Catalysis B: Environmental, 125 (2012) 398-408.
[58] K.-H. Kim, S.-K. Ihm, Heterogeneous catalytic wet air oxidation of refractory organic pollutants in industrial wastewaters: A review, Journal of Hazardous Materials, 186 (2011) 16-34.
[59] A. Sadana, J.R. Katzer, Involvement of free radicals in the aqueous-phase catalytic oxidation of phenol over copper oxide, Journal of Catalysis, 35 (1974) 140-152.
[60] A. Pintar, J. Levec, Catalytic oxidation of organics in aqueous solutions: I. Kinetics of phenol oxidation, Journal of Catalysis, 135 (1992) 345-357.

[61] R. Robert, S. Barbati, N. Ricq, M. Ambrosio, Intermediates in wet oxidation of cellulose: identification of hydroxyl radical and characterization of hydrogen peroxide, Water Research, 36 (2002) 4821-4829.
[62] P.D. Vaidya, V.V. Mahajani, Insight into sub-critical wet oxidation of phenol, Advances in Environmental Research, 6 (2002) 429-439.
[63] B. Stöffler, G. Luft, Influence of the Radical Scavenger t-Butanol on the Wet Air Oxidation of p-Toluenesulfonic Acid, Chemical Engineering & Technology, 22 (1999) 409-412.
[64] F.J. Beltrán, F.J. Rivas, L.A. Fernández, P.M. Álvarez, R. Montero-de-Espinosa, Kinetics of catalytic ozonation of oxalic acid in water with activated carbon, Industrial and Engineering Chemistry Research, 41 (2002) 6510-6517.
[65] J. Hoigné, Inter-calibration of OH radical sources and water quality parameters, Water Science and Technology, 35 (1997) 1-8.
[66] J. Méndez-Díaz, M. Sánchez-Polo, J. Rivera-Utrilla, S. Canonica, U. von Gunten, Advanced oxidation of the surfactant SDBS by means of hydroxyl and sulphate radicals, Chemical Engineering Journal, 163 (2010) 300-306.
[67] P.C.C. Faria, J.J.M. Órfão, M.F.R. Pereira, Activated carbon and ceria catalysts applied to the catalytic ozonation of dyes and textile effluents, Applied Catalysis B: Environmental, 88 (2009) 341-350.
[68] D.F.M. Santos, O.S.G.P. Soares, A.M.T. Silva, J.L. Figueiredo, M.F.R. Pereira, Catalytic wet oxidation of organic compounds over N-doped carbon nanotubes in batch and continuous operation, Applied Catalysis B: Environmental, 199 (2016) 361-371.
[69] N. Yan, F. Liu, W. Huang, Interaction of oxidants in siderite catalyzed hydrogen peroxide and persulfate system using trichloroethylene as a target contaminant, Chemical Engineering Journal, 219 (2013) 149-154.
[70] T. Olmez-Hanci, I. Arslan-Alaton, Comparison of sulfate and hydroxyl radical based advanced oxidation of phenol, Chemical Engineering Journal, 224 (2013) 10-16.
[71] X.Y. Xu, G.M. Zeng, Y.R. Peng, Z. Zeng, Potassium persulfate promoted catalytic wet oxidation of fulvic acid as a model organic compound in landfill leachate with activated carbon, Chemical Engineering Journal, 200-202 (2012) 25-31.
[72] J. Criquet, N.K.V. Leitner, Degradation of acetic acid with sulfate radical generated by persulfate ions photolysis, Chemosphere, 77 (2009) 194-200.
[73] J.A. Khan, X. He, H.M. Khan, N.S. Shah, D.D. Dionysiou, Oxidative degradation of atrazine in aqueous solution by UV/H2O2/Fe2+, UV//Fe2+ and UV//Fe2+ processes: A comparative study, Chemical Engineering Journal, 218 (2013) 376-383.
[74] S.S. Abu Amr, H.A. Aziz, M.N. Adlan, M.J.K. Bashir, Pretreatment of stabilized leachate using ozone/persulfate oxidation process, Chemical Engineering Journal, 221 (2013) 492-499.

[75] P. Neta, R.E. Huie, A.B. Ross, Rate Constants for Reactions of Inorganic Radicals in Aqueous Solution, Journal of Physical and Chemical Reference Data, 17 (1988) 1027-1284.
[76] S. Yang, X. Yang, X. Shao, R. Niu, L. Wang, Activated carbon catalyzed persulfate oxidation of Azo dye acid orange 7 at ambient temperature, Journal of Hazardous Materials, 186 (2011) 659-666.
[77] H.R. Devlin, I.J. Harris, Mechanism of the oxidation of aqueous phenol with dissolved oxygen, Industrial & Engineering Chemistry Fundamentals, 23 (1984) 387-392.
[78] R.V. Shende, J. Levec, Wet Oxidation Kinetics of Refractory Low Molecular Mass Carboxylic Acids, Industrial & Engineering Chemistry Research, 38 (1999) 3830-3837.
[79] R.V. Shende, V.V. Mahajani, Kinetics of Wet Air Oxidation of Glyoxalic Acid and Oxalic Acid, Industrial & Engineering Chemistry Research, 33 (1994) 3125-3130.
[80] P. Gallezot, N. Laurain, P. Isnard, Catalytic wet-air oxidation of carboxylic acids on carbon-supported platinum catalysts, Applied Catalysis B: Environmental, 9 (1996) L11-L17.
[81] D.-K. Lee, D.-S. Kim, Catalytic wet air oxidation of carboxylic acids at atmospheric pressure, Catalysis Today, 63 (2000) 249-255.
[82] S. Roy, A.K. Saroha, Ceria promoted [gamma]-Al2O3 supported platinum catalyst for catalytic wet air oxidation of oxalic acid: kinetics and catalyst deactivation, RSC Advances, 4 (2014) 56838-56847.
[83] B.B. Pruden, H. Le, Wet air oxidation of soluble components in waste water, The Canadian Journal of Chemical Engineering, 54 (1976) 319-325.
[84] M.T. Harris, G.E. Oswald, R.L. Jolley, Wet oxidation of phenol and naphthalene in aqueous and sludge solutions: applicability for the treatment of phenolics and PAHs found in coal conversion wastewater and biological sludge, ; Oak Ridge National Lab., TN (USA)1983.
[85] A. Quintanilla, C.M. Dominguez, J.A. Casas, J.J. Rodriguez, Emerging catalysts for wet air oxidation process, Focus on Catalysis Research: New Developments2012, pp. 237-259.
[86] M.E. Suárez-Ojeda, J. Carrera, I.S. Metcalfe, J. Font, Wet air oxidation (WAO) as a precursor to biological treatment of substituted phenols: Refractory nature of the WAO intermediates, Chemical Engineering Journal, 144 (2008) 205-212.
[87] Y.I. Matatov-Meytal, M. Sheintuch, Catalytic Abatement of Water Pollutants, Industrial & Engineering Chemistry Research, 37 (1998) 309-326.
[88] S. Imamura, Catalytic and Noncatalytic Wet Oxidation, Industrial & Engineering Chemistry Research, 38 (1999) 1743-1753.
[89] A.B. Ayusheev, O.P. Taran, I.A. Seryak, O.Y. Podyacheva, C. Descorme, M. Besson, L.S. Kibis, A.I. Boronin, A.I. Romanenko, Z.R. Ismagilov, V. Parmon, Ruthenium nanoparticles supported on nitrogen-doped carbon nanofibers for the catalytic wet air oxidation of phenol, Applied Catalysis B: Environmental, 146 (2014) 177-185.

[90] B. Larruy, A. Ayude, J. Font, A. Fortuny, C. Bengoa, A. Fabregat, F. Stüber, Gas feed composition modulation in phenol CWAO over active carbon, Chemical Engineering Science, 62 (2007) 5564-5566.
[91] A. Eftaxias, J. Font, A. Fortuny, A. Fabregat, F. Stüber, Catalytic wet air oxidation of phenol over active carbon catalyst: Global kinetic modelling using simulated annealing, Applied Catalysis B: Environmental, 67 (2006) 12-23.
[92] F. Stüber, I. Polaert, H. Delmas, J. Font, A. Fortuny, A. Fabregat, Catalytic wet air oxidation of phenol using active carbon: performance of discontinuous and continuous reactors, Journal of Chemical Technology & Biotechnology, 76 (2001) 743-751.
[93] A. Eftaxias, J. Font, A. Fortuny, A. Fabregat, F. Stüber, Kinetics of phenol oxidation in a trickle bed reactor over active carbon catalyst, Journal of Chemical Technology & Biotechnology, 80 (2005) 677-687.
[94] K.M. de Lathouder, E. Crezee, F. Kapteijn, J.A. Moulijn, Carbon Monoliths in Catalysis, Carbon Materials for Catalysis, John Wiley & Sons, Inc.2008, pp. 401-427.
[95] E. Garcia-Bordeje, Y. Liu, D.S. Su, C. Pham-Huu, Hierarchically structured reactors containing nanocarbons for intensification of chemical reactions, Journal of Materials Chemistry A, 5 (2017) 22408-22441.
[96] H. Ba, Y. Liu, L. Truong-Phuoc, C. Duong-Viet, X. Mu, W.H. Doh, T. Tran-Thanh, W. Baaziz, L. Nguyen-Dinh, J.-M. Nhut, I. Janowska, D. Begin, S. Zafeiratos, P. Granger, G. Tuci, G. Giambastiani, F. Banhart, M.J. Ledoux, C. Pham-Huu, A highly N-doped carbon phase "dressing" of macroscopic supports for catalytic applications, Chemical Communications, 51 (2015) 14393-14396.

(This page intentionally left blank)

PART V

Conclusions and Future Work

CONTENT

Conclusions

Future Work

(This page intentionally left blank)

Conclusions

Carbon-based materials, namely carbon nanotubes (CNTs), carbon xerogels (CXs) and graphene-based materials (rGOs) were prepared or modified by suitable chemical and thermal treatments in order to improve their catalytic performance in liquid-phase reactions, namely the oxidation of organic compounds by catalytic wet air oxidation (CWAO) and the acid catalysed reaction of esterification of acetic acid with ethanol. Controllable tuning of the surface chemistry allowed to obtain stable and highly active catalysts thus providing a reliable alternative to the metal-based and homogeneous catalysts traditionally used in the selected reactions.

The modifications promoted by liquid/gas-phase or mechanical treatments, allowed to obtain carbon materials with different oxygen, nitrogen, and sulphur functional groups, preserving, in most cases, the textural properties of the materials.

O-functionalities were incorporated by liquid-phase treatments with concentrated nitric acid (HNO_3) at boiling temperature, or by hydrothermal treatment with diluted HNO_3. Acidic carbon samples can be obtained by these methods, due to the functionalization of the carbon surface with acidic O-surface groups (carboxylic acids, anhydrides, phenols and lactones). Neutral or basic groups like carbonyl and quinone groups were also incorporated. The hydrothermal treatment with diluted HNO_3 has the advantage to allow a finer control of the amount of O-containing groups incorporated as function of the acid concentration used (0.05 – 0.30 mol L^{-1}). The basicity of the carbon surface can be recovered by thermal treatments under inert atmosphere at specific temperatures after

oxidation with HNO_3, in order to selectively remove some of the groups previously introduced during oxidation.

The basicity of carbon materials was improved by doping the surface with nitrogen functionalities. Post-treatments were developed, including hydrothermal functionalization using urea as nitrogen precursor and a novel method involving a mechanical treatment under ball milling, followed by thermal treatment. Several parameters were studied to optimize this new method. Among the N-precursors tested, melamine was the most effective for the incorporation of large amounts of pyridine (N6), pyrrole (N5) and quaternary nitrogen (NQ), avoiding the use of solvents and production of wastes. The new approach was successfully tested to incorporate N6, N5, NQ onto the surfaces of CNT and rGO samples.

Strongly acidic sulphonic groups ($-SO_3H$) were successfully incorporated on the graphitic network of CNT and CX samples by liquid-phase treatments using sulphuric acid (H_2SO_4) or a mixture of H_2SO_4/HNO_3. Larger amounts of $-SO_3H$ were incorporated on CX samples (up to 3.2 % wt., determined by XPS). The use of H_2SO_4 alone was found to be more adequate for the incorporation of $-SO_3H$ groups than the simultaneous use of H_2SO_4/HNO_3, which led to the incorporation of large amounts of O-functionalities, in the case of CNTs.

The role of the incorporated surface groups was evaluated in liquid-phase reactions catalysed by the prepared carbon materials. Esterification of acetic acid with ethanol was investigated using acidic CNT and CX samples. The S-doped samples, and particularly CX samples, were found to be more effective for the formation of ethyl acetate than the acidic O-containing groups incorporated by oxidation with HNO_3. An ethyl acetate yield higher than 50 % was obtained in 6 h of reaction using the CX samples

with the highest concentration of -SO_3H groups, being competitive with other carbon-based materials reported in the literature. A good correlation was found between the ethyl acetate rate formation and the concentration of -SO_3H groups.

Investigation of the catalytic activity of carbon materials under CWAO was performed using oxalic acid and phenol as model pollutants. Their resistance to oxidation can be overcome by using carbon materials as catalysts in the reaction. The most promising catalyst, the melamine treated sample CNT-BM-M, allowed full oxalic acid conversion in 5 min of reaction (140 °C; 40 bar of total pressure; initial oxalic acid concentration of 1000 mg L^{-1}) and a phenol degradation of 97 % in 2 h. CNT, CX and rGO samples with O-, N- and S-functionalities were tested. It was found that the apparent initial first order reaction rate constants for CWAO of oxalic acid correlate with the point of zero charge of the CNT samples. In addition, the absence of acidic O-containing groups, such as carboxylic acids and anhydrides, is beneficial for the reactions (the conversion of model pollutants increased as the amount of O-containing surface groups present on the catalyst surface released as CO_2 decreased). S-doped CNTs modified with H_2SO_4 or H_2SO_4/HNO_3, despite their strong acidic character (low pH_{PZC}), showed an unexpected good performance, ascribed to the presence of S-containing surface groups that may originate strong oxidant species in the liquid-phase, such as sulphate radicals. However, the low decomposition temperature of the -SO_3H surface groups compromises their reuse in cyclic experiments. The increase of the surface basicity by incorporation of nitrogen led to improved catalytic activity of the carbon materials, except in the case of the rGO-U sample. Using N-doped CX samples, a positive correlation between the apparent reaction rate

constant of oxalic acid oxidation and the amount of nitrogen determined by XPS was obtained, highlighting the improvement of the catalytic performance by N-doping. In general, N-doped CNT samples performed better than N-doped CX and rGO samples, particularly samples prepared by the novel solvent-free approach involving ball milling followed by thermal treatment. N-species were stable in cyclic evaluations without loss or modifications of the species. Mechanistic clarification experiments performed with the radical scavenger *tert*-butanol suggested that hydroxyl radicals in solution were not the main species involved in the oxidation mechanism when N-doped carbon materials were used. The reaction was proposed to occur at the surface of carbon materials between the adsorbed pollutant and the active species resulting from the decomposition of oxygen, leading to the oxidation of the organic compound. The role of N-groups was explained by the enhanced chemisorption and activation of oxygen molecules on the carbon surface.

The fine tuning of the carbon surface, providing adequate active sites in the graphitic lattice, was of paramount importance for the observed good performance of the carbon materials in the catalytic reactions studied.

The present work discloses the potentialities of carbon materials in liquid phase reactions offering a promising perspective towards the use of carbon catalysts in industrial applications.

Future Work

The quest for metal-free carbon catalysts suitable for industrial processes cannot cease, and several opportunities should be explored in the near future.

This work demonstrated the application of sulfonated carbon materials as catalysts for the esterification of acetic acid, but other Fischer esterification reactions could be attempted using the acidic samples. In addition, there are several other acid catalysed reactions where the same or similar acidic materials may perform well. These include reactions like etherification, hydration, hydrolysis, alkylation, acetalization and isomerisation, where some interesting results have already been reported in the literature.

The same is valid for the N-doped carbon materials prepared. In addition to the CWAO of oxalic acid and phenol, further studies should be carried out using: other short-chain carboxylic acids as model compounds, like maleic, fumaric, malonic, acetic and formic acids, which are typically refractory under non-catalytic conditions; as well as compounds containing nitrogen bonds, like ammonia, oxamic acid and aniline to evaluate the catalyst efficiency to produce nitrate and elemental nitrogen. Catalytic performance studies should also be extended to halogen-, sulphur- and phosphorous-containing compounds, before testing with real wastewaters. Since CWAO is a wastewater treatment, additional parameters, such as toxicity and biodegradability, should be analysed at the end of the experiments, to ensure that the treated streams are not more dangerous for human health than the original ones.

The N-doped carbon materials can also be applied to other environmental oxidation processes, such as ozonation. Some preliminary results with N-doped carbon materials showed that N-functionalities may favour the reduction of ozone.

In addition, N-doped materials can perform well in other fields: as catalysts in organic synthesis, such as Knoevenagel condensation, where traditionally homogeneous bases are used.

In the energy conversion field, particularly in the replacement of platinum-based catalysts at the cathode of fuel cells (where the oxygen reduction reaction takes place); or even, in the energy storage field, particularly in the development of carbon-based electrodes for supercapacitors that could surpass batteries, an area that gained special relevance in recent years.

In addition to exploring other possible applications of the materials developed herein, doping and functionalization methodologies should not be forgotten. Ball milling may be a promising tool to develop new S-,B-,P-doped materials offering more simple and easy to handle methods, avoiding the use of solvents. Exploratory experiments have been already performed in this context. Thiourea, sodium thiosulphate and sodium sulphite are among the S-precursors already tested.

Ball milling can also be used for doping other carbon materials, in addition to the CNT and rGO samples tested in this work. Further efforts and studies should also be carried out to develop additional methodologies for the incorporation of carbon materials into hierarchical structures, which are more adequate for their industrial application.

In addition to the advances made during this work, new frontiers for carbon materials can be open.

Recent advances in the development of reliable methods for tuning the physicochemical properties and the available reliable methods for a better understanding of the carbon surface chemistry, provide a major asset to correlate the catalytic properties of the carbon materials with their surface chemistry. Active sites should be promptly identified and quantified and turnover frequencies, if possible, calculated, and used to benchmark the novel metal-free catalysts with those currently used. However, this is not the general rule, because characterization techniques have their own weak points and clear qualitative and quantitative identification of the actives sites remains elusive. In addition, not always all surface groups are acting as active sites or available for reaction, due to the chemical environment of the surface. It is advisable to develop studies to increase our knowledge in this area. A new prospect to fostering carbon materials application deals with their characterization by well-defined model reactions. The kinetic profiling of carbon materials in model reactions may support other characterization techniques in distinguishing between the presence of surface functionalities and the real available active sites.

(This page intentionally left blank)

APPENDIX

Supporting Information

(This page intentionally left blank)

Supporting information for *Chapter* 4 *Nitrogen-containing surface groups* (PART II)

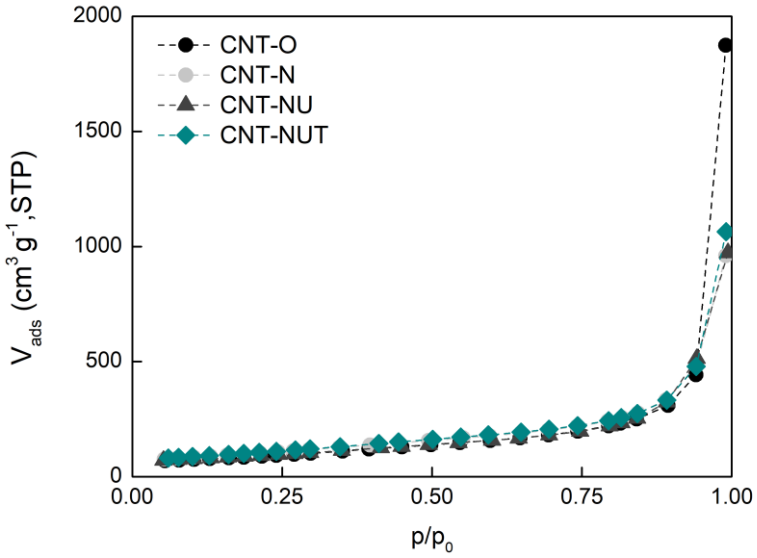

Figure A. 1 N_2 adsorption isotherms at -196 °C of pristine and modified CNT samples during the hydrothermal treatment steps[58].

[58] Adapted from Applied Catalysis B Environmental 104 (2011) 330–336.

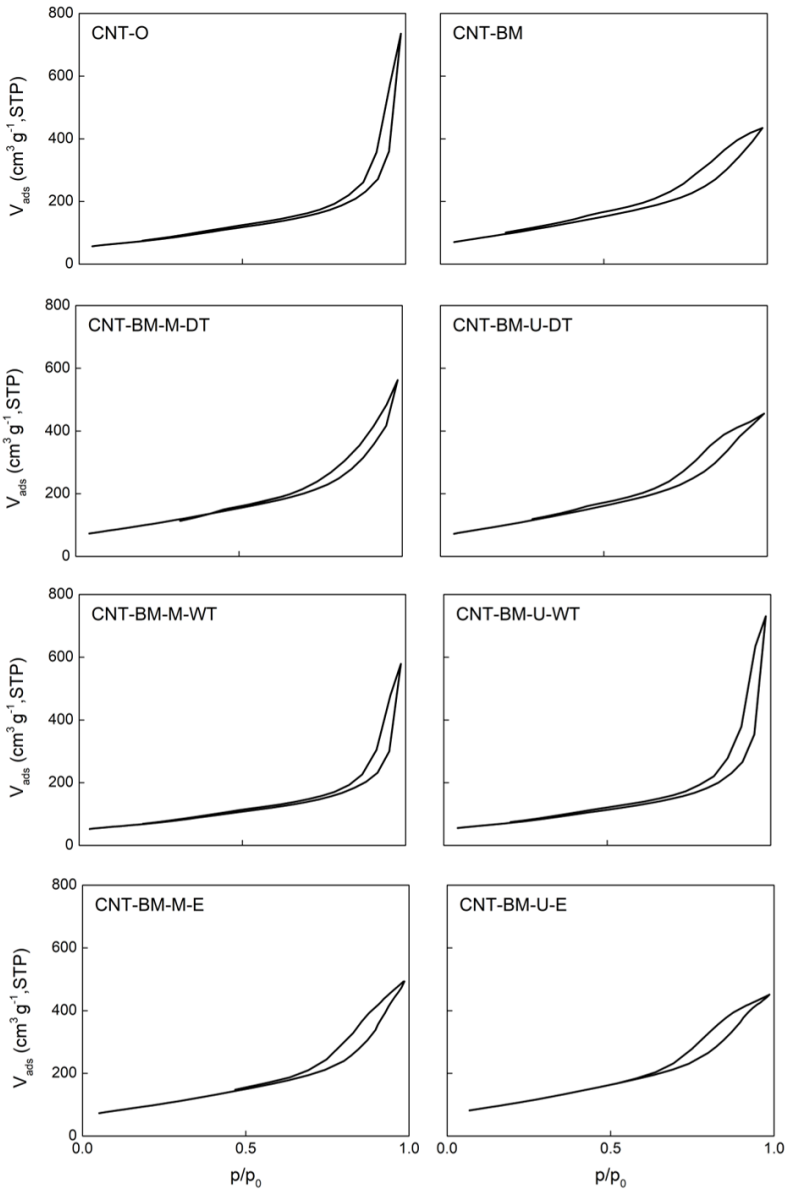

Figure A. 2. N_2 adsorption–desorption isotherms at -196 °C of pristine and ball milled CNT samples prepared by wet, dry or external methodologies[59].

[59] Adapted from Carbon 91 (2015) 114-121.

Appendix ii

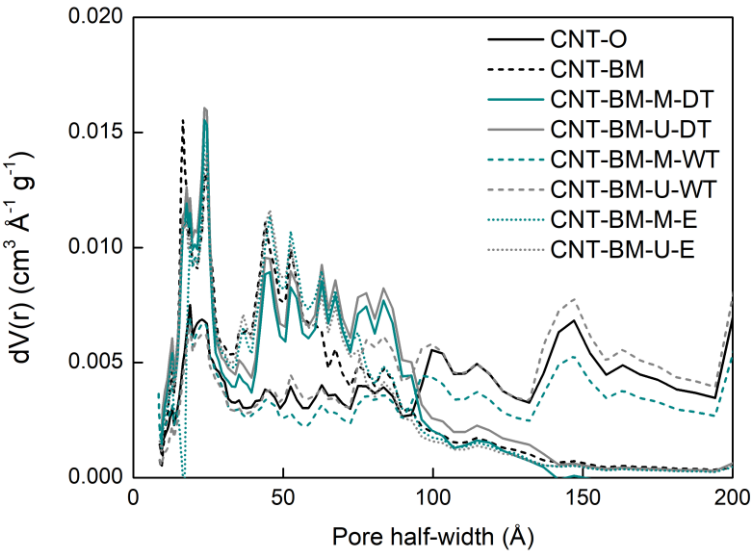

Figure A. 3 Pore size distributions obtained by NLDFT for pristine and ball milled CNT samples prepared by wet, dry or external methodologies[60].

[60] Adapted from Carbon 91 (2015) 114-121.

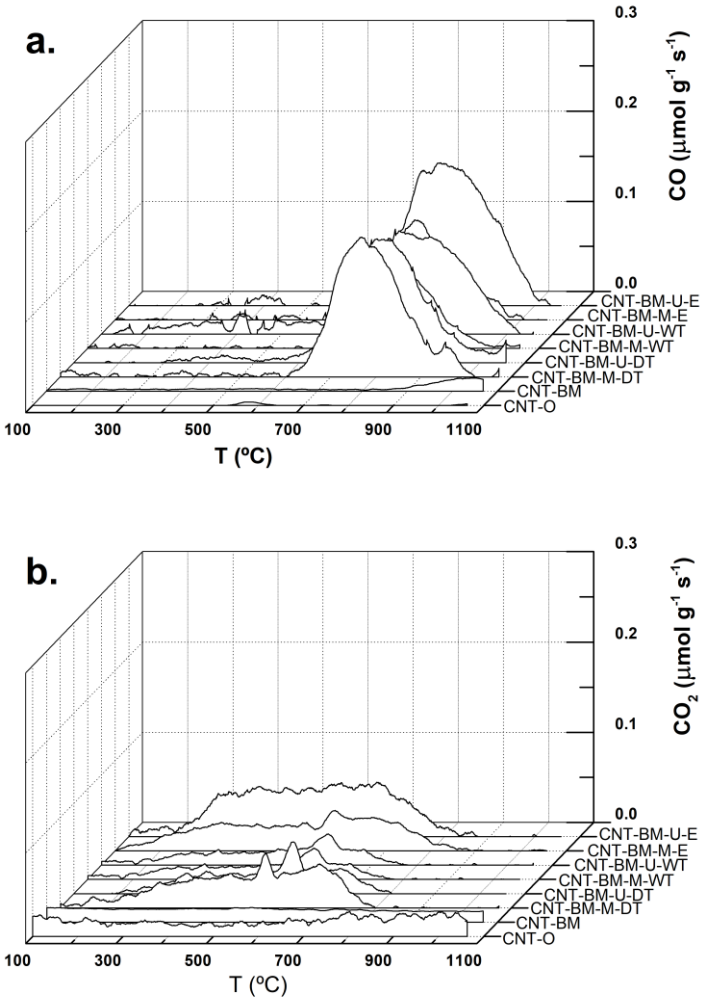

Figure A. 4 CO (a) and CO_2 (b) evolutions in TPD experiments of pristine and ball milled CNT samples prepared by wet, dry or external methodologies[61].

[61] Adapted from Carbon 91 (2015) 114-121.

There comes a point in your life when you need to stop reading other people's books and write your own

- Albert Einstein –

I hope to have accomplished the challenge.

- Raquel Rocha -